RATIONAL SYNTHESIS OF LINEAR AND BRANCHED OLIGOGERMANES

By

MONIKA LAKSHMIE AMADORUGE

Bachelor of Science in Chemistry

University of Kelaniya

Kelaniya, Sri Lanka

2003

Submitted to the Faculty of the
Graduate College of the
Oklahoma State University
in partial fulfillment of
the requirements for
the Degree of
DOCTOR OF PHILOSOPHY
July, 2010

RATIONAL SYNTHESIS OF LINEAR AND

BRANCHED OLIGOGERMANES

Dissertation Approved:

Charles S. Weinert

Dissertation Adviser

Dr. Allen Apblett

Dr. Richard A. Bunce

Dr. LeGrande M. Slaughter

Dr. John N. Veenstra

Dr. Mark E. Payton

Dean of the Graduate College

DEDICATION

I dedicate this dissertation to my loving parents Luwis Amadoru and Wimala Makandana for their inspiration and unconditional love. Your love and guidance helped me to build a strong foundation in life. I owe all my accomplishments and accolades to the two of you. Thank you so much and I love you with all my heart and soul.

ACKNOWLEDGEMENT

The past five years at Oklahoma State University have been a dream come true for me. During this time, I learned valuable lessons as a graduate student and as well as a professional. I would like to take this opportunity to thank everyone who was instrumental in helping me successfully complete this program. First, I would like to thank my advisor Dr. Charles S. Weinert for all his support, supervision, advice, teachings and encouragement. You were always there to guide me whenever needed. You taught me how to write manuscripts, review papers and make presentations to large audiences among many other invaluable teachings that I can ever thank you for. Also, thank you for giving me the opportunity to attend the Gordon conference.

I would also like to thank my thesis committee: Dr. Allen Apblett, Dr. Richard Bunce, Dr. LeGrande Slaughter and Dr. John Veenstra. Thank you very much for your advice, guidance, comments and reviewing my work. I am also very thankful to our

collaborators for their assistance. Thank you Dr. Claude Yoder (Franklin and Marshall College) for your help with the ^{73}Ge NMR analysis. I am also thankful to Dr. James Gardinier (Marquette University) for helping with the Density Functional Calculations. Thank you, Dr. Arnold Rheingold, for helping with the X-ray crystallography. Also, thank you Dr. Iob, for your assistance with the instrumentations. Thank you, Gianna, for training me for NMR and helping me with all NMR issues and mostly for your friendship. I would also like to thank Dr. Bunce, Dr. Ohrtman and Dr. Materer for providing me with the chemicals I needed.

Also, I would like to thank all the current and former members of Dr. Weinert's research group. Thank you, Dr. Tony and Rebecca, for being such a nice lab family; but you left me here for another year. I really miss the two of you. Thank you Esla, Dr. Christian, Erin, Aaron, Kim, Courtney and Hope for your friendship, making the lab a nice working environment and all the help you have given me. I would like to thank the faculty and the staff at the chemistry department for giving me the opportunity to pursue my PhD and for all the support. Thank you to all my friends that I met here and wish you the best of luck.

Last, but not least,I am very much grateful to my family: my parents, my two brothers and my sister. Thank you for all the love, encouragement and prayers you gave me to achieve my goals. Although you are far from me distance wise, I never felt that way because you are always in my heart. Finally, I would like to thank my fiancé Mike and his family for their love and support. You were always by my side and never let me down. Whenever frustration set in, you listened to me, supported me and encouraged me. Thank you so much and I love you.

TABLE OF CONTENTS

Chapter **Page**

Chapter 5 Page

LIST OF TABLES

Table **Page**

Chapter 1

Chapter 2

Chapter 3

Chapter 4

Chapter 5

LIST OF FIGURES

Figure Page

Chapter 1

Chapter 2

Chapter 3

Chapter 4

Chapter 5

LIST OF SCHEMES

Scheme Page

Chapter 1

Chapter 2

Chapter 3

Chapter 5

CHAPTER ONE

INTRODUCTION

Catenated compounds of the heavier group 14 elements are of significant interest. Although these singly bonded molecules structurally resemble saturated hydrocarbons, the bonding electrons in the element-element backbone are not localized between two atoms, but rather are delocalized across the entire backbone. This phenomenon is known as σ-delocalization.[1-3] A *trans* conformation along the element-element backbone is required for this σ delocalization to occur which imparts unusual physical characteristics, particularly in the electronic and optical properties of these compounds. Therefore, these compounds more closely resemble π-conjugated unsaturated hydrocarbons rather than their saturated hydrocarbon analogues. In these systems, the highest occupied molecular orbital is regarded as σ bonding while the lowest unoccupied molecular orbital is σ* antibonding. The HOMO- LUMO electron transition corresponds to the promotion of an electron from σ to the σ* molecular orbital[2] and the interesting optical attributes of these compounds are due to this electronic transition. Other potentially useful physical properties exhibited by these compounds include conductivity, thermochromism, and non-linear optical properties.[4-7]

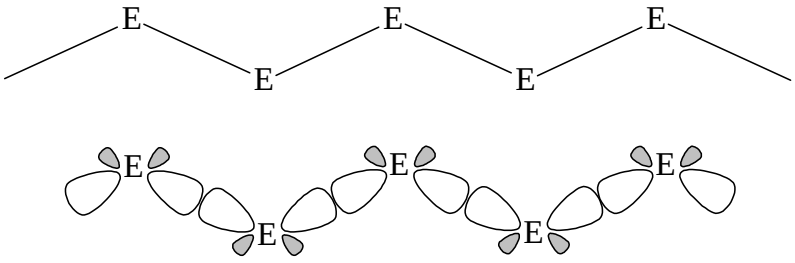

Figure 1.1: Basis set orbitals in a σ-conjugated linear chain of interacting sp^3 orbitals in group 14 catenates.[1,8]

Among the heavier group 14 catenates, studies of the synthesis, properties and chemistry are well developed for silicon-[9-19] and tin-[20-37] containing compounds. In the case of germanium, however, the synthesis, chemistry, and properties are less understood. This is due to the difficulties encountered in the reactions involving the formation of germanium-germanium bonds. Compounds containing Si-Si and Sn-Sn bonds can be readily prepared using several facile synthetic methods in good to excellent yields, but the synthesis of singly bonded germanium compounds is complicated due to the formation of product mixtures and/or low yields. A detailed investigation of the relationship between the composition of catenated germanium compounds and their physical properties has been hampered due to the lack of available methods to prepare discrete oligogermanium compounds. Those structure/property investigations have been conducted in significant detail for silicon and tin catenates. Although, in the past 80 years, some progress has been made in the synthesis and characterization of oligogermanes, the scope of these investigations has not approached the magnitude of those directed at the related silicon and tin containing compounds. The focus of this chapter is to provide a brief survey of the synthetic methods, structures and properties of singly bonded oligogermanes that have been reported prior to our investigation.

Germanium was discovered by Clemens Winkler in 1886 in Freiburg in Germany.[38-39] One year after of the discovery of the element, the first organometallic germanium compound, Et_4Ge, was reported.[40] Methods for the formation of germanium-germanium bonds were first described in 1925 and the first compound to have a germanium-germanium single bond was $Ph_3GeGePh_3$.[41] The normal germanium-

germanium single bond distance in these systems are regarded to be within the range 2.43-2.47 Å.[42] Unlike the carbon-containing hydrocarbons, these compounds require organic side groups or halogens to stabilize the germanium-germanium single bond. For example, the hydride-substituted digermane, H_3GeGeH_3, which is the germanium analogue of ethane, is highly pyrophoric.[43-47] The previous methods used to form germanium-germanium bonds include Wurtz-type coupling reactions involving germanium(IV) halides by alkali metals, the insertion of germylenes :GeR_2 into Ge-X bonds (X = N, O or a halogen), thermal decomposition of germylmercury compounds, or treatment of germanium halides with organolithium or Grignard reagents.[42-47] The latter methods provided a series of perphenylated linear oligogermanes $Ph(GePh_2)_nPh$ (n = 2 - 5)[48-49] as well as the cyclic derivatives $(Ph_2Ge)_n$ (n = 4-6),[50] although the desired products were typically isolated in low yields in most cases. Significant improvements in yields have also been recently achieved by using SmI_2 as the reducing agent for the coupling of organohalogermanes.[51-52]

Digermanes

Wurtz-type coupling reactions of trialkyl germanium halide using alkali metals can furnish Ge-Ge single bonds.[53] The first digermane $Ph_3GeGePh_3$ (**1**) was prepared in modest yield by the coupling of Ph_3GeBr and sodium metal (Scheme 1.1).[41] Later, similar symmetric hexaalkyl substituted digermanes R_3GeGeR_3 were synthesized with slight deviation of the Wurtz-type coupling reaction.[54-55] The first alkyl substituted digermane $Et_3GeGeEt_3$ was prepared from Et_3GeBr and sodium metal in 1932[54] and, the hexamethyl derivative, $Me_3GeGeMe_3$ was produced from Me_3GeBr and potassium in 1953,[55] while an alternate method for its preparation was reported in 1976.[53]

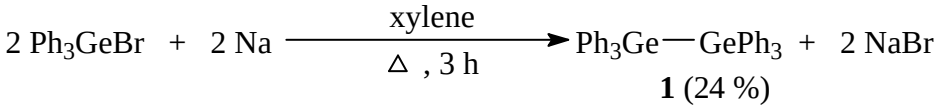

Scheme 1.1: Synthesis of $Ph_3GeGePh_3$ (**1**) by the Wurtz-type coupling of Ph_3GeBr with sodium metal.

Reaction of germanium halides with Grignard or organolithium reagents provides digermanes in low yields as a component of a product mixture, where the outcome of the reaction depends on the reaction conditions and stoichiometry employed.[41,56-59] For example, treatment of $GeBr_4$ with a large excess of PhMgBr in Et_2O[41] failed to furnish digermane $Ph_3GeGePh_3$ (**1**). Instead **1** was obtained in 69 % yield from the reaction of $GeCl_4$ with 7.8 equivalents of PhMgBr in THF that contained a 20 mol % excess magnesium metal.[56] When using a 14:4 mole ratio of PhMgBr:$GeCl_4$, hexaphenyl digermane (**1**) was obtained in 59 % yield, [60] and it was also found that the formation of the trigermane $Ph_3GeGePh_2GePh_3$ (**2**) and the tetragermane $Ph_3GeGePh_2GePh_2GePh_3$ (**3**) occurred under similar conditions when THF was used as the solvent.[57]

The reaction pathway for the formation of compound **1**, **2**, and **3** has been rationalized by considering the reaction pathway for the formation of Ph_4Ge from $GeCl_4$ and PhMgBr (Scheme 1.2 and 1.3). Scheme 1.2 shows the stepwise formation of $GePh_4$ from $GeCl_4$. Once Ph_3GeCl is formed it can react with excess magnesium present to form germyl Grignard reagent $Ph_3GeMgCl$, which also can be generated from the reaction of Ph_3GeCl with PhMgBr itself (Scheme 1.3). This species then reacts with the other phenylchlorogermanes present as intermediates in the stepwise formation of Ph_4Ge to

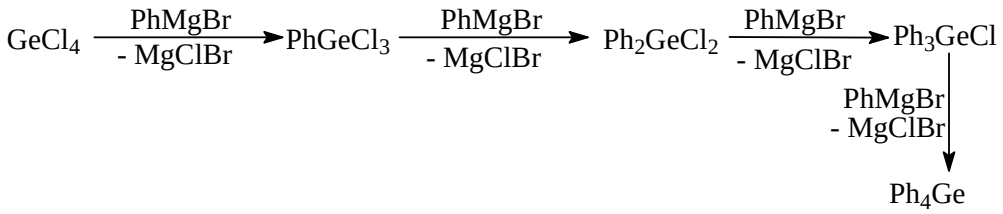

Scheme 1.2: Reaction pathway for the formation of Ph_4Ge from $GeCl_4$ and PhMgBr.

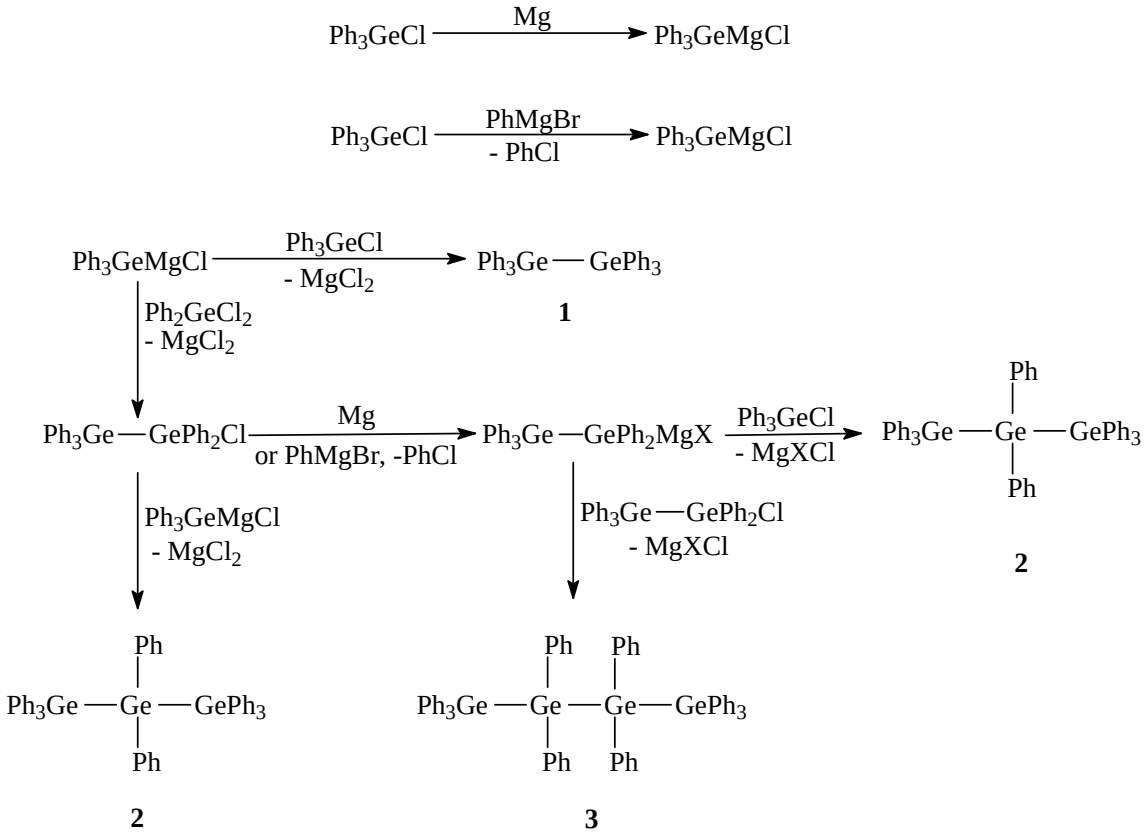

Scheme 1.3: Stepwise formation of oligogermanes **1**, **2**, and **3**.

provide the two higher oligomeric products Ph_8Ge_3 and $Ph_{10}Ge_4$ (Scheme 1.3). The three oligogermanes can be formed in the presence or absence of excess magnesium metal in the Grignard reaction, and the choice of solvent is of importance, since yields of the tri-

and tetragermanes are diminished if Et_2O/toluene is used instead of THF as the reaction medium. Generation of intermediate germyl Grignard reagents resulting from the presence of an excess of magnesium, has been reported to result in the isolation of other digermanes, including hexavinyldigermane[59] and three isomeric hexatolyldigermanes[58].

An ORTEP diagram of the first structurally characterized digermane $Ph_3GeGePh_3$ is shown in Figure 1.2, which was obtained as rhombohedral form (**1a**) from benzene at 25 °C.[61] It was also shown that the morphology of the crystals of **1** depends on the crystallization conditions employed. A hexagonal form of $Ph_3GeGePh_3$ (**1b**)[62] resulted from crystallization using CH_2Cl_2 at 25 °C, while crystallization from CH_2Cl_2 at -15 °C furnished a triclinic form of $Ph_3GeGePh_3$ (**1c**).[62] The geometries around germanium atoms in these three structures are nearly tetrahedral and the Ge-Ge bond distances were found as 2.437(2) Å for the unsolvated triclinic form (**1c**) and 2.446(1) Å for the solvated rhombohedral form (**1a**).[61]

Functionalized digermanes, having functional substituents on the germanium atoms rather than alkyl and aryl groups, are important because these compounds can serve as precursor materials for the synthesis of higher oligogermanes. The dihalogenated digermane $BrPh_2GeGePh_2Br$ (**4**) was produced in 1960[63] (Scheme 1.4) and it can be converted to other useful products by treating with various reagents as shown in Scheme 1.4.[64]

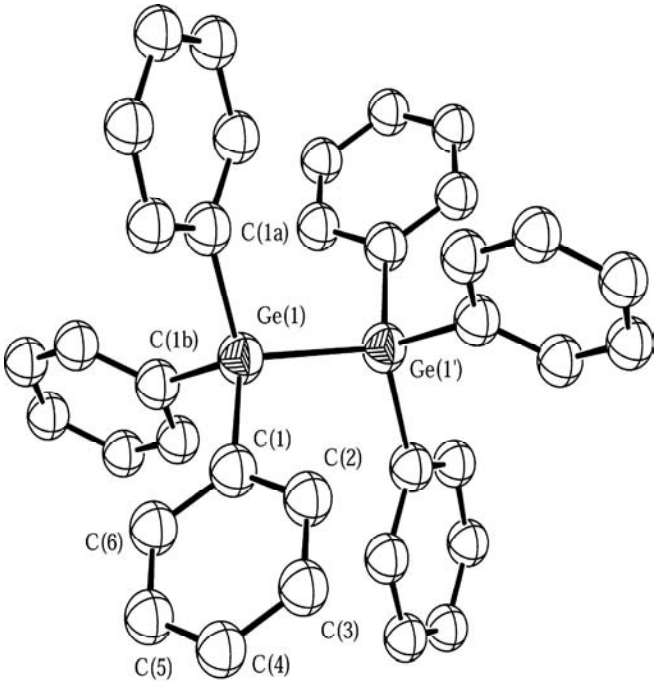

Figure 1.2: ORTEP diagram of $Ph_3GeGePh_3 \cdot 2C_6H_6$ (**1a)** with benzene solvates omitted. Selected bond distances (Å) and angles (˚): Ge(1)-Ge(1'), 2.446(1); Ge(1)-C(1), 1.963(1); C(1)-Ge(1)-C(1a), 108.11(1); C(1)-Ge(1)-Ge(1'), 110.80(1).[61]

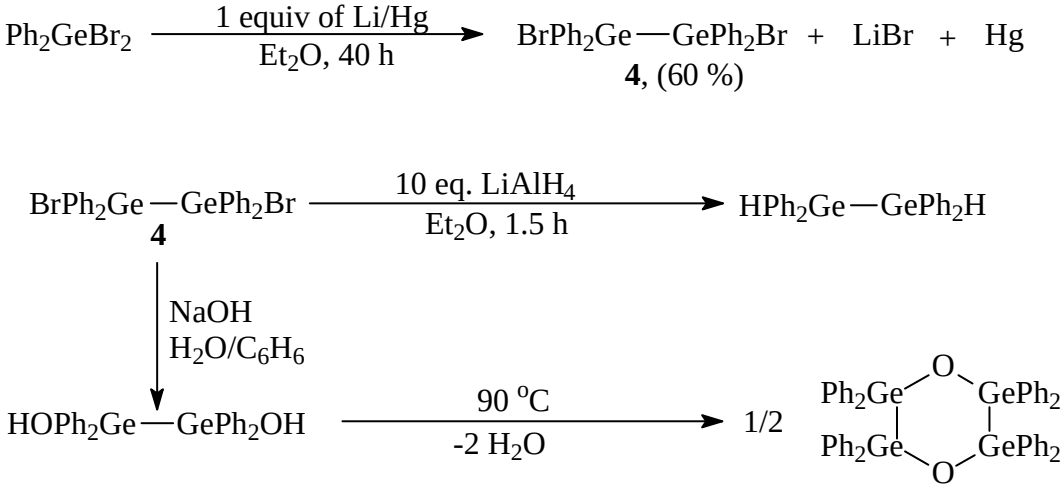

Scheme 1.4: Synthesis of 1, 2-dibrominated digermane **(4)** and reactions of compound **4**

Direct functionalization of digermanes has also been described. Hexaalkylated digermanes R_3GeGeR_3 (R= Pr^n, Bu^n, Et) react with $GeCl_4$ to yield halogenated digermanes where the number of halogen atoms depends on the stoichiometry ratio of the reactants.[65] Scheme 1.5 shows the selective chlorination of $Et_3GeGeEt_3$ with $GeCl_4$ at 200 ^oC.[65]

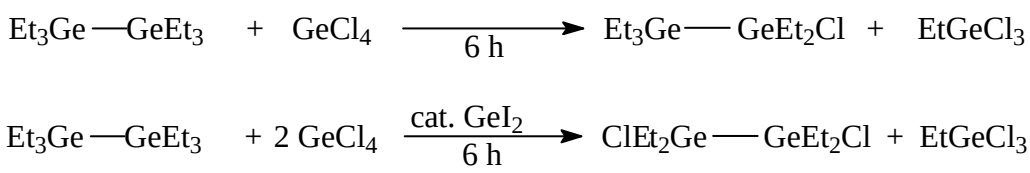

Scheme 1.5: Synthesis of chloride-substituted digermane by direct functionalization of $Et_3GeGeEt_3$ with $GeCl_4$ at 200 ^oC

A dichlorinated derivative of hexamethyldigermane $ClMe_2GeGeMe_2Cl$ was obtained using sulfuric acid and NH_4Cl; and subsequent treatment of $ClMe_2GeGeMe_2Cl$ with Bu^tLi has been shown to produce a polymeric mixture of products containing small amounts of *tert*-butyl substituted digermanes as well as other trace products (Scheme 1.6).[53]

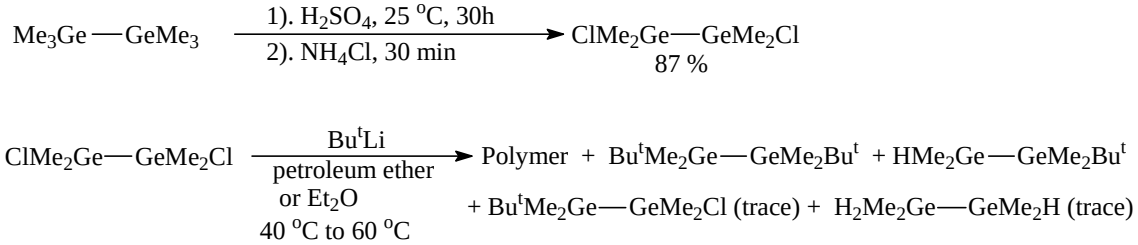

Scheme 1.6: The dichlorination of $Me_3GeGeMe_3$ and its reaction with Bu^tLi.

Several studies have been reported for the synthesis of chlorinated digermanes from hexaphenyldigermane. Treating $Ph_3GeGePh_3$ with anhydrous HCl or HBr furnishes tetrahalogenated digermanes $Cl_2PhGeGePhCl_2$ and $Br_2PhGeGePhBr_2$ in nearly quantitative yields.[66] Direct functionalization of **1** using liquid HCl under pressure produces dichlorinated product $ClPh_2GeGePh_2Cl$ (**5**) as shown in Scheme 1.7 and the yields of the more halogenated species increase as the pressure is increased.[67]
The tetrachlorinated digermane $Cl_2PhGeGePhCl_2$ (**6**) can also be prepared quantitatively using 44:1 molar ratio of HCl to **1** as shown in Scheme 1.7.[67] Compound **6** contains a relatively short Ge-Ge bond length of 2.413(1) Å due to the presence of two electronegative Cl atoms attached to each germanium center.[67]

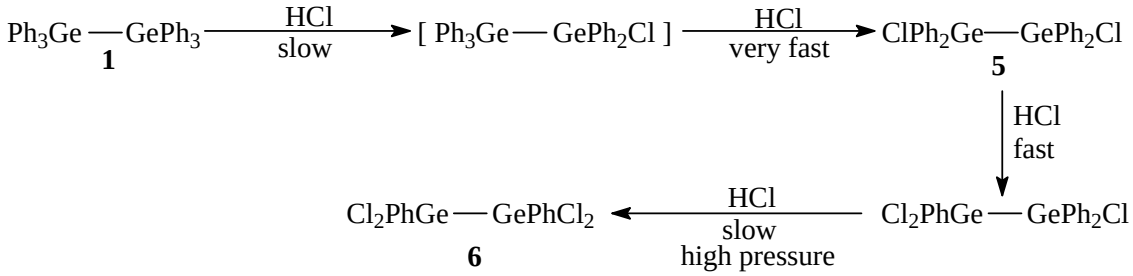

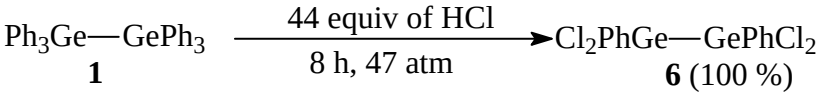

Scheme 1.7: Direct halogenations of $Ph_3GeGePh_3$ with HCl .

Compound **1** can also be directly functionalized using trihaloacetic acids, which was first described in 1973,[68] and the resulting product can be subsequently used for the preparation of different materials.[68-69] The functionalized digermane **7** was obtained by the reaction of **1** with five equivalents of trichloroacetic acid. Trichloroacetic acid selectively cleaves one phenyl group from each Ge atom of **1** (Scheme 1.8),[69] and the dichlorinated digermane **5** was obtained by subsequent treatment of **7** with concentrated HCl in acetone. (Scheme 1.8)[69]

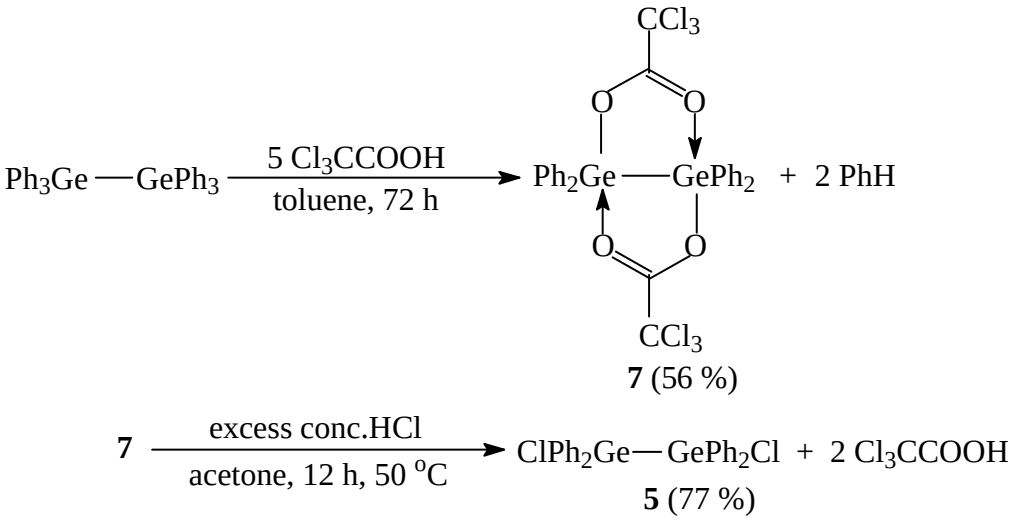

Scheme 1.8: Reaction of trichloroacetic acid with $Ph_3GeGePh_3$

An ORTEP diagram of compound **7** is shown in Figure 1.3 and it contains a very short Ge-Ge bond [2.393(2) Å]. In this molecule, coordination of the two carbonyl oxygens to the opposite germanium atoms results the Ge-Ge bond contraction from the normal Ge-Ge bond length of 2.43-2.47.[69]

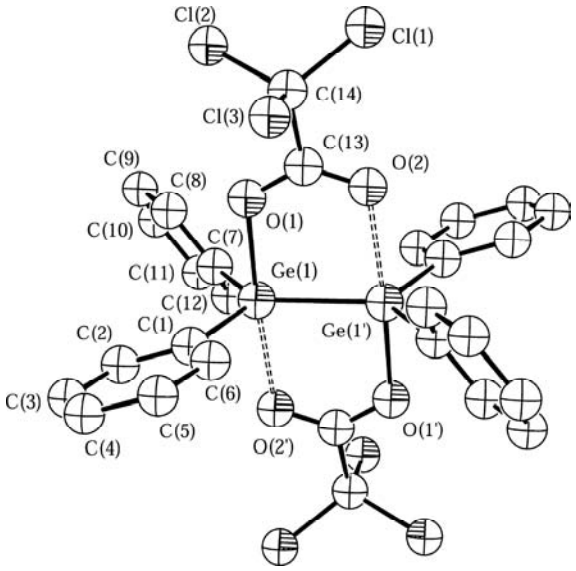

Figure 1.3: ORTEP diagram of 7. Selected bond distances (Å) and angles (˚): Ge(1)-Ge(1'), 2.393(2); Ge(1)-O(1), 2.073(3); Ge(1)-O(2'), 2.314(3); Ge(1)-C(1), 1.935(4); Ge(1)-C(7), 1.219(5); C(1)-Ge(1)-C(7), 116.4(2); C(1)-Ge(1)-O(1), 91.1(2); C(1)-Ge(1)-O(2'), 89.5(2); C(1)-Ge(1)-Ge(1'), 120.2(1); C(7)-Ge(1)-O(1), 93.5(2); C(7)-Ge(1)-O(2'), 90.3(2); C(7)-Ge(1)-Ge(1'), 123.0(1); O(1)-Ge(1)-O(2'), 175.4(1); O(1)-Ge(1)-Ge(1'), (91.9(1); O(2')-Ge(1)-Ge(1'), 83.8(1).[69]

Digermanes, having functionalized substituents combined with sterically encumbered substituents has also been reported. Synthesis of three different tetramesityl substituted digermanes **8-10**[70-71] is shown in Scheme 1.9.

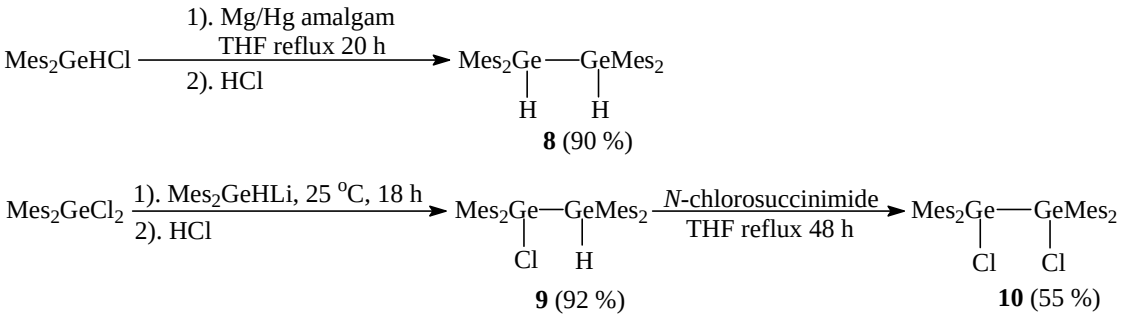

Scheme 1.9: Synthesis of three sterically encumbered functionalized digermanes

Finally the more sterically encumbered fluorenyl digermane **12** (Scheme 1.11) was synthesized starting from the tetrahydride precursor compound **11** which was obtained via the catalytic coupling of $MesGeH_3$ using Wilkinson's catalyst[72] (Scheme 1.10)

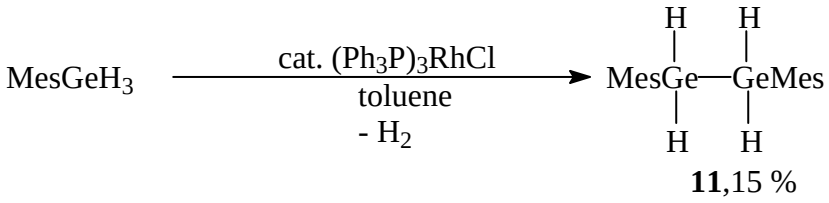

Scheme 1.10: Synthesis of compound 11 using Wilkinson's catalyst.

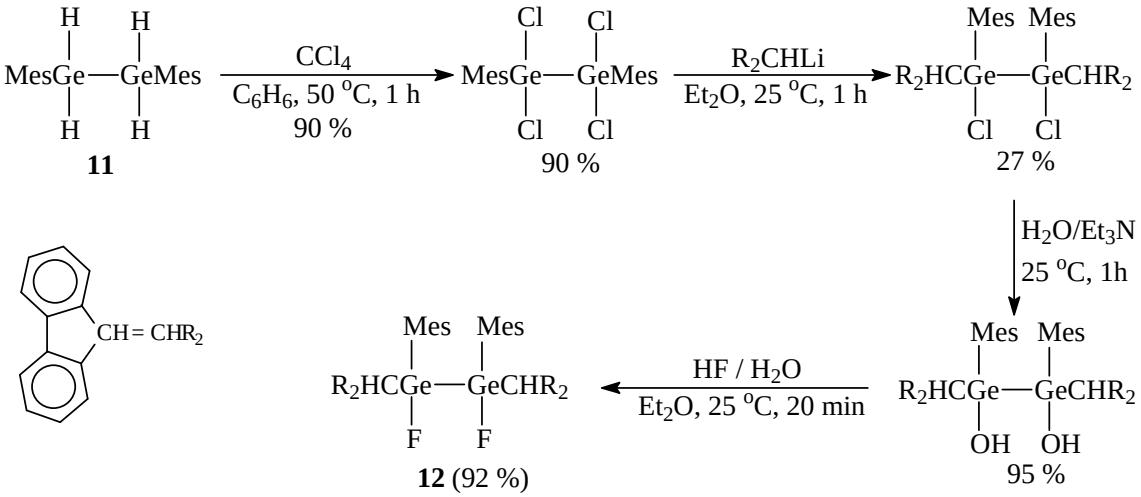

Scheme 1.11: Formation of compound **12** starting from compound **11**.

Linear Trigermanes

Perphenyl substituted trigermane $Ph_3GeGePh_2GePh_3$ (**2**) was originally prepared by using Ph_3GeNa and Ph_2GeCl_2 via a nucleophillic substitution reaction.[73] Later, the same compound was obtained by the reaction of Ph_3GeLi with Ph_2GeCl_2 in high yield

(91 %).[74] Using similar methods, the synthesis of trigermanes, $Ph_3GeGeEt_2GePh_3$[74] and $Et_3GeGeMe_2GeEt_3$,[75] were also described (Scheme 1.12).

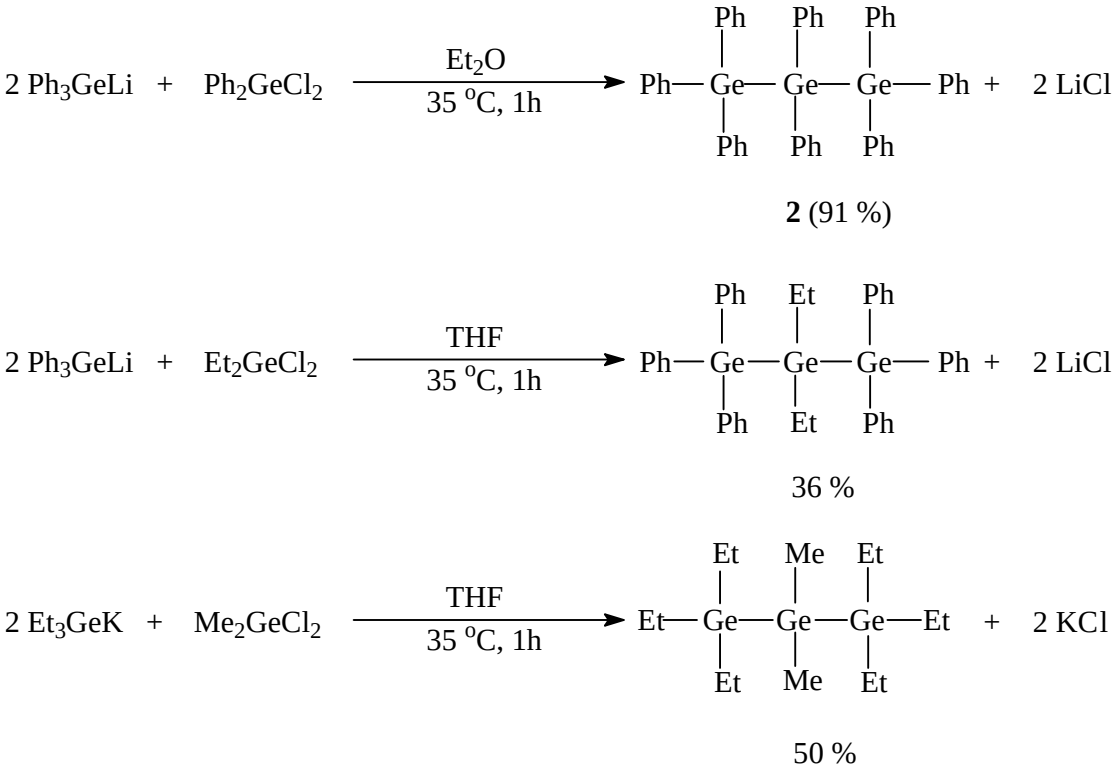

Scheme 1.12: Synthesis of trigermanes using nucleophillic substitution reaction of Ph_3GeM with R_2GeCl_2, (M = Li, K, R = Ph, Et, Me).

Trigermane **2** was also isolated as one of the products from the Grignard reaction of $GeCl_4$ with PhMgBr in a maximum yield of 11 % (Scheme 1.3). This was achieved by using THF as the solvent and excess Mg metal was removed by filtration during the reaction.[57] The structure of trigermane **2** was obtained and the ORTEP diagram is shown in Figure 1.4. It was found that the molecule adopts a *trans* conformation about the central Ge atom and the Ge-Ge bond distances are 2.438(2) and 2.441(2) Å, while the

Ge-Ge-Ge bond angle is 121.3(1)°.[57] The environment around each germanium atom is nearly tetrahedral.

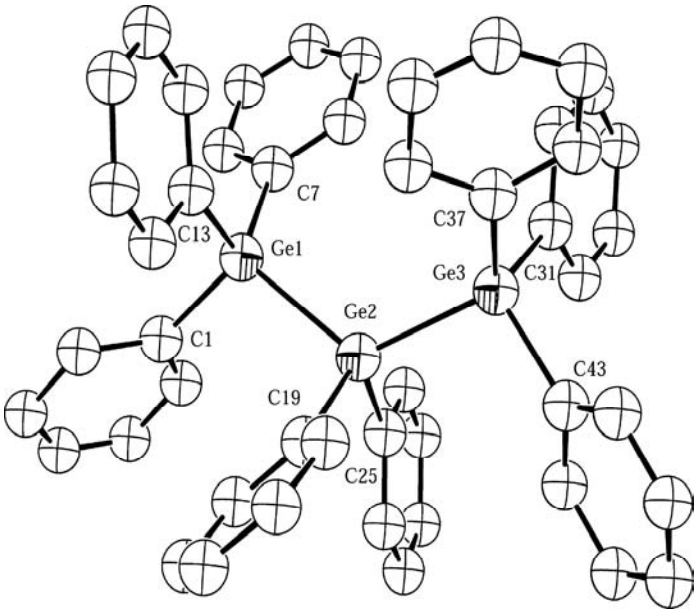

Figure 1.4: ORTEP diagram of **2**. Selected bond distances (Å) and angles (˚): Ge(1)-Ge(2), 2.438(2); Ge(2)-Ge(3), 2.441(2); Ge-C_{avg}, 1.960(1); Ge(1)-Ge(2)-Ge(3), 121.3(1); Ge-Ge-C_{avg}, 108.7(3); C-Ge-C_{avg}, 108.8(5).[57]

Subsequently, compound **2** was obtained in increased yield (34 %) starting from hexaphenyldigermane and using hexamethylphosphorous triamide (HMPT) as shown in Scheme 1.13. Use of HMPT is very important in this reaction because it suppresses the nucleophilic attack of the Ph_3Ge^- anion at the Ge-Ge bond of the intermediate digermane species $Ph_3GeGePh_2Cl$ and promotes the nucleophillic attack at the Ge-Cl bond of intermediate $Ph_3GeGePh_2Cl$ increasing the formation of product **2** rather than **1** (Scheme 1.14).

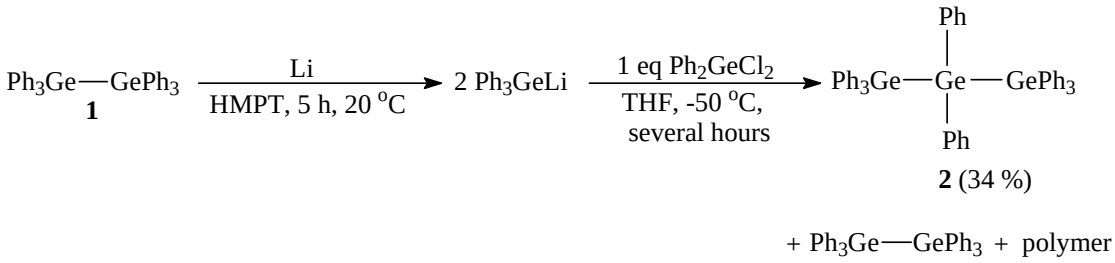

Scheme 1.13: Synthesis of trigermane $Ph_3GeGePh_2GePh_3$ using HMPT as the solvent

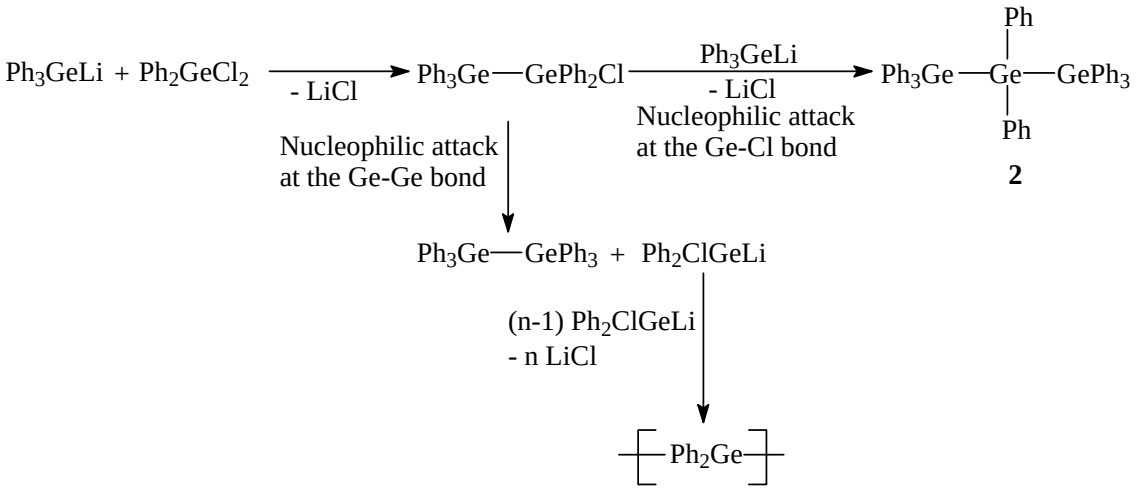

Scheme1.14: Reaction pathway for the formation of $Ph_3GeGePh_2GePh_3$ (**2**)

Similarly, the trigermane $Ph_3GeGeMe_2GePh_3$ (**13**) was obtained in 44 % yield (Scheme 1.15)[76] and its crystal structure was also obtained. The compound **13** exhibits a C_2 symmetry. The two Ge-Ge bond distances are identical [2.429(1) Å] and are shorter than those of molecule **2** due to the presence of the two methyl groups attached to the central Ge atom.[76] Compound **13** also shows a *trans* conformation about Ge atoms having Ge-Ge-Ge bond angle of 120.3(1)°.[76]

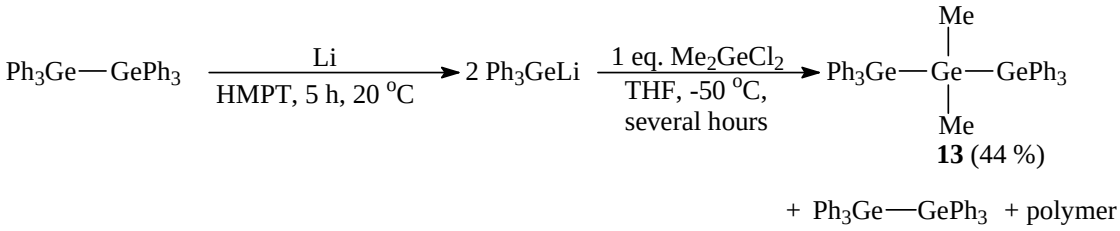

Scheme1.15: Synthesis of mixed alkyl/aryl trigermane $Ph_3GeGeMe_2GePh_3$

Recently, the use of SmI_2 for the synthesis of catenated germanium compounds has been described, and several discrete trigermane compounds were produced in good yields (Table 1.1) using organogermanium halides R_3GeCl and R'_2GeBr_2 with 10 equivalents of SmI_2 as the reducing agent.[52] The general reaction scheme for this synthesis is shown in Scheme 1.16.[52]

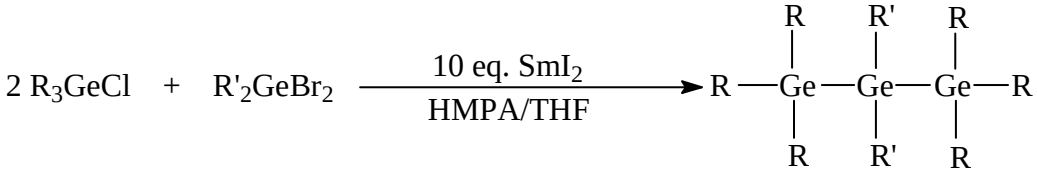

Scheme 1.16: Synthesis of trigermanes using SmI_2 as the reducing agent

Table 1.1: Experimental data for the scheme 1.16[52]

R_3GeCl	R'_2GeBr_2	Trigermane product	Yield (%)
Me_3GeCl	Ph_2GeBr_2	$Me_3GeGePh_2GeMe_3$	87
Et_3GeCl	Ph_2GeBr_2	$Et_3GeGePh_2GeEt_3$	94
Pr^i_3GeCl	Ph_2GeBr_2	$Pr^i_3GeGePh_2GePr^i_3$	30
Bu^n_3GeCl	Ph_2GeBr_2	$Bu^n_3GeGePh_2GePh_3$	87
Et_3GeCl	$MePhGeBr_2$	$Et_3GeGeMePhGeEt_3$	70

The synthesis of functionalized trigermanes has also been reported. For example, the chloride substituted trigermane **14** was isolated from the reaction of Ph_2GeHCl with NEt_3 (Scheme1.17).[77] Tetragermane **15**, trigermane **14** and digermane **5** were also formed during this reaction, and the product ratio depends on the stoichiometry of the reaction.[77]

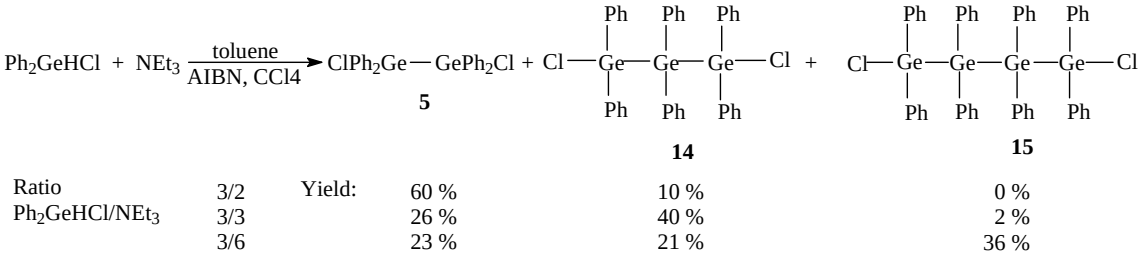

Ratio Ph_2GeHCl/NEt_3		Yield:	**5**	**14**	**15**
	3/2		60 %	10 %	0 %
	3/3		26 %	40 %	2 %
	3/6		23 %	21 %	36 %

Scheme 1.17: Synthesis of chlorinated oligogermanes $Cl(GePh_2)_nCl$, n = 2, 3, 4**.**

The reaction pathway for this conversion is shown in Scheme 1.18 and involves the generation of germylene, Ph_2Ge: from Ph_2GeHCl, followed by insertion of the germylene into the Ge-Cl bond of Ph_2GeHCl. A similar insertion reaction of PhGeCl into Ge-Cl bond of $PhGeCl_3$ has also been reported and a mixture of products was obtained from this reaction as well as shown in Scheme 1.19, which includes a digermane, trigermane and a branched tetragermane.[78]

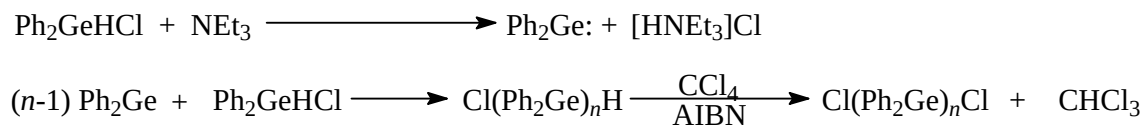

Scheme 1.18: The reaction pathway for the formation of $Cl(GePh_2)_nCl$, n = 2, 3, 4.

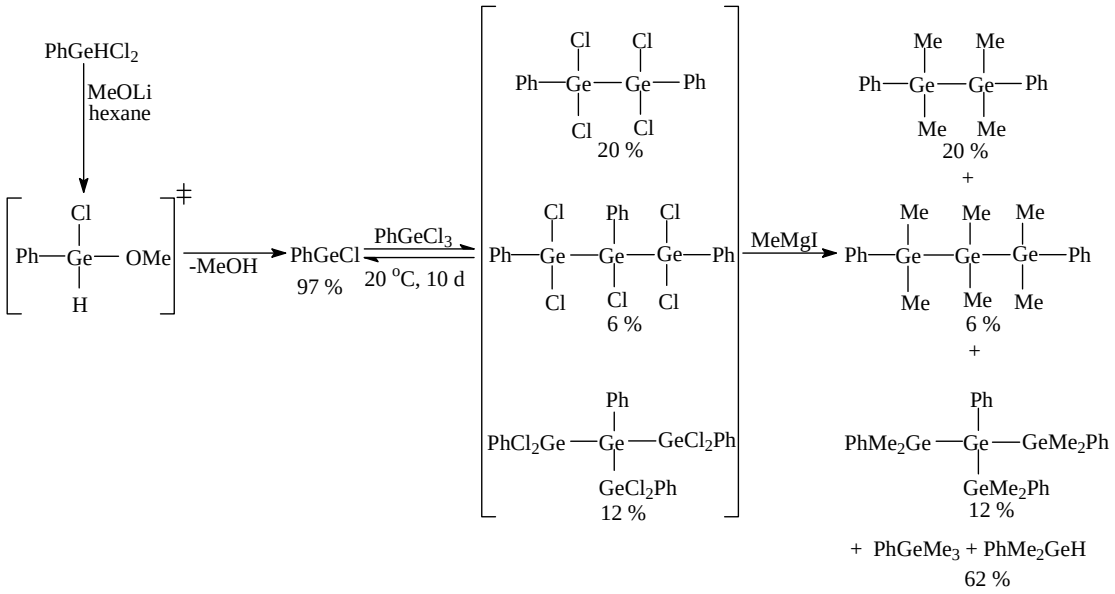

Scheme 1.19: Formation of a mixture of compounds after treating the chlorinated product from the insertion of PhGeCl into Ge-Cl bond.

The structure of compound **14** ($ClPh_2GeGePh_2GePh_2Cl$) was obtained and it contains two crystallographically independent molecules.[77] In one molecule (**14a**), the Cl-Ge_3-Cl chain is arranged in a *gauche-gauche* conformation while, in the second molecule (**14b**), it is in *anti-gauche* conformation (Figure 1.5). The Ge-Ge bond distance and Ge-Ge-Ge bond angles are different in each case. In molecule **14a**, the Ge-Ge bond distances were 2.437(2) and 2.419(1) Å while those were 2.413(2) and 2.423(2) Å in molecule **14b**. These are shorter than in Ph_8Ge_3 (**2)** due to the presence of the two electron withdrawing chlorine atoms attached to the terminal Ge atoms. The Ge-Ge-Ge bond angles in **14a** [110.4(1)˚] and **14b** [116.7(1)˚] are more acute than those in **2** due to the presence of the less sterically encumbering chlorine atoms in **14a** and **14b** versus two phenyl groups in **2**.[77]

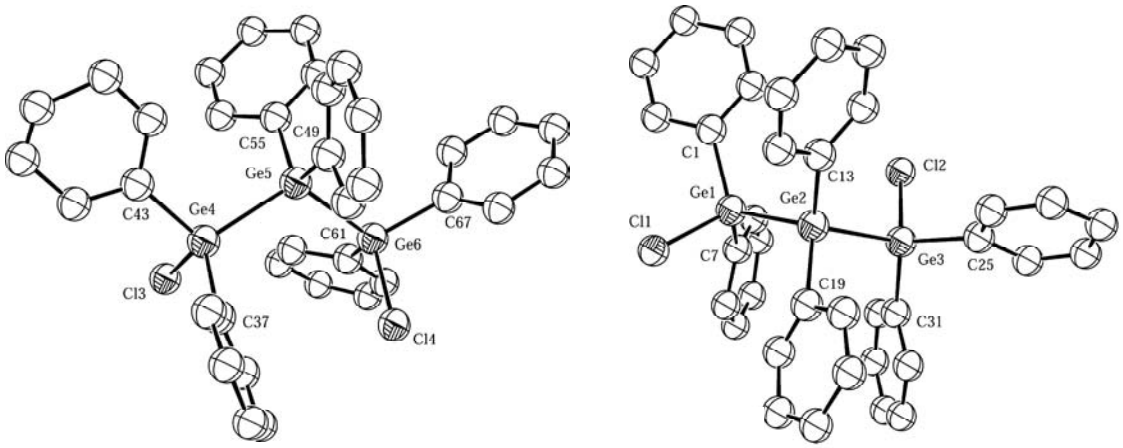

Compound **14a** Compound **14b**

Figure 1.5: ORTEP diagram of **14a** and **14b**. Selected bond distances (Å) and angles (˚) for **14a**: Ge(1)-Ge(2), 2.437(2); Ge(2)-Ge(3), 2.419(1); Ge(1)-Cl(1), 2.187(6); Ge(3)-Cl(3), 2.194(4); Ge-C_{avg}, 1.95(1); Cl(1)-Ge(1)-Ge(2), 104.4(2); Ge(1)-Ge(2)-Ge(3), 110.4(1); Ge(2)-Ge(3)-Cl(3), 105.8(1). Selected bond distances (Å) and angles (˚) for **14b**: Ge(4)-Ge(5), 2.413(2); Ge(5)-Ge(6), 2.423(2); Ge(4)-Cl(4), 2.192(6); Ge(6)-Cl(6), 2.196(6); Ge-C_{avg}, 1.95(1); Cl(4)-Ge(4)-Ge(5), 109.9(1); Ge(4)-Ge(5)-Ge(6), 116.7(1); Ge(5)-Ge(6)-Cl(6), 108.1(1).[77]

Linear tetragermanes:

The perphenylated tetragermane $Ph_3GeGePh_2GePh_2GePh_3$ (**3**) was obtained in 18 % yield as a product of the synthesis of $GePh_4$ by using PhMgBr and $GeCl_4$ in THF.[57] This was achieved by variation of the process shown in Scheme 1.3, when excess magnesium metal was not removed by filtration. The structure of the tetragermane **4** is shown in Figure 1.6. In this molecule, four germanium atoms are arranged in a staggered conformation and the molecule contains a center of symmetry located along the Ge(2)-

Ge(2′) bond. The two unique Ge-Ge bond distances are nearly identical [2.463(2) and 2.461(3) Å], and the Ge-Ge-Ge bond angle is 117.8(1)˚.[57]

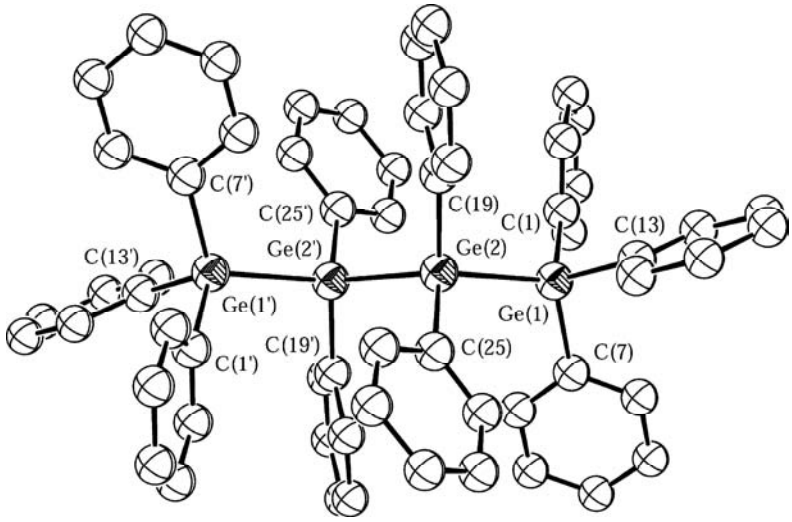

Figure 1.6: ORTEP diagram of $Ph_3GeGePh_2GePh_2GePh_3$ (**3)**. Selected bond distances (Å) and angles (˚): Ge(1)-Ge(2), 2.463(2); Ge(2)-Ge(2'), 2.461; Ge-C_{avg}, 1.968(5); Ge(1)-Ge(2)-Ge(2'), 117.8(1); Ge-Ge-C_{avg}, 109.5(2); C-Ge-C_{avg} 107.1(5).[57]

The synthesis of a related tetragermane $Ph_3Ge(GeEt_2)_2GePh_3$ from Ph_3GeLi and $ClEt_2GeGeEt_2Cl$, in 25 % yield[74] has also been described, and the functionalized tetragermane $Cl(GePh_2)_4Cl$ was prepared and isolated according to Scheme 1.17.[77] The later compound contains a center of symmetry similar to perphenylated derivative **3** with Ge-Ge distances of 2.450(4) and 2.442(3) Å and a Ge-Ge-Ge angle of 116.2(1)˚.[77]

Very recently, the preparation of tetragermanium dihydride $HPh_2Ge(GePh_2)_2GePh_2H$ from diarylgermane Ph_2GeH_2 has been described.[79] This was achieved using the bis(germyl)platinum complex, which was treated with slight excess of

H_2GePh_2 to form four-membered and five-membered germaplatinacyles. Cleavage of Ge-Pt bonds of the cyclic complexes produced both a trigermane dihydride and a tetragermane dihydride. (Scheme 1.20)

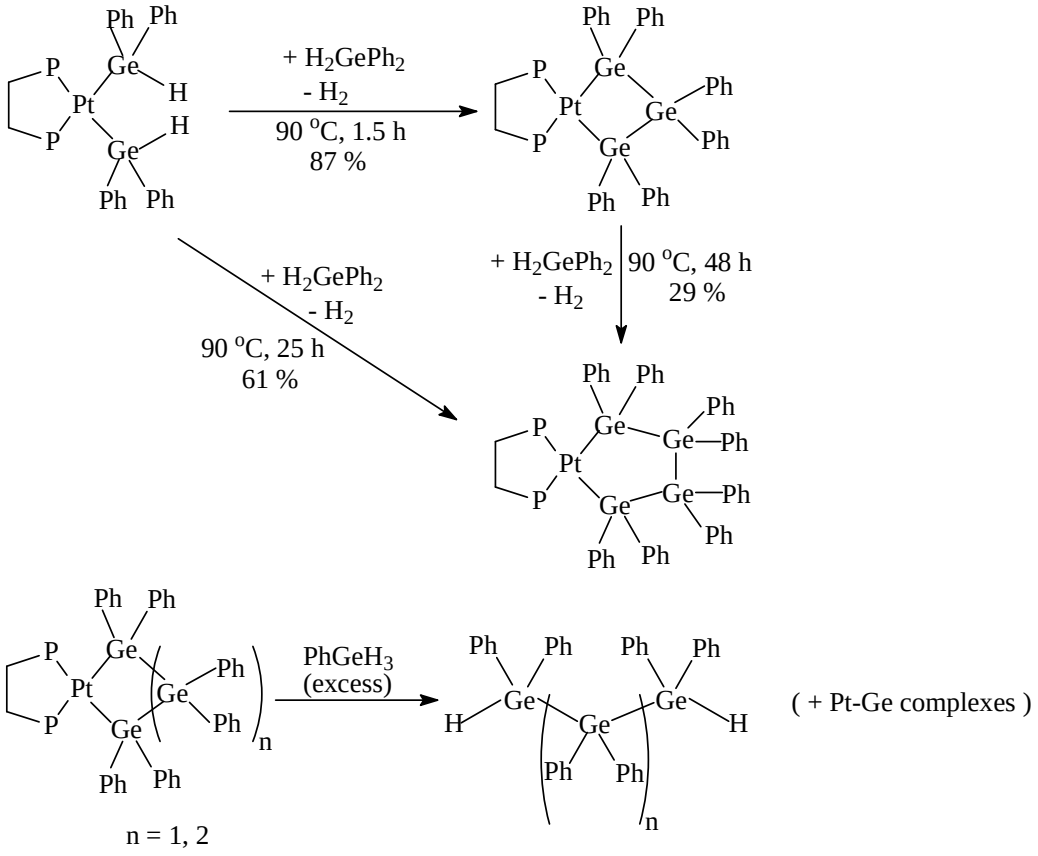

Scheme 1.20: Synthesis of $H(GePh_2)_nH$ (n = 1, 2) from Bis(germyl)platinum complex

Linear Pentagermanes

The syntheses of a few pentagermanes have been described. Diphenyl methylpentagermane (**15**) was prepared along with some other lower oligomers starting from $PhMe_2GeCl$ and $PhMe_2GeLi$ (Scheme 1.21).[80] This involves a cleavage of a Ge-Ph bond using HCl followed by the metathesis reaction with the organolithium reagent

$PhMe_2GeLi$ to produce the desired product where the mixture of oligomers was separated by fractional distillation and individually characterized by ^{1}NMR and elemental analyses.[80]

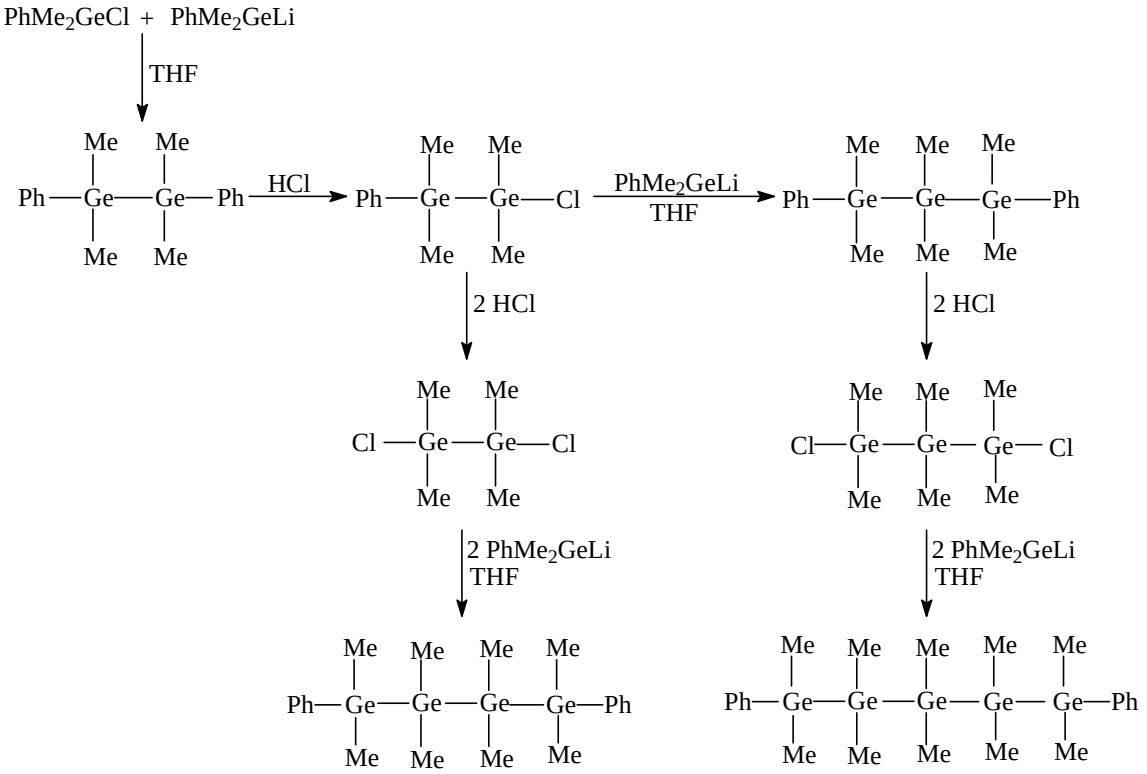

Scheme 1.21: Synthesis of diphenylmethyl pentagermane

Wurtz-type coupling reactions can also be used to synthesize higher oligogermanes. For example, the perethyl-substituted pentagermane **16** was obtained in 43 % yield by several sequential Wurtz-type coupling reactions (Scheme1.22).[81-82] In this synthesis, it was necessary to use excess organogermanium halide to prevent Ge-Ge bond cleavage by the alkali metal and compound **16** was isolated after separating the trigermane by-product. By a similar reaction using Ph_3GeLi and $ClEt_2Ge(GeEt_2)GeEt_2Cl$,

a related heteroleptic pentagermane $Ph_3Ge(GeEt_2)_3GePh_3$ was isolated in 59% yield.[74]

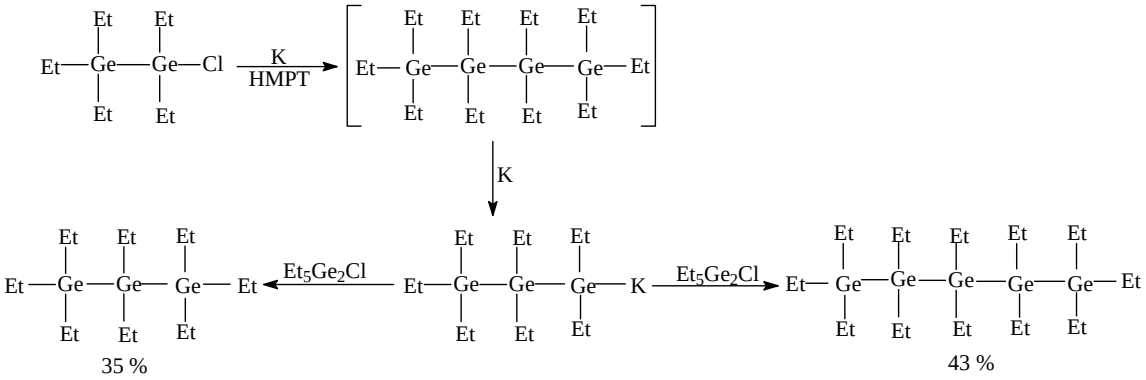

Scheme 1.22: Synthesis of perethyl-substituted pentagermane

The perphenyl-substituted pentagermane $Ph_3Ge(GePh_2)_3GePh_3$ (**17**) was obtained in 0.5 % yield as the main product of the reaction of $LiPh_2GeGePh_3$ with Cl_2GePh_2 after separation of short chained-polygermanes (Scheme 1.23).[48] The structure of **17** is shown in Figure 1.7 and this represents the longest structurally characterized linear oligogermane to date. The molecule **17** does not adapt any of the three normal conformation of *n*-pentane (*anti-anti*, *gauche-gauche*, or *anti-gauche*), but rather it is antiperiplaner-anticlinal (with torsion angles 179.3(2) and 114.4(2)˚) along the Ge5 chain with the average Ge-Ge distances of 2.476(3) (central) and 2.443(4) (terminal) Å.[48]

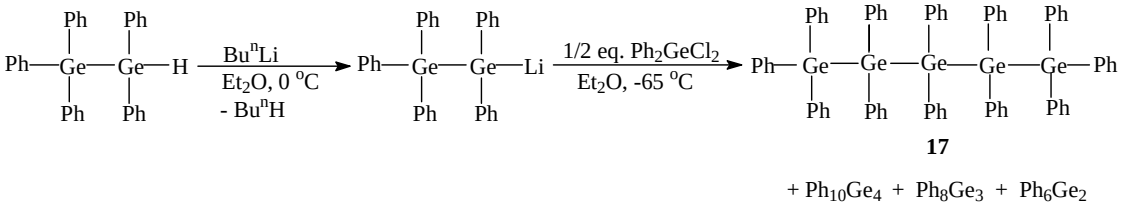

Scheme1.23: Synthesis of perphenyl substituted pentagermane.

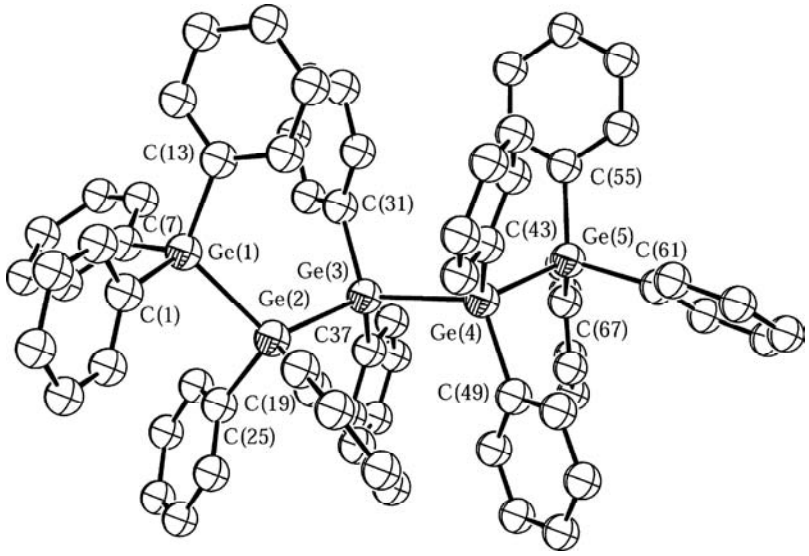

Figure 1.7: ORTEP diagram of **17.** Selected bond distances (Å) and angles (˚): Ge(1)-Ge(2), 2.447(4); Ge(2)-Ge(3), 2.485(4); Ge(3)-Ge(4), 2.468(4); Ge(4)-Ge(5), 2.439(4); Ge-C_{avg}, 1.96(1); Ge(1)-Ge(2)-Ge(3), 116.7(2); Ge(2)-Ge(3)-Ge(4), 114.0(2); Ge(3)-Ge(4)-Ge(5), 116.0(2); Ge-Ge-C_{avg}, 109.0(6); C-Ge-C_{avg}, 108.1(8).[48]

Branched oligogermanes

To date, only a very few syntheses of branched oligogermanes have been reported. The branched tetragermane $(Ph_3Ge)_3GeH$ was obtained from the reaction of Ph_3GeLi with I_2 in 36 % yield as shown in Scheme 1.24.[83] The lithiated reagent Ph_3GeLi was prepared *in situ* from $Ph_3GeGePh_3$ and excess Li metal[83] and the methyl-substituted

species $(Ph_3Ge)_3GeCH_3$ was obtained in 54 % yield by subsequent reaction of $(Ph_3Ge)_3GeH$ with Bu^nLi followed by alkylation with MeI.[83] A branched tetragermane $(PhMe_2Ge)_3GePh$ was isolated in 12 % yield after methylation of the product obtained by the insertion reaction of phenylchlorogermylene PhGeCl into the Ge-Cl bond of $PhGeCl_3$.[78] Also this reaction generated a digermane ($PhMe_2GeGeMe_2Ph$, 20 %) and a trigermane [$(PhMe_2Ge)_2GePhMe$, 6 %] besides $PhMe_2GeH$ and $PhGeMe_3$ as well.[78]

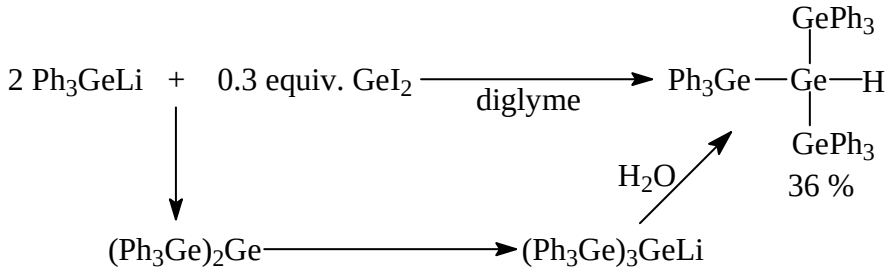

Scheme1.24: Synthesis of branched tetragermane $(Ph_3Ge)_3GeH$

Higher Oligomers

Syntheses of linear oligogermanes containing more than five germanium atoms in the Ge-Ge backbone have been reported, although none of these has been structurally characterized. For example, the permethyl-substituted hexagermane $Me_{14}Ge_6$ was isolated from the reaction of $GeCl_4$ with large excess of Me_3Al in the presence of NaCl.[84] In addition to $Me_{14}Ge_6$, lower oligogermanes, $Me_{12}Ge_5$, $Me_{10}Ge_4$, and Me_8Ge_3 was also generated. In a similar reaction, a mixture of $Me_{16}Ge_7$, $Me_{14}Ge_6$ and $Me_{12}Ge_5$ were obtained from Me_3Al and GeI_2. This reaction was assumed to proceed through generation of germanium/aluminum intermediates.[84] The synthesis of linear hexagermanes,

$Et_3Ge(GeEt_2)_4GeEt_3$[81] and $Ph_3Ge(GeEt_2)_4GePh_3$[74] have also been reported. In addition, the permethylated oligogermanes Me_6Ge_2 (18 %), Me_8Ge_3 (20 %), $Me_{10}Ge_4$ (10 %), and $Me_{12}Ge_5$ (4 %)[85] as well as $Me_{22}Ge_{10}$[86] were obtained by a Wurtz coupling reaction of Me_3GeCl and Me_2GeCl_2 with lithium metal in THF.

Properties of oligogermanes

The physical properties of oligogermanes have been investigated using electrochemistry and UV/vis spectroscopy, and depend on the chain length of the oligogermanes. Some of the physical data that has been reported are shown in Table 1.2. For example, as the length of the Ge-Ge chain increases, the permethylated species Ge_nMe_{2n+2} exhibit a bathachromic shift in their absorption maxima. Additionally, the ionization and oxidation potentials decrease in energy as the chain length increases.

Table 1.2: Physical data for permethylated oligogermanes with absorbance (λ_{max}) values reported in nanometers.

Compound	Ionization Potential (eV)	Electrochemical oxidation potential (V)[b]	λ_{max} (neutral oligomer)	λ_{max} (TCNE charge transfer complex	λ_{max} (radical anion)
Me_6Ge_2	8.58[a]	1.28	197[c]	427[a]	267, 305[d]
Me_8Ge_3	8.15[a]	0.93	217[c]	485[a]	291, 345[d]
$Me_{10}Ge_4$	7.80[a]	0.72	233[c]	550[a]	n/a
$Me_{12}Ge_5$	7.67[a]	0.61	246[c]	565[a]	330, 545[d]
$Me_{22}Ge_{10}$	5.55[d]	n/a	286[c]	n/a	400, 900[d]

[a]Taken from ref [85] [b]Data from ref [87] [c]Data from ref [88] [d]From ref [89]

Table 1.3: UV/Visible data for oligogermanes with absorbance (λ_{max}) in nanometers

Compound	λ_{max}	ref	compound	λ_{max}	ref
Digermanes			**Trigermanes**		
$Me_3GeGeMe_3$	197	87	Me_8Ge_3	218	39
$PhMe_2GeGeMe_3$	228	74	Et_8Ge_3	218	23
$PhMe_2GeGeMe_2Ph$	233	15	$Ph(GeEt_2)_3Ph$	241	15
$Ph_3GeGeMe_3$	233	15	$Ph_3Ge(GeEt_2)GePh_3$	247	15
$Ph_3GeGeMe_2Ph$	234	15	$Ph_3Ge(GeMe_2)GePh_3$	245	15
$Ph_2MeGeGeMe_2Ph$	237	15	$Ph_3Ge(GePhMe)GePh_3$	250	15
$Ph_3GeGePh_3$	241	15	$Ph_3Ge(GePh_2)GePh_3$	250	15
$Ph_3GeGeClPh_2$	236	15	Mes_6Ge_3	273	36
$Ph_2FGeGeFPh_2$	226	15			
$Ph_2ClGeGeClPh_2$	225	15	**Tetragermanes**		
$Ph_2BrGeGeBrPh_2$	231	15	$Me_{10}Ge_4$	233	39
$Ph_2IGeGeIPh_2$	240	15	$Et_{10}Ge_4$	234	23
$PhCl_2GeGeCl_2Ph$	230	15	$Ph(GeEt_2)_4Ph$	248	15
$Et_3GeGeEt_3$	202	81	$Ph_3Ge(GeEt_2)_2GePh_3$	256	15
$(Me_3Si)_3GeGe(SiMe_3)_3$	209	90	$(Pr^i_2Ge)_4$	280	36
$Ph(GeEt_2)_2Ph$	233	15	$(Ph_2Ge)_4$	280	36
Pentagermanes			**Hexagermanes**		
$Me_{12}Ge_5$	246	91	$Me_{14}Ge_6$	255	39
$Et_{12}Ge_5$	248	23	$Et_{14}Ge_6$	258	23
$Ph_3Ge(GeEt_2)_3GePh_3$	269	15	$Ph(GeEt_2)_6Ph$	264	15
$Ph(GeEt_2)_5Ph$	256	15	$Ph_3Ge(GeEt_2)_4GePh_3$	278	15
$(Me_2Ge)_5$	270	88	$(Me_2Ge)_6$	250	36
$(Ph_2Ge)_5$	272	36	$(Ph_2Ge)_6$	270	36

It should also be noted that the variation of the organic substituents attached to the germanium centers has an effect on the position of the λ_{max} in these compounds. UV/vis absorption data for some of the oligogermanes are collected in Table 1.3, and these

absorption features correspond to the HOMO-LUMO electronic transition in the molecule.

Therefore, the physical properties of these compounds can be tuned by varying the number of germanium atoms of the backbone as well as varying the organic substituent groups. The lack of good synthetic procedures to prepare discrete oligogermanes in high yields to date has prevented a detailed investigation of the relationship between their physical and structural properties. Therefore, the development of new methods for the preparation of oligomeric germanium compounds, which reduces common difficulties involved in previous synthetic methods, such as low yields, and the formation of product mixtures, is of significant interest. Recently we have developed a preparative synthetic method to generate Ge-Ge bonds that involves a reaction between a germanium amide and a germanium hydride, this is known as the hydrogermolysis reaction. The following chapters focus the synthesis of singly bonded discrete linear and branched oligogermanes using this method, and the characterization of the compounds, and the investigation of their physical properties, using CV, UV/vis, DFT calculations and ^{73}Ge NMR.

CHAPTER TWO

SYNTHESIS, STRUCTURES, AND CHARACTERIZATION OF LINEAR OLIGOGERMANES

INTRODUCTION

The study of structure property relationships of catenated germanium compounds has been less developed compared to the silicon and tin catenates due to the difficulties (low yields of the products and/or the formation of mixtures of products which required extensive separation procedures) encountered in available methods to form Ge-Ge bonds (as described in Chapter 1).

Germanium-nitrogen compounds are potentially good starting materials for the formation of germanium-germanium bonded compounds.[92] Generally, in singly bonded germanium nitrogen compounds, the Ge-N bond behaves as a dipole in which the metal is an electrophile and the nitrogen as a nucleoplile.[92] It has been known that Ge-N bond in germanium amide ($R_3GeNR'_2$) can be cleaved by protic species such as ROH (R = H, alkyl, or aryl), R_2P-H, R_2S-H, R_3Ge-H, RC≡C-H and R'_2N-H.[92] With acetonitrile, R_3GeNMe_2 produces an α-germylated nitrile, which contains a labile Ge-C bond resulting from cleavage of the Ge-N bond (Scheme 2.1).

$$R_3Ge{-}NMe_2 + CH_3{-}C{\equiv}N \xrightarrow{\text{Carius tube}} R_3Ge{-}CH_2{-}C{\equiv}N + (R_3Ge)_2CH{-}C{\equiv}N + Me_2NH$$

Scheme 2.1: Reaction of a germanium amide with acetonitrile

It has also been reported that triethylgermanium amide reacts with perfluorinated triphenylgermanium hydride in hexane at 100 ºC resulting a digermane and a trigermane

as shown in Scheme 2.2.[93] It has also been found that the common germanium hydride (R_3GeH) does not react with germanium amide (R_3GeNR_2) to provide germanium-germanium bonded compound in similar way (under similar experimental conditions).[94]

$$(C_6F_5)_{4-n}GeH_n + n\ Et_3GeNEt_2 \xrightarrow{100\ ^oC} (C_6F_5)_{4-n}Ge(GeEt_3)_n + n\ Et_2NH \quad (n = 1, 2)$$

Scheme 2.2: Reaction of perfluorotriphenyl germane with triethylgermyl amide

In contrast, as an approach to develop a rational synthetic procedure to synthesize discrete oligogermanes in high yield, the hydrogermolysis reaction has been investigated. This synthetic procedure also employs a reaction between a germanium amide and a germanium hydride. The reaction proceeds via the formation of an α-germyl nitrile, which is the active species in the Ge - Ge bond forming reaction. The α-germyl nitrile is formed by the reaction of a germanium amide with acetonitrile as the solvent (Scheme 2.3). This method can be used for the synthesis of small molecules containing two or three Ge atoms or for the stepwise construction of linear oligomeric chains via combination with a hydride protection/deprotection strategy using DIBAL-H as the hydrogen transfer reagent. This allows for the addition of the individual germanium atoms one at a time, permitting for the first time a systematic variation of the organic substituents attached to the Ge−Ge backbone. This study describes the structure and characterization of a series of linear oligogermanes, which were synthesized using the hydrogermolysis reaction.

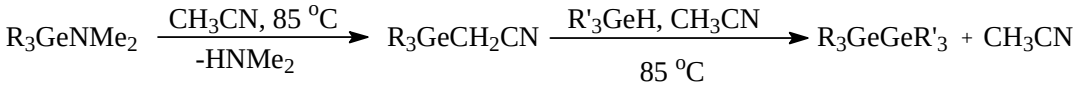

Scheme 2.3: The reaction of germanium amide and germanium hydride in acetonitrile.

RESULTS AND DISCUSSION:

The reaction of germanium amides R_3GeNMe_2 with germanium hydrides in the presence of acetonitrile solvent produces a Ge-Ge bond via the hydrogermolysis reaction. Several digermane compounds were prepared by this method and are shown in Scheme 2.4. The first attempt to synthesize digermane $Ph_3GeGeBu_3$ (**1**) reacting Bu_3GeNMe_2 and Ph_3GeH in benzene at room temperature was unsuccessful.[95] The desired product was not detected even using a longer reaction time of up to a week. Similar attempts to synthesize **1** using different solvents and reaction conditions including refluxing in benzene or toluene were unsuccessful. When refluxing the reaction mixture in acetonitrile as the solvent, however, the reaction was successful and compound **1** was obtained in 83 % yield after 48 h.

The digermanes shown in Scheme 2.4 were prepared by sealing an acetonitrile solution of the reactants in a Schlenk tube and heating at 80-90 ºC for 48 h in an oil bath. The isolated yields of the digermanes **1-6** that were prepared using this method are generally higher than the yields obtained via other previously reported methods (Scheme 2.4). For example, $Bu^t_3GeGeBu^t_3$ (16 %) was isolated via the reduction of Bu^t_3GeCl with lithium naphthalenide,[96] $Ph_3GeGePh_3$ (69 %) was obtained from the reaction of PhMgBr with $GeCl_4$,[58,56] $Bu^n_3GeGePh_3$ (~60 %) was obtained from the coupling reaction of Bu^n_3GeK and Me_3GeCl.[97] However by the use of SmI_2 as the reductant, digermanes can

be synthesized from corresponding trialkylgermanium hydride in 39-96 % yield. For example, $Et_3GeGePh_3$ and $Me_3GeGeBu_3$ were isolated in 96 % and 39 % respectively.[51-52]

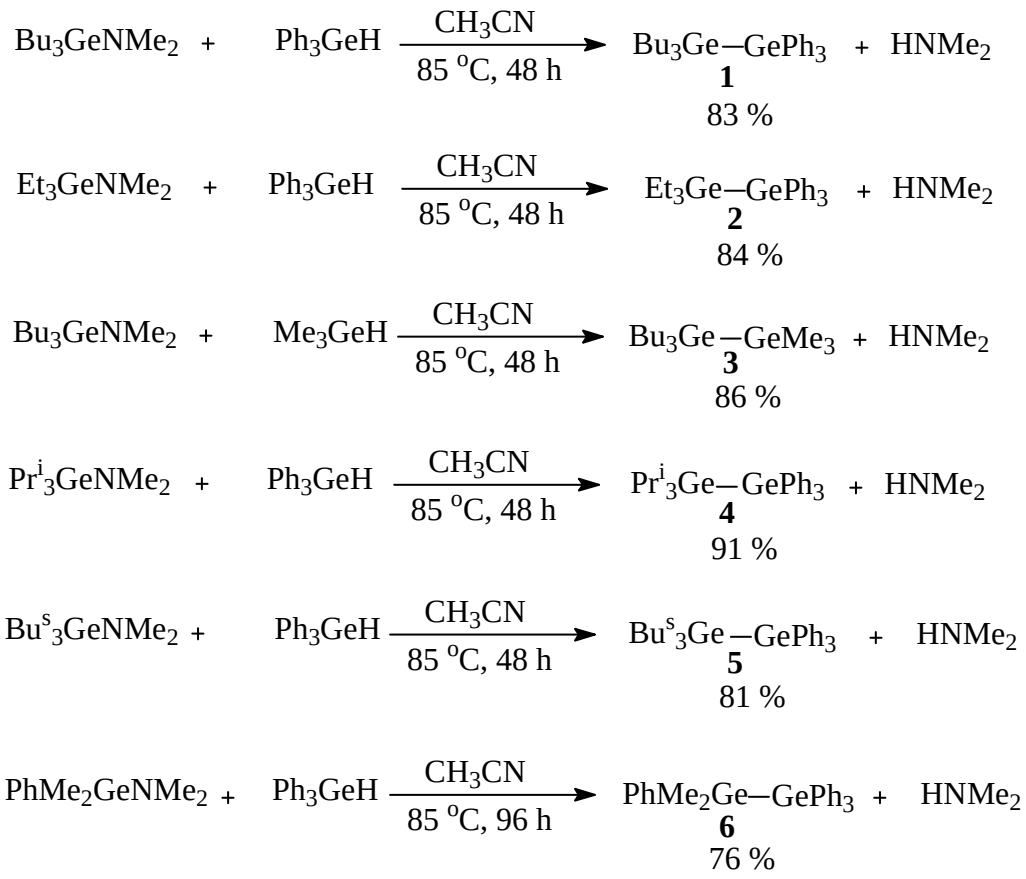

Scheme 2.4: Synthesis of digermanes using the hydrogermolysis reaction

The use of acetonitrile as the reaction medium is necessary for the formation of the Ge-Ge bond using hydrogermolysis reaction. It has been shown that germanium amides ($R_3GeNR'_2$) react with acetonitrile to produce α-germylated nitriles R_3GeCH_2CN. Bisgermylated nitriles $(R_3Ge)_2CHCN$ can also be formed as a product, but the relative yields percentage of depend on the experimental conditions used.[98,99,100] This type of

reaction is observed around 150 ºC in the presence of large excess of acetonitrile and the reaction can be catalyzed by adding small amounts of Lewis acids such as $ZnCl_2$. The reactions of these α-germylated nitriles have been studied[98] For example, hydrolysis and reduction reactions proceeded via opening of the –C≡N bond of the α-germylated nitrile as the first step while addition reactions were observed with organometallic compounds such as RMgX or RLi. The Ge-C bond cleavage reactions were observed with organic halogenated derivatives RX (R = Me, C_6H_5; X = Br, I) indicating the relative lability of the Ge-C bond of the α-germylated nitrile.[98] To determine the role of acetonitrile in the use of hydrogermolysis reaction, the reaction of $Bu^n_3GeNMe_2$ with Ph_3GeH was investigated (Scheme 2.5).[95] The reaction was performed in acetonitrile-d_3 solvent and was monitored by ^1H NMR spectroscopy.

$$Bu_3GeNMe_2 + CD_3CN \xrightarrow[-\ DNMe_2]{90\ ^oC,\ 1\ h} Bu_3GeCD_2CN \xrightarrow[90\ ^oC,\ 36\ h]{Ph_3GeH} \underset{\mathbf{1}}{Bu_3GeGePh_3} + HCD_2CN$$

Scheme 2.5: Reaction of Bu_3GeNMe_2 with Ph_3GeH in acetonitrile

Initially the sample of Bu_3GeNMe_2 prepared in CD_3CN, exhibited a sharp resonance at δ 2.45 ppm in ^1H NMR spectrum and a peak at δ 41.5 ppm in the ^{13}C NMR spectrum that corresponded to the carbon atoms of the amide group in $Bu^n_3GeNMe_2$. These features nearly disappeared after heating the sample for 1 h at 90 ºC and a new peak appeared at δ 2.29 ppm. This observation indicated the conversion of the amide to $Bu^n_3GeCD_2CN$ and the formation of $DNMe_2$. At this point, 1 equivalent of Ph_3GeH was added to the NMR tube with a small amount of Me_4Ge (ca. 5 mg) as an internal standard. The progress of the reaction was monitored by integrating the Ge-*H* resonance at δ 5.64

ppm for Ph_3GeH versus the peak at δ 0.14 ppm for $GeMe_4$. After heating for 3 h at 90 ºC, ^1H spectra indicated the decreasing intensity of the resonance at δ 5.64 ppm and the formation of digermane **1**. The progress of the reaction was monitored at regular time intervals and the result showed that Ph_3GeH was being continuously consumed while compound **1** was being continuously generated. Approximately 50 % of the Ph_3GeH had reacted after 20 h, and only a small amount (ca 5 %) remained after 50 h. The clean formation of **1,** in the sample, was clearly indicated by both the ^1H and ^{13}C NMR spectra.

$$CH_3CN \xrightarrow[THF,\ 30\ min]{LiNPr^i_2} LiCH_2CN \xrightarrow[\substack{THF,\ 2\ h \\ -\ LiCl}]{Bu_3GeCl} Bu_3GeCH_2CN$$

Scheme 2.6: Synthesis of Bu_3GeCH_2CN

To further investigate the importance of the α-germylnitrile intermediate in the Ge-Ge bond formation reaction, Bu_3GeCH_2CN was synthesized and characterized (Scheme 2.6).[101] The formation of Bu_3GeCH_2CN was confirmed by the ^{13}C NMR spectrum, which exhibited a broadened resonance at δ 16.0 ppm arising from the α-carbon of $-CH_2CN$ group and a resonance at δ 118.6 ppm for the carbon of the cyano group. A reaction mixture containing Bu_3GeCH_2CN and 1 equivalent of Ph_3GeH was prepared in CD_3CN solvent and the progress of the reaction was monitored by NMR spectroscopy. The ^1H and ^{13}C NMR signals indicated the formation of compound **1** approximately 10 min after mixing the reagents at room temperature and also indicated the completion of the reaction after 50 min of heating at 90 ºC. Digermane **1** was also synthesized on a preparative scale

in 89 % yield starting from Bu_3GeCH_2CN under these conditions as shown in Scheme 2.7. It was found that Bu_3GeCH_2CN does not react with Ph_3GeH in other solvents including toluene even in the presence of a catalytic amount of acetonitrile. These results confirmed that the hydrogermolysis reaction only yields the desired product when acetonitrile is used as the reaction medium. Therefore, acetonitrile serves as the solvent, as well as a reagent, which converts germanium amide to an activated α-germylated nitrile intermediate. This also revealed that the production of Ge-Ge bonds from germanium hydride and Bu_3GeCH_2CN is faster than the reaction of germanium hydride with R_3GeNMe_2. The later process requires a reaction time of 48 h and was shown to proceed by reaction of the amide with CH_3CN to generate the α-germylated nitrile as an intermediate formed *in situ* which subsequently reacts with the hydride to furnish the Ge-Ge bond.

$$Bu_3GeCH_2CN + Ph_3GeH \xrightarrow[90\ ^oC,\ 50\ min]{CH_3CN} \underset{\mathbf{1}}{Bu_3GeGePh_3} + CH_3CN$$

Scheme 2.7: The reaction of Bu_3GeCH_2CN with Ph_3GeH

In addition to the Bu_3GeCH_2CN, several other α-germylated nitriles were prepared and similar experiments were conducted in order to study their reactivity with Ph_3GeH. The compounds Ph_3GeCH_2CN (**7a**), $Pr^i{}_3GeCH_2CN$ (**4a)**, and $Bu^t{}_3GeCH_2CN$ (**8a**) were prepared in good to excellent yields from the corresponding monochlorides and $LiCH_2CN$ as shown in Scheme 2.8**.**

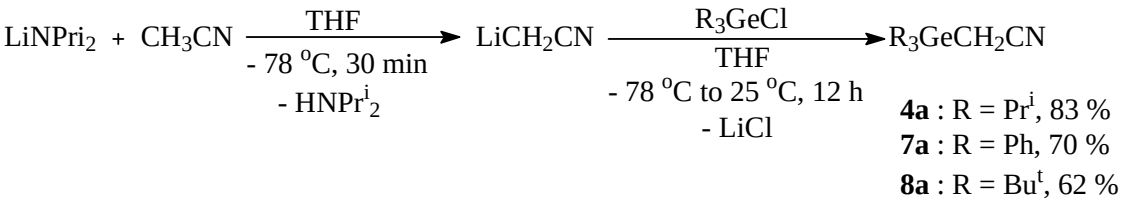

Scheme 2.8: Synthesis of α-germylated nitriles from trialkylgermanium halides.

The starting monochloride Bu^t_3GeCl used for the synthesis of **8a** was produced by treating $GeCl_4$ with Bu^tLi according to the literature procedure.[102] This resulted in a mixture of oligomeric and polymeric materials from which the desired product could not be separated. This obstacle was overcome by using the milder organocuprate $LiCu(CN)Bu^t$ as the alkylating agent and the desired product was purified by vacuum distillation at a higher temperature than that condition published in the literature (150 °C).[103]

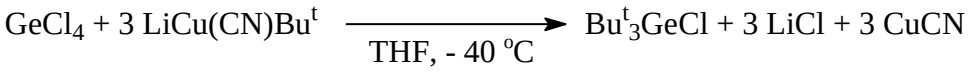

Scheme 2.9: Synthesis of Bu^t_3GeCl

Although the three α-germyl nitriles synthesized were shown to be pure by NMR spectroscopy, satisfactory elemental analyses could not be obtained. This is assumed to be due to their thermal instability. These species could be isolated and stored at -35 °C in the glove box for several days. Resonances for the –C*H*$_2$CN protons were visible in the ^{1}H NMR spectra of these compounds in C_6D_6 at δ 1.43 (**4a**), 1.98 (**7a**), 1.43 (**8a**) ppm. The ^{13}C NMR spectra contain resonances for the terminal –CN groups in the range δ 115-125 ppm (δ 118.4 ppm for **4a**, δ 124.2 ppm for **7a**, and δ 123.2 ppm for **8a**) and

resonances for the α-carbons between δ 20-30 ppm. These values are similar to those for the structurally characterized compound $[(CH_3Si)_2CH]_2Ge(H)(CH_2CN)$ which showed a resonance for the –CN group at δ 119.84 ppm although the α-carbon resonances for **4a**, **7a** and **8a** are shifted downfield relative to that for this species.

To investigate the reaction of Ph_3GeCH_2CN with Ph_3GeH, an NMR scale reaction was performed adding 1 equivalent of Ph_3GeH to a solution of Ph_3GeCH_2CN (**7a**) in CD_3CN. The reaction progress was monitored by ^1H NMR spectroscopy and similar results were observed as seen with Bu_3GeCH_2CN (Figure 2.1). Compound **7a** exhibits a singlet at δ 2.20 ppm arising from the $–CH_2CN$ protons in CD_3CN solution. The intensity of this peak began to decrease and a new resonance at δ 2.08 ppm began to appear immediately upon addition of Ph_3GeH. The singlet at δ 2.08 ppm steadily increased in intensity during the course of the experiment while the intensity of the feature at δ 2.20 ppm decreased. The resonance at δ 2.20 ppm completely disappeared after 6 h of reaction time indicating the completion of the reaction while the resonance at δ 2.08 ppm resonances remained. At this time, the peak that corresponds to the Ph_3GeH was also absent (Figure 2.2). The resonance at δ 2.08 ppm matches exactly with ^1H NMR feature observed for a sample of CH_3CN in CD_3CN solution, which clearly indicates the formation of CH_3CN in this process. However, this reaction proceeds slower than that between Bu_3GeCH_2CN and Ph_3GeH, which was complete in 50 min.[95] In order to confirm the generation of $Ph_3GeGePh_3$ (**7**), the reaction was carried out on a preparative scale resulting in the isolation of **7** in 88 % yield which was confirmed by elemental analysis.

$$Ph_3GeCH_2CN + Ph_3GeH \xrightarrow[85\ ^oC,\ 6h]{CD_3CN} \underset{\mathbf{7}}{Ph_3GeGePh_3} + CH_3CN$$

Scheme 2.10: Reaction of Ph_3GeCH_2CN with Ph_3GeH

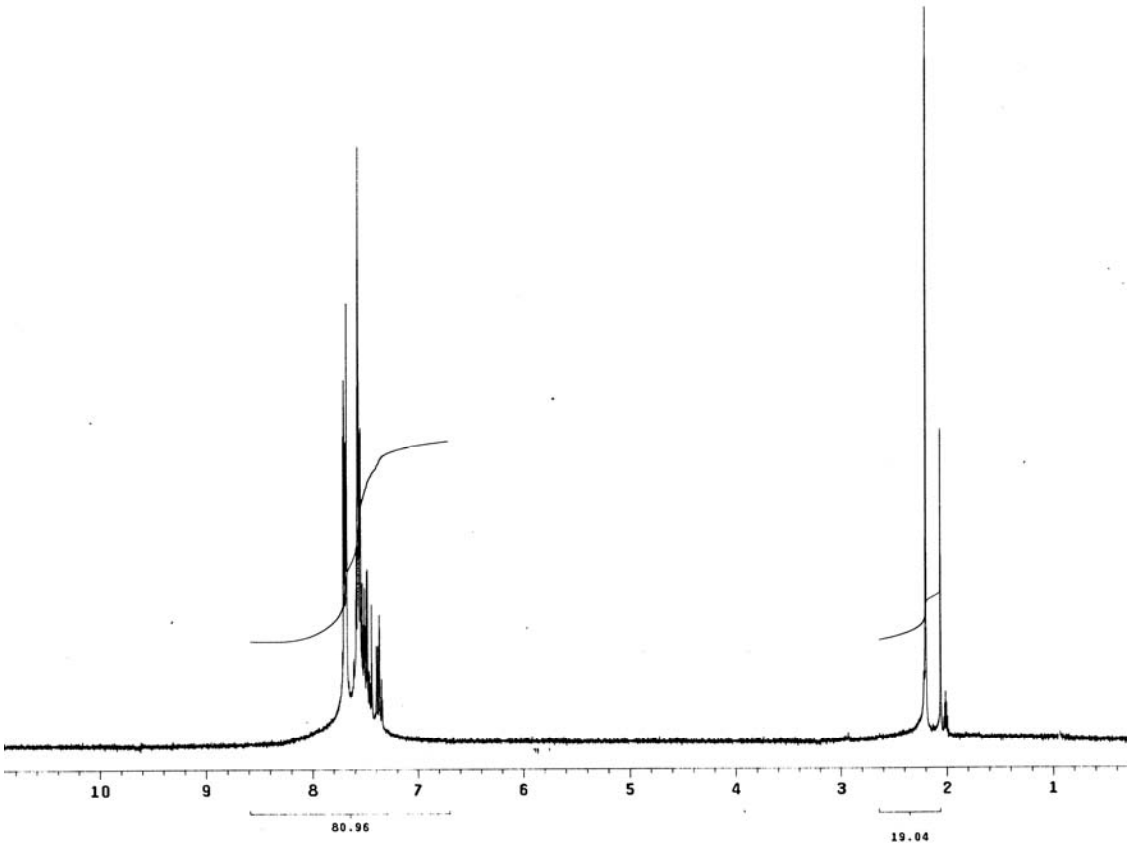

Figure 2.1: ^{1}H-NMR of Ph_3GeCH_2CN in CD_3CN

(**a**)

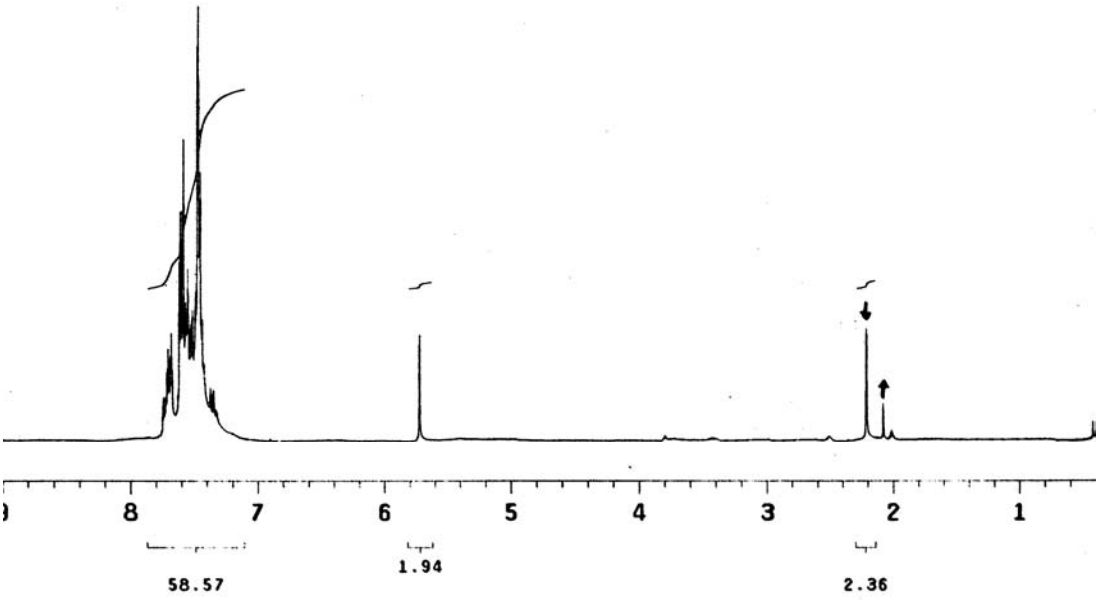

(**b**)

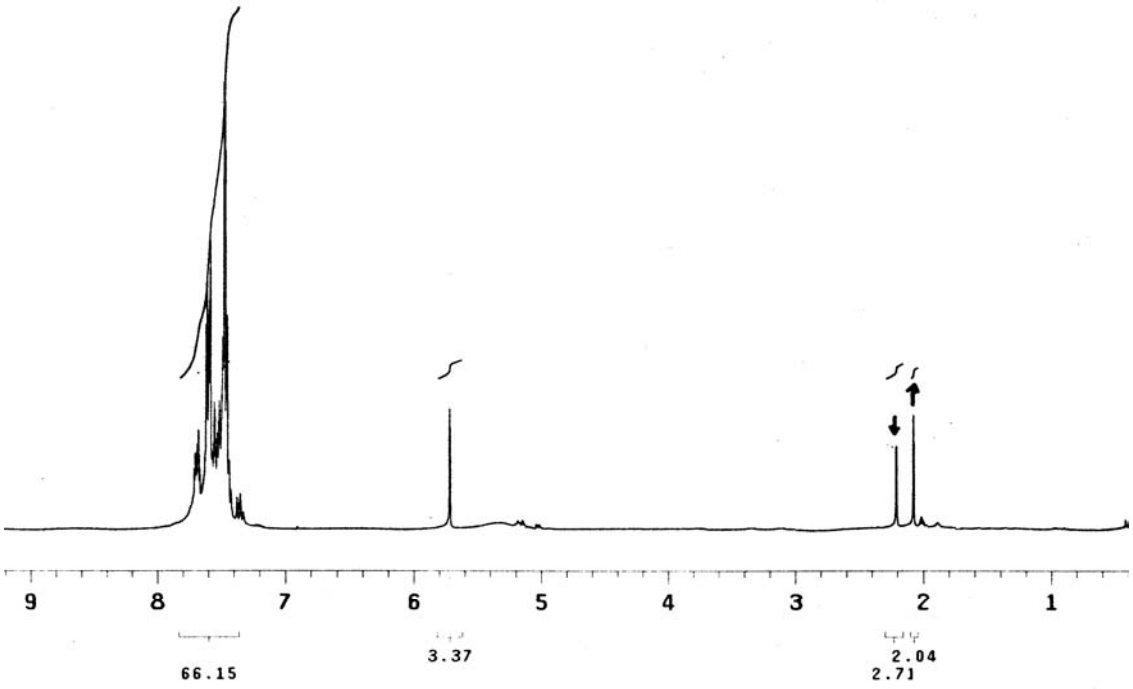

(**c**)

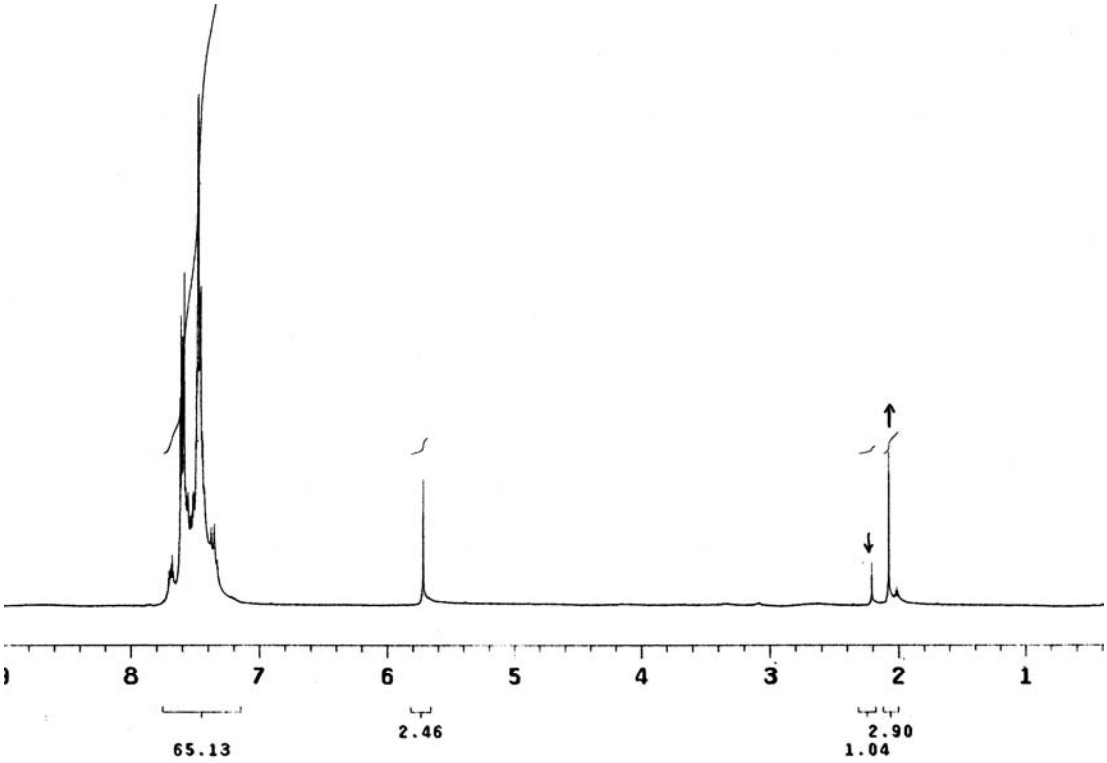

(**d**)

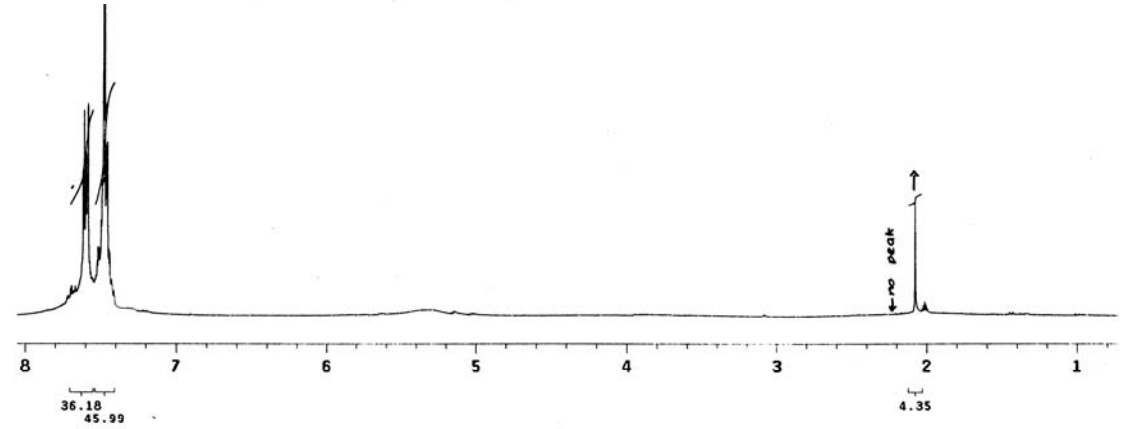

Figure 2.2: ^{1}H-NMR of the reaction of Ph_3GeCH_2CN with Ph_3GeH in CD_3CN (a) just after mixing, (b) after 1.5 h, (c) after 3 h, (d) after 24 h

A similar experiment was performed to investigate the reactivity of $Pr^{i}_{3}GeCH_2CN$ with Ph_3GeH. Treatment of $Pr^{i}_{3}GeCH_2CN$ with 1 equivalent of Ph_3GeH in CD_3CN clearly generated $Pr^{i}_{3}GeGePh_3$(**4**) in high yield (87 %). However, this reaction required a reaction time of between 32 h to 36 h for the complete consumption of the starting materials. Therefore, the reaction of $Pr^{i}_{3}GeCH_2CN$ with Ph_3GeH proceeded significantly slower than that involving the phenyl derivative. An attempt to synthesize $Bu^{t}_{3}GeGePh_3$ (**8**) from $Bu^{t}_{3}GeCH_2CN$ (**8a**) was unsuccessful and no evidence was observed for the formation of **8;** instead, an unexpected 3-amidocrotononitrile product was isolated from the reaction (*vide infra*). The reactivity of Et_3GeCH_2CN with various small molecules has been investigated to demonstrate the lability of the Ge-CH_2CN bond in this compound.[98] The reactivity of the other α-germylated nitriles has not previously been described. The reported lability of the Ge-C bonds in these compounds appears to be highly dependent on the substituents attached to germanium center. The reaction times required for the complete conversion of α-germylated nitrile to the corresponding digermanes are summarized in Table 2.1. These data indicate that, the presence of sterically demanding groups can significantly retard reactions involving cleavage of the Ge-C bond.

Table 2.1: Reaction time required for the R_3GeCH_2CN to react with Ph_3GeH.

$Bu^{n}_{3}GeCH_2CN$ (**1a**)	50 min
Ph_3GeCH_2CN (**7a**)	6 h
$Pr^{i}_{3}GeCH_2CN$ (**4a**)	32-36 h
$Bu^{t}_{3}GeCH_2CN$ (**8a**)	No reaction

The preparation of the α-germylated nitriles is more difficult than the preparation of the corresponding amides. Additionally, these materials do not generally provide the Ge-Ge bonded species more rapidly than the corresponding amides. Hence, there is little advantage to employing the $–CH_2CN$ versus the $–NMe_2$ ligand in reagents for the construction of Ge-Ge bonds. Therefore, the germanium amide reagents $Pr^i_3GeNMe_2$ (**4b**) and $Bu^t_3GeNMe_2$ (**8b**) were also prepared by the metathesis reaction of the corresponding chloride and $LiNMe_2$. The isopropyl derivative (**4b**) could be synthesized in benzene or THF as the solvent at room temperature but synthesis of Bu^tGeNMe_2 (**8b**) required refluxing the two reagents in THF for 24 h, due to the steric crowding about the germanium atom in Bu^tGeCl. These compounds were characterized by ^1H NMR spectroscopy, which showed characteristic resonances at δ 2.67 ppm (**4b**) and 2.71 (**8b**) ppm in C_6D_6 for the protons of the amide methyl groups [$-N(CH_3)_2$]. Also, elemental analyses for both of these compounds were successfully obtained. The digermane $Pr^i_3GeGePh_3$ (**4**) was obtained in slightly higher yield (91 %) using the amide reagent (**4b**) versus the reaction of $Pr^i_3GeCH_2CN$ with Ph_3GeH (see Scheme 2.11.)

$$\underset{\textbf{4b}}{Pr^i_3GeNMe_2} + Ph_3GeH \xrightarrow[85\ ^oC,\ 48\ h]{CH_3CN} \underset{\textbf{4}}{Pr^i_3Ge-GeMe_3} + HNMe_2$$

91 %

Scheme 2.11: Synthesis of digermane **4** from $Pr^i_3GeNMe_2$

The starting trialkylchlorogermane precursor Bu^s_3GeCl used for the preparation of corresponding amide $Bu^s_3GeNMe_2$, was synthesized from $GeCl_4$ and Bu^sMgCl. This resulted in the formation of a mixture of products $Bu^s_nGeCl_{4-n}$ as well as a polymeric material. Analytically pure Bu^s_3GeCl was separated from this crude reaction mixture in 27 % yield via fractional distillation at 47 ºC (0.25 Torr), which is consistent with the previously reported boiling point of 93 ºC (3 Torr).[104] The ^{1}H NMR of Bu^s_3GeCl in benzene-d_6 is complex since each of the three α-carbon atoms of the *sec*-butyl groups is chiral, resulting in eight possible diastereomers of this species. Resonances for the protons of the α-carbon, the methylene group, and the β-methyl group appear as multiplets centered at δ 1.71, 1.35, and 1.11 ppm (respectively), while that for the γ-methyl group appears as a broad triplet at δ 0.89 ppm (J = 9.6 Hz). The ^{13}C NMR spectrum of Bu^s_3GeCl in benzene-d_6 recorded at 100.6 MHz exhibits only eight resolved resonances (*vide infra*) instead of the predicted 32 peaks since several of these features overlap (as expected) due to their nearly identical magnetic environments.

Treatment of Bu^s_3GeCl with $LiNMe_2$ yielded the amide $Bu^s_3GeNMe_2$ in 78 % yield (Scheme 2.12). As found for Bu^s_3GeCl, three of the four resonances for the *sec*-butyl groups in the ^{1}H NMR spectrum of $Bu^s_3GeNMe_2$ appear as multiplets centered at δ 1.73, 1.34, and 1.12 ppm, while the peak for the γ-methyl group is a broad triplet at δ 0.89 ppm (J = 7.2 Hz) (Figure 2.3). Three separate resonances for the $-N(CH_3)_2$ protons of the amide groups were visible at δ 2.67, 2.66, and 2.65 ppm in an intensity ratio of 1: 1.3: 3 and the expected eight individual peaks could not be resolved at a spectrometer frequency of 600 MHz. The alkyl region of the ^{13}C NMR spectrum of $Bu^s_3GeNMe_2$ resembles that

of Bu^s_3GeCl, having eight resolved peaks, while two broad features at δ 42.4 and 42.1 ppm correspond to the carbon atoms of the $–N(CH_3)_2$ groups.

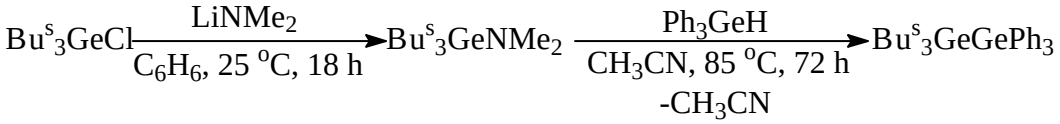

Scheme 2.12: Synthesis of $Bu^s_3GeGePh_3$ (**5**) starting from Bu^s_3GeCl

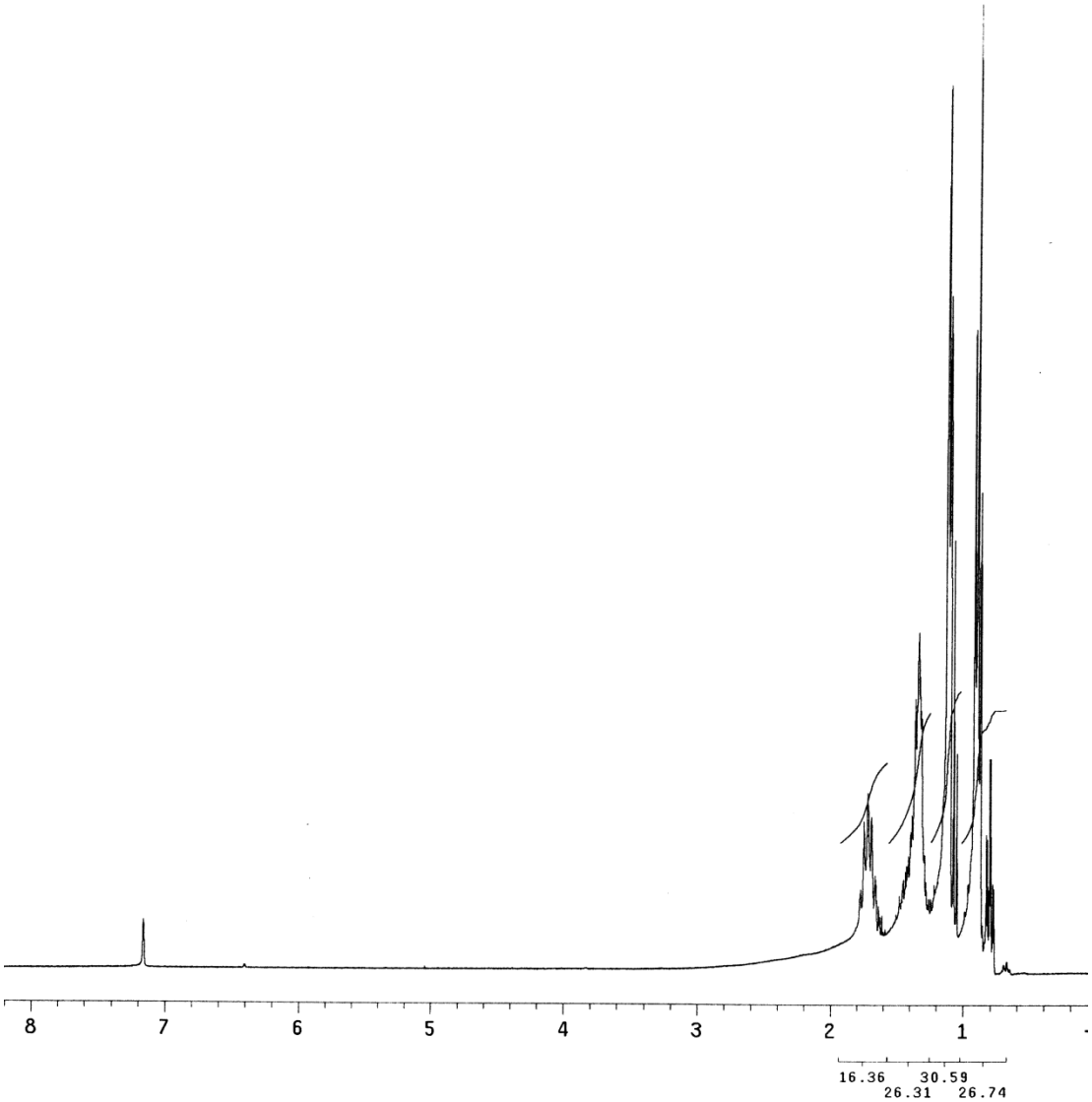

Figure 2.3: ^1H NMR of Bu^s_3GeCl

The hydrogermolysis reaction of $Bu^{s}_{3}GeNMe_2$ with Ph_3GeH in CH_3CN yielded the digermane $Bu^{s}_{3}GeGePh_3$ (**5**) in 81 % yield (Scheme 2.12). In contrast with most digermanes of the general formula $R_3GeGePh_3$, compound **5** is a highly viscous oil at room temperature instead of a solid, which can be attributed to the presence of multiple diastereomers of **5** due to the chiral nature of the *sec*-butyl groups. The aromatic region of the ^{1}H NMR spectrum of **5** is similar to that of other digermanes $R_3GeGePh_3$, with a triplet and a doublet at δ 7.68 (*J* = 7.2 Hz, *para*-H) and 7.63 (*J* = 7.2 Hz, *ortho*-H) ppm (respectively), and a multiplet centered at δ 7.11 ppm (*meta*-H). The alkyl region is again complex, with three multiplets centered at δ 1.75, 1.41, and 1.08 ppm and a broad triplet at δ 0.77 (*J* = 7.6 Hz) ppm (Figure 2.4). The alkyl region of the ^{13}C NMR of **5** exhibits six clearly resolved resonances at δ 28.8, 28.6, 26.8, 14.5, 14.4, and 13.8 ppm.

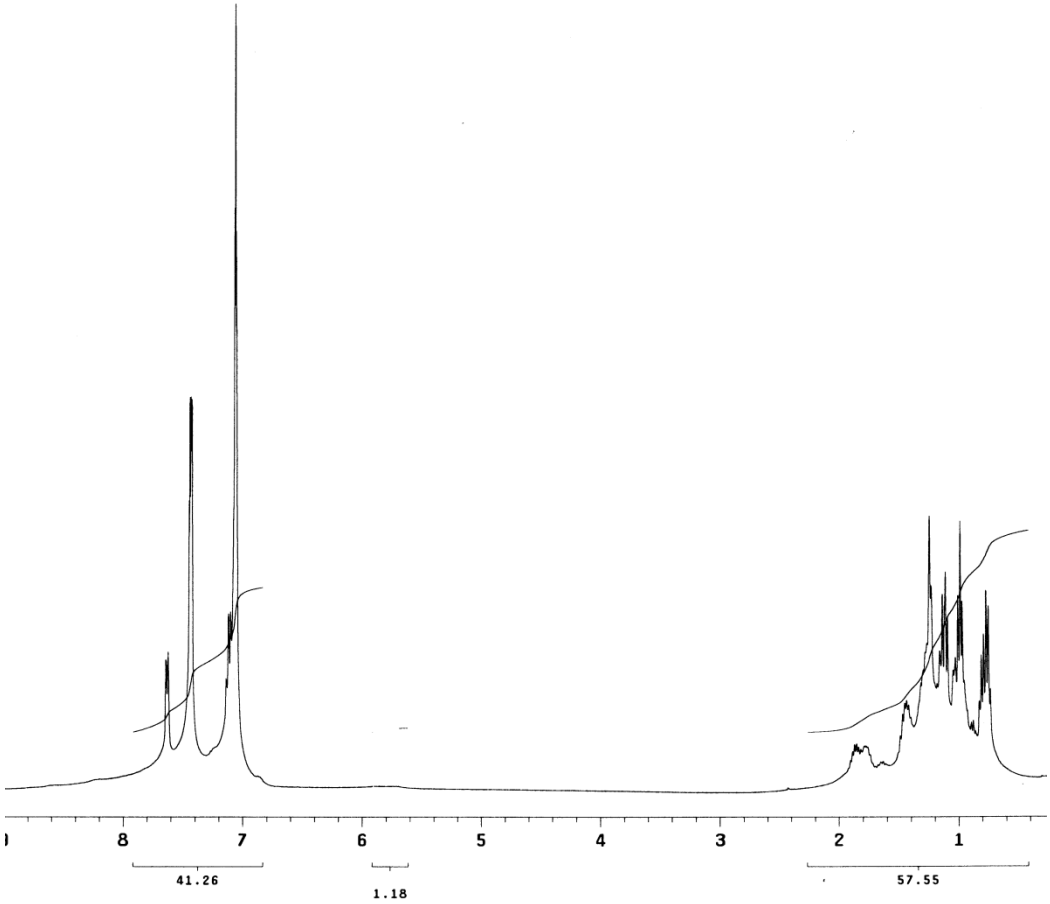

Figure 2.4: ^{1}H-NMR of $Bu^{s}_{3}GeGePh3$

Similarly, the amides Et_3GeNMe_2 and $PhMe_2GeNMe_2$ were prepared starting from the corresponding commercially available germanium halides in 57 % and 75 % yields respectively. Digermanes $Et_3GeGePh_3$ (**2**) and $PhMe_2GeGePh_3$ (**6**) were obtained in yields of 84 % for **2** and 76 % for **6** treating the amides with Ph_3GeH, and each was characterized by ^{1}H NMR, ^{13}C NMR and elemental analyses.

The X-ray crystal structures of digermanes **1**, **2**, **4**, and **6** were obtained. An ORTEP diagram of compound **1** is shown in Figure 2.5 and selected bond distances and angles are collected in Table 2.2. Compound **1** contains two crystallographically independent molecules in the unit cell which have an average Ge-Ge distance of 2.421(8) Å. The average Ge-C_{ipso} bond distances are 1.955(4) Å for **1′a** and 1.954(4) Å for **1′b**. The average Ge-$C_{aliphatic}$ distances are 1.943(5) Å for **1′a** and 1.958(5) Å for **1′b** and Ge(2)-C(9) bond is slightly elongated [2.006(7) Å] over the other Ge-$C_{aliphatic}$ bond distances. The geometry around Ge(1) and Ge(2) are nearly tetrahedral, which has average C-Ge(1)-C bond angles of 107.8(2)˚ for **1′a** and 107.4(2)˚ for **1′b** while the C-Ge(2)-C bond angels are slightly more obtuse than at Ge(1) (average C-Ge(2)-C, 109.0(3)˚ for **1′a** and 108.2(2)˚ for **1′b**).

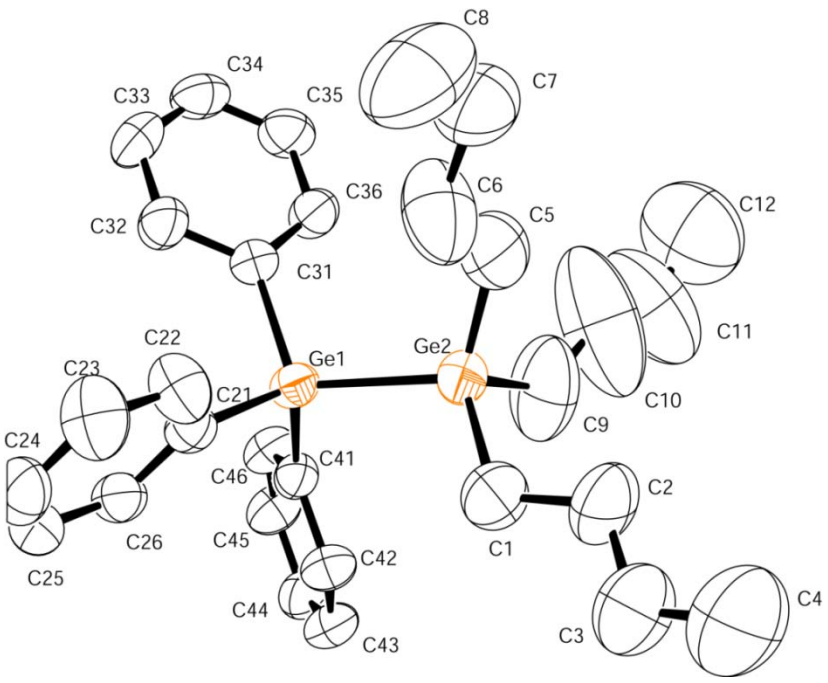

Figure 2.5: ORTEP diagram of one of the crystallographically independent molecules of $Bu_3GeGePh_3$ (**1′a**). Thermal ellipsoids are drawn at 50 % probability.

Table 2.2: Selected bond distance **(Å)** and angles (˚) for the two crystallographically independent molecules of $Bu_3GeGePh_3$ **(1)**

1′a		**1′b**		average
Ge(1)-Ge(2)	2.415(8)	Ge(1′)-Ge(2′)	2.4270(8)	2.421(8)
Ge(1)-C(21)	1.956(4)	Ge(1′)-C(21′)	1.954(4)	1.955(4)
Ge(1)-C(31)	1.956(4)	Ge(1′)-C(31′)	1.955(4)	1.956(4)
Ge(1)-C(41)	1.953(4)	Ge(1′)-C(41′)	1.952(4)	1.953(4)
Ge(2)-C(1)	1.921(5)	Ge(2′)-C(1′)	1.947(4)	1.934(4)
Ge(2)-C(5)	1.902(5)	Ge(2′)-C(5′)	1.941(5)	1.922(5)
Ge(2)-C(9)	2.006(7)	Ge(2′)-C(9′)	1.987(6)	1.997(6)
C(21)-Ge(1)-C(31)	107.2(2)	C(21′)-Ge(1′)-C(31′)	106.8(2)	107.0(2)
C(21)-Ge(1)-C(41)	107.8(2)	C(21′)-Ge(1′)-C(41′)	108.5(2)	108.2(2)
C(31)-Ge(1)-C(41)	108.3(2)	C(31′)-Ge(1′)-C(41′)	106.9(2)	107.6(2)
C(21)-Ge(1)-C(2)	115.0(1)	C(21′)-Ge(1′)-C(2′)	111.7(1)	113.4(1)
C(31)-Ge(1)-C(2)	111.3(1)	C(31′)-Ge(1′)-C(2′)	110.3(1)	110.8(1)
C(41)-Ge(1)-C(2)	107.1(1)	C(41′)-Ge(1′)-C(2′)	112.3(1)	109.7(1)
C(1)-Ge(1)-C(5)	113.8(3)	C(1′)-Ge(1′)-C(5′)	109.9(2)	111.9(2)
C(1)-Ge(1)-C(9)	105.9(3)	C(1′)-Ge(1′)-C(9′)	106.8(2)	106.4(2)
C(5)-Ge(1)-C(9)	107.3(4)	C(5′)-Ge(1′)-C(9′)	107.5(3)	107.4(3)
C(1)-Ge(1)-C(1)	110.0(2)	C(1′)-Ge(1′)-C(1′)	108.9(1)	109.5(1)
C(5)-Ge(1)-C(1)	112.5(2)	C(5′)-Ge(1′)-C(1′)	112.3(1)	112.4(1)
C(9)-Ge(1)-C(1)	106.9(2)	C(9′)-Ge(1′)-C(1′)	111.3(2)	109.1(2)

The Ge-Ge bond distance of compound **2** is 2.425(7) Å, which is fairly close to that of compound **1.** The three phenyl and three ethyl substituents in compound **2** are symmetry related by a C_3 axis and the ORTEP diagram of compound **2** and the selected bond distances are shown in Figure 2.6 and Table 2.3 respectively. The Ge-C bond distances at each germanium are similar which has Ge(1)-C_{ipso} bond distances of 1.954(2) Å and Ge(2)-$C_{aliphatic}$ distance of 1.959(2).The C-Ge-C bond angles at Ge(2) and very closely match the ideal tetrahedral angle of 109.5º while the C-Ge-C angles at Ge(1) are acute. Also, the C-Ge-C bond angles at each germanium center are similar.

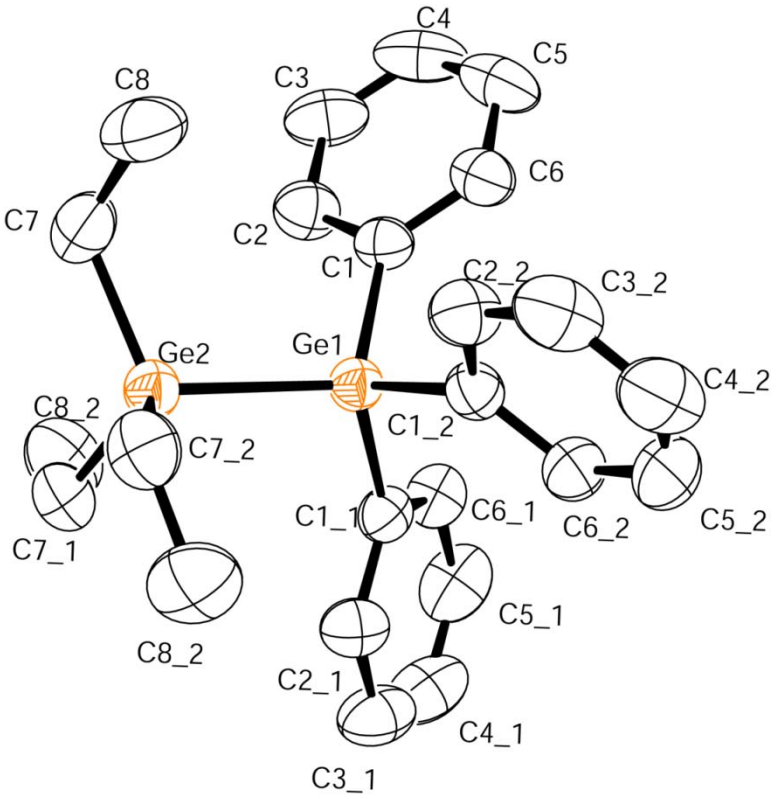

Figure 2.6: ORTEP diagram of $Et_3GeGePh_3$ (**2**). Thermal ellipsoids are drawn at 50 % probability.

Table 2.3: Selected bond distances (Å) and angles (˚) for $Et_3GeGePh_3$ (**2**)

Ge(1)-Ge(2)	2.4253(7)
Ge(1)-C(1)	1.954(2)
Ge(1)-C(1_1)	1.954(2)
Ge(1)-C(1_2	1.954(2)
Ge(2)-C(7)	1.959(2)
Ge(2)-C(7_1)	1.959(2)
Ge(2)-C(7_2)	1.959(2)
C(7)-C(8)	1.510(4)
C(1)-Ge(1)-C(1_2)	107.78(7)
C(1)-Ge(1)-C(1)	107.78(7)
C(1_1)-Ge(1)-C(1_2)	107.78(7)
C(7)-Ge(2)-C(7_1)	109.75(9)
C(7)-Ge(2)-C(7_2)	109.75(9)
C(7_1)-Ge(2)-C(7_2)	109.75(9)
C(1-1)-Ge(1)-Ge(2)	111.11(7)
C(1_2)-Ge(1)-Ge(2)	111.11(7)
C(1)-Ge(1)-Ge(2)	111.11(7)
Ge(1)-Ge(2)-C(7)	109.19(9)
C(7_1)-Ge(2)-Ge(1)	109.19(9)

The Ge-Ge bond distance of other digermanes (alkyl and aryl substituted) which have been previously reported are shown in Table 2.4. The bond lengths of these digermanes are dependent on the steric and electronic properties of the organic substituents including their size and electron-withdrawing or -donating ability. Thus hexa-phenyl and hexa-*tert*-butyl derivatives are expected to exhibit longer bond lengths than that of $Me_3GeGePh_3$ and compounds **1** and **2** due to more bulky phenyl and more electron donating *tert*-butyl groups. The electron donating ability and the relative size of the alkyl groups of the compound **1** and **2** are the same and exhibit similar Ge-Ge bond distances as expected.

Table 2.4: The Ge-Ge, average Ge-$C_{aliphatic}$, and average Ge-C_{ipso} bond lengths of previously reported alkyl and phenyl substituted digermanes in (Å)

	Ge-Ge	Ge-$C_{aliphatic}$	Ge-C_{ipso}
$Ph_3GeGePh_3$(**7**)	2.446(1)[61,105]		1.954(2)
$^tBu_3GeGe^tBu_3$(**9**)	2.710(1)[62]	2.076(5)	
$Ph_3GeGeMe_3$(**10**)	2.428(1)[103]	1.943(4)	1.957(2)

The X-ray crystal structure of $^iPr_3GeGePh_3$ (**4**) was determined and an ORTEP diagram is shown in Figure 2.7 while selected bond distances and bond angles are collected in Table 2.5. The three sterically encumbering isopropyl groups in **4** result in a Ge-Ge distance of 2.4637(7) Å, that is longer than the corresponding bond lengths of $Me_3GeGePh_3$ [**10,** 2.418(1) Å], $Et_3GeGePh_3$ [**2**, 2.4253(7) Å], $Bu^n_3GeGePh_3$ [**1**, 2.4212(8) Å] and $Ph_3GeGePh_3$ [**7**, 2.446(1) Å]. The average Ge-$C_{aliphatic}$ distance in **4** is 1.985(2) Å which is significantly longer than those of **1** and **2**, which range from 1.943 to 1.959 Å.

The average Ge-C_{ipso} distance of compound **4** is 1.985(2) Å, which is elongated over those in **1**, **2**, **8** and **7** that range from 1.954(2) to 1.957(2) Å. The average C-Ge-C angles among **4 3**, **2**,and **1** for the aliphatic substituents approach normal values for a tetrahedral geometry at germanium ranging from 108.7(1)˚ to 109.75(9)˚, while those for the phenyl substituents in **7**, **4**, **1**, **2**, and **3** are generally more obtuse ranging from 108.1(3)˚ to 115.51(6)˚.

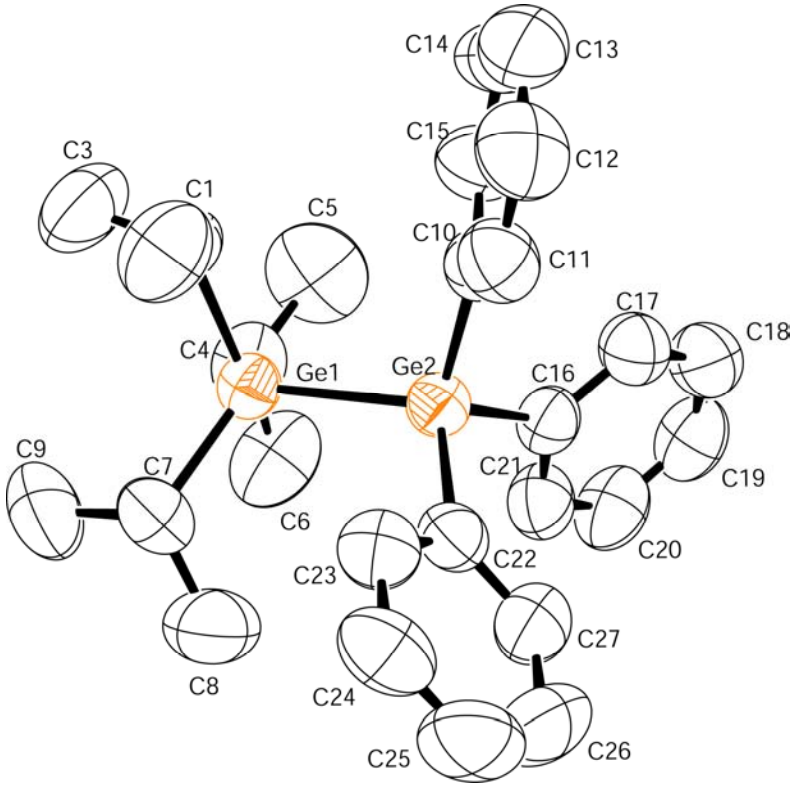

Figure 2.7: ORTEP diagram of $Pr^{i}_{3}GeGePh_3$ (**4**). Thermal ellipsoids are drawn at 50 % probability.

Table 2.5: Selected bond distances (Å) and angles (˚) for compound $Pr^{i}_{3}GeGePh_3$ (**4**)

Ge(1)-Ge(2)	2.4637(7)	C(1)-Ge(1)-C(7)	110.27(9)
Ge(1)-C(1)	1.990(2)	C(4)-Ge(1)-C(7)	111.60(9)
Ge(1)-C(4)	1.980(2)	C(1)-Ge(1)-C(7)	110.27(9)
Ge(1)-C(7)	1.986(2)	C(4)-Ge(1)-C(7)	111.60(9)
Ge(2)-C(10)	1.964(2)	C(1)-Ge(1)-Ge(2)	105.04(6)
Ge(2)-C(16)	1.960(2)	C(4)-Ge(1)-Ge(2)	113.64(6)
Ge(2)-C(22)	1.961(2)	C(7)-Ge(1)-Ge(2)	110.11(6)
		C(10)-Ge(2)-C(16)	107.01(8)
		C(10)-Ge(2)-C(22)	107.34(8)
		C(16)-Ge(2)-C(22)	107.90(8)
		C(10)-Ge(2)-Ge(1)	107.95(6)
		C(16)-Ge(2)-Ge(1)	115.14(6)
		C(22)-Ge(2)-Ge(1)	111.16(6)

An ORTEP diagram for the digermane $PhMe_2GeGePh_3$ (**6**) is shown in Figure 2.8 and selected bond distances and angles are collected in Table 2.6. The Ge-Ge bond distance in **6** is 2.4216(4) Å, which is slightly longer than those in the related compounds $Me_3GeGePh_3$ [**10**, 2.418(1) Å], but shorter than the Ge-Ge bond distance in $Et_3GeGePh_3$ [**2**, 2.4253(7) Å]. The ethyl and phenyl substituents in **2** are *eclipsed*, resulting in the

longer Ge-Ge distance, while the substituents at each of the germanium atoms in **6** is in an *anti* conformation.

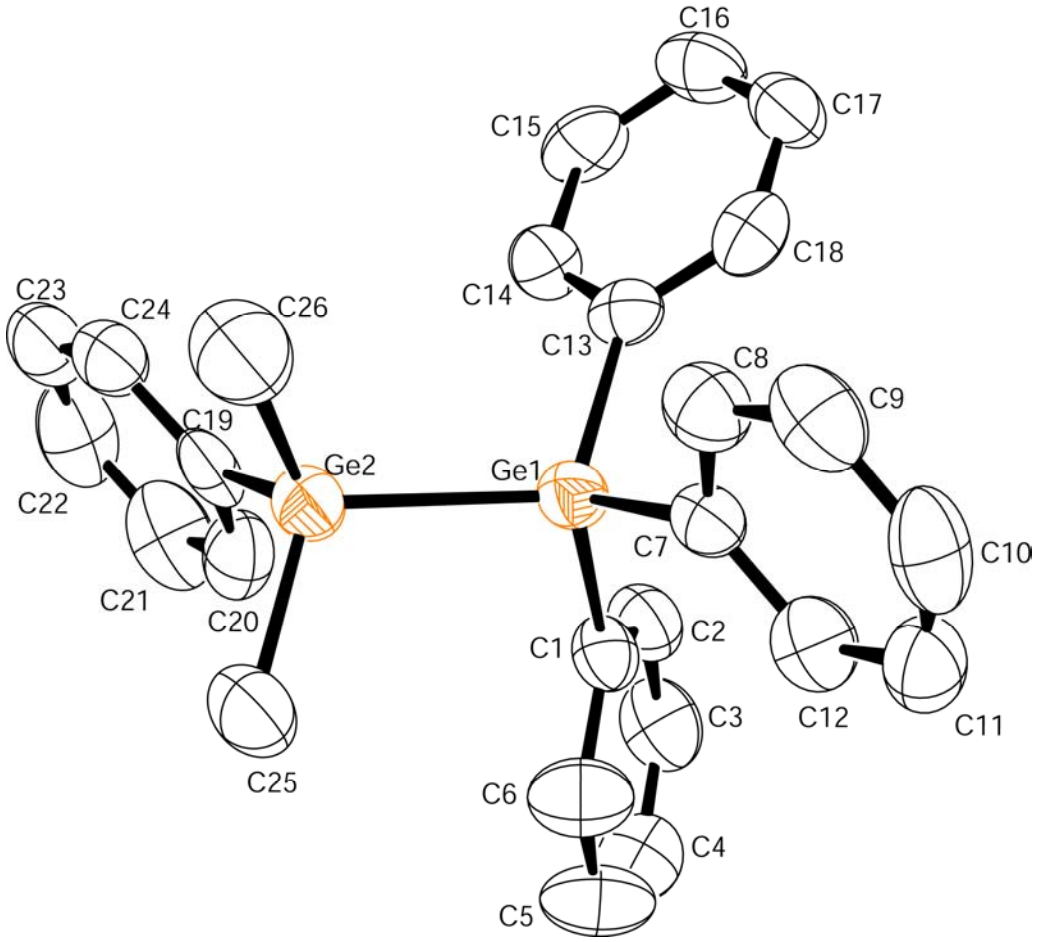

Figure 2.8: ORTEP diagram of $PhMe_2GeGePh_3$ (**6**). Thermal ellipsoids are drawn at 50 % probability

Table 2.6: Selected bond distances (Å) and bond angles (˚) for $PhMe_2GeGePh_3$ (**6**)

Ge(1)-Ge(2)	2.4216 (4)	C(1)-Ge(1)-C(7)	109.5(2)
Ge(1)-C(1)	1.965(4)	C(1)-Ge(1)-C(13)	109.7(1)
Ge(1)-C(7)	1.953(3)	C(7)-Ge(1)-C(13)	106.9(2)
Ge(1)-C(13)	1.955(4)	C(19)-Ge(2)-C(25)	107.6(2)
Ge(2)-C(19)	1.959(3)	C(19)-Ge(2)-C(26)	111.3(2)
Ge(2)-C(25)	1.955(4)	C(25)-Ge(2)-C(26)	108.6(2)
Ge(2)-C(26)	1.951(4)	C(1)-Ge(1)-Ge(2)	106.7(1)
		C(7)-Ge(1)-Ge(2)	111.5(9)
		C(13)-Ge(1)-C(2)	112.3(1)
		C(19)-Ge(2)-Ge(1)	107.1(2)
		C(25)-Ge(2)-Ge(1)	109.0(1)
		C(26)-Ge(2)-Ge(1)	113.2(1)

The elongation of the Ge-Ge bond in **6** relative to that of $Me_3GeGePh_3$, $Bu^n{}_3GeGePh_3$ and $Et_3GeGePh_3$ results due to the presence of a phenyl group at Ge(2), while the other three derivatives have three relatively less bulky methyl, *n*-butyl and ethyl groups attached to Ge(2). Two of the C-Ge-C bond angles at Ge(1) very closely match the ideal angle of 109.5˚, while the third is slightly more acute. The C-Ge-C bond angles at Ge(2) are highly distorted from the ideal tetrahedral geometry, although the average bond angle is 109.2˚. These distortions result from the steric interaction of the single phenyl substituent at Ge(2) with the three phenyl groups attached to Ge(1).

The synthesis of $Bu^t_3GeGePh_3$ (**8**) starting from amide $Bu^t_3GeNMe_2$ (**8b**) and Ph_3GeH was attempted, but no evidence for the formation of **8** was found. A viscous yellow oil was obtained after treating **8b** with $PhGeH_3$ at 85 ºC for 72 h. Vacuum distillation of this crude product mixture at 120 ºC afforded a small amount (0.025 g) of unreacted **8b.** Continued distillation of the crude material at 180 ºC resulted in the isolation of a yellow solid material which, upon recrystallization from cold hexane, furnished $Bu^t_3Ge[NHC(CH_3)CHCN]$ (**11**) (Scheme 2.13) as a minor product with a maximum yield of 6 % over three separate trials. Unreacted Ph_3GeH and $Bu^t_3GeCH_2CN$ were also contained in this second fraction as shown by ^1H NMR spectroscopy.

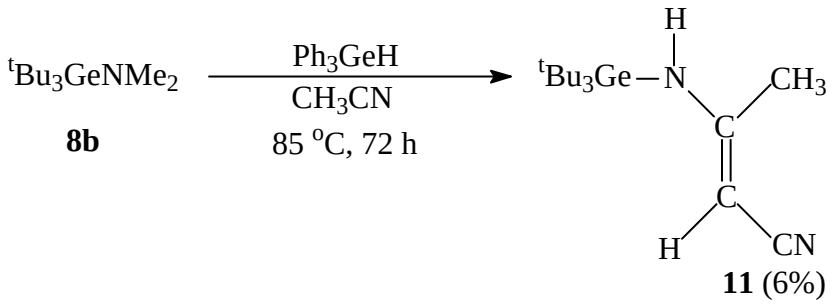

Scheme 2.13: Reaction of $Bu^t_3GeNMe_2$ with Ph_3GeH

A sample of **8b** was prepared in CD_3CN and used to probe the pathway of this reaction using ^{13}C NMR spectroscopy. The results indicated that the presence of Ph_3GeH is necessary for the generation of both $Bu^t_3GeCH_2CN$ and compound **11**. The appearance of the ^{13}C NMR spectrum was unchanged after heating **8b** alone in CD_3CN for 6 days at 85 ºC. However, heating the sample for 24 h after the addition of 1 equivalent of Ph_3GeH resulted a significant decrease in intensity of this feature as well as the corresponding

resonance for the *tert*-butyl groups of **8b**. After continued heating for 72 h, the appearance of peaks at δ 135.8, 130.3, and 129.5 ppm indicated the presence of the deuterated analog of **11**, and features for Ph_3GeH and $Bu^t_3GeCD_2CN$ were also present. The appearance of the ^{13}C NMR spectrum remained unchanged upon heating the sample for a further 72 h. These results are consistent with those obtained from the preparative scale reaction where a small amount of unreacted **8b** was recovered in the low boiling fraction (*vide supra*).

It is likely that compound **11** is generated by a variation of the Thorpe reaction used for the dimerization of nitriles which requires the presence of a base in either catalytic or stoichiometric amounts.[106] Although Ph_3GeH cannot be considered a base, it is required for the generation of both the α-germylated nitrile **8a** and compound **11** from Bu^t_3GeCl, but is not consumed to any significant degree in the process and so appears to function as a catalyst. Although the exact role of Ph_3GeH is not known, a proposed pathway for the formation of **11** is shown in Scheme 2.14.

The ^1H NMR spectrum of **11** in C_6D_6 contains a single resonance at δ 1.08 ppm for the *tert*-butyl groups as well as sharp signals at δ 1.94 and δ 4.33 ppm corresponding to the protons of the methyl group and the single olefinic proton (respectively), while a broad singlet at δ 3.18 ppm arises from the proton bound to nitrogen. The presence of only one feature for each type of proton in the 3-amidocrotononitrile ligand in **11** indicates the substituents about the C=C double bond are present in only one conformation. In order to ascertain the exact confirmation of the ligand, the X-ray crystal

structure of **11** was determined. An ORTEP diagram is shown in Figure 2.9 and selected bond distances and angles are collected in Table 2.7.

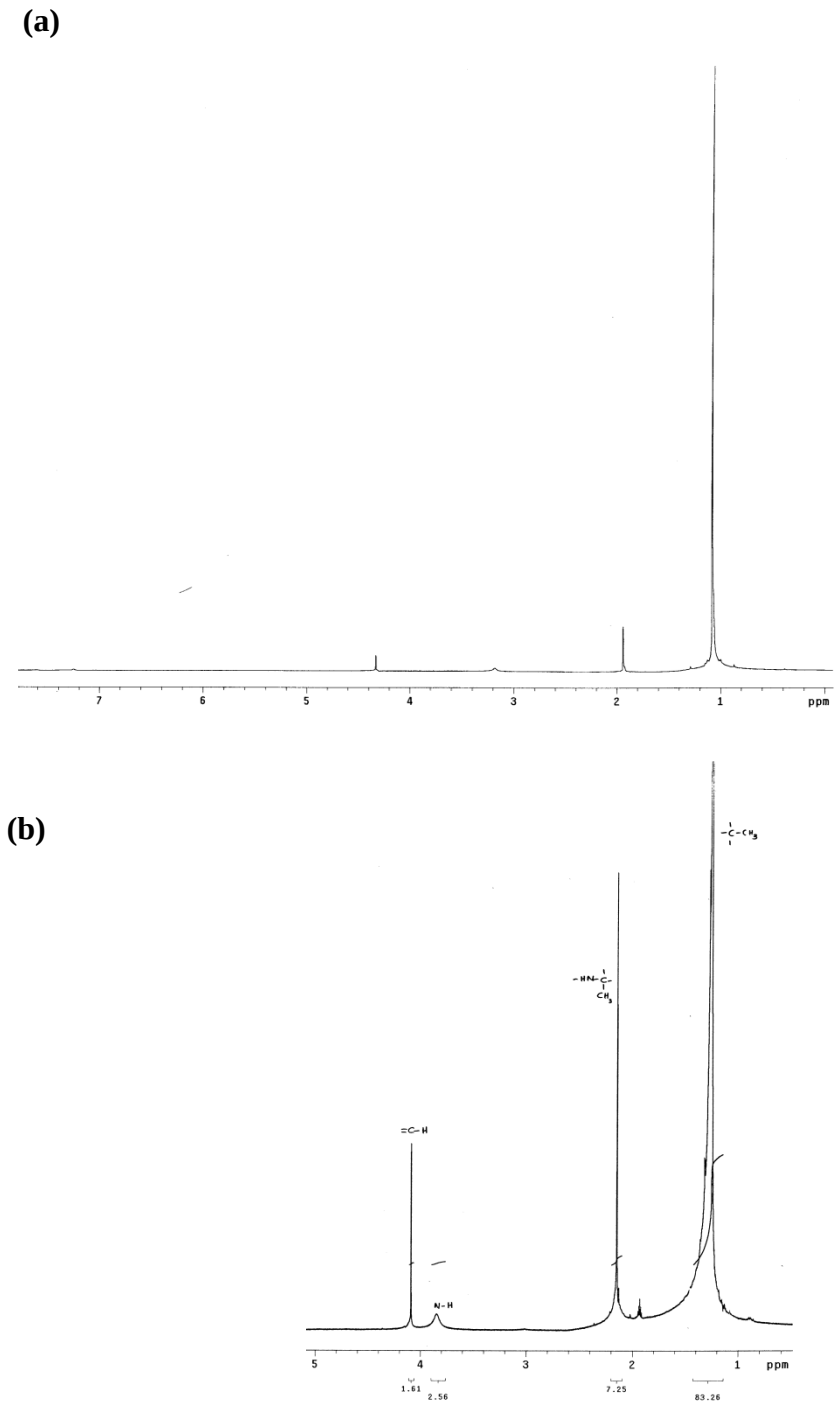

Figure 2.9: ^{1}H-NMR of compound **11** in CD_3CN (a) and in C_6D_6 (b).

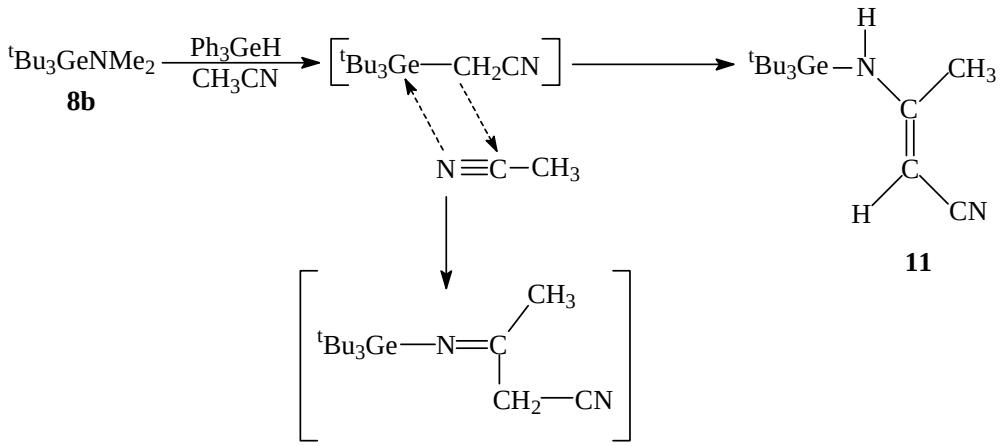

Scheme 2.14: Proposed mechanism for the formation of $Bu^{t}_{3}GeNHC(CH_3)CHCN$ (**11**) form $Bu^{t}_{3}GeNMe_2$ and Ph_3GeH

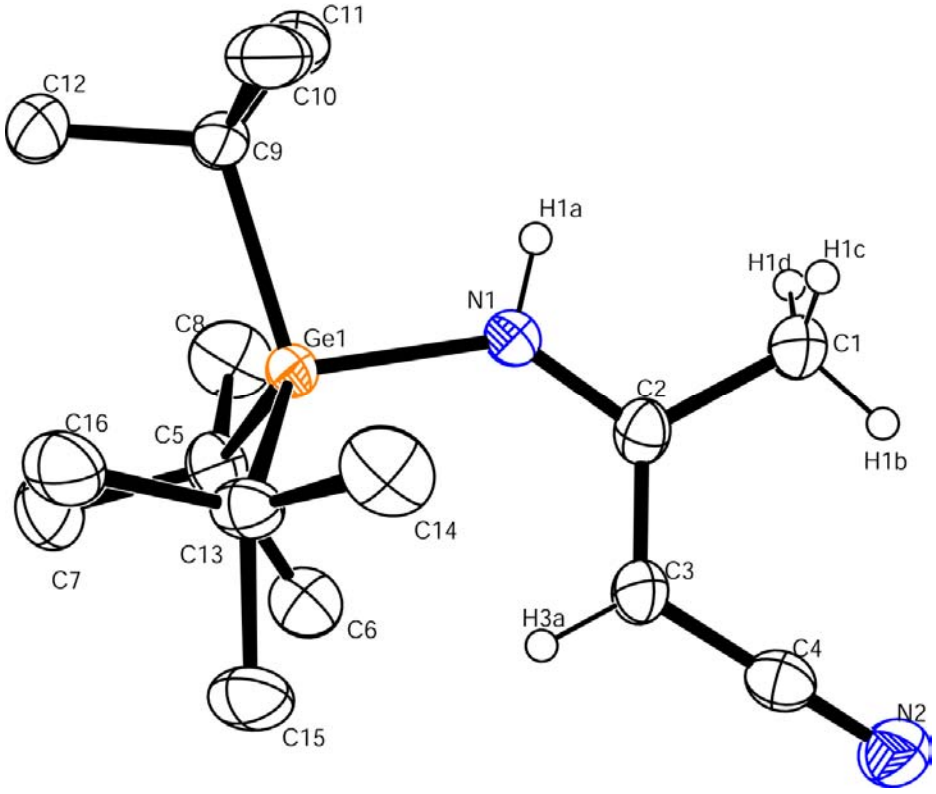

Figure 2.10: ORTEP diagram of $Bu^{t}_{3}GeNHC(CH_3)CHCN$ (**11**).Thermal ellipsoids are drawn at 50 % probability.

Table 2.7: Selected bond distances (Å) and angles (˚) for $Bu^t_3GeNHC(CH_3)CHCN$ (**11**).

Ge(1)-N(1)	1.895(2)	N(1)-Ge(1)-C(5)	108.76(8)
Ge(1)-C(5)	2.006(2)	N(1)-Ge(1)-C(9)	99.25(7)
Ge(1)-C(9)	2.015(2)	N(1)-Ge(1)-C(13)	108.90(8)
Ge(1)-C(13)	2.018(2)	C(5)-Ge(1)-C(9)	112.76(9)
N(1)-C(2)	1.36093)	C(5)-Ge(1)-C(13)	113.61(8)
C(1)-C(2)	1.509(3)	C(9)-Ge(1)-C(13)	112.47(9)
C(2)-C(3)	1.361(3)	Ge(1)-N(1)-C(2)	135.4(1)
C(3)-C(4)	1.414(3)	N(1)-C(2)-C(1)	115.6(2)
C(4)-N(2)	1.152(3)	N(1)-C(2)-C(3)	125.0(2)
		C(1)-C(2)-C(3)	119.5(2)
		C(2)-C(3)-C(4)	121.4(2)
		C(3)-C(4)-N(2)	179.6 (3)

The 3-amidocrotononitrile ligand exclusively adopts an (*E*)-configuration about the C=C double bond which measures 1.361(3) Å. Crystallographically characterized Ge compounds bearing a single Ge-N bond are rare, and this distance in **11** is 1.895(2) Å which is longer than the Ge-N distance of 1.854(3), 1.818(2), and 1.824(9) Å in the primary germyl amines Mes_3GeNH_2[107], $(RGe)_2(NH_2)_4(NH)$ ($R=Pr^i_2C_6H_3NSiMe_3$),[108] and $[(2,6\text{-}Pr^i_2C_6H_3)NSiMe_3Ge(NH_2)NH]_3$[109] respectively. However, the Ge-N bond length in **11** is similar to those in the germanium(IV) compounds $[(Me_3Si)_2N]_3GeBr$ (1.848(3) Å)

and $[(Me_3Si)_2N]_3GeBu$ (1.890(2) Å)[110], and also compares well with the Ge-N distances in the germanium(II) amides $Ge[N(SiMe_3)_2]_2$[111] and $Ge[NC_5H_6(CH_3)_4\text{-}2,2,6,6]_2$[112] which are 1.875(5) and 1.88(5) Å respectively. The environment about the germanium atom in **11** is distorted tetrahedral with the largest perturbation occurring in the C-Ge-C angles which average 112.95(8)˚. This distortion occurs due to the presence of the three bulky *tert*-butyl groups which also results in the long average Ge-C bond length of 2.013(2) Å. This distance is elongated by 0.07 Å relative to typical Ge-C single bonds (1.94 Å),[113] but is significantly shorter than the average Ge-C bond length in $Bu^t_3GeGeBu^t_3$ which is 2.076(7) Å.[103]

The hydrogermolysis reaction can be used to synthesize not only digermanes but also oligogermanes having Ge-Ge chains. In order to construct oligomeric germanium chains systematically, amide containing synthons have been used.[95] The preparation of the synthons is shown in Scheme 2.15 starting from the germanium dihydride reagents.[114] Monochlorinated products of R_2GeH_2 were prepared in high yields using a published procedure[114] and converted to the corresponding chlorides **12a**, **12b**, and **12c** by the hydrogermylation of ethyl vinyl ether in the presence of AIBN as the radical initiator. In the hydrogermylation reaction, the germanium-hydrogen bond is added across the vinyl group in the anti-Markovnikov fashion. The chloride reagents can be subsequently converted to an amide **13a**,**13b**, and **13c** by reacting with $LiNMe_2$. Relative to the starting material R_2GeHCl, the overall yields of the germanium amides are 82 % (**13a**), 75 % (**13b**), and 57 % (**13c**). These compounds were characterized by ^1H NMR spectroscopy, and they exhibit a characteristic feature at δ 2.57 ppm (**13a**), δ 2.60 ppm (**13b**), and 2.78 ppm (**13c**) for the protons of the $–NMe_2$ group, which was very important for monitoring

the reaction progress (Figure 2.11).

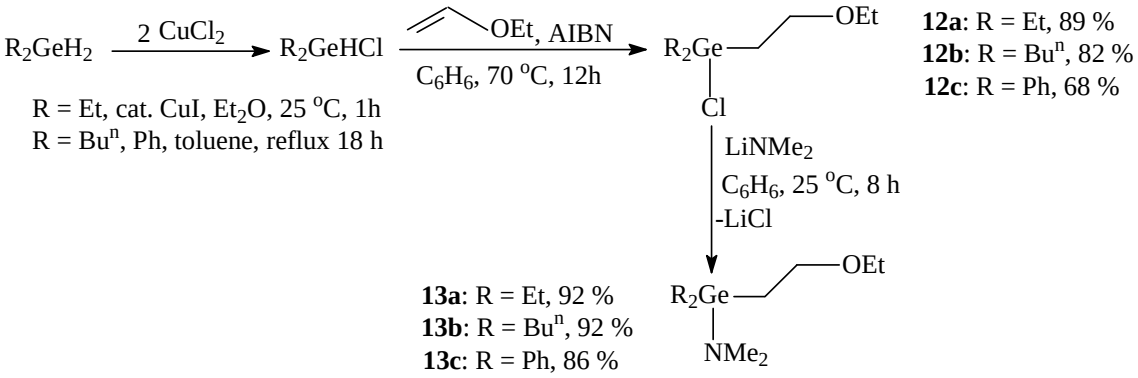

Scheme 2.15: Preparation of $R_2Ge(NMe_2)CH_2CH_2OEt$ from R_2GeH_2

(a)

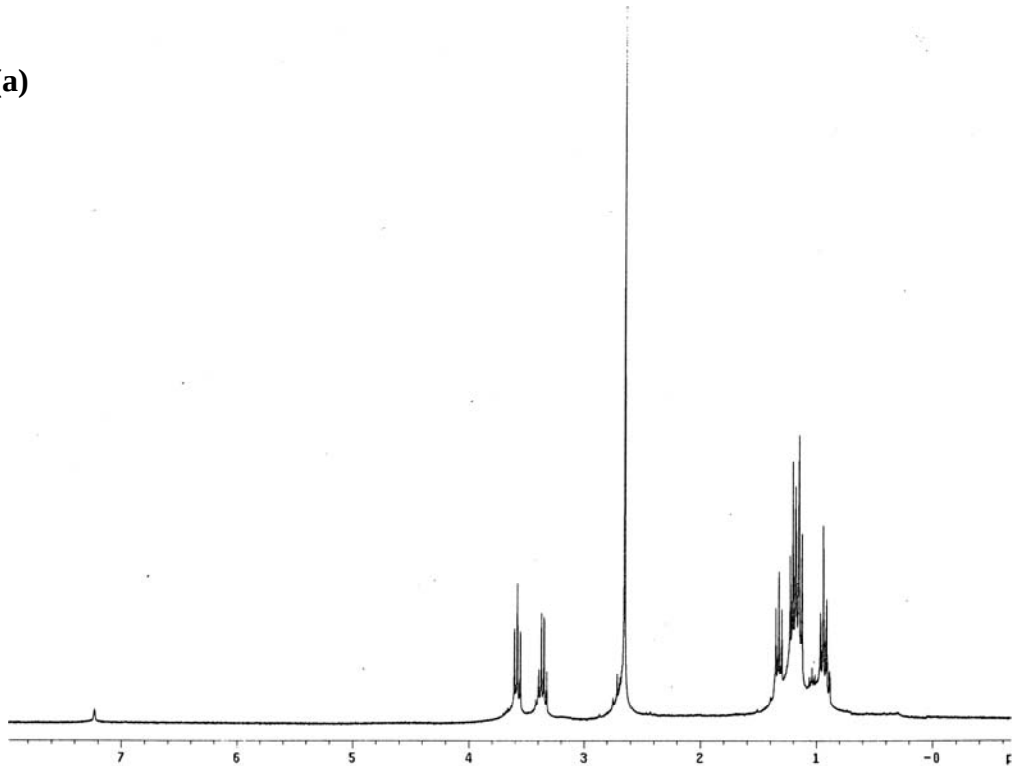

(b)

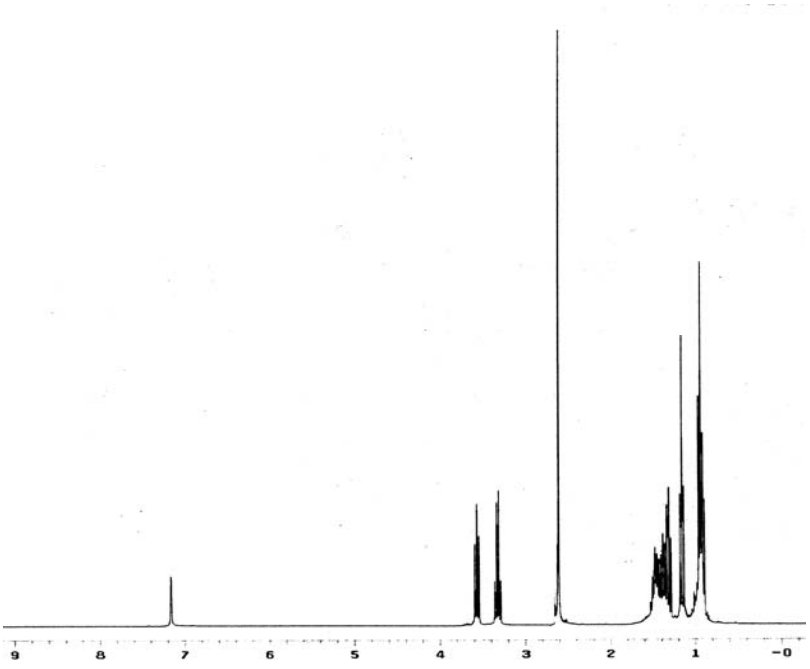

(c)

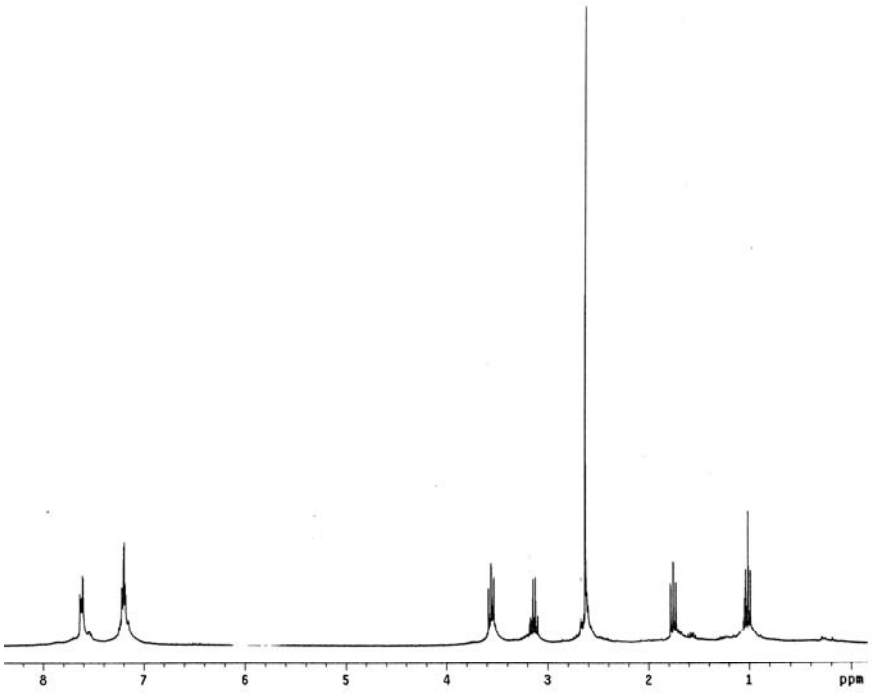

Figure 2.11: ^{1}H-NMR of compounds of **13a** (a), **13b** (b), **13c** (c).

The germanium amide synthons **13a**, **13b**, and **13c** were reacted with a slight excess of Ph_3GeH in a sealed Schlenk tube in acetonitrile over 48 h at 90 °C to form the digermanes **14a**, **14b**, and **14c**. After removing excess Ph_3GeH via Kugelrohr distillation, purified digermanes were obtained in high yields of 75 % (**14a**), 76 % (**14b**), and 92 % (**14c**) (Scheme 2.16). Compound **14a** is substantially more volatile than **14b** or **14c** and can co-distill with the Ph_3GeH. Therefore, care must be taken when distilling this product. These compounds were characterized by NMR spectroscopy and elemental analysis. In the ^1H NMR spectra, these species each exhibit a triplet and a quartet arising from the protons of the methylene groups bound to the oxygen atom of the ethoxyethyl substituents at δ 3.44 ppm (t, J = 7.8 Hz) and δ 3.14 ppm (q, J = 6.9 Hz) for **14a**, δ 3.51 ppm (t, J = 7.2 Hz) and δ 3.18 (q, J = 7.2 Hz) for **14b** (Figure 2.12), and δ 3.59 ppm (t, J = 7.8 Hz) and δ 3.03 ppm (q, J = 6.9 Hz) for **14c**.

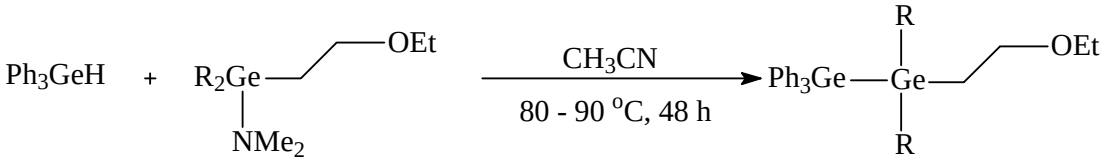

13 a: R = Et,
13 b: R = Bu^n
13 c: R = Ph

14 a: R = Et, 75 %
14 b: R = Bu^n, 76 %
14 c: R = Ph, 92 %

Scheme 2.16: Synthesis of digermane $Ph_3GeGe(R)_2CH_2CH_2OEt$ using amide synthon.

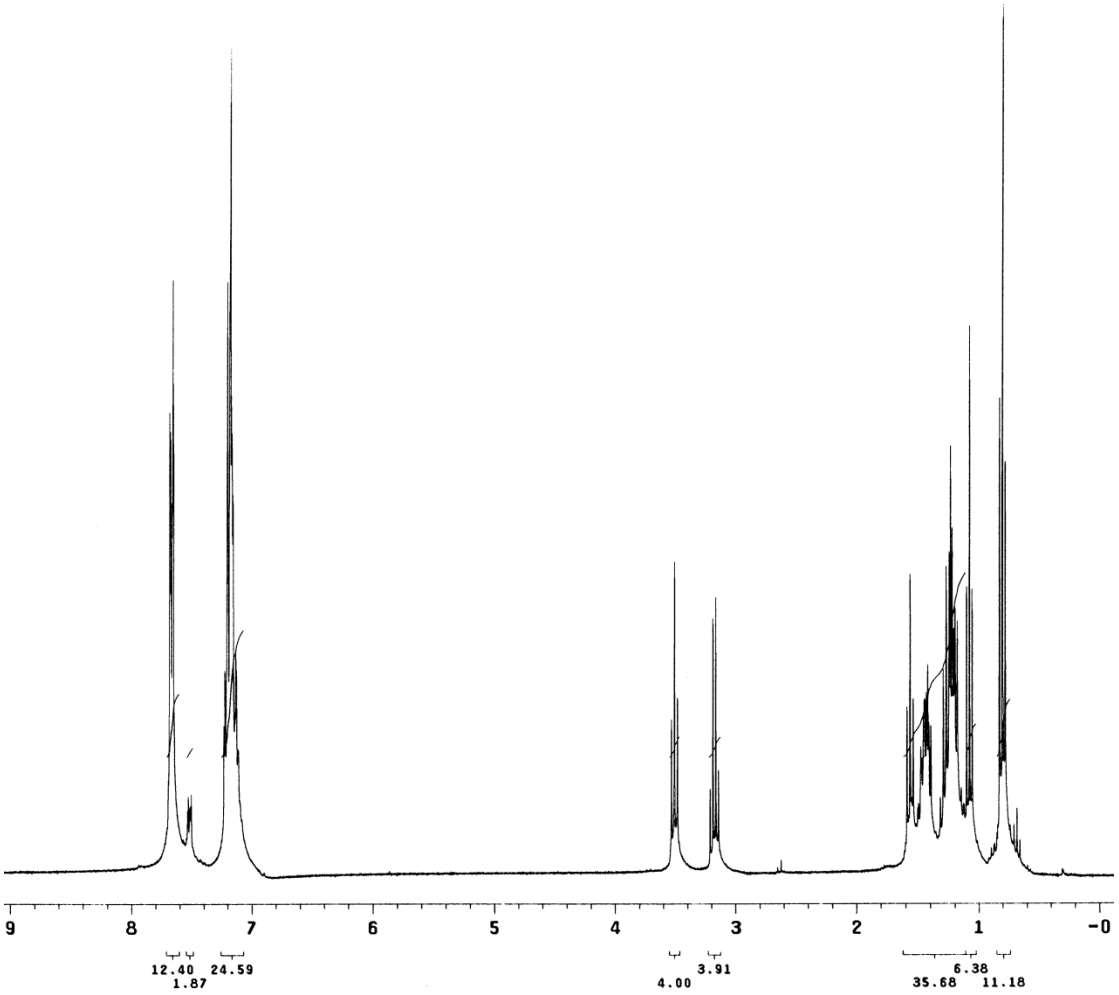

Figure 2.12: ^{1}H-NMR of **14b**

In digermanes **14a-c**, the ethoxyethyl group serves as a protecting group and that can be cleaved using diisobutylaluminium hydride (DIBAL-H) to produce the hydride-terminated digermanes **15a**, **15b**, and **15c** as shown in Scheme 2.17. This method is very similar to that used by Sita for the related tin compounds[20], but in the case of germanium more vigorous conditions were required. Organostananes can be converted to the

corresponding hydrides in 1 h reacting with DIBAL-H at room temperature in hexane[20], but organogermanes required a 12-h reflux time in benzene to obtain the corresponding hydride species. The reaction pathway for the hydride deprotection by DIBAL-H is shown in Scheme 2.18. This reaction proceeds through the formation of a six-membered transition-state. During the reaction, gas evolution was observed indicating the release of $H_2C{=}CH_2$ and the other by-product formed was diisobutylaluminum ethoxide. The pure hydrides were separated from the crude product mixture by passing through a short silica gel column using benzene as the eluent. Although this process removes the aluminum-containing by-product, subsequent distillation was required to remove all other contaminants to obtain analytically pure hydrides. The hydride **16c** could not be obtained from starting digermane **14c** using this method. This is presumed to be due to either steric interactions between the phenyl substituents on the digermane and the isobutyl groups of the DIBAL-H, or due to electronic effects (*vide infra*). The yields of the hydride **15a** and **15b** are moderate. Different hydride transfer reagents have been tried including using $LiBH_4$ and $LiBHEt_3$ to overcome this difficulty and to improve the yield of the reaction compared to the yield obtained using DIBAL-H.[95] Even though various reaction conditions were employed including refluxing in benzene, toluene, or THF for 48 h, none of these reagents served as a better hydride transfer reagent to improve the yields or to convert **14a-c** to **15a-c**.

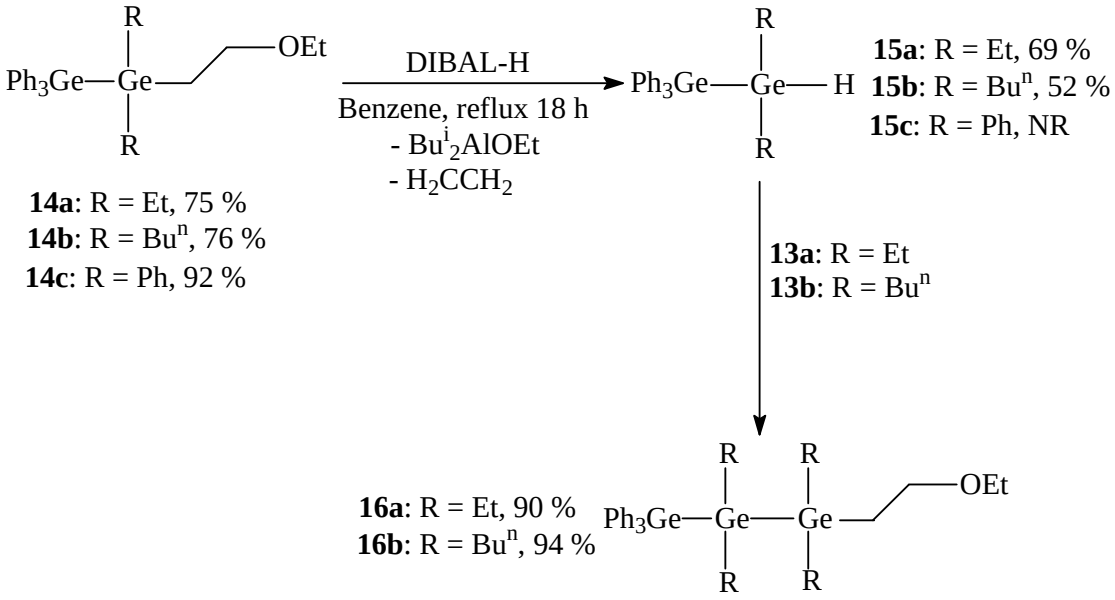

Scheme 2.17: Synthesis of trigermanes from digermane **14a**, **14b**, and **14c**

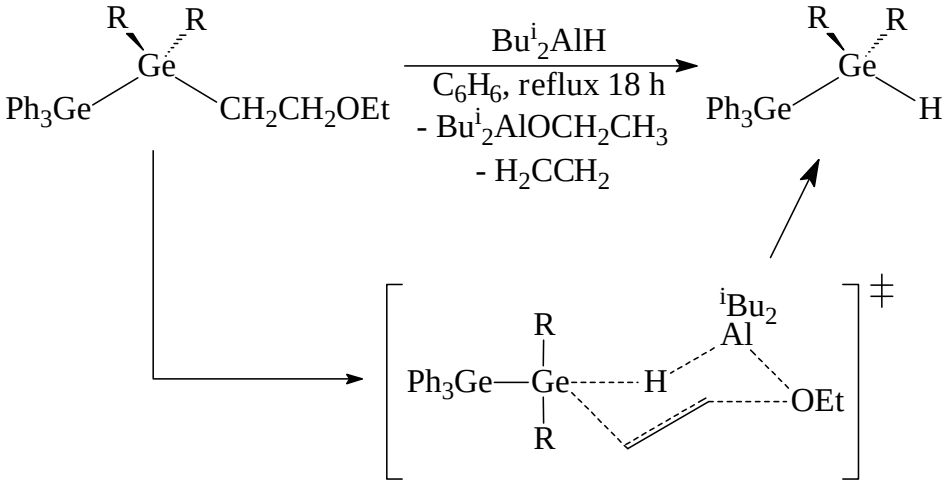

Scheme 2.18: The reaction pathway for the cleavage of ethoxyethyl group by DIBAL-H

The hydride compounds **15a** and **15b** were characterized by infrared spectroscopy and these compounds exhibited characteristic Ge-H stretching bands at 1996 cm^{-1} (**15a**) and 2036 cm^{-1}(**15b**) which are similar to other Ge-H stretching frequencies reported in the literature.[115] The terminal hydride in each of these compounds exhibits a pentet in their ^{1}H NMR spectrum which was observed at δ 4.91 ppm (J = 3.0 Hz) for **17a** and δ 4.40 ppm (J = 3.6 Hz) for **17b**. The absence of the methylene peaks of the ethoxy ethyl group that were observed in the ^{1}H NMR of **14a** and **14b** indicates the complete conversion of these species to corresponding hydride **15a** and **15b**.

By the addition of another equivalent of the amide synthon to the digermane hydride, the germanium chain can be lengthened by one germanium atom at a time. Accordingly, trigermanes **16a** and **16b** were synthesized in high yield [90 % (**16a**) and 94% (**16b**)] by treating hydrides **14a** and **14b** (respectively) with an additional equivalent of the germanium amide **13a** and **13b** as shown in Scheme 2.17. The resulting trigermanes were characterized by ^{1}H NMR spectroscopy and characteristic features for the ethoxyethyl groups appeared at δ 3.28 ppm (t, J = 6.6 Hz) and 3.14 ppm (q, J = 6.9 Hz) for **16a** and 3.51 ppm (t, J = 7.5 Hz) and 3.18 ppm (q, J = 6.9 Hz) for **16b,** which were similar to the chemical shifts observed for **14a** and **14b**.

The product compositions of compounds **14a**, **b** and **16a**,**b** were confirmed by elemental analysis and ^{13}C NMR spectroscopy. In addition, the initial purity of these materials can be assessed by integration of the aromatic versus the alkyl region in the ^{1}H NMR spectra. The alkyl region includes resonances for all protons contained in the alkyl side groups, such as ethyl or butyl, as well as the terminal methyl group and the α-

methylene group of the ethoxyethyl substituent.[95] For compound **14a**, the integrated ratio of the alkyl versus the aromatic regions of the ^{1}H NMR was almost exactly 1:1 as expected. It was 1.67:1 for compound **16a** which is consistent with the predicted. The results obtained for compound **14b** and **16b,** that are the butyl analogs of **14a** and **16a,** closely matched the calculated values (1.57:1, calculated 1.53:1) for **14b** and (2.80:1, calculated 2.73:1) for **16b**.

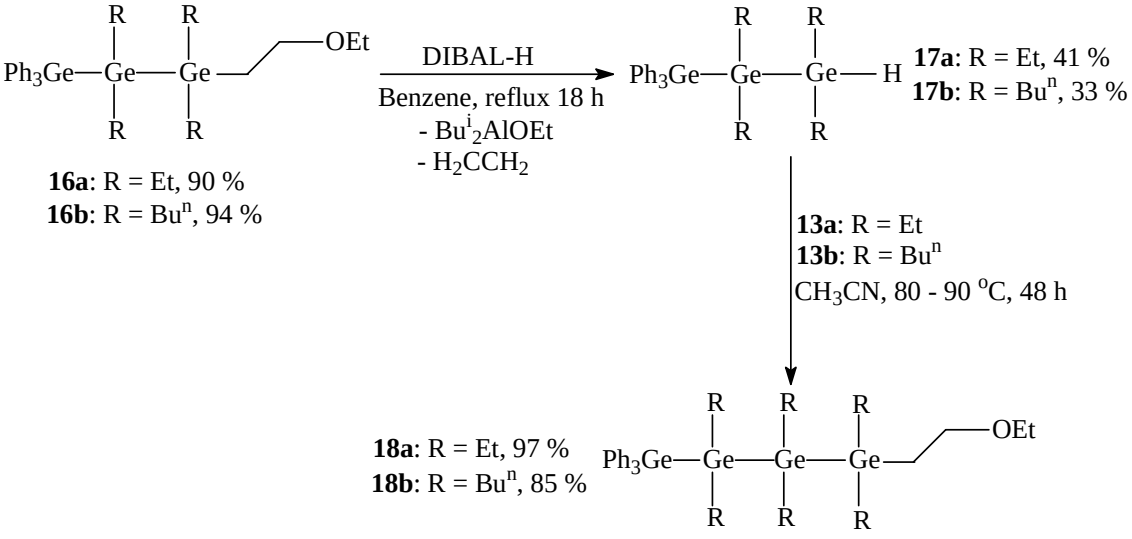

Scheme 2.19: Preparation of tetragermanes **18a** and **18b**

Trigermane **16a** and **16b** can be converted to the corresponding hydride **17a** and **17b** by using DIBAL-H as shown in Scheme **2.19**, but the yields of these compounds were relatively low compared to the yields of **14a** and **14b**. These compounds also exhibit the characteristic Ge-H stretching frequencies at 1996 cm^{-1} for **17a** and at 2000 cm^{-1} for **17b** in their infrared spectra. The Ge-H resonances appeared at δ 4.31 ppm (J = 3.2 Hz) for **17a** and 4.91 ppm (J = 3.0 Hz) for **17b** in their ^{1}H NMR spectra, which

indicated the presence of the terminal hydrogen atom. An extensive purification procedure was required to obtain product **17a** and **17b** in analytically pure form. The crude product was first washed on a short silica gel column followed by vacuum distillation and the resulting material was again washed on a short silica column. This extensive purification is likely the reason for the diminished yields of **17a** and **17b**. Hydrides **17a** and **17b** were reacted with an additional equivalent of the amide synthon **13a** or **13b** to furnish the corresponding tetragermanes **18a** and **18b** in yields of 97 % and 85 % respectively. Compounds **18a** and **18b** were characterized by ^{1}H NMR, ^{13}C NMR and elemental analyses. The integration ratio of the alkyl versus the aromatic on protons in their ^{1}H NMR again was used as an initial estimate of their purity, and were 2.32:1 for **18a** (calculated value 2.33:1) and 3.99:1 for **18b** (calculated value 3.93:1). The resonances for the methylene protons in the ^{1}H NMR spectra were observed at 3.59 ppm (t, J = 7.5 Hz) and 3.30 ppm (q, J = 6.8 Hz) for **18a** and 3.35 ppm (t, J = 7.2 Hz) and 3.19 (q, J = 6.0 Hz) for **18b**.

It has been found that the overall yields of the tri- and tetragermanes can be improved by reacting the intermediate hydride directly with the amide synthon without isolating and purifying the hydride.[95] For example, tetragermane **18b** was obtained in 75 % yield by reacting the material from the DIBAL-H reaction directly with **13b,** and this was a substantial improvement over the 28 % overall yield achieved when the hydride **17b** was isolated and purified. In conclusion, the aluminum byproduct $Bu^{i}_{2}AlOEt$ and excess DIBAL-H that formed in the hydride transfer reaction does not interfere with the hydrogermolysis reaction.

As described above, this method can be used to vary the peripheral substituents according to the amide synthon used. The trigermane **19** was prepared starting from digermane **14b** as shown in Scheme 2.20. First, the digermane **14b** was reacted with DIBAL-H and the intermediate hydride generated was neither isolated nor purified, but rather treated with the germanium amide **13c** in acetonitrile solution to obtain trigermane **19**. The yield of the trigermane **19** was moderate (63 %) and purification required washing on a silica gel column. The identity of **19** was confirmed by ^{1}H NMR, ^{13}C NMR, and elemental analysis. The characteristic features at 3.48 ppm (t, J = 7.5 Hz) and 3.14 ppm (q, J = 6.6 Hz) were observed for the protons of the methylene groups of the ethoxy ethyl group attached to germanium in ^{1}H NMR (Figure 2.13).

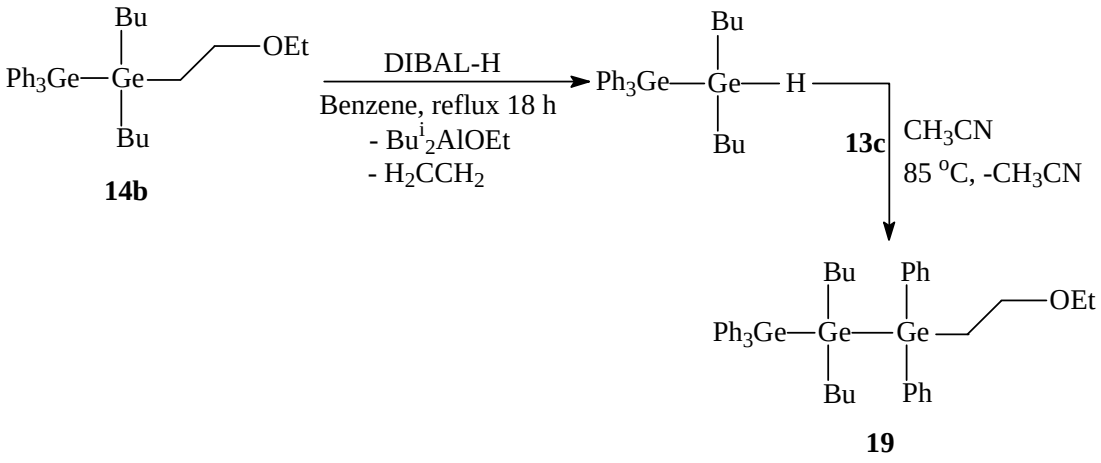

Scheme 2.20: Synthesis of tetragermane **19** from **14b** and **13c**

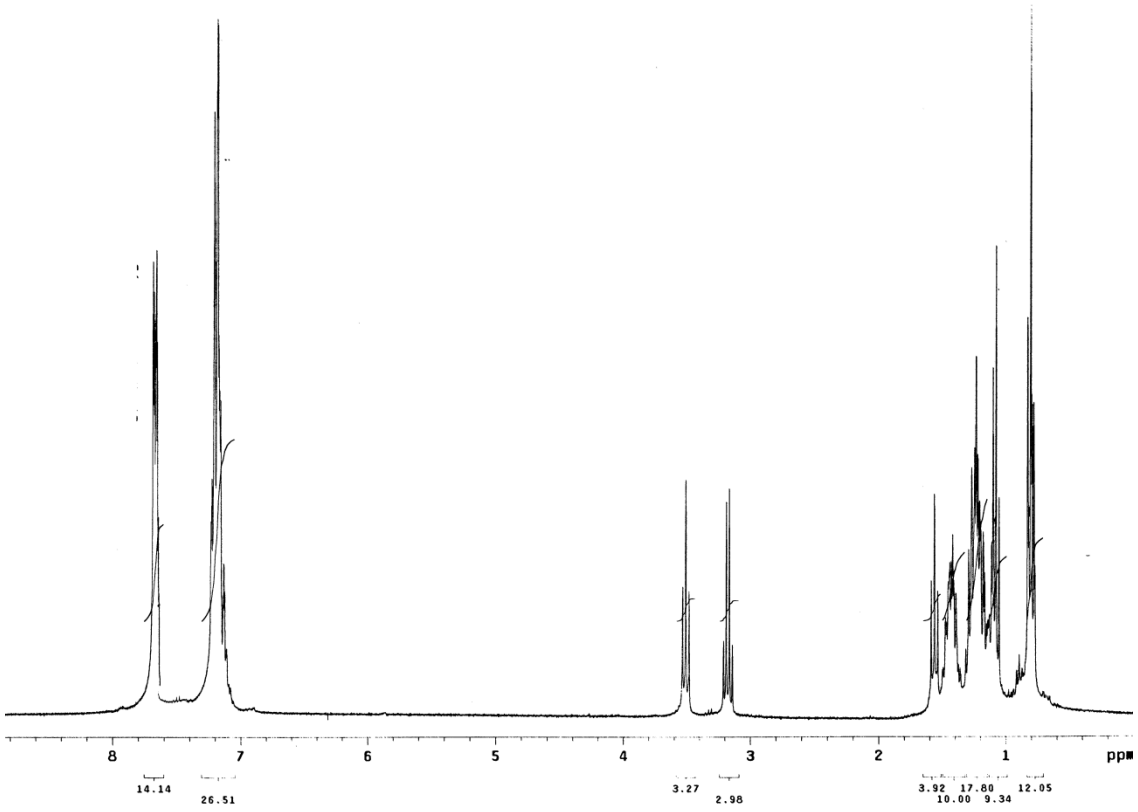

Figure 2.13: ^{1}H-NMR of compound **19**

Compound **19** was subsequently used for the preparation of tetragermanes **20a** and **20b** as shown in Scheme 2.21. The intermediate hydride generated in the reactions of the trigermane with the diisobutylaluminium hydride (DIBAL-H) was again not isolated, but was treated in crude form with the germanium amide in CH_3CN solution in order to provide the desired products **20a** and **20b**. After removing by-products by washing through a silica gel column **20a** and **20b** were obtained in 83 % and 85 % yield respectively. Both tetragermanes were characterized using ^{1}H NMR ,^{13}C NMR and elemental analyses and characteristic resonances for methylene protons of the ethoxy

ethyl substituent appeared at δ 3.42 ppm (t, J = 7.2 Hz) and δ 3.09 ppm (J = 6.8 Hz) for **20a** and **20b** (Figure 2.14). The reaction of $Ph_3GeGePh_2CH_2CH_2OEt$ with DIBAL-H was previously found to be unsuccessful,[95] but the ethoxyethyl group of **19** can readily be cleaved by DIBAL-H to furnish the intermediate trigermane hydride $Ph_3GeGe(Bu_2)Ge(Ph_2)H$, which was then subsequently converted to the tetragermanes **20a** and **20b**. The differences in reactivity of $Ph_3GeGePh_2CH_2CH_2OEt$ and **19** therefore appeared to be electronic rather than steric in nature, since compound **19** contains electron-donating *n*-butyl groups located between the two phenyl-substituted Ge centers.

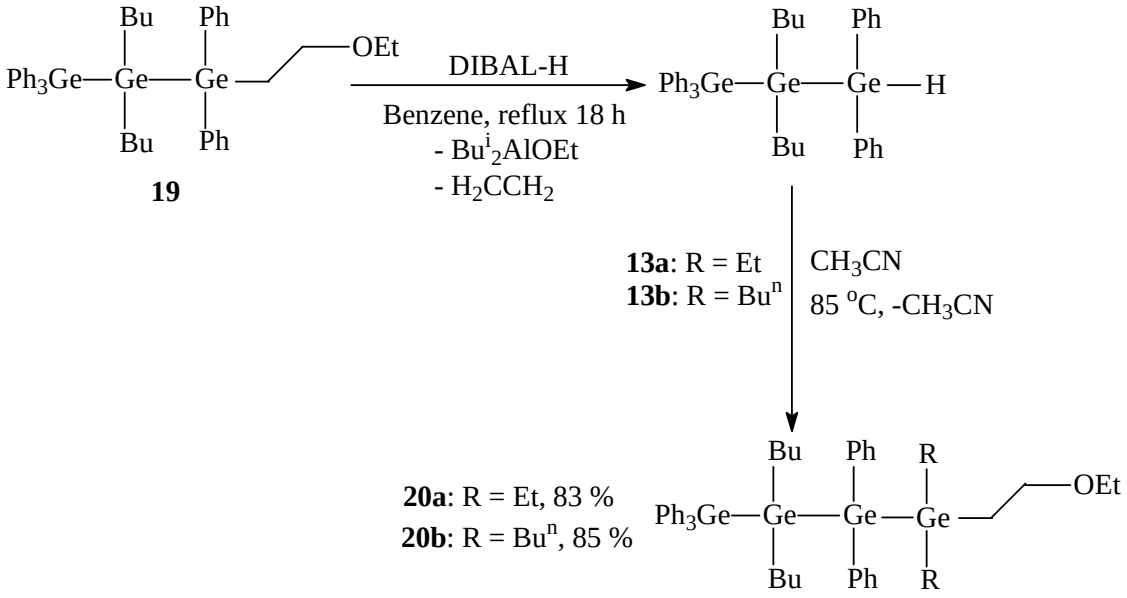

Scheme 2.21: Synthesis of tetragermane **20a** and **20b**

(a)

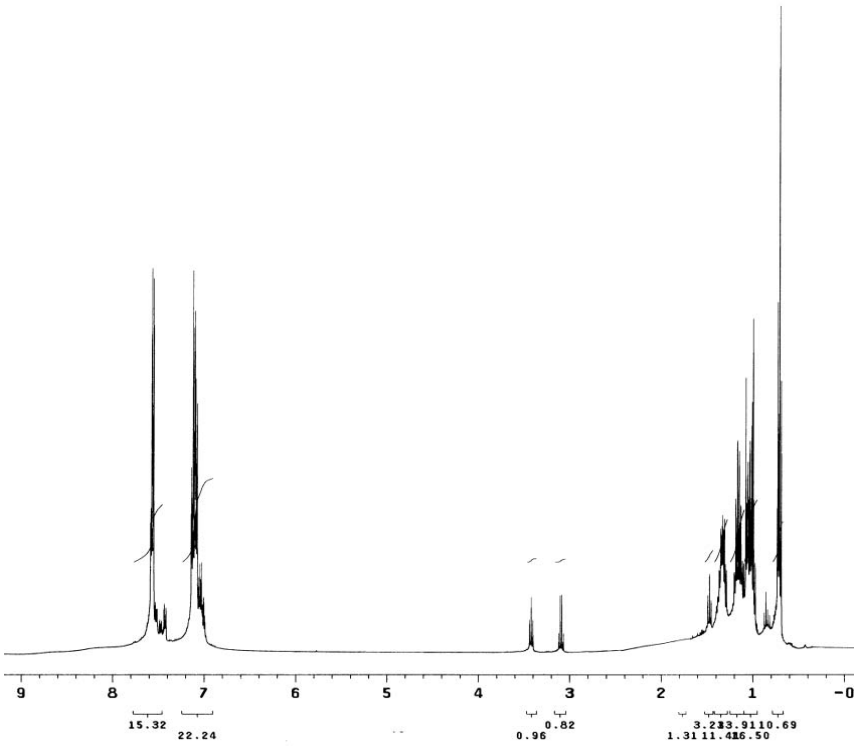

(b)

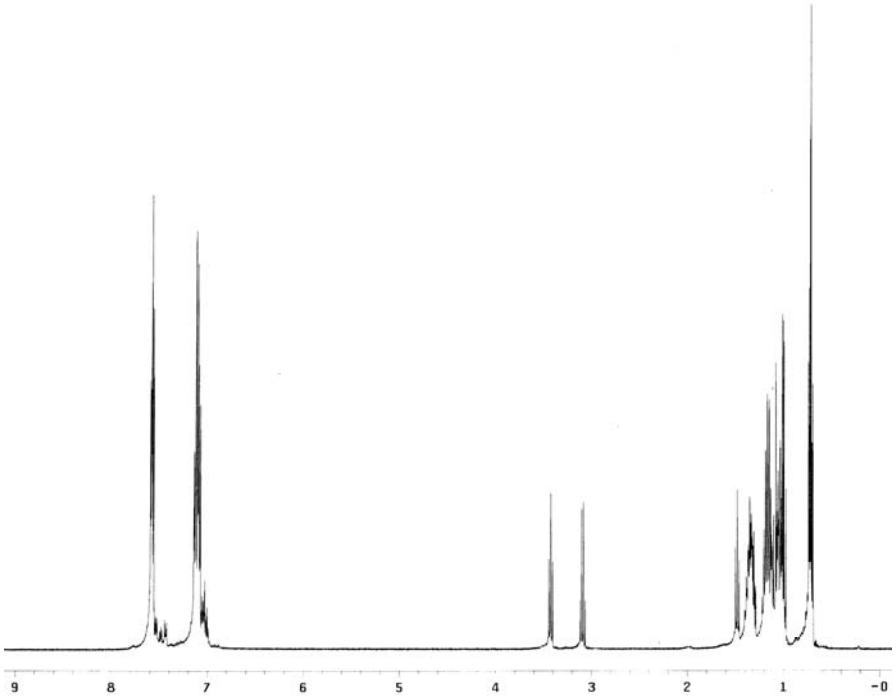

Figure 2.14: ^{1}H-NMR of compound **20a** (a) and compound **20b** (b)

All of the oligogermanes and digermanes discussed above were synthesized using a germanium amide and a germanium hydride which only has only one hydride functional group. The hydrogermolysis reaction also works for germanium hydrides which have two functional hydrogen atoms attached to one Ge center. Three trigermanes **21a**, **21b**, and **21c** were synthesized in excellent yields starting from Ph_2GeH_2 and the three synthons $R_2Ge(NMe_2)CH_2CH_2OEt$ (where R= Et, Bu^n, Ph) as shown in Scheme 2.22. The amide synthon **13a**, **13b**, and **13c** were each reacted with 0.5 equiv of Ph_2GeH_2 in a sealed Schlenk tube using acetonitrile as the solvent over 48 h at 80-85 ºC After Kugelrohr distillation to remove any unreacted Ph_2GeH_2, trigermane **21a**, **21b**, **21c** were obtained in 72 %, 83 %, and 92 % yield, respectively (See Figure 2.15). The ethyl-substituted derivative **21a** is volatile, and care must be taken when distilling the crude product under vacuum to remove excess Ph_2GeH_2.

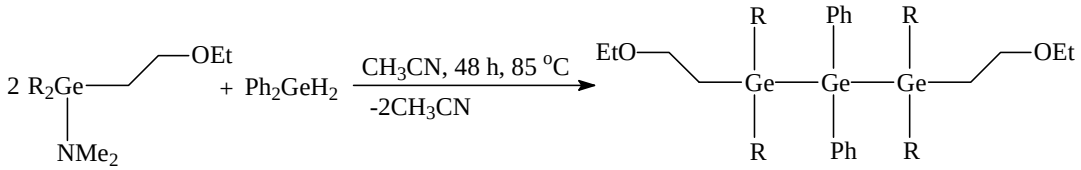

13a : R= Et
13b : R = Bu
13c : R = Ph

21a : R = Et, 72 %
21b : R = Bu, 83 %
21c : R = Ph, 92 %

Scheme 2.22: Synthesis of symmetric trigermanes from Ph_2GeH_2

a)

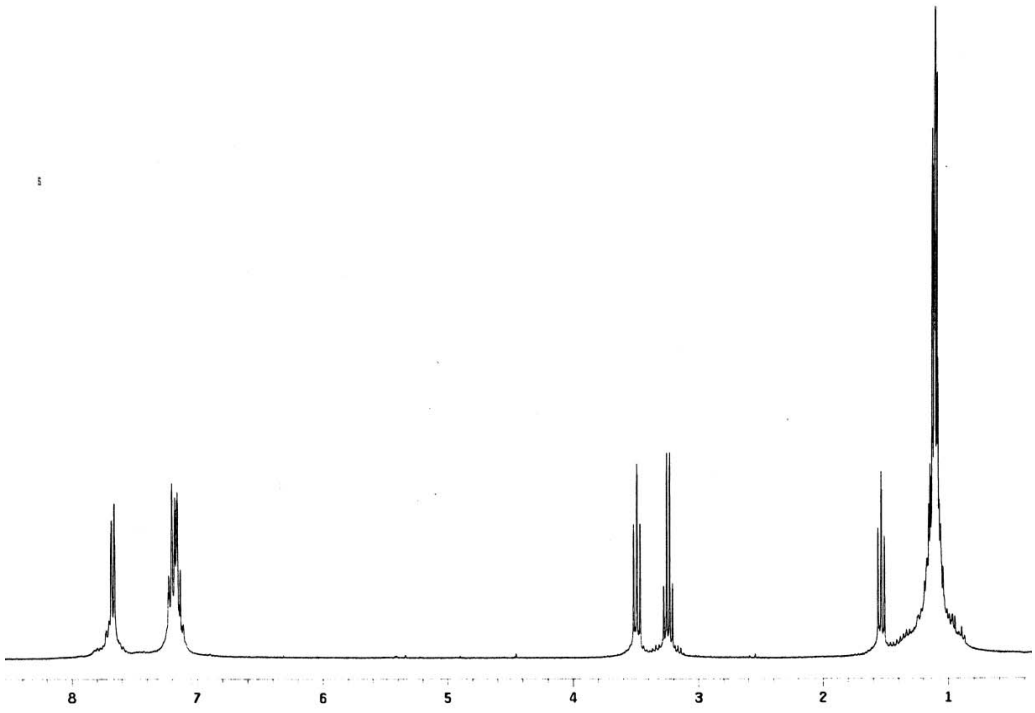

b)

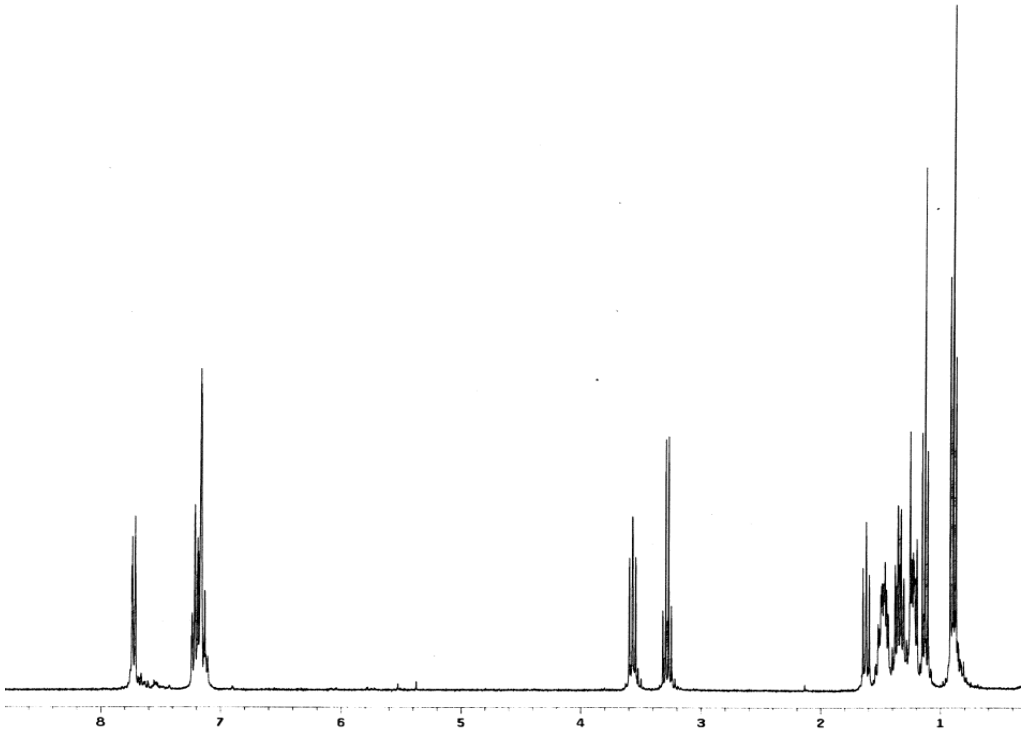

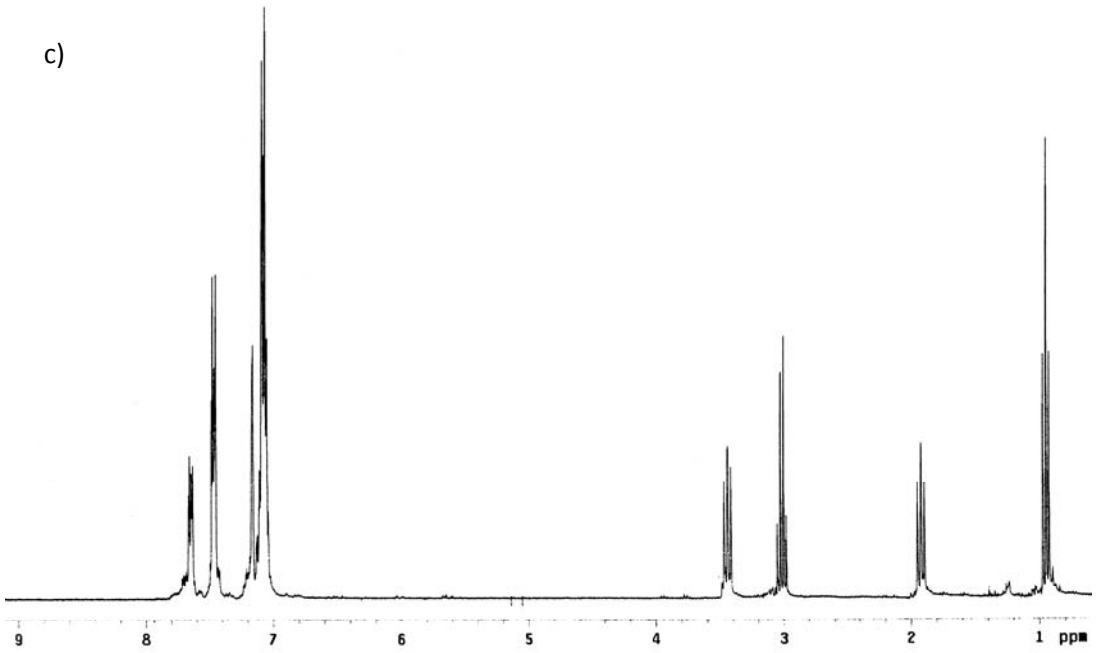

Figure 2.15: ^{1}H NMR of compounds **21a** (a), **21b** (b), **and 21c** (c).

CONCLUSIONS

The hydrogermolysis reaction between a germanium amide and a germanium hydride furnishes a Ge-Ge bond when acetonitrile is used as the solvent. The reaction proceeds in acetonitrile solution via the conversion of germanium amide R_3GeNMe_2 into an α-germyl nitrile R_3GeCH_2CN which is the active species in the Ge-Ge bond forming reaction. The intermediate R_3GeCH_2CN reagents, which can also be directly synthesized from the chlorides R_3GeCl and $LiCH_2CN$, react with the germanium hydride Ph_3GeH to furnish the Ge-Ge bond. The lability of the Ge-C bond in the α-germylated nitriles appears to depend on the steric and/or electronic attributes of the organic substituents attached to germanium, with reactions involving the butyl-substituted derivative proceeding more rapidly than those of the phenyl or isopropyl substituted species.

Treatment of either $Bu^t_3GeCH_2CN$ or $Bu^t_3GeNMe_2$ with Ph_3GeH did not result in isolation of the expected digermane $^tBu_3GeGePh_3$ but rather generated the 3-amidocrotononitrile-containing germane $Bu^t_3Ge[NHC(CH_3)CHCN]$ as a minor product. The nitrogen-containing substituent in this compound results from reaction of $Bu^t_3GeCH_2CN$ with a further equivalent of CH_3CN and the 3-amidocrotonitrile ligand is present exclusively in the (*E*) configuration.

The methods used in this study allow for the stepwise preparation of oligogermanes, where the organic substituents attached to the germanium center can be systematically varied. The use of the hydrogermolysis reaction with the hydride protection and deprotection technique is useful to extend the Ge-Ge backbone by adding one germanium atom at a time. The advantages of this method over previously used synthetic techniques to prepare oligogermanes include improved yields, formation of discrete molecules rather than product mixtures, and direct control over the substituents attached to the germanium backbone.

EXPERIMENTAL:

General considerations: All manipulations were carried out under an inert N_2 atmosphere using a standard Schlenk, syringe, and glovebox techniques.[116] Solvents were purified using Glass Contour solvent purification system. The starting reagents Et_3GeCl, Bu_3GeCl, Me_3GeH, $GeCl_4$, Pr^i_3GeCl, Ph_3GeCl, Ph_3GeH, $PhMe_2GeCl$ and Ph_2GeH_2 were purchased from Gelest and used without further purification and ethyl vinyl ether, AIBN, $LiNMe_2$, CuCN, Bu^sMgCl (2.0 M in Et_2O) DIBAL-H (1.0 M in hexanes) and Bu^tLi (1.7 M in pentane) were purchased from Aldrich. The hydrochlorides R_2GeHCl (R = Et, Bu, Ph) were prepared using the method of Kunai *et al.*[117] The reagent $LiNPr^i_2$ was prepared in situ from $HNPr^i_2$ and Bu^nLi while $LiCH_2CN$ was prepared according to a literature procedure.[101] The starting material $Bu_3{}^tGeCl$ was produced by modifying the reported synthetic method.[118] The compounds Et_3GeNMe_2,[119] Bu_3GeNMe_2,[120] $Bu_3GeGePh_3$,[82,115,121] $Et_3GeGePh_3$[115,121-122] and $Bu_3GeGeMe_3$[82] have been previously reported but are now fully characterized, and their complete characterization is described here. NMR spectral data were recorded using a Varian Gemini 2000 spectrometer operating at 300 MHz (^1H) or 75.5 MHz (^{13}C) and were referenced to resonances for the solvent. Elemental analyses were conducted by Desert Analytics (Tucson, AZ) or Midwest Microlabs (Indianapolis, IN).

Synthesis of Et_3GeNMe_2

A flask was charged with Et_3GeCl (2.302 g, 11.79 mmol) dissolved in benzene (30 mL). To this was added solid $LiNMe_2$ (0.789 g, 15.5 mmol). The resulting suspension

was stirred for 12 h and then filtered through Celite to yield a clear solution. The volatiles were removed *in vacuo* to yield a slightly turbid oil, which was distilled using a Kugelrohr oven (oven temp = 100 °C at 0.11 Torr) to yield Et_3GeNMe_2 (1.371 g, 57 %) as a clear oil. ^{1}H NMR (C_6D_6, 25 °C): δ 2.58 (s, 6H, GeN(C*H*$_3$)$_2$), 1.07 (t, *J* = 8.4 Hz, 9H, GeCH$_2$C*H*$_3$), 0.80 (m, *J* = 8.4 Hz, 6H, GeC*H*$_2$-CH$_3$). ^{13}C NMR (C_6D_6, 25°C): δ 41.4 (-N(*C*H$_3$))$_2$, 9.3 (Ge(CH$_2$*C*H$_3$)$_3$), 4.6 (Ge(*C*H$_2$CH$_3$)$_3$) ppm.

Synthesis of Bu_3GeNMe_2

A flask was charged with 1.583 g (5.666 mmol) of Bu_3GeCl dissolved in benzene (30 mL). To this was added solid $LiNMe_2$ (0.354 g, 6.94 mmol). The resulting suspension was stirred for 12 h and then filtered through Celite to yield a clear solution. The volatiles were removed *in vacuo* to yield a slightly turbid oil, which was distilled using a Kugelrohr oven (oven temp = 105 °C at 0.0.09 Torr) to yield Bu_3GeNMe_2 (1.469 g, 90 %) as a clear oil. ^{1}H NMR (C_6D_6, 25 °C): δ 2.62 (s, 6H, GeN-(C*H*$_3$)$_2$), 1.52-1.30 (m, 12H, GeCH$_2$C*H*$_2$C*H*$_2$CH$_3$), 0.93 (t, *J* = 7.2 Hz, 9H, GeCH$_2$CH$_2$CH$_2$C*H*$_3$), 0.89 (m, 6H, GeC*H*2). ^{13}C NMR (C_6D_6, 25 °C): δ 41.5 (-N(*C*H$_3$)$_2$), 27.4, 26.9, 14.1 (butyl group carbons), 13.2 (-*C*H$_2$CH$_2$CH$_2$CH$_3$) ppm. *Anal*. Calcd. for $C_{14}H_{33}GeN$: C, 58.38; H, 11.55. Found: C, 58.28; H, 11.79.

Synthesis of $Bu_3GeGePh_3$ (1)

A flask was charged with 0.770 g (2.67 mmol) of Bu_3GeNMe_2, and acetonitrile (15 mL). To the resulting solution was added a solution of Ph_3GeH (0.864 g, 2.83 mmol) in acetonitrile (10 mL). The reaction mixture was refluxed under N_2 for 48 h, then allowed to cool, and the volatiles were removed in *vacuo*. Kugelrohr oven distillation (oven temp = 180 °C at 0.10 Torr) of the crude material to remove excess Ph_3GeH yielded **1** (1.21 g 83 %) as a white solid. ^{1}H NMR (C_6D_6, 25 °C): δ 7.72-7.64 (m, 6H, *meta*-H), 7.24-7.16 (m, 9H, *ortho*-H and *para*-H), 1.52-1.39 (m, 6H, $GeCH_2$), 1.27 (sextet, J = 7.8 Hz, 6H, $GeCH_2CH_2CH_2CH_3$), 1.21-1.15 (m, 6H, $GeCH_2CH_2CH_2CH_3$), 0.81 (t, J = 6.9 Hz, 9H, $GeCH_2CH_2CH_2CH_3$). ^{13}C NMR (C_6D_6, 25 °C): δ 139.7, 135.7, 128.7, 128.6 (aromatic carbons), 28.8, 26.8, 14.5, 13.8 (butyl group carbons) ppm. *Anal*. Calcd. for $C_{30}H_{42}Ge_2$: C, 65.77; H, 7.73. Found: C, 65.74; H, 7.80.

Synthesis of $Et_3GeGePh_3$(2)

To a solution of Et_3GeNMe_2 (0.471 g, 2.00 mmol) in acetonitrile (15 mL) in a Schlenk tube was added Ph_3GeH (0.637 g, 2.10 mmol) in acetonitrile (15 mL). The tube was sealed with a Teflon plug, and the reaction was heated at 85 °C for 48 h. The solution was transferred to a Schlenk flask, and the volatiles were removed *in vacuo*. The crude product was distilled in a Kugelrohr oven (oven temp = 100 °C, P = 0.05 Torr) to remove excess Ph_3GeH to yield **2** as a white solid (0.247 g, 84 %). ^{1}H NMR (C_6D_6, 25 °C): δ 7.64-7.61 (m, 6H, *meta*-H), 7.23-7.16 (m, 9H, *ortho*-H and *para*-H), 1.03 (m, 15H, $Ge(CH_2CH_3)_3$) ppm. ^{13}C NMR (C_6D_6, 25 °C): δ 139.2, 135.6, 128.7, 128.6 (aromatic

carbons), 10.2, 6.1 (ethyl group carbons) ppm. *Anal*. Calcd. for $C_{24}H_{30}Ge_2$: C, 62.16; H, 6.52. Found: C, 61.96; H, 6.61.

Synthesis of $Bu_3GeGeMe_3$ (3)

A solution of Me_3GeH (0.113 g, 0.952 mmol) in acetonitrile (10 mL) was added to a solution of Bu_3GeNMe_2 (0.226 g, 0.785 mmol) in acetonitrile (10 mL) in a Schlenk tube. The tube was sealed with a Teflon plug, and the reaction mixture was heated to 85 °C for 48 h. The solution was transferred to a Schlenk flask, and the volatiles were removed in *vacuo*. The crude product was distilled in a Kugelrohr oven (oven temp = 85 °C, P = 0.05 Torr) to remove excess starting material to yield **3** as a colorless oil (0.244 g, 86 %). ^{1}H NMR (C_6D_6, 25 °C): δ 1.58-1.51 (m, 6H, $GeCH_2CH_2CH_2CH_3$), 1.42 (pent, J = 5.7 Hz, 6H, $GeCH_2CH_2CH_2CH_3$), 0.96 (m, 15H, $GeCH_2CH_2CH_2CH_3$ and $GeCH_2CH_2CH_2CH_3$), 0.26 (s, 9H, $GeCH_3$) ppm. ^{13}C NMR (C_6D_6, 25 °C): δ 27.0, 26.8, 18.2, 14.0 (butyl groups), 1.4 ($GeCH_3$) ppm. *Anal*. Calcd. for $C_{15}H_{36}Ge_2$: C, 49.81; H, 10.03. Found: C, 50.11; H, 10.08.

Synthesis of Bu_3GeCH_2CN (2a)

To a solution of $HN(Pr^i)_2$ (0.70 mL, 5.0 mmol) in THF (20 mL) was added a 2.5 M solution of Bu^nLi in hexane (2.04 mL, 5.1 mmol) at -78 °C. The solution was stirred for 30 min, and acetonitrile (0.27 mL, 5.2 mmol) was added. The resulting suspension was placed in a -30 °C bath, and a solution of Bu_3GeCl (1.391 g, 4.97 mmol) in THF (15

mL) was added at this temperature. The reaction mixture was allowed to come to room temperature and was stirred for 12 h. The volatiles were removed *in vacuo* to yield a white solid, which was dissolved in hexane (15 mL) and filtered through Celite. Removal of the volatiles yielded Bu_3GeCH_2CN (**1a**), 1.19 g (84 %). ^1H NMR (C_6D_6, 25 °C): δ 1.82-1.49 (m, 20H, $Ge(CH_2CH_2CH_2CH_3)_3$ and $GeCH_2CN$), 1.08 (t, J = 7.2 Hz, 9H, $Ge(CH_2CH_2CH_2CH_3)_3$) ppm. ^{13}C NMR (C_6D_6, 25 °C): δ 118.6 ($-CH_2CN$), 28.4, 27.5, 25.7, (butyl group carbons), 16.0 ($GeCH_2CN$), 14.3 ($-CH_2CH_2CH_2CH_3$) ppm.

Synthesis of $Ph_3GeGeBu_3$ (1) from Bu_3GeCH_2CN (2a)

A Schlenk tube was charged with Bu_3GeCH_2CN (0.253 g, 0.890 mmol) in acetonitrile (10 mL).To this was added a solution of Ph_3GeH (0.270 g, 0.885 mmol) in acetonitrile (10 mL). The tube was sealed with a Teflon plug and was heated at 90 °C for 50 min, and the solution was transferred to a Schlenk flask. The volatiles were removed *in vacuo*, yielding 0.434 g (89 %) of **1**. The identity of **1** was confirmed by NMR (^1H and ^{13}C spectroscopy.

Synthesis of Bu^t_3GeCl

To a suspension of CuCN (11.5 g, 0.129 mol) in THF (75.5 mL) cooled to -25 °C in a *meta*-dichlorobenzene/liquid N_2 bath was added a solution of 1.7 M Bu^tLi in pentane (75.8 mL, 0.129 mol) drop wise over 1h. The resulting suspension was cooled to - 40 °C using a CH_3CN/liquid N_2 bath and neat $GeCl_4$ (9.25 g, 0.043 mmol) was slowly added.

The THF was removed *in vacuo* and exchanged for 65 mL of a 1:1 mixture of hexane and benzene. The insoluble salts were removed by filtration and the solvent was distilled off under N_2. The resulting oil was vacuum distilled at 0.010 torr and 150 °C to yield Bu^{t}GeCl (4.311 g, 36 %) as a colorless oil. ^{1}H NMR (C_6D_6, 25 °C): δ 1.11 (s, 27 H, -C(CH_3)$_3$) ppm. ^{13}C NMR (C_6D_6, 25 °C): δ 29.8 (-*C*(CH_3)$_3$), 31.3 (-C(*C*H_3)$_3$) ppm.

Synthesis of Ph_3GeCH_2CN (7a)

A solution of $LiCH_2CN$ was prepared from CH_3CN (0.10 mL, 1.91 mmol) and LiNPr$^i_2$ (0.212 g, 1.98 mmol) and stirred at -78 °C for 30 min. To this was added a solution of Ph_3GeCl (0.666 g, 1.96 mmol) in THF (20 mL) at -78 °C. The reaction mixture was warmed to room temperature and stirred for 12 h. The volatiles were removed *in vacuo* to yield a white semisolid which was suspended in hexane and filtered through Celite. Removal of the solvent furnished Ph_3GeCH_2CN (0.472 g, 70 %) as a white solid. ^{1}H NMR (C_6D_6, 25 °C): δ 7.43 (d, 6H, *o*-C_6H_5), 7.08-7.00 (m, 9H, aromatics), 1.98 (s, 2H, -C*H*$_2$CN) ppm. ^{13}C NMR (C_6D_6, 25 °C): δ 132.5, 128.4, 126.9, 125.1, 124.2, 20.2 ppm.

Synthesis of Pr$^i_3$GeCH$_2$CN (4a)

The same procedure for the preparation of Ph_3GeCH_2CN was used for Pr$^i_3$GeCH$_2$CN starting with Pr$^i_3$GeCl (0.422 g, 1.78 mmol), CH_3CN (95 µL, 1.82 mmol) and LiNPr$^i_2$ (0.195 g, 1.82 mmol) and 4a was isolated as a colorless oil. Yield = 0.358 g,

83 %. ^{1}H NMR (C_6D_6, 25 °C): δ 1.62 (sept, *J* = 7.2 Hz, 3H, $(CH_3)_2CH$-), 1.43 (s, 2H, -CH_2CN), 1.18 (d, *J* = 7.2, 18H, $(CH_3)_2$CH-) ppm. ^{13}C NMR (C_6D_6, 25 °C): δ 118.4 (-CH_2CN), 24.6 (-CH_2CN), 19.3 ($(CH_3)_2$CH-), 14.8 ($(CH_3)_2$CH-) ppm.

Synthesis of $Bu^t_3GeCH_2CN$ (8a)

The same procedure for the preparation of Ph_3GeCH_2CN was used for $Bu^t_3GeCH_2CN$ starting with Bu^t_3GeCl (0.225 g, 0.805 mmol), CH_3CN (44 µL, 0.84 mmol) and $LiNPr^i_2$ (0.090 g, 0.84 mmol) and $Bu^t_3GeCH_2CN$ was isolated as a colorless oil. Yield = 0.147 g, 64 %. ^{1}H NMR (C_6D_6, 25 °C): δ 1.59 (s, 2H, -CH_2CN), 1.06 (s, 27H, -$C(CH_3)_3$) ppm. ^{13}C NMR (C_6D_6, 25 °C): δ 123.2 (-CH_2CN), 31.4 (-$C(CH_3)_3$), 30.2 (-$C(CH_3)_3$), 28.3 (-CH_2CN) ppm.

Preparation of $Ph_3GeGePh_3$ (7) from Ph_3GeCH_2CN (7a)

To a solution of Ph_3GeCH_2CN (0.315 g, 0.916 mmol) in acetonitrile (20 mL) in a Schlenk tube was added a solution of Ph_3GeH (0.282 g, 0.925 mmol) in acetonitrile (10 mL). The tube was sealed and the reaction mixture was heated at 85 °C for 48 h. The volatiles were removed *in vacuo* and the product was distilled in a Kugelrohr oven (180 °C, 0.05 torr) to remove excess Ph_3GeH. Yield = 0.488 g, 88 %. The identity of **7** was confirmed by NMR (^{1}H and ^{13}C spectroscopy. *Anal*. Calcd for $C_{36}H_{30}Ge_2$: C, 71.14; H, 4.97. Found: C, 71.02; H, 5.04.

Preparation of $Ph_3GeGePr^i_3$ (4) from $Pr^i_3GeCH_2CN$ (4a)

To a solution of $Pr^i_3GeCH_2CN$ (0.255 g, 1.05 mmol) in acetonitrile (20 mL) in a Schlenk tube was added a solution of Ph_3GeH (0.332 g, 1.09 mmol) in acetonitrile (10 mL). The tube was sealed and the reaction mixture was heated at 85 °C for 48 h. The volatiles were removed *in vacuo* and the product was distilled in a Kugelrohr oven (180 °C, 0.05 torr) to remove excess Ph_3GeH. Yield = 0.461 g, 87 %. The identity of **4** was confirmed by NMR (^1H and ^{13}C) spectroscopy.

Preparation of $Pr^i_3GeNMe_2$

To a solution of Pr^i_3GeCl (1.00 g, 4.21 mmol) in benzene (15 mL) was added a suspension of $LiNMe_2$ (0.225 g, 4.42 mmol) in benzene (20 mL). The resulting suspension was stirred for 24 h and then filtered through Celite. The volatiles were removed from the filtrate *in vacuo* to yield $Pr^i_3GeNMe_2$ as a colorless oil. ^1H NMR (C_6D_6, 25 °C): δ 2.67 (s, 6H, -N(CH_3)$_2$), 1.42 (sept, J = 7.2 Hz, 3H, CH_3CHCH_3), 1.10 (d, J = 7.2 Hz,18H, CH_3CHCH_3) ppm. ^{13}C NMR (C_6D_6, 25 °C): δ 42.2 (-N(CH_3)$_2$, 18.8 (CH_3CHCH_3), 15.7 (CH_3CHCH_3) ppm. *Anal*. Calcd for $C_{11}H_{27}GeN$: C, 53.72; H, 11.07. Found: C, 53.81; H, 11.11.

Preparation of $Bu^t_3GeNMe_2$

To a solution of Bu^t_3GeCl (0.500 g, 1.79 mmol) in THF (20 mL) was added a solution of $LiNMe_2$ (0.091 g, 1.79 mmol) in THF (10 mL). The reaction mixture was refluxed for 18 h and the solvent was removed *in vacuo*. The resulting solid was dissolved in benzene, filtered through Celite, and the volatiles were removed *in vacuo* to yield a pale yellow semisolid. The crude product was distilled in a Kugelrohr oven (125 °C, 0.07 torr) to yield $Bu^t_3GeNMe_2$ (0.315 g, 61 %) as a colorless oil. ^{1}H NMR (C_6D_6, 25 °C): δ 2.71 (s, 6H, -N(CH_3)$_2$), 1.19 (s, 27H, -C(CH_3)$_3$) ppm. ^{1}H NMR (CD_3CN, 25 °C): δ 2.63 (s, 6H, -N(CH_3)$_2$), 1.27 (s, 27H, -C(CH_3)$_3$) ppm. ^{13}C NMR (C_6D_6, 25 °C): δ 41.9 (-N(*C*H_3)$_2$), 32.8 (-*C*(CH_3)$_3$), 29.9 (-C(*C*H_3)$_3$) ppm. ^{13}C NMR (CD_3CN, 25 °C): δ 42.2 (-N(*C*H_3)$_2$), 31.6 (-*C*(CH_3)$_3$), 30.2 (-C(*C*H_3)$_3$) ppm. *Anal*. Calcd for $C_{14}H_{33}GeN$: C, 58.38; H, 11.55. Found: C, 58.03; H, 11.67.

Preparation of $Pr^i_3GeGePh_3$ (4) from $Pr^i_3GeNMe_2$

To a solution of $Pr^i_3GeNMe_2$ (0.778 g, 3.16 mmol) in acetonitrile (20 mL) in a Schlenk tube was added to a solution of Ph_3GeH (1.239 g, 4.062 mmol) in acetonitrile (10 mL). The tube was sealed and the reaction mixture was heated at 85 °C for 48 h. The volatiles were removed *in vacuo* and the crude product was distilled in a Kugelrohr oven (180 °C, 0.05 torr) to remove excess Ph_3GeH which furnished **4** (1.451 g, 91 %) as a colorless solid. ^{1}H NMR (C_6D_6, 25 °C): δ 7.72-7.68 (m, 6H, *meta*-H), 7.20-7.15 (m, 9H, *para*- and *ortho*-H), 1.67 (sept, *J* = 7.5 Hz, 3H, CH_3C*H*CH_3), 1.18 (d, *J* = 7.5 Hz, 18H, C*H*$_3$CHC*H*$_3$) ppm. ^{13}C NMR (C_6D_6, 25 °C): δ 139.8 (*ipso*-C), 135.9 (*ortho*-C), 128.6

(*meta*-C), 128.5 (*para*-C), 21.3 (CH$_3$CHCH$_3$), 16.8 (CH$_3$$CHCH_3$) ppm. UV/visible λ_{max} 234 nm (br, ε 3.82 × 10^4 cm^{-1} M^{-1}). *Anal*. Calcd for $C_{27}H_{36}Ge_2$: C, 64.12; H, 7.17. Found C, 63.88; H,6.97.

Preparation of Bu$^t_3$Ge[NHC(CH$_3$)CHCN] (11)

To a solution of Bu$^t_3$GeNMe$_2$ (0.281 g, 0.976 mmol) in CH$_3$CN (5 mL) was added a solution of Ph$_3$GeH (0.299 g, 0.981 mmol) in CH$_3$CN (10 mL). The reaction mixture was sealed in a Schlenk tube and was heated at 85 °C for 72 h. The solvent was removed *in vacuo* to yield a yellow oil. The crude material was distilled in a Kugelrohr oven (120 °C, 0.050 torr) resulting in the collection of a clear oil which was isolated (0.147 g) and identified to be pure Bu$^t_3$GeN(CH$_3$)$_2$. A new receiving flask was attached to the apparatus and distillation was continued (180 °C, 0.05 torr) resulting in the isolation of a yellow oil (0.338 g) which consisted of a mixture of **9** , Bu$^t_3$GeNMe$_2$, and Ph$_3$GeH as shown by ^{1}H NMR spectroscopy. Recrystallization of the product from hexane (~3 mL) at -35 °C afforded **9** as colorless crystals (0.020 g, 6.3 %). ^{1}H NMR (C$_6$D$_6$, 25 °C): δ 4.33 (s, 1H, C=CHCN), 3.18 (br, s, 1H, Ge-NH), 1.94 (s, 3H, H_3C-C=C), 1.08 (s, 28H, -C(CH_3)$_3$) ppm. ^{1}H NMR (CD$_3$CN, 25 °C): δ 4.09 (s, 1H, C=CHCN), 3.84 (br, s, 1H, GeNH), 2.14 (s, 3H, H_3C-C=C), 1.25 (s, 28H, -C(CH_3)$_3$), ppm. ^{13}C NMR (C$_6$D$_6$, 25 °C): δ 135.8 (-CN), 130.2 (N-C=C), 129.4 (N-C=C), 66.0 (C=C-CH$_3$), 31.5 (C(CH$_3$)$_3$) 30.7 (-C(CH$_3$)$_3$) ppm. *Anal*. Calcd for $C_{16}H_{32}GeN_2$: C, 59.13; H, 9.92. Found: C, 58.92; H, 9.97.

NMR tube reaction of $Bu^t_3GeNMe_2$ with Ph_3GeH

A solution of $Bu^t_3GeNMe_2$ (0.025 g, 0.087 mmol) in CD_3CN (0.5 mL) was prepared in a Kontes screw-cap NMR tube. The sample was heated at 85 °C for 6 days during which time the ^{13}C NMR spectrum was recorded at regular intervals. After this time, Ph_3GeH (0.027 g, 0.088 mmol) was added to the tube and the sample was heated at 85 °C for 24 h. The ^{13}C NMR spectrum was recorded and the sample was heated at 85 °C for a further 72 h.

Synthesis of Bu^s_3GeCl

A solution of Bu^s_3MgCl (44.0 mL, 2.0 M in Et_2O, 88.0 mmol) was added to a solution of $GeCl_4$ (6.25 g, 29.1 mmol) in Et_2O (140 mL) at 0 °C over 30 min. the reaction mixture was stirred at 0 °C for 1 h, and the volatiles were removed *in vacuo*. The resulting material was dissolved in hexane (100 mL) and treated with 50 mL of 1.0 M HCl. The organic layer was separated and the aqueous layer was extracted with hexane (3 × 15 mL). The combined organic layer and extracts were dried over anhydrous $MgSO_4$ and filtered, and the volatiles were removed *in vacuo* to yield a colorless oil. ^1H NMR (C_6D_6, 25 °C): δ 1.77-1.66 (m, 3H, $CH_3CHCH_2CH_3$), 1.38-1.31 (m, 6H, $CH_3CHCH_2CH_3$), 1.12-1.07 (m, 9H, $CH_3CHCH_2CH_3$), 0.89 (t, J = 9.6 Hz, 9H,$CH_3CHCH_2CH_3$) ppm. ^{13}C NMR (C_6D_6, 25 °C): δ 27.00, 26.97, 26.94 ($CH_3CHCH_2CH_3$), 25.95, 25.32 ($CH_3CHCH_2CH_3$), 15.01, 14.96 ($CH_3CHCH_2CH_3$), 13.4 ($CH_3CHCH_2CH_3$) ppm. Anal. Calcd for $C_{12}H_{27}ClGe$: C, 51.59; H, 9.74. Found: C, 51.69; H, 9.50.

Preparation of $Bu^s_3GeNMe_2$

A flask was charged with 0.274 g (0.981 mmol) of Bu^s_3GeCl dissolved in benzene (10 mL). To this was added $LiNMe_2$ (0.057 g, 1.12 mmol) in benzene (10 mL).The resulting suspension was stirred 36 h and then filtered through Celite to yield a clear solution. The volatiles were removed *in vacuo* to yield $Bu^s_3GeNMe_2$ (0.221 g, 78 %) as a slightly turbid colorless oil. ^{1}H NMR (C_6D_6, 25 °C): δ 2.67, 2.66, 2.65 (s, 6H, -N(CH_3)$_2$), 1.78-1.70 (m, 3H, $CH_3CHCH_2CH_3$), 1.36-1.30 (m, 6H, $CH_3CHCH_2CH_3$), 1.16-1.11 (m, 9H, $CH_3CHCH_2CH_3$), 0.89 (t, *J* = 7.2 Hz, 9H, $CH_2CHCH_2CH_3$), ppm. ^{13}C NMR (C_6D_6, 25 °C): δ 42.44, 42.11 (-N(CH_3)$_2$), 27.03, 26.98 ($CH_3CHCH_2CH_3$), 25.93 ($CH_3CHCH_2CH_3$), 15.04, 14.86 ($CH_3CHCH_2CH_3$), 13.61, 13.44, 13.27 ($CH_3CHCH_2CH_3$) ppm. *Anal*. Calcd for $C_{14}H_{33}GeN$: C, 58.38; H,11.55. Found: C, 58.32; H, 11.24.

Preparation of $PhMe_2GeNMe_2$

To a solution of $PhMe_2GeCl$ (1.000 g, 4.646 mmol) in Et_2O (15 mL) was added a solution of $LiNMe_2$ (0.249 g, 4.88 mmol) in Et_2O (10 mL). The reaction mixture was stirred for 18 h, and the ether was removed to yield a yellow oil, which was dissolved in hexane and filtered through Celite. The volatiles were removed from the filtrate to yield $PhMe_2GeNMe_2$ (0.775 g, 75 %) as a colorless oil. ^{1}H NMR (C_6D_6, 25 °C): δ 7.61 (d, *J* = 6.4 Hz, 2H, *m*-H), 7.37-7.32 (m, 3H, *o*-H and *p*-H), 2.64 (s, 6H, -N(CH_3)$_2$), 0.49 (s, 6H, -CH_3) ppm. ^{13}C NMR (C_6D_6, 25 °C): δ 133.79 (*ipso*-C), 129.20 (*ortho*-C), 128.40 (*meta*-C), 128.08 (*para*-C), 40.94 (-N(CH_3)$_2$), 4.33 (-CH_3) ppm. Anal. Calcd for $C_{10}H_{17}GeN$: C, 53.66; H, 7.65. Found: C, 53.36; H, 7.41.

Preparation of $Bu^{s}_{3}GeGePh_3$ (5)

To a solution of $Bu^{s}_{3}GeNMe_2$ (0.201 g, 0.698 mmol) in acetonitrile (5 mL) was added a solution of Ph_3GeH (0.220 g, 0.721 mmol) in acetonitrile (10 mL). The reaction mixture was sealed in a Schlenk tube and heated at 90 °C for 72 h. The volatiles were removed *in vacuo* to yield a viscous yellow oil, which was Kugelrohr distilled (135 °C, 0.05 Torr) to yield $Bu^{s}_{3}GeGePh_3$ (0.308 g, 81 %) as a colorless oil. ^{1}H NMR (C_6D_6, 25 °C): δ 7.68 (t, *J* = 7.2 Hz, 3H, *para*-H), 7.63 (d, *J* = 7.2 Hz, 6H, *ortho*-H), 7.13-7.08 (m, 6H, *meta*-H), 1.78-1.73 (m, 3H, $CH_3CHCH_2CH_3$), 1.46-1.23 (m, 6H, $CH_3CHCH_2CH_3$), 1.13-1.04 (m, 9H, $CH_3CHCH_2CH_3$), 0.77 (t, *J* = 7.6 Hz, 9H, $CH_3CHCH_2CH_3$) ppm. ^{13}C NMR (C_6D_6, 25 °C): δ 138.9 (*ipso*-C), 135.33 (*ortho*-C), 128.83 (*meta*-C), 128.44 (*para*-C), 28.80, 28.64 ($CH_3CHCH_2CH_3$), 26.83 ($CH_3CHCH_2CH_3$), 14.49, 14.46 ($CH_3CHCH_2CH_3$), 13.78 ($CH_3CHCH_2CH_3$) ppm. *Anal*. Calcd for $C_{30}H_{42}Ge_2$: C, 65.77; H, 7.73. Found: C, 65.72; H, 7.88.

Synthesis of $PhMe_2GeGePh_3$ (6)

To a solution of $PhMe_2GeNMe_2$ (0.220 g, 0.983 mmol) in acetonitrile (10 mL) was added a solution of Ph_3GeH (0.302 g, 0.990 mmol) in acetonitrile (10 mL). The reaction mixture was stirred at 85 °C for 96 h, and the volatiles were removed *in vacuo* to yield a yellow viscous oil. The crude product was vacuum distilled (120 °C, 0.05 Torr) to yield $PhMe_2GeGePh_3$ (0.360 g, 76 %) as a colorless solid. ^{1}H NMR (C_6D_6, 25 °C): δ 7.58-7.55 (m, 6H, *m*-$(C_6H_5)_3$), 7.44-7.41 (m, 2H, *m*-C_6H_5), 7.17-7.14 (m, 9H, *o*-$(C_6H_5)_3$ and *p*-$(C_6H_5)_3$), 7.12-7.09 (m, 3H, *o*-C_6H_5 and *p*-C_6H_5), 0.64 (s, 6H, -CH_3) ppm. ^{13}C

NMR (C_6D_6, 25 °C): δ 135.80 (*ipso*-C), 134.19 (*ipso*-C), 129.00 (*ortho*-C), 128.72 (*ortho*-C), 128.39 (*meta*-C), 128.22 (*meta*-C), 128.76 (*para*-C), 128.68 (*para*-C), 1.94 (-*C*H_3) ppm. *Anal*. Calcd for $C_{26}H_{26}Ge_2$: C, 64.57; H, 5.42. Found: C, 64.28; H, 5.64.

Synthesis of $Et_2Ge(Cl)CH_2CH_2OEt$ (12a)

To a solution of Et_2GeHCl (1.90 g, 11.4 mmol) in benzene (30 mL in a Schlenk tube was added ethyl vinyl ether (1.35 mL, 13.7 mmol) via syringe. A solution of AIBN (0.038 g, 0.23 mmol) in benzene (2 mL) was added to the reaction mixture. The tube was sealed with a Teflon plug and heated at 85 °C for 18 h. The solution was transferred to a Schlenk flask, and the volatiles were removed *in vacuo* to yield 2.41 g (89 %) of **11a** as a clear oil. ^{1}H NMR (C_6D_6, 25 °C): δ 3.33 (t, *J* = 6.6 Hz, 2H, -GeCH_2CH_2O), 3.10 (q, *J* =7.2 Hz, 2H, -OCH_2CH_3), 1.41 (t, *J* = 7.2 Hz, -OCH_2CH_3), 1.16-1.04, (m, 6H, (CH_3CH_2)$_2$Ge and GeCH_2CH_2O-), 0.97 (t, *J* = 6.6 Hz, 6H, Ge(CH_2CH_3)$_2$) ppm. ^{13}C NMR (C_6D_6, 25 °C): δ 66.8 (-O*C*H_2CH_3), 66.0 (GeCH_2*C*H_2O-), 20.2, 15.2, 12.1, 8.2 (aliphatic carbons) ppm. *Anal*. Calcd for $C_8H_{19}ClGeO$: C, 40.15; H, 8.00. Found: C, 39.25; H, 8.10.

Synthesis of $Bu_2Ge(Cl)CH_2CH_2OEt$ (12b)

To a solution of Bu_2GeHCl (1.28 g, 5.74 mmol) in benzene (20 mL) in a Schlenk tube was added ethyl vinyl ether (1.00 mL, 10.2 mmol) via syringe. A solution of AIBN (0.016 g, 0.097 mmol) in benzene (4 mL) was added to the reaction mixture. The solution was sealed with a Teflon plug and heated at 85 °C for 18 h. The solution was transferred

to a Schlenk flask, and the volatiles were removed *in vacuo* to yield 1.40 g (82 %) of **12b** as a clear oil. ^{1}H NMR (C_6D_6, 25 °C): δ 3.41 (t, *J* = 7.2 Hz, 2H, -GeCH$_2$C*H*$_2$O), 3.15 (q, *J* = 6.9 Hz, 2H, -OC*H*$_2$CH$_3$), 1.58 – 1.49 (m, 4H, GeCH$_2$C*H*$_2$CH$_2$CH$_3$), 1.47 (t *J* = 6.9 Hz, 4H, -GeC*H*$_2$CH$_2$CH$_2$CH$_3$), 1.32 (sext, *J* = 7.2 Hz, 4H, GeCH$_2$CH$_2$C*H*$_2$CH$_3$), 1.17-1.11 (m, 2H, GeC*H*$_2$CH$_2$O-), 1.01 (t, *J* = 6.9 Hz, 3H, -OCH$_2$C*H*$_3$), 0.89 (t, *J* = 7.2 Hz, 6H, GeCH$_2$CH$_2$CH$_2$C*H*$_3$) ppm. ^{13}C NMR (C_6D_6, 25 °C): δ 66.9 (- O*C*H$_2$CH$_3$), 66.1 (GeCH$_2$*C*H$_2$O-), 26.6, 26.1, 21.1, 20.0, 15.3, 13.8 (aliphatic carbons) ppm. *Anal*. Calcd for $C_{12}H_{27}ClGeO$: C, 48.79; H, 9.21. Found: C, 48.13; H, 8.74.

Synthesis of Ph$_2$Ge(Cl)CH$_2$CH$_2$OEt (12c)

To a solution of Ph$_2$GeHCl (0.590 g, 1.82 mmol) in benzene (15 mL) in a Schlenk tube was added ethyl vinyl ether (0.20 mL, 2.0 mmol) via syringe. A solution of AIBN (0.0090 g, 0.055 mmol) in benzene (2 mL) was added to the reaction mixture. The tube was sealed with a Teflon plug and heated at 85 °C for 24 h. The solution was transferred to a Schlenk flask, and the volatiles were removed *in vacuo* to yield 0.493 g (66 %) of **12c** as a clear oil. ^{1}H NMR (C_6D_6, 25 °C): δ 7.64-7.61 (m, 4H, *meta*-H), 7.18-7.07 (m, 6H, *ortho*-H and *para*-H), 3.58 (t, *J* = 7.5 Hz, 2H, -GeCH$_2$C*H*$_2$O), 3.10 (q, *J* = 7.2 Hz, 2H, -OC*H*$_2$CH$_3$), 1.90 (t, *J* = 7.5 Hz, 2H, GeC*H*$_2$CH$_2$O-), 1.00 (t, *J* = 7.2 Hz, 3H, -OCH$_2$C*H*$_3$) ppm. ^{13}C NMR (C_6D_6, 25 °C): δ 136.7, 134.0, 130.2, 128.5, (aromatic carbons), 66.1 (-O*C*H$_2$CH$_3$), 66.0 (Ge*C*H$_2$CH$_2$O-), 22.0, 15.0, (aliphatic carbons) ppm. *Anal*. Calcd for $C_{16}H_{19}ClGeO$: C, 57.30; H, 5.71. Found: C, 57.47; H, 5.81.

Synthesis of $Et_2Ge(NMe_2)CH_2CH_2OEt$ (13a)

To a solution of **12a** (2.36 g, 9.86 mmol) in benzene (35 mL) was added solid $LiNMe_2$ (0.509 g, 9.98 mmol). The resulting suspension was stirred at room temperature for 7 h and was then filtered through Celite. The volatiles were removed from the filtrate *in vacuo* to yield 2.25 g (92 %) of **13a** as a clear oil. ^{1}H NMR (C_6D_6, 25 °C): δ 3.50 (t, *J* = 7.5 Hz, 2H, $GeCH_2CH_2O$), 3.29 (q, *J* = 7.2 Hz, 2H, - OCH_2CH_3), 2.57 (s, 6H, - $N(CH_3)_2$), 1.24 (t, *J* = 7.2 Hz, 3H, -OCH_2CH_3), 1.17-1.05 (m, 6H, $(CH_3CH_2)_2Ge$ and $GeCH_2CH_2O$-), 0.87 (t, *J* = 7.2Hz, 6H, $Ge(CH_2CH_3)_2$) ppm. ^{13}C NMR (C_6D_6, 25 °C): δ 67.8 (-OCH_2CH_3), 65.8 ($GeCH_2CH_2O$-), 41.4 (-$N(CH_3)_2$), 15.5, 14.2, 8.8, 5.6, (aliphatic carbons) ppm. *Anal*. Calcd for $C_{10}H_{25}GeNO$: C, 48.44; H, 10.16. Found: C,47.55; H,10.51.

Synthesis of $Bu_2Ge(NMe_2)CH_2CH_2OEt$ (13b)

To a solution of **12b** (1.324 g, 4.482 mmol) in benzene (35 mL) was added solid lithium dimethylamide (0.234 g, 4.59 mmol). The resulting suspension was stirred 8 h, followed by filtration through Celite to yield a clear solution. Removed of the volatiles *in vacuo* yielded **13b** (1.42 g, 92 %) as a clear oil. ^{1}H NMR (C_6D_6, 25 °C): δ 3.54 (t, *J* = 7.8 Hz, 2H, $GeCH_2CH_2O$), 3.31 (q, *J* = 6.9 Hz, 2H, OCH_2CH_3), 2.60 (s, 6H, $N(CH_3)_2$), 1.53-1.26 (m, 6H), 1.43 (t, *J* = 6.9 Hz, 3H, OCH_2CH_3), 0.92 (t, *J* = 6.9 Hz, 6H, $GeCH_2CH_2CH_2CH_3$), 0.89 (m, 4H, $GeCH_2CH_2CH_2CH_3$) ppm. ^{13}C NMR (C_6D_6, 25 °C): δ 68.0 (-OCH_2CH_3), 65.8 ($GeCH_2CH_2O$-), 41.4 (-$N(CH_3)_2$), 27.3, 26.9, 15.6, 15.0, 14.0,

13.6 (aliphatic carbons) ppm. *Anal* Clad for $C_{14}H_{33}GeNO$: C, 55.31; H, 10.94. Found: C, 54.91; H, 11.0.

Synthesis of $Ph_2Ge(NMe_2)CH_2CH_2OEt$ (13c)

To a solution of **12c** (0.493 g, 1.47 mmol) in benzene (25 mL) was added solid $LiNMe_2$ (0.093 g, 1.8 mmol). The resulting suspension was stirred at room temperature for 15 h and was then filtered through Celite. The volatiles were removed from the filtrate *in vacuo* to yield 0.436 g (86 %) of **13c** as a clear oil. ^{1}H NMR (C_6D_6, 25 °C): δ 7.70-7.67 (m, 4H, *meta*-H), 7.21-7.17 (m, 6H, *ortho*-H and *para*-H), 3.58 (t, *J* = 7.8 Hz, 2H, $GeCH_2CH_2O$), 3.10 (q, *J* = 6.9 Hz, 2H, $-OCH_2CH_3$), 2.78 (s, 6H, $-N(CH_3)_2$), 1.89 (t, *J* = 7.8 Hz, 2H, $GeCH_2CH_2O$-), 1.00 (t, *J* = 6.9 Hz, 3H, OCH_2CH_3) ppm. ^{13}C NMR (C_6D_6, 25 °C): δ 136.9, 134.9, 129.3, 128.3, (aromatic carbons), 67.2 ($-OCH_2CH_3$), 65.7 ($GeCH_2CH_2O$-), 41.4 ($-N(CH_3)_2$), 15.8, 15.3 (aliphatic carbons) ppm. *Anal*. Calcd. For $C_{18}H_{25}GeNO$: C, 62.85; H, 7.32. Found: C, 63.01; H, 7.54.

Synthesis of $Ph_3GeGe(Et_2)CH_2CH_2OEt$ (14a)

To a solution of **13a** (0.762 g, 3.07 mmol) in acetonitrile (15 mL) in a Schlenk tube was added Ph_3GeH (0.945 g, 3.10 mmol) in acetonitrile (10 mL). The tube was sealed with a Teflon stopper, and the reaction mixture was heated at 90 °C for 36 h. The solution was transferred to a Schlenk flask, and the volatiles were removed *in vacuo*, yielding a pale yellow oil. Kugelrohr distillation of the crude product afforded 1.179g (75

%) of **14a** as a clear oil. ^{1}H NMR (C_6D_6, 25 °C): δ 7.66-7.60 (m, 6H, aromatics), 7.24-7.14 (m, 9H, aromatics) 3.44 (t, *J* = 7.8 Hz, 2H, $GeCH_2CH_2O$), 3.14 (q, *J* = 6.9 Hz, 2H, -OCH_2CH_3), 1.49 (t, *J* = 6.9 Hz, 3H, -OCH_2CH_3), 1.17-1.01 (m, 12H, $(CH_3CH_2)_2Ge$, $(CH_3CH_2)_2Ge$ and $GeCH_2CH_2O$-) ppm. ^{13}C NMR (C_6D_6, 25 °C): δ 139.2, 135.7, 128.7, 128.6 (aromatic carbons), 68.7 (-OCH_2CH_3), 65.7 ($GeCH_2CH_2O$-), 15.5, 15.4, 10.3, 7.2 (aliphatic carbons) ppm. *Anal*. Calcd for $C_{26}H_{34}Ge_2O$: C, 61.50; H, 6.75. Found: C, 61.18; H, 6.96.

Synthesis of $Ph_3GeGe(Bu)_2CH_2CH_2OEt$ (14b)

To a solution of **13b** (0.633 g, 2.18 mmol) in acetonitrile (15 mL) was added Ph_3GeH (0.670 g, 2.20 mmol) in acetonitrile (10 mL). The solution was refluxed for 48 h, and the volatiles were removed *in vacuo* to yield a yellow oil. The material was distilled in a Kugelrohr oven to remove the remaining Ph_3GeH, and the pot residue was isolated to yield 0.930 g (76 %) of **14b** as a pale yellow oil. ^{1}H NMR (C_6D_6, 25 °C): δ 7.68-7.65 (m, 6H, aromatics), 7.24-7.14 (m, 9H, aromatics), 3.51 (t, *J* = 7.2 Hz, 2H, $GeCH_2CH_2OEt$), 3.18 (q, *J* = 7.2 Hz, OCH_2CH_3), 1.56 (t, *J* = 7.5 Hz, 2H, $GeCH_2CH_2O$), 1.49-1.41 (m, 4H, aliphatics), 1.31-1.18 (m, 8H, aliphatics), 1.08 (t, *J* = 6.9 Hz, 3H, OCH_2CH_3), 0.80 (t, *J* = 7.2 Hz, 6H, -$(CH_2)_3CH_3$) ppm. ^{13}C NMR (C_6D_6, 25 °C): δ 139.1, 135.7, 128.7, 128.5 (aromatic carbons), 68.9 (-OCH_2CH_3), 65.6 ($GeCH_2CH_2O$-), 28.7, 26.7, 16.2, 15.4, 14.9, 13.7 (aliphatic carbons) ppm. *Anal*. Calcd for $C_{30}H_{42}Ge_2O$: C, 63.90; H, 7.51. Found: C, 63.55; H, 7.48.

Synthesis of $Ph_3GeGe(Ph)_2CH_2CH_2OEt$ (14c)

To a solution of **13c** (1.511 g, 4.392 mmol) in acetonitrile (40 mL) was added Ph_3GeH (1.339 g, 4.391 mmol) in acetonitrile (25 mL). The solution was refluxed for 48 h, and the volatiles were removed *in vacuo* to yield a yellow oil. The material was distilled in a Kugelrohr oven to remove the remaining Ph_3GeH, and the pot residue was isolated to yield 2.443 g (92 %) of **14c** as a white solid. ^{1}H NMR (C_6D_6, 25 °C): δ 7.64-7.52 (m, 10H, *meta*-H), 7.13-7.02 (m, 15H, *ortho*- and *para*-H), 3.59 (t, *J* = 7.8 Hz, 2H, $GeCH_2CH_2O$-), 3.03 (q, *J* = 6.9 Hz, 2H, $-OCH_2CH_3$), 2.08 (q, *J* = 7.8 Hz, 2H, $GeCH_2CH_2O$-), 0.95 (t, *J* = 6.9 Hz, 3H, $-OCH_2CH_3$) ppm. ^{13}C NMR (C_6D_6, 25 °C): δ 138.4, 138.1, 135.9, 135.5, 129.0, 128.9, 128.6, 128.5 (aromatic carbons) ppm. *Anal.* Calcd for $C_{34}H_{34}Ge_2O$: C, 67.63; H, 5.67. Found: C, 67.37; H, 5.44.

Synthesis of $Ph_3GeGe(Et)_2H$ (15a)

To a solution of **14a** (0.600 g, 1.18 mmol) in benzene (20 mL) was added a 1.0 M solution of DIBAL-H in hexane (1.22 mL, 1.22 mmol). The solution was refluxed for 36 h, and the volatiles were removed *in vacuo* to yield a pale yellow oil. The crude material was filtered through a 1 in. × 1 in. silica gel column using 25 mL of a 9:1 benzene/acetonitrile solution as the eluent to yield 0.357 g (69 %) of **15a** as a cloudy white liquid after removal of the solvent. ^{1}H NMR (C_6D_6, 25 °C): δ 7.67-7.61 (m, 6H, aromatics), 7.23-7.16 (m, 9H, aromatics), 4.91 (pent, *J* = 3.0 Hz, 1H, Ge-*H*), 1.07-1.01 (m, 10H, $Ge(CH_2CH_3)_2$) ppm. ^{13}C NMR (C_6D_6, 25 °C): δ 139.2, 135.7, 128.7, 128.6

(aromatic carbons), 10.2, 6.2 (aliphatic carbons) ppm. IR (Nujol): 1996.1 cm^{-1} (ν_{Ge-H}). *Anal*. Calcd: for $C_{22}H_{26}Ge_2$: C, 60.65; H, 6.01. Found: C, 60.81; H, 6.42.

Synthesis of $Ph_3GeGe(Bu)_2H$ (15b)

To a solution of **14b** (1.286 g, 2.280 mmol) in benzene (15 mL) was added a 1.0 M solution of diisobutylaluminum hydride (2.5 mL, 2.5 mmol) via syringe. The resulting solution was refluxed for 18 h. The volatiles were removed *in vacuo* to yield a clear viscous oil. The crude material was dissolved in hexane (5 mL) and filtered through a short column (1 in.) of silica gel using 45 mL of hexane as the eluent. The solvent was removed *in vacuo* to yield 0.585 g (52 %) of **15b** as a clear oil. ^{1}H NMR (C_6D_6, 25 °C): δ 7.67-7.64 (m, 6H, aromatics), 7.24-7.16 (m, 9h, aromatics), 4.40 (pent, *J* = 3.6 Hz, 1H, Ge-*H*), 1.47-1.34 (m,4H, aliphatics), 1.24 (sext, *J* = 7.8 Hz, 4H, $GeCH_2CH_2CH_2CH_3$), 1.17-1.08 (m, 4H, aliphatics), 0.80 (t, *J* = 7.5 Hz, 6H, $GeCH_2CH_2CH_2CH_3$) ppm. ^{13}C NMR (C_6D_6, 25 °C): δ 139.3, 135.7, 128.7, 128.6, (aromatic carbons), 28.7, 26.7, 14.0, 13.7, (aliphatic carbons) ppm. IR (Nujol): 2036.2 cm^{-1} (ν_{Ge-H}). *Anal*. Calcd for $C_{26}H_{34}Ge_2$: C, 63.50; H, 6.96. Found: C, 63.60; H, 7.10.

Synthesis of $Ph_3GeGe(Et)_2Ge(Et)_2CH_2CH_2OEt$ (16a)

To a solution of **15a** (0.322 g, 0.739 mmol) in acetonitrile in (10 mL) was added a solution of **13a** (0.185 g, 0.746 mmol) in acetonitrile (5 mL). The reaction was sealed in a Schlenk tube and heated to 90 °C for 72 h. The volatiles were removed *in vacuo* to yield

0.425 g (90 %) of **16a** as a pale yellow liquid. ^{1}H NMR (C_6D_6, 25 °C): δ 7.62-7.58 (m, 6H, aromatics), 7.22-7.14 (m, 9H, aromatics), 3.28 (t *J* = 6.6 Hz, 2H, $GeCH_2CH_2OEt$), 3.14 (q, *J* = 6.9 Hz, 2H, $-OCH_2CH_3$), 1.04-0.97 (m, 17H, $Ge(CH_2CH_3)_2$ and $-OCH_2CH_3$), 0.90 (t, 6H, $Ge(CH_2CH_3)_2$), 0.74 (t, 2H, *J* = 6.6 Hz, $GeCH_2CH_2OEt$) ppm. ^{13}C NMR (C_6D_6, 25 °C): δ 139.2, 135.6, 128.7, 128.5, (aromatic carbons), 67.2 ($-OCH_2CH_3$), 65.9 ($GeCH_2CH_2O$-) 15.3, 14.0, 10.2, 8.6, 6.1, 5.6 (aliphatic carbons) ppm. *Anal*. Calcd for $C_{30}H_{44}Ge_3O$: C, 56.43; H, 6.94. Found: C, 57.23; H, 6.86.

Synthesis of $Ph_3GeGe(Bu)_2Ge(Bu)_2CH_2CH_2OEt$ (16b)

To a solution of **15b** (1.777 g, 3.62 mmol) in acetonitrile (20 mL) was added a solution of **13b** (1.208 g, 3.98 mmol) in acetonitrile (10 mL). The reaction mixture was sealed in a Schlenk tube equipped with a Teflon plug and was heated at 85 °C for 48 h. The solution was transferred to a Schlenk flask, and the volatiles were removed *in vacuo*. The crude product was distilled in a Kugelrohr oven (oven temp = 100 °C, *P* = 0.08 Torr) for 3h to remove excess **13b**. Yield of **16b** = 2.555 g (94 %). ^{1}H NMR (C_6D_6, 25 °C): δ 7.73-7.65 (m, 6H, aromatics), 7.23-7.12 (m, 9H, aromatics), 3.51 (t, *J* = 7.5 Hz, 2H, $GeCH_2CH_2OEt$), 3.18 (q, *J* = 6.9 Hz, 2H,$-OCH_2CH_3$), 1.62-1.04 (m, 24H, aliphatics), 0.98-0.72 (m, 17H, aliphatics) ppm. ^{13}C NMR (C_6D_6, 25 °C): δ 139.1, 135.8, 128.7, 128.5 (aromatic carbons), 68.8 ($-OCH_2CH_3$), 65.7 ($GeCH_2CH_2O$-), 31.9, 28.8, 26.8, 20.0, 16.3, 15.0, 14.0, 13.8, 10.4, 7.1 (aliphatic carbons) ppm. *Anal*. Calcd for $C_{38}H_{60}Ge_4O$: C, 60.79; H, 8.05. Found: C, 60.43; H, 8.39.

Synthesis of $Ph_3GeGe(Et)_2Ge(Et)_2H$ (17a)

A solution of **16a** (0.217 g, 0.340 mmol) in benzene (15 mL) was treated with a 1.0 M hexane solution of DIBAL-H (0.35 mL, 0.35 mmol), and the mixture was refluxed under N_2 for 18 h. The volatiles were removed *in vacuo* to yield a clear oil, which was washed on a silica column (1 in. h × 1 in. dia) using benzene as the eluent (30 mL). The benzene was removed *in vacuo*, and the resulting oil was distilled using a Kugelrohr oven (oven temp = 115 °C, *P* = 0.07 Torr) to remove any remaining impurities for 3 h to yield **17a** as a clear oil (0.079 g, 41 %). ^{1}H NMR (C_6D_6, 25 °C): δ 7.64-7.61 (m, 6H, aromatics), 7.22-7.17 (m, 9H, aromatics), 4.31 (pent, *J* = 3.2 Hz, 1H, Ge-*H*), 1.03 (m, 20H, aliphatics) ppm. ^{13}C NMR (C_6D_6, 25 °C): δ ?? IR (Nujol) 1996.4 cm^{-1} ($\nu_{Ge\text{-}H}$). We were not able to obtain a satisfactory elemental analysis for **17a.**

Synthesis of $Ph_3GeGe(Bu_2)Ge(Bu_2)H$ (17b)

A solution of **16b** (1.965 g, 2.61 mmol) in benzene (40 mL) was treated with a 1.0 M hexane solution of DIBAL-H (2.88 mL), and the mixture was refluxed under N_2 for 48 h. The volatiles were removed *in vacuo* to yield a clear oil, which was washed on a silica column (1 in. h × 1 in. dia) using benzene as the eluent (45 mL). The benzene was removed *in vacuo*, and the resulting oil was distilled using a Kugelrohr oven (oven temp = 110 °C, P = 0.005 Torr) for 5 h to remove impurities to yield **17b** as a clear oil (0.580 g, 33 %). ^{1}H NMR (C_6D_6, 25 °C): δ 7.74-7.63 (m, 6H, aromatics), 7.23-7.12 (m, 9H, aromatics), 4.91 (pent, *J* = 3.0 Hz, 1H, Ge-*H*), 1.61-1.09 (m, 24H, aliphatics), 0.80 (t, *J* = 7.2 Hz, 12H, -$CH_2CH_2CH_2CH_3$) ppm. ^{13}C NMR (C_6D_6, 25 °C): δ 139.2, 135.7, 128.7,

128.5 (aromatic carbons), 30.6, 28.7, 26.7, 26.2, 14.0, 13.7, 10.3, 7.05 (aliphatic carbons) ppm. IR (Nujol): 2000.0 cm^{-1} (ν Ge-H). We were not able to obtain a satisfactory elemental analysis for **17b**.

Synthesis of $Ph_3GeGe(Et)_2Ge(Et)_2Ge(Et)_2CH_2CH_2OEt$ (18a)

To a solution of **17a** (0.056 g, 0.099 mmol) in acetonitrile (10 mL) was added a solution of **13a** (0.056 g, 0.104 mmol) in acetonitrile (10 mL). The reaction mixture was sealed in a Schlenk tube equipped with a Teflon plug, and the reaction mixture was heated at 85 °C for 48 h. The solution was transferred to a Schlenk flask, and the volatiles were removed *in vacuo*. The crude product was distilled in a Kugelrohr oven (oven temp = 115 °C, P = 0.07 Torr) to remove excess **13a** yielding **18a** (0.073 g, 97 %) as a viscous clear oil. ^{1}H NMR (C_6D_6, 25 °C): δ 7.62-7.59 (m, 6H, aromatics), 7.25-7.12 (m, 9H, aromatics), 3.59 (t, *J* = 7.5 Hz, 2H, $GeCH_2CH_2OEt$), 3.30 (q, *J* = 6.8 Hz, 2H, -OCH_2CH_3), 1.36 (t, *J* = 7.8 Hz, 3H, -OCH_2CH_3), 1.18-0.89 (m, 32H, aliphatics) ppm. ^{13}C NMR (C_6D_6, 25 °C): δ 139.2, 135.6, 128.7, 128.6, 67.5 (-OCH_2CH_3), 65.8 ($GeCH_2CH_2$-), 19.1, 15.5, 14.0, 10.5, 10.2, 8.6, 8.3, 6.1 (aliphatic carbons) ppm. UV/visible: λ_{max} 241 ($\varepsilon = 1.8 \times 10^4$ L mol^{-1} cm^{-1}). *Anal*. Calcd for $C_{34}H_{54}Ge_4O$: C, 53.09; H, 7.08. Found: C, 53.29; H, 7.22.

Synthesis of $Ph_3GeGe(Bu)_2Ge(Bu)_2Ge(Bu)_2CH_2OEt$ (18b)

To a solution of **17b** (0.370 g, 0.540 mmol) in acetonitrile (10 mL) was added a solution of **13b** (0.174 g, 0.570 mmol) in acetonitrile (10 mL). The reaction mixture was sealed in a Schlenk tube equipped with a Teflon plug, and the reaction mixture was heated at 85 °C for 48 h. The solution was transferred to a Schlenk flask, and the volatiles were removed *in vacuo*. The crude product was distilled in a Kugelrohr oven (oven temp = 105 °C, P = 0.03 Torr) to remove excess **13b**, yielding **18b** (0.430 g, 85 %) as a viscous clear oil. ^{1}H NMR (C_6D_6, 25 °C): δ 7.70-7.58 (m, 6H, aromatics), 7.23- 7.08 (m, 9H, aromatics), 3.35 (t, *J* = 7.2 Hz, 2H, $GeCH_2C\mathit{H}_2OEt$), 3.19 (q, *J* = 6.0 Hz, 2H, -$OC\mathit{H}_2CH_3$), 1.52-1.02 (m, 29H, aliphatics), 0.94-0.72 (m, 30H, aliphatics) ppm. ^{13}C NMR (C_6D_6, 25 °C): δ 139.2, 135.6, 128.7, 128.5, 68.5 (-OCH_2CH_3), 31.9, 28.7, 28.6, 26.7, 22.9, 16.2, 15.4, 15.0, 14.4, 14.2, 14.0, 13.7, 10.3 7.0 (aliphatic carbons) ppm. UV/visible: λ_{max} 235 ($\varepsilon = 1.4 \times 10^4$ L mol^{-1} cm^{-1}). *Anal*. Calcd for $C_{46}H_{78}Ge_4O$: C, 58.93; H, 8.38. Found: C, 58.85; H, 8.11.

Synthesis of $Ph_3GeGe(Bu_2)Ge(Bu_2)Ge(Bu_2)CH_2CH_2OEt$ (18b) directly from $Ph_3GeGe(Bu_2)Ge(Bu_2)CH_2CH_2OEt$ (16b)

To a solution of **16b** (0.94 g, 1.14 mmol) in benzene (30 mL) in a Schlenk flask was added a 1 M solution of DIBAL-H in hexane (1.50 mL, 1.50 mmol). The resulting solution was refluxed under N_2 for 24 h and allowed to cool, and the volatiles were removed *in vacuo*, yielding a pale yellow oil. The product was directly transferred to a Schlenk tube, where a solution of **13b** (0.380 g, 1.25 mmol) in acetonitrile (30 mL) was

added. The volatiles were removed *in vacuo*, resulting in an orange oil. The crude material was filtered through a 1 in. × 1 in. silica gel column using 40 mL of benzene as the eluent to yield 0.876 g (75 %) of **18b** as a pale yellow liquid after removal of the solvent. The identity of **18b** was confirmed by NMR (^{1}H and ^{13}C) spectroscopy.

Preparation of $Ph_3Ge(GeBu_2)(GePh_2)CH_2CH_2OEt$ (19)

To a solution of $Ph_3Ge(GeBu_2)CH_2CH_2OEt$ (0.672 g, 1.19 mmol) in benzene (15 mL) was added a solution of 1.0 M DIBAL-H in hexane (1.31 mL). The reaction mixture was refluxed under N_2 for 24 h, after which time the solvent was removed *in vacuo* to yield viscous oil. The oil was dissolved in acetonitrile (20 mL), transferred to a Schlenk tube, and treated with a solution of $Ph_2Ge(NMe_2)CH_2CH_2OEt$ (**13c**) (0.409 g, 1.19 mmol) in acetonitrile (10 mL). The tube was sealed, and the reaction mixture was heated at 90 °C for 4 days. The volatiles were removed *in vacuo*, and the crude product mixture was washed through a 1 in. × 3 in. silica gel column using benzene (35 mL). The solvent was removed *in vacuo* to yield **19** (0.595 g, 63 %) as thick colorless oil. ^{1}H NMR (C_6D_6, 25 °C): δ 7.65-7.61 (m, 10 H, aromatics, *meta*-H), 7.20-7.08 (m, 15H, aromatics, *ortho*-H and *para*-H), 3.48 (t, *J* = 7.5 Hz, 2H, -CH_2CH_2O-), 3.14 (q, *J* = 6.6 Hz, 2H, -OCH_2CH_3), 1.53 (t, *J* = 7.5 Hz, 2H, -CH_2CH_2O-), 1.39 (m, 4H, aliphatics), 1.15 (m, 8H, aliphatics), 0.77 (t, 3H, *J* = 6.6 Hz, -OCH_2CH_3), 0.76 (t, *J* = 7.2 Hz, 6H, -$CH_2CH_2CH_2CH_3$). ^{13}C NMR (C_6D_6, 25 °C): δ 139.3 (*ipso*-C), 139.2 (*ipso*-C), 136.0 (*ortho*-C) 135.7 (*ortho*-C), 128.7, 128.5 (2 *meta*- and 2 *para*-C), 68.8 (-OCH_2CH_3), 65.7 (-$GeCH_2CH_2O$-), 28.7 (-OCH_2CH_3), 26.8 (-$CH_2CH_2CH_2CH_3$), 14.0 (-$CH_2CH_2CH_2CH_3$), 13.8 (-$CH_2CH_2CH_2CH_3$),

10.4 (Ge*C*H_2CH_2O-), 7.1 (-*C*$H_2CH_2CH_2CH_3$) ppm. UV/visible: λ_{max} 232 nm (br, ε =4.02 × 10^4 cm^{-1} M^{-1}). *Anal*. Calcd for $C_{42}H_{52}Ge_3O$: C, 63.80; H, 6.63. Found: C, 64.11; H, 7.15.

Preparation of $Ph_3Ge(GeBu_2)(GePh_2)(GeEt_2)CH_2CH_2OEt$ (20a)

To a solution of $Ph_3Ge(GeBu_2)(GePh_2)CH_2CH_2OEt$ (**19**) (0.525g, 0.664mmol) in benzene (20 mL) was added a solution of 1.0 M DIBAL-H in hexane (0.75 mL, 0.75 mmol). The reaction mixture was refluxed under N_2 for 24 h, after which time the solvent was removed in vacuo to yield a thick opaque oil. The oil was dissolved in acetonitrile (25 mL), transferred to a Schlenk tube and treated with a solution of $Et_2Ge(NMe_2)CH_2CH_2OEt$ (**13a)** (0.165 g, 0.666 mmol) in acetonitrile (15 mL). The tube was sealed, and the reaction mixture was heated at 90 °C for 48 h. The volatiles were removed *in vacuo*, and the crude product mixture was washed through a 1 in. × 3 in. silica gel column using benzene (50 mL). The solvent was removed *in vacuo* to yield **20a** (0.508 g, 83 %) as a thick colorless oil. ^{1}H NMR (C_6D_6, 25 °C): δ7.70-7.54 (m, 10H, aromatics, *meta*-H), 7.19-7.03 (m,15H,aromatics, *ortho* and *para*-H), 3.42 (t, *J* = 7.2 Hz, 2H, $GeCH_2CH_2O$-), 3.09 (q, *J* = 6.8 Hz, 2H, -OCH_2CH_3), 1.48 (t, *J* = 7.2 Hz, 2H, $GeCH_2CH_2O$-), 1.44-1.28 (m, 4H, aliphatics), 1.19-1.13 (m, 4H, aliphatics), 1.09-0.98 (m, 14H, aliphatics), 0.73 (t, *J* = 6.8 Hz, 3H, -OCH_2CH_3), 0.71 (t, *J* = 7.2 Hz, 6H, $Ge(CH_2CH_2CH_2CH_3)_2$) ppm. ^{13}C NMR (C_6D_6, 25 °C): δ139.1 (*ipso*-C), 139.0 (*ipso*-C), 136.0 (*ortho*-C), 135.6 (*ortho*-C), 128.6, 128.5 (2 *meta* and 2 *para* C), 68.7 (-OCH_2CH_3), 65.6 ($GeCH_2CH_2O$-), 28.5 (-OCH_2CH_3), 26.6 (-$Ge(CH_2CH_2CH_2CH_3)_2$), 14.0 (-$Ge(CH_2CH_3)_2$), 13.7 (-$Ge(CH_2CH_2CH_2CH_3)_2$), 10.3 ($Ge(CH_2CH_2CH_2CH_3)_2$) 8.6 ($GeCH_2CH_2O$-), 7.0 (-$Ge(CH_2CH_2CH_2CH_3)_2$), 5.6 ($Ge(CH_2CH_3)_2$ ppm. UV/visible: λ_{max}

248 nm (v br, $\varepsilon = 2.97 \times 10^4$ cm^{-1} M^{-1}). *Anal*. Calcd for $C_{46}H_{62}Ge_4O$: C, 59.97; H, 6.78 Found: C, 60.10; H, 6.90.

Preparation of $Ph_3Ge(GeBu_2)(GePh_2)(GeBu_2)CH_2CH_2OE$ (20b)

To a solution of $Ph_3Ge(GeBu_2)(GePh_2)CH_2CH_2OEt$ **(19)** (0.211 g, 0.267 mmol) in benzene (10 mL) was added a solution of 1.0 M solution of DIBAL-H in hexane (0.28 mL, 0.28 mmol). The reaction mixture was refluxed under N_2 for 24 h, after which time the solvent was removed *in vacuo* to yield a thick opaque oil. The oil was dissolved in acetonitrile (10 mL), transferred to a Schlenk tube, and treated with a solution of $Bu_2Ge(NMe_2)CH_2CH_2OEt$ (**13b**) (0.083 g, 0.27 mmol) in acetonitrile (10 mL). The tube was sealed and the reaction mixture was heated at 90 °C for 48 h. The volatiles were removed *in vacuo*, and the crude product mixture was washed through a 1 in. × 3 in. silica gel column using benzene (45 mL). The solvent was removed *in vacuo* to yield **20b** (0.224 g, 86 %) as a thick pale yellow oil. ^{1}H NMR (C_6D_6, 25 °C): δ 7.60-7.56 (m, 10H, *meta*-H), 7.14-7.07 (m,25H, *ortho* and *para*-H), 3.42 (t, *J* = 7.6 Hz, 2H, $GeCH_2CH_2O$-), 3.09 (q, *J* = 6.8 Hz, 2H, $-OCH_2CH_3$), 1.48 (t, *J* = 6.8 Hz, 2H, $GeCH_2CH_2O$-), 1.40-1.26 (m, 4H, aliphatics), 1.21-0.97 (m, 13H, aliphatics), 0.71 (m, 12H, $(GeCH_2CH_2CH_2CH_3)_4$) ppm. ^{13}C NMR (C_6D_6, 25 °C): δ139.1 (ipso-C), 139.0 (*ipso*-C), 135.6 (*ortho*-C), 135.3 (*ortho*-C), 128.6 (2 *meta* and 2 *para* C), 68.7 ($-OCH_2CH_3$), 65.6 ($-GeCH_2CH_2O$-), 28.6 ($-OCH_2CH_3$), 26.6 ($-Ge(CH_2CH_2CH_2CH_3)_2$), 16.1 ($-Ge(CH_2CH_2CH_2CH_3)_2$), 15.3 ($-Ge(CH_2CH_2CH_2CH_3)_2$), 14.9 ($Ge(CH_2CH_2CH_2CH_3)_2$), 13.9 ($-CH_2CH_2CH_2CH_3$), 13.6 ($-GeCH_2CH_2O$-), 10.2 ($GeCH_2CH_2CH_2CH_3$), 6.9 ($GeCH_2CH_2CH_2CH_3$) ppm. *Anal*. Calcd for $C_{50}H_{70}Ge_4O$: C, 61.44; H, 7.22 Found: C, 64.41; H, 7.42.

Preparation of $EtOCH_2CH_2(GeEt_2)(GePh_2)(GeEt_2)CH_2CH_2OEt$ (21a)

To a solution of $Et_2Ge(NMe_2)CH_2CH_2OEt$ (**13a**) (0.535 g, 2.16 mmol) in acetonitrile (20 mL) in a Schlenk tube was added Ph_2GeH_2 (0.250 g, 1.09 mmol) in acetonitrile (10 mL). The tube was sealed and heated in an oil bath at 85 °C for 48 h, after which time the volatiles were removed *in vacuo*. Residual Ph_2GeH_2 was removed by Kugelrohr distillation (110 °C, 0.05 Torr) to yield 0.498 g (72 %) of **21a** as a thick colorless liquid. ^{1}H NMR (C_6D_6, 25 °C): δ 7.68 (d, *J* = 6.3 Hz, 4H, *m*-H), 7.23-7.13 (m, 6H, *p*- and *o*-H), 3.49 (t, *J* = 7.8 Hz, 4H, $GeCH_2CH_2O$-), 3.24 (q, *J* = 7.2 Hz, 4H, -OCH_2CH_3), 1.54 (t, *J* = 7.8 Hz, 4H, $GeCH_2CH_2O$-), 1.15-1.06 (m, 26H, aliphatics) ppm. ^{13}C NMR (C_6D_6, 25 °C): δ 140.2 (*ipso*-C), 135.9 (*ortho*-C), 128.4 (*meta*-C), 128.0 (*para*-C), 68.7 (-OCH_2CH_3), 65.6 (-$GeCH_2CH_2$-O), 15.8 (-OCH_2CH_3), 15.5 ($Ge(CH_2CH_3)_2$), 10.2 ($GeCH_2CH_2O$-), 7.4 ($Ge(CH_2CH_3)_2$) ppm. UV/visible: λ_{max} 243 nm (v, br, $\varepsilon = 2.05 \times 10^4$ cm^{-1} M^{-1}). *Anal*. Calcd for $C_{28}H_{48}Ge_3O_2$: C, 53.01; H, 7.63. Found: C, 52.93; H, 7.25.

Preparation of $EtOCH_2CH_2(GeBu_2)(GePh_2)(GeBu_2)CH_2CH_2OEt$ (21b)

To a solution of $Bu_2Ge(NMe_2)CH_2CH_2OEt$ (**13b**) (1.505 g, 4.950 mmol) in acetonitrile (25 mL) in a Schlenk tube was added Ph_2GeH_2 (0.569 g, 2.49 mmol) in acetonitrile (10 mL). The tube was sealed and heated in an oil bath at 80 °C for 48 h, after which time the volatiles were removed *in vacuo*. Residual Ph_2GeH_2 was removed by Kugelrohr distillation to yield 1.535 g (83 %) of **21b** as a thick pale yellow liquid. ^{1}H NMR (C_6D_6, 25 °C): δ 7.73 (d, *J* = 7.8 Hz, 4H, *meta*-H,), 7.23-7.11 (m, 6H, *para* and *ortho*-H), 3.57 (t, *J* = 7.5 Hz, 4H, $GeCH_2CH_2O$-), 3.28 (q, *J* = 7.2Hz, 4H, -OCH_2CH_3),

1.62 (t, J = 7.5 Hz, 4H, GeC$H_2$$CH_2$O-), 1.48 (m, 8H, Ge($CH_2CH_2$$CH_2$$CH_3$)$_2$), 1.35 (pent, *J* = 6.8 Hz, 8H Ge($CH_2$$CH_2CH_2$$CH_3$)$_2$), 1.25 (t, *J* = 7.5 Hz, 8H, Ge(C$H_2$$CH_2$$CH_2$$CH_3$)$_2$), 1.13 (t, *J* = 7.5 Hz, 6H, -OCH_2CH_3), 0.89 (t, *J* = 6.8 Hz, 12H, Ge($CH_2$$CH_2$$CH_2CH_3$)$_2$) ppm. ^{13}C NMR ($C_6D_6$, 25 °C): δ 140.4 (*ipso*-C), 138.0 (*ortho*-C), 128.4 (*meta*-C), 128.1 (*para*-C), 68.9 (-O$CH_2$$CH_3$), 65.7 (-Ge$CH_2$$CH_2$O-), 28.8 (-O$CH_2$$CH_3$), 27.0 (Ge($CH_2$$CH_2$$CH_2$$CH_3$)$_2$), 16.6 (Ge($CH_2$$CH_2$$CH_2$$CH_3$)$_2$), 15.8 (Ge($CH_2$$CH_2$$CH_2$$CH_3$)$_2$), 15.4 (Ge$CH_2$$CH_2$O-), 13.8 (Ge($CH_2$$CH_2$$CH_2$$CH_3$)$_2$) ppm. UV/visible: λ_{max} 243 nm (v br, ε = 1.57 × 10^4 cm^{-1} M^{-1}). *Anal*. Calcd for $C_{36}H_{64}Ge_3O_2$: C, 57.91; H,8.64. Found: C,58.06; H, 8.78.

Preparation of EtO$CH_2$$CH_2$($GePh_2$)($GePh_2$)($GePh_2$)$CH_2$$CH_2$OEt (21c)

To a solution of Ph_2GeH_2 (0.510 g, 2.23 mmol) in acetonitrile (15 mL) in a Schlenk tube was added Ph_2Ge(NMe_2)$CH_2$$CH_2$OEt (**13c**) (1.52 g, 4.42 mmol) in acetonitrile (10 mL). The tube was sealed and heated in an oil bath at 85 °C for 48 h, after which time the volatiles were removed *in vacuo* to yield a thick viscous liquid, which was distilled in a Kugelrohr oven (140 °C, 0.05 Torr) to yield 1.681 g (92 %) of **21c** as a white solid. ^{1}H NMR (C_6D_6, 25 °C): δ 7.68-7.64 (m, 4H, *meta*-H) 7.49-7.45 (m, 8H, *meta*-H), 7.17 (m, 6H, *para*-H and *ortho*-H), 7.11-7.05(m, 12H, *para* and *ortho*-H), 3.45 (t, *J* = 7.8 Hz, 4H, GeCH_2CH_2O-), 3.02 (q, *J* = 6.9 Hz, 4H, -OC$H_2$$CH_3$), 1.93 (t, *J* = 7.8 Hz, 4H, GeC$H_2$$CH_2$O-), 0.95 (t, *J* = 6.9 Hz, 6H, -OCH_2CH_3) ppm. ^{13}C NMR (C_6D_6, 25 °C): δ 138.2 (*ipso*-C), 136.5 (*ortho*-C), 135.6 (*ortho*-C), 139.0 (*ipso*-C), 128.8, 128.5, 128.4, 128.3, (*meta*- and *para*-C), 68.0 (-O$CH_2$$CH_3$), 65.4 (-Ge$CH_2$$CH_2$O-), 17.3 (-O$CH_2$$CH_3$), 15.3 (Ge$CH_2$$CH_2$O-) ppm. UV/visible: λ_{max} 247 nm (v br, ε = 1.98 × 10^4 cm^{-1} M^{-1}). *Anal*. Calcd for $C_{44}H_{48}Ge_3O_2$: C, 63.93; H, 5.85. Found: C, 63.51; H, 5.69.

X-ray crystal structure of compound 1 and 2

Diffraction intensity data were collected with a Siemens P4/CCD diffractometer. Crystallographic data and details of X-ray studies are shown in Table 2.8. Absorption corrections were applied for all data by SADABS. The structures were solved using direct methods, completed by difference Fourier syntheses, and refined by full matrix least squares procedures on F^2. All non-hydrogen atoms were refined with anisotropic displacement coefficients and hydrogen atoms were treated as idealized contributions. All software and sources of scattering factors are contained in the SHEXTL (5.10) program package (G. Sheldrick, Bruker XRD, Madison, WI). ORTEP diagrams were drawn using the ORTEP3v2 program (L. J. Farrugia, Glasgow)

Table 2.8: Crystal data and structure refinement details for **1** and **2**

Compound	***1***	***2***
Empirical formula	$C_{30}H_{42}Ge_2$	$C_{24}H_{27}Ge_2$
Space group	*P*1	*R*3
a (Å)	10.051(3)	15.533(1)
b (Å)	15.141(4)	15.533(1)
c (Å)	20.970(6)	16.275(3)
α (˚)	109.043(4)	90
β (˚)	100.239(4)	90
γ (˚)	98.645(4)	120
Volume ($Å^3$)	2893.1(1)	3400.4(7)
Z,*Z´*	4, 2	6, 1
Calculated density (g/cm^3)	1.258	1.350
Temperature (K)	215(2)	213(2)
Radiation	Mo Kα	Mo Kα
Wavelength (Å)	0.71073	0.71073
R	0.0485	0.0333
Rw	0.1199	0.0932

X-ray Crystal structure of 6

Diffraction intensity data were collected with a Siemens P4/CCD diffractometer. Crystallographic data for the of X-ray analysis of **6** are collected in Table 2.9. Crystal-to-detector distance was 60 mm and exposure time was 20s per frame using a scan with of 0.5º. data collection was 100.0% complete to 25.00º in θ. The data were integrated using the Bruker SAINT software program and scaled using SADABS software program. Solution by direct methods (SIR-2004) produced a complete heavy atom phasing model consistent with the proposed structure. All non-hydrogen atoms were refined anisotropically by full matrix least-squares (SHELXL-97). All hydrogen atoms were placed using a riding model. Their positions were constrained relative to their parent atom using the approximate HFIX command in SHELXK-97.

Table 2.9: Crystallographic data for **6**

Empirical formula	$C_{26}H_{26}Ge_2$
FW (g mol^{-1})	483.65
Crystal size (mm)	0.07 × 0.07 × 0.02
Crystal system	orthorhombic
Space group	*P*na2
a (Å)	24.7570(3))
b (Å)	7.7560(5)
c (Å)	11.701(1)
α (˚)	90
β (˚)	90
γ (˚)	90
Volume ($Å^3$)	2246.8(3)
Z	4
Calculated density (g/cm^3)	1.430
Absorption coefficient (mm^{-1})	2.684
F(000)	984
θ range for data collection (o)	1.65-28.20
Index ranges	$-30 \leq h \leq 31$
	$-10 \leq k \leq 10$
	$-15 \leq l \leq 15$
Reflections collected	29 898

Independent reflections	5198 (R_{int} = 0.0567)
Completeness to θ	25.00 (100.0%)
Absorption correction	Semiempirical from equivalents
Maximum and minimum transmission	0.9483 and 0.8344
Refinement method	Full-matrix least-squares on F^2
Data/restraints/parameters	5198/1/255
Goodness of fit on F^2	1.048
Temperature (K)	100(2)
Radiation	Mo Kα
Wavelength (Å)	0.71073
R	0.0332
R_w	0.0655
Largest difference in peak and hole (e Å^{-3})	0.952 and -0.324

X-ray crystal structures of compound 4 and 11

Diffraction intensity data were collected with a Siemens P4/CCD diffractometer. Crystallographic data and details of X-ray studies are shown in Table 2.10. Absorption corrections were applied for all data by SADABS. The structures were solved using direct methods, completed by difference Fourier syntheses, and refined by full matrix least squares procedures on F^2. All non-hydrogen atoms were refined with anisotropic displacement coefficients and hydrogen atoms were treated as idealized contributions. All software and sources of scattering factors are contained in the SHEXTL (5.10) program package (G. Sheldrick, Bruker XRD, Madison, WI). ORTEP diagrams were drawn using the ORTEP3v2 program (L. J. Farrugia, Glasgow).

Table 2.10: Crystal data and structure refinement details for **4** and **11**

Compound	***4***	***11***
Empirical formula	$C_{27}H_{36}Ge_2$	$C_{16}H_{32}GeN_2$
Formula weight (g/mol)	505.74	325.03
Temperature (K)	208(2)	100(2)
Wavelength (Å)	0.71073	0.71073
Crystal system	Triclinic	Monoclinic
Space group	$P\bar{1}$	$P2_1/c$
a (Å)	8.786(2)	14.2022(8)
b (Å)	9.361(3)	8.4666(5)
c (Å)	15.544(4)	14.9069(8)
α (˚)	90.138(5)	90
β (˚)	90.176(5)	93.932(1)
γ (˚)	102.212(5)	90
Volume (Å^3)	1249.5(6)	1788.2(2)
Z	2	4
Calculated density (g/cm^3)	1.344	1.207
Absorption coefficient (mm^{-1})	2.416	1.705
F(000)	524	696
Crystal size (mm)	0.14 × 0.10 × 0.07	0.35 × 0.30 × 0.28
Crystal size and shape	Colorless block	Colorless block
θ range for data collection (o)	2.23-28.27	1.44-28.21
Index ranges	$-11 \le h \le 11$ $-12 \le k \le 12$ $-20 \le l \le 20$	$-14 \le h \le 17$ $-10 \le k \le 10$ $-19 \le l \le 19$
Reflections collected	15365	12764
Independent reflections	5760 (R_{int} = 0.0316)	3935 (R_{int} = 0.0279)
Completeness to θ	25.00 (99.8%)	25.00 (97.6%)
Absorption correction	Semi-empirical from equivalents	Multi-scan
Maximum and minimum transmission	0.8491 and 0.7285	0.6467 and 0.5867
Refinement method	Full-matrix least-squares on F^2	Full-matrix least-squares on F^2
Data/restraints/parameters	5760/0/268	3935/0/172
Goodness of fit on F^2	1.067	1.020
Final R indices ($I > 2\sigma(I)$)		
R_1	0.0335	0.0296
wR_2	0.0892	0.0689
Final R indices (all data)		
R_1	0.0376	0.0388
wR_2	0.0923	0.0733
Largest difference in peak and hole (e Å^{-3})	1.126 and -0.817	0.486 and -0.436

CHAPTER THREE

BRANCHED OLIGOGERMANES

INTRODUCTION

Branched group 14 catenates can be regarded as a two-dimensional array of elements where the presence of branching results in an overall increase in the σ-delocalization in these molecules versus related linear systems.[123] This is attributed to the interaction of the individual arms of the branched system giving rise to different electronic and optical properties than their corresponding linear catenates.[124-125] Group 14 branched oligomers are rare and only a few examples have been reported for tin containing species which include $RSn(SnMe_3)_3$ (R = Me, Et, Bu^n, Bu^i, C_5H_{11} or Ph)[126] as well as the lithium salt $LiSn(SnMe_3)_3$[127] and the neopentyl analogues $Sn(SnR_3)_4$ (R = Me[126] or Ph[128]). A series of longer chain branched perbutyl polystannanes has also been reported.[129]

In the case of germanium, the branched species are even more uncommon, and only a few examples have been reported to date which include $HGe(GePh_3)_3$.[83] $MeGe(GePh_3)_3$[83] and $PhGe(GeX_2Ph)_3$ (R = Cl or Me).[130] The hydride $HGe(Ph_3)_3$ was obtained by the reaction of Ph_3GeLi with GeI_2 and the subsequent treatment of $HGe(Ph_3)_3$ with Bu^nLi followed by the addition of MeI furnished the methyl derivative, $MeGe(GePh_3)_3$. A schematic diagram of these syntheses are shown in Scheme **3.1**. The ^{13}C NMR spectroscopy data in $CDCl_3$ for the branched oligogermanes $PhGe(GePh_3)_3$ and $Ge(GePh_3)_4$ have been reported, but the details regarding their synthesis were not described.[131]

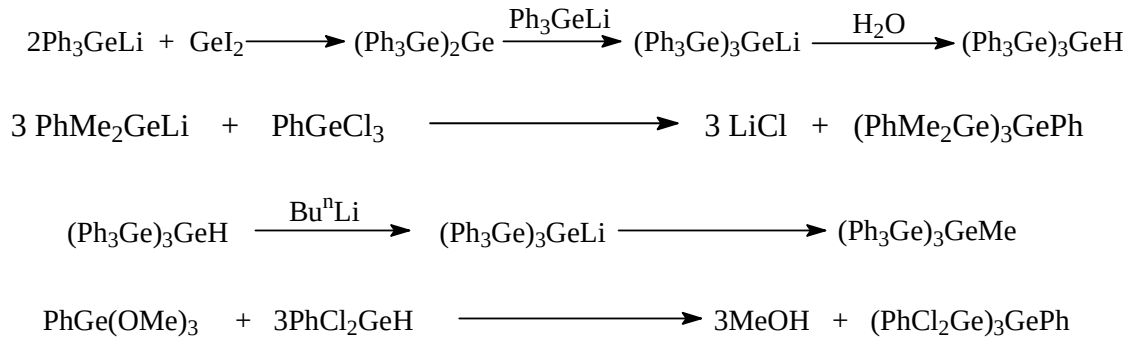

Scheme 3.1: Synthesis of previously reported branched oligogermanes

This study describes the use of the hydrogermolysis reaction for the preparation of discrete branched oligogermanes including the first structurally characterized species, $PhGe(GePh_3)_3$.[132] We also have demonstrated the synthesis of functionally substituted branched tetragermanes which subsequently can be used for the synthesis of branched heptagermanes via implementation of our hydride protection/deprotection strategy. Preparation of a highly branched dendritic oligogermane is also described.

RESULTS AND DISCUSSION

The branched tetragermane $PhGe(GePh_3)_3$ (**1**) was prepared by reaction of $PhGeH_3$ with 3 equivalents of Ph_3GeNMe_2 in CH_3CN solution for 48 h at 85 ºC. The reaction proceeds through the formation of the intermediate α-germyl nitrile Ph_3GeCH_2CN as shown in Scheme 3.2. The ^1H NMR spectrum of **1** in C_6D_6 contains two distinct doublets at δ 7.66 (J = 7.5 Hz) and δ 7.26 (J = 7.5 Hz) ppm in an integrated ratio of 1:9 due to the *ortho*-protons of the mono and triphenylgermyl groups, respectively

(Figure 3.1). The ^{13}C NMR spectrum of **1** in C_6D_6 exhibits eight resonances for the eight different carbons present in the molecule. The resonances for the two different types of ipsocarbon atoms of the phenyl groups appear at 138.9 and 138.6 ppm, where the upfield peak corresponds to the *ipso*-carbon of the monophenyl germyl group. This is due to a slight shielding effect of the three $–GePh_3$ groups attached to the central Ge atom. These ^{13}C NMR chemical shift values are similar to the estimated chemical shift values for **1** in CD_3Cl which has been reported as 138.3 ppm (Ph_3Ge-) and 137.3 ppm (PhGe-).[131]

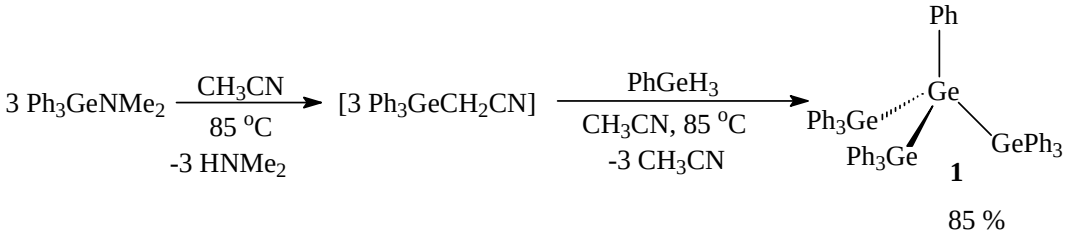

Scheme 3.2: Synthesis of $PhGe(GePh_3)_3$

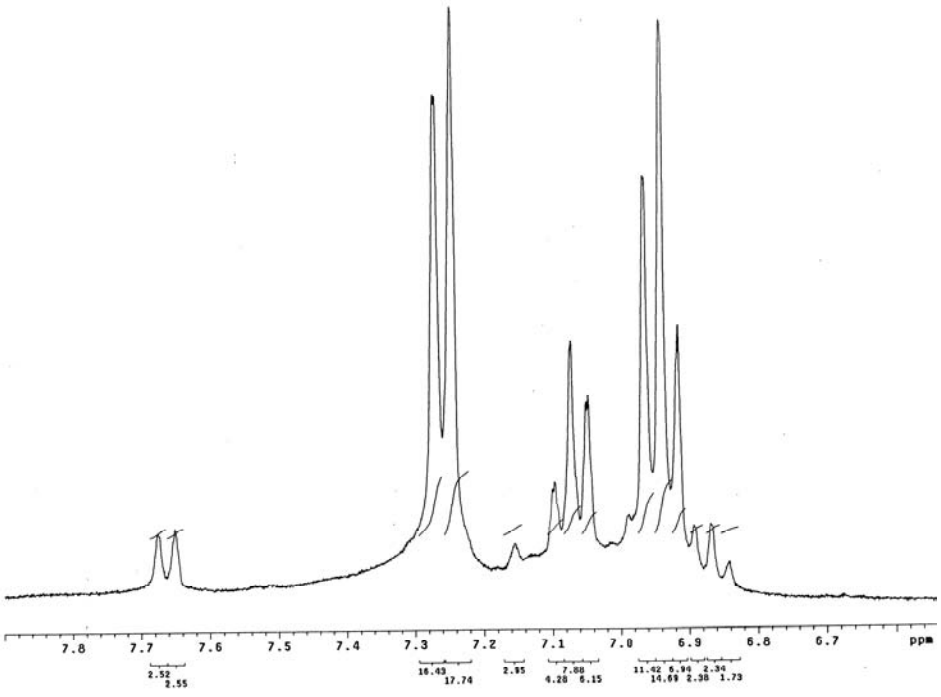

Figure 3.1: ^1H NMR spectrum of **1** (expanded)

The X-ray crystal structure of **1** was obtained and an ORTEP diagram is shown in Figure 3.2 while, selected bond lengths and bond angles are collected in Table 3.1. Compound **1** contains a significantly distorted tetrahedral environment at Ge(1) with an average Ge-Ge-Ge bond angle of 112.72(1)˚. The Ge(2)-Ge(1)-Ge(3) angle is more acute than the other two Ge-Ge-Ge bond angles at Ge(1) by approximately 8˚, which is due to the steric repulsion of the phenyl groups bound to Ge(4) with those attached to Ge(2) and Ge(3). The average C-Ge(1)-Ge angle is acute [105.90(7)˚] and two of these bond angles [C(1)-Ge(1)-Ge(2), 107.51(7)˚ and C(1)-Ge(1)-Ge(4), 107.12(7)˚] are more obtuse than the remaining one [C(1)-Ge(2)-C(19), 103.07˚]. The geometries at each of the three germanium atoms of the -$GePh_3$ groups are very similar and each Ge atom is also present in a distorted tetrahedral environment, although the degree of distortion is less in these three cases than that observed at Ge(1). The average C-Ge-C and C-Ge-Ge angles among Ge(2), Ge(3), and Ge(4) fall into the narrow ranges of 107.2(1)-107.8˚(7) and 111.1(1)-111.6(1)˚, respectively.

The average Ge-Ge bond distance in **1** is 2.469(4) Å, which is elongated relative to both linear and cyclic oligogermanes bearing similar organic substituents. The series of digermanes (discussed in Chapter 2) $R_3GeGePh_3$ (R= Me, Et, Pr^i, Bu^n, Ph) have average Ge-Ge distances in the range 2.418(1)-2.4637(7) Å while the series of higher linear oligogermanes Ge_nPh_{2n+2} have average Ge-Ge bond lengths of 2.440(2) (n = 3),[57] 2.462(3) (n = 4),[57] and 2.460(4) Å (n = 5).[48] The average Ge-Ge distances in the series of cyclic oligomers Ge_nPh_{2n} (n = 4-6) are slightly longer than the related linear species ranging from 2.457(2) to 2.465(2) Å.[133-135] The elongated Ge-Ge distances in **1** are a manifestation of the steric crowding present about the Ge_4 skeleton. The Ge-C distances

to the ipsocarbon atoms of the phenyl substituents in **1** are typical and range from 1.954(2) to 1.971(2) Å, where the longest Ge-C bond is that in the central monophenyl germanium group, which is likely elongated due to electronic effects resulting from the attachment of Ge(1) to three other germanium atoms.

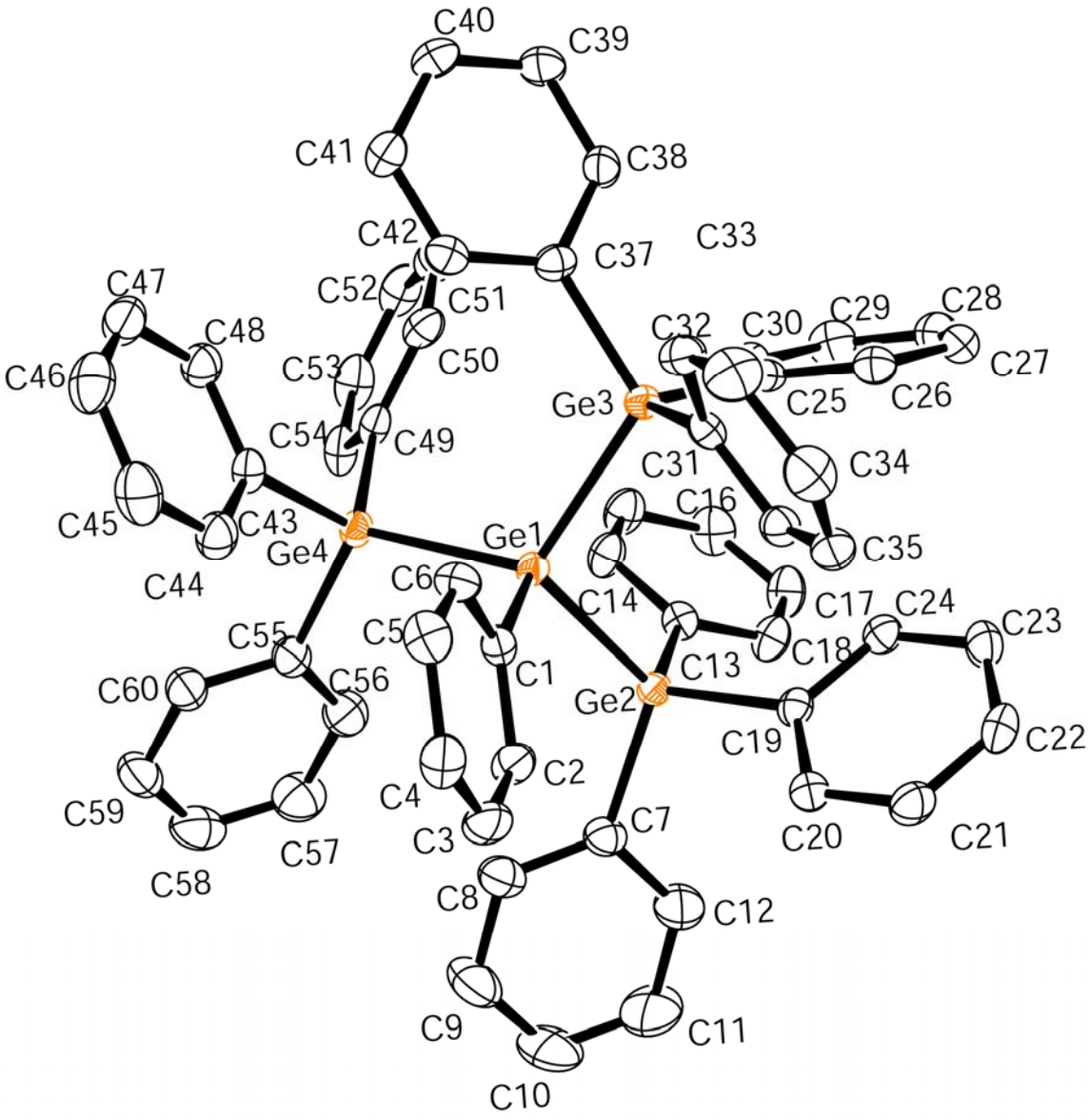

Figure 3.2: ORTEP diagram of $PhGe(GePh_3)_3.C_7H_8$ (**1**·C_7H_8). Thermal ellipsoids are drawn at 50 % probability. The molecule of toluene is not shown.

Table 3.1: Selected bond distances (Å) and angles (˚) for $PhGe(GePh_3)_3 \cdot C_7H_8$ (**1**$\cdot C_7H_8$)

Ge(1)-Ge(2)	2.4552(4)	Ge(2)-Ge(1)-Ge(3)	107.41 (1)
Ge(1)-Ge(3)	2.4753(4)	Ge(2)-Ge(1)-Ge(4)	115.70 (1)
Ge(1)-Ge(4)	2.4772(4)	Ge(3)-Ge(1)-Ge(4)	115.06 (1)
Ge(1)-C(1)	1.971(2)	C(1)-Ge(1)-Ge(2)	107.51 (7)
Ge(2)-C(7)	1.961(2)	C(1)-Ge(1)-Ge(3)	103.07 (7)
Ge(2)-C(13)	1.954(2)	C(1)-Ge(1)-Ge(4)	107.12 (7)
Ge(2)-C(19)	1.961(2)	C(7)-Ge(2)-C(13)	109.0 (1)
Ge(3)-C(25)	1.959(3)	C(7)-Ge(2)-C(19)	103.9 (1)
Ge(3)-C(31)	1.959(2)	C(13)-Ge(2)-C(19)	108.7 (1)
Ge(3)-C(37)	1.959(2)	C(7)-Ge(2)-Ge(1)	116.6 (8)
Ge(4)-C(43)	1.962(2)	C(13)-Ge(2)-Ge(1)	109.3 (7)
Ge(4)-C(49)	1.963(3)	C(19)-Ge(2)-Ge(1)	109.0 (7)
Ge(4)-C(55)	1.965(2)	C(25)-Ge(3)-C(31)	107.7 (1)
		C(25)-Ge(3)-C(37)	106.4 (1)
		C(31)-Ge(3)-C(37)	108.0 (1)
		C(25)-Ge(3)-Ge(1)	113.90 (7)
		C(31)-Ge(3)-Ge(1)	106.29 (7)
		C(37)-Ge(3)-Ge(1)	114.26 (7)
		C(43)-Ge(4)-C(49)	109.8 (1)
		C(43)-Ge(4)-C(55)	106.8 (1)
		C(49)-Ge(4)-C(55)	106.7 (1)
		C(43)-Ge(4)-Ge(1)	108.51 (7)
		C(49)-Ge(4)-Ge(1)	112.28 (7)
		C(55)-Ge(4)-Ge(1)	112.63 (7)

The longer Ge-C distance of the monophenyl germanium group in **1** suggests that this bond might be weaker than the other nine Ge-C_{ipso} bonds. Triflic acid has been shown to selectively cleave an aromatic Ge-C bond in the presence of aliphatic Ge-C bonds. The selectivity of this reaction in the presence of different aryl groups has also been described.[136-137] Studies conducted on a small scale and a large preparative scale indicated that reaction of **1** with exactly 1 equivalent of triflic acid furnished a monotriflate compound presumed to be $(F_3CO_2SO)Ge(GePh_3)_3$ (**2**) that exhibited a single resonance at δ -77.7 ppm in its ^{19}F NMR spectrum (Scheme 3.3 and Figure 3.3). The free triflate anion has C_{3v} symmetry and coordination to a metal center reduces the symmetry to C_s, resulting in the expected appearance of two bands in its IR spectrum for $\nu_{as}(SO_3)$ stretching modes as opposed to one feature in the free ion. The IR spectrum of **2** in a Nujol mull exhibited bands at 1305 and 1261 cm^{-1} corresponding to the $\nu_{as}(SO_3)$ stretching modes. Sharp features at 1200 and 1150 cm^{-1} for the $\nu_s(CF_3)$ and $\nu_{as}(CF_3)$ modes, respectively, and a band at 937 cm^{-1} due to the $\nu_s(SO_3)$ stretching mode were also observed, where assignments for these bands are based on those for $Ph_3GeOSO_2CF_3$,[138] $AgOSO_2CF_3$,[139] $NaOSO_2CF_3$,[140] and the normal coordinate analysis conducted for $[Bu_4N][OSO_2CF_3]$.[141]

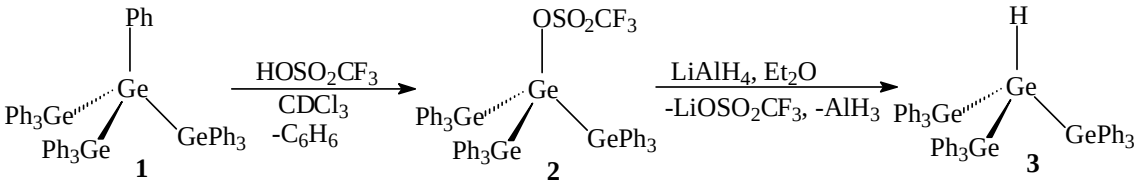

Scheme 3.3: Synthesis of $HGe(GePh_3)_3$ from $PhGe(GePh_3)_3$

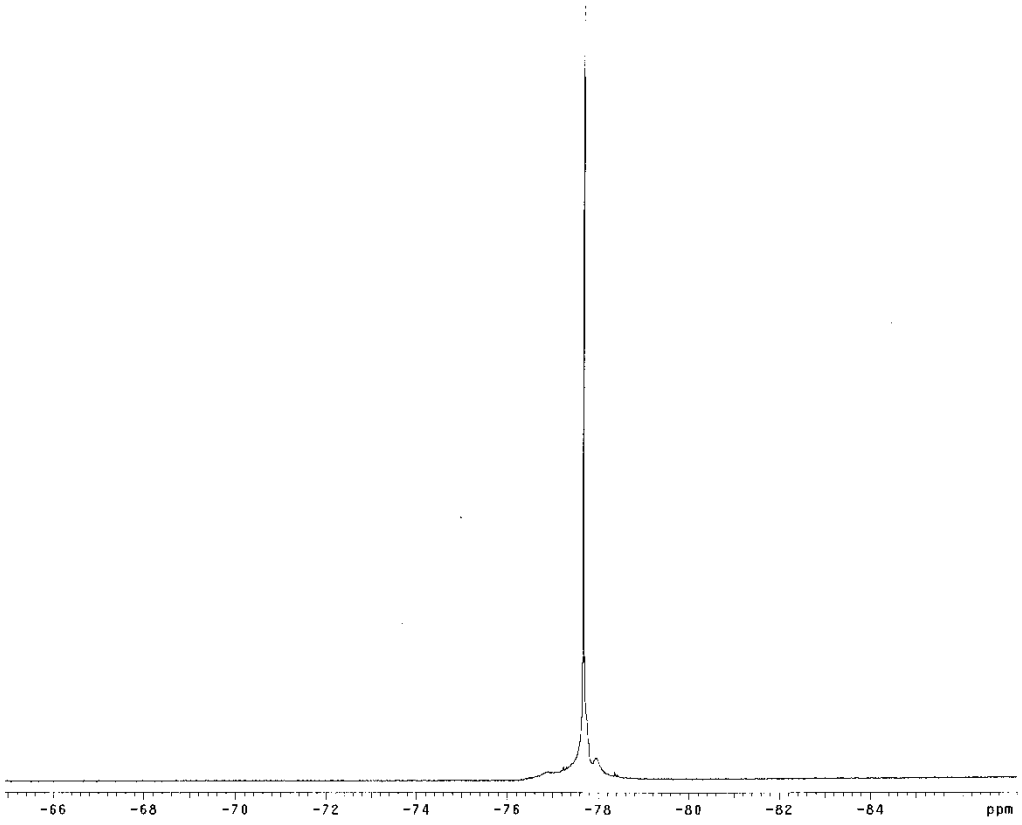

Figure 3.3: ^{19}F NMR of $(F_3CO_2SO)Ge(GePh_3)_3$

Subsequent treatment of **2** with an ethereal solution of $LiAlH_4$ generated the hydride $HGe(GePh_3)_3$ (**3**) as shown by ^1H NMR and IR spectroscopy and elemental analysis. The ^1H NMR spectrum of **3** contains a single hydride resonance at δ 4.58 ppm and a doublet for the *ortho*-hydrogen atoms of the $–GePh_3$ groups is clearly visible at 7.26 (J = 8.1 Hz) ppm. The IR spectrum of **3** contains a Ge-H stretching band at 1953 cm^{-1} and this feature is identical with the value reported in the literature for $HGe(GePh_3)$.[83] Crystals of **3** were obtained and the ORTEP diagram is shown in Figure 3.4 while selected bond distances and bond angles are collected in Table 3.2.

As expected the average Ge-Ge bond distance in **3** is 2.430(5) Å which is shorter than the average Ge-Ge bond distance of **1** [2.469(4) Å]. This is due to the diminished steric crowding around the central Ge atom in **3** compared to the central Ge atom of **1.** Also, the average Ge-Ge bond distance in **3** is slightly longer than the Ge-Ge bond distance of digermanes $R_3GeGePh_3$ [R = Me, (2.418 Å), Bu^n, (2.4212 Å), Et, (2.4253 Å), $PhMe_2$, (2.4216 Å)] but shorter than that of $Pr^i_3GeGePh_3$ (2.4637 Å), $Ph_3GeGePh_3$ (2.437 Å), higher linear oligomers Ge_nPh_{2n+2} (n = 3-5) [2.440(2) (n = 3),[57] 2.462(3) (n = 4),[57] 2.460(4) Å (n = 5)[48]] and cyclic oligomers Ge_nPh_{2n} (n = 4-6) ranging from 2.457(2) to 2.465(2) Å.[133-135]

The Ge-Ge-Ge bond angles at Ge(1) are obtuse and distorted from the expected tetrahedral geometry with an average bond angle of 115.49(17)˚. Similar to compound **1**, the geometries around each of the three Ge atoms of the –$GePh_3$ groups in **3** are similar with average bond angles ranging from 108.02(12)˚ to 109.5(12)˚ but each germanium atom is distorted from the idealized tetrahedral geometry at each Ge center. Two of these C-Ge-C bond angles are more acute than the remaining C-Ge-C angle, with the more obtuse angles at each of the three Ge centers being C(7)-Ge(2)-(C13), C(19)-Ge(3)-C(25), and C(43)-Ge(4)-C(37) angles. This is due to the diminished steric repulsion arising from the hydrogen atom attached to the Ge(1) in **3** compared with the Ph group attached to the Ge(1) in **1.**

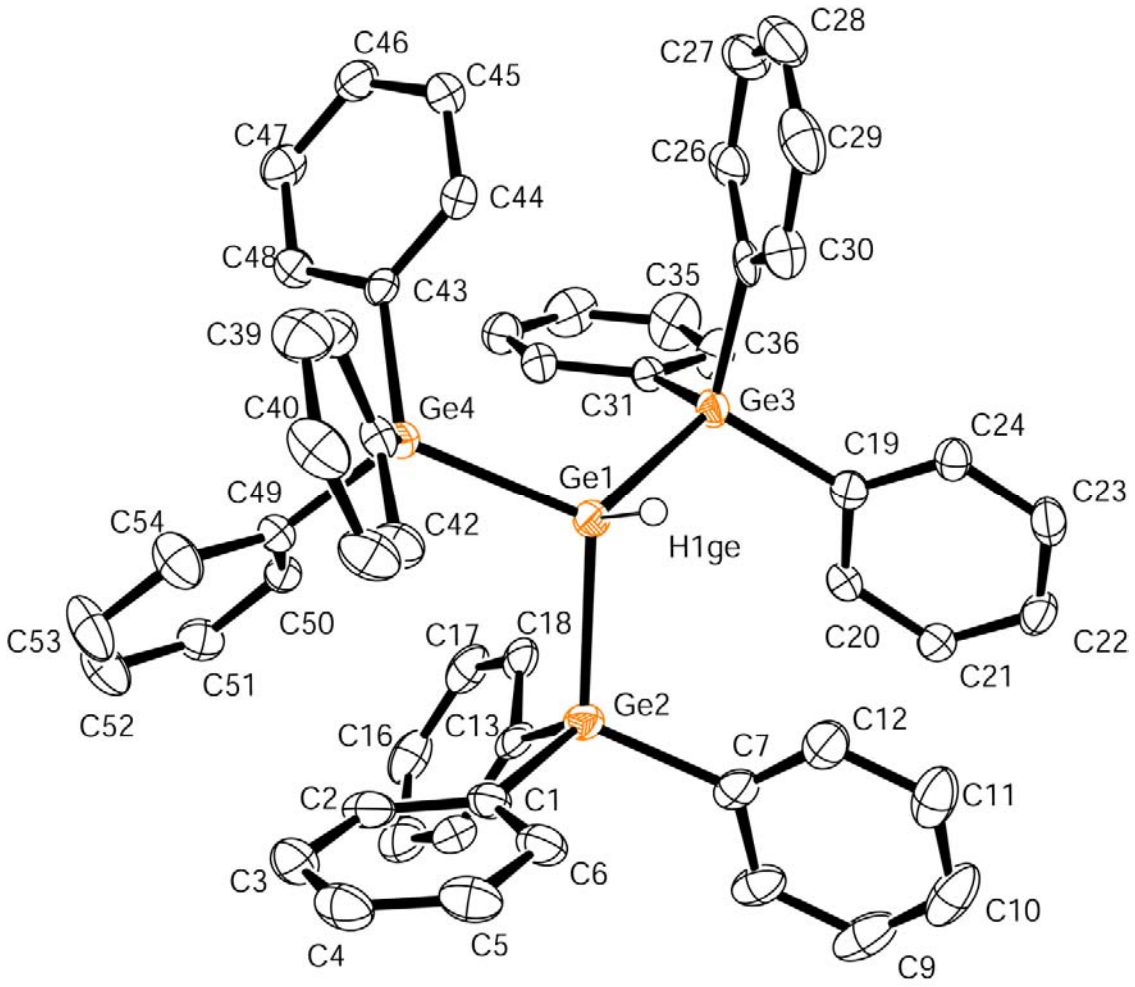

Figure 3.4: ORTEP diagram of $HGe(GePh_3)_3$ **(3)**. Thermal ellipsoids are drawn at 50 % probability. The molecule of toluene is not shown.

Table 3.2: Selected bond distances (Å) and angles (˚) for $HGe(GePh_3)_3$ (**3**)

Ge(1)-Ge(2)	2.4271(5)	Ge(2)-Ge(1)-Ge(3)	116.112(18)
Ge(1)-Ge(3)	2.4298(5)	Ge(2)-Ge(1)-Ge(4)	112.490(17)
Ge(1)-Ge(4)	2.4360(5)	Ge(3)-Ge(1)-Ge(4)	117.893(17)
Ge(2)-C(1)	1.953(3)	C(7)-Ge(2)-C(13)	111.97(12)
Ge(2)-C(7)	1.950(3)	C(7)-Ge(2)-C(1)	107.21(12)
Ge(2)-C(13)	1.951(3)	C(13)-Ge(2)-C(1)	109.567(13)
Ge(3)-C(19)	1.948(3)	C(1)-Ge(2)-Ge(1)	106.58(8)
Ge(3)-C(25)	1.953(3)	C(7)-Ge(2)-Ge(1)	110.27(9)
Ge(3)-C(31)	1.949(3)	C(13)-Ge(2)-Ge(1)	111.04(8)
Ge(4)-C(37)	1.948(3)	C(19)-Ge(3)-C(25)	110.21(12)
Ge(4)-C(43)	1.947(3)	C(19)-Ge(3)-C(31)	107.79(12)
Ge(4)-C(49)	1.951(3)	C(31)-Ge(3)-C(25)	107.00(12)
		C(19)-Ge(3)-Ge(1)	108.68(8)
		C(31)-Ge(3)-Ge(1)	115.50(9)
		C(25)-Ge(3)-Ge(1)	107.63(9)
		C(43)-Ge(4)-C(37)	111.61(11)
		C(43)-Ge(4)-C(49)	106.57(12)
		C(37)-Ge(4)-C(49)	105.88(12)
		C(43)-Ge(4)-Ge(1)	112.07(9)
		C(37)-Ge(4)-Ge(1)	107.78(9)

Compound **3** contains a hydride functionality, which might be treated with another germanium amide to extend the branched framework by adding another Ge atom to the central Ge. Attempts to synthesize the neopentyl analogue of germanium $Ge(GePh_3)_4$ (**4**) by treating an acetonitrile solution of **3** with one equivalent of Ph_3GeNMe_2 for 48 h at 85 °C was unsuccessful. Only **3** and Ph_3GeCH_2CN were detected in the ^1H NMR spectrum of the product mixture. The synthesis of compound **4** was attempted by the use of germane gas GeH_4 and amide Ph_3GeNMe_2. To a slight excess of GeH_4 was added four equivalent of Ph_3GeNMe_2 in acetonitrile and the reaction mixture was heated at 85 °C for 48 hours which resulted a yellow solid material as the crude product. Subsequent distillation of the crude material in a Kugelrohr oven resulted in the isolation of $HGe(GePh_3)_3$, instead of the desired neopentyl analogue $Ge(GePh_3)_4$. Accordingly, it can be concluded that the hydride $HGe(GePh_3)_3$ is not very reactive towards the hydrogermolysis reaction. The ^1H NMR resonance obtained for $HGe(GePh_3)_3$ is highly upfield (δ 4.58 ppm) compared to that of Ph_3GeH (δ 5.64 ppm). This is due to the electronic effect caused by the surrounding three Ph_3Ge- groups attached to the central Ge atom.

The tetragermane $PhGe(GeBu_3)_3$ (**5)** which is the butyl analog of compound **1** was prepared by the reaction of 3 equivalent of Bu_3GeNMe_2 with $PhGeH_3$ and isolated in 98 % yield as shown in Scheme 3.4. The reaction time required for the formation of **5** was 72 h which is longer than the time required for **1**. This species is a viscous colorless oil at room temperature. The formation of **5** was confirmed by NMR and elemental analysis (Figure 3.5).

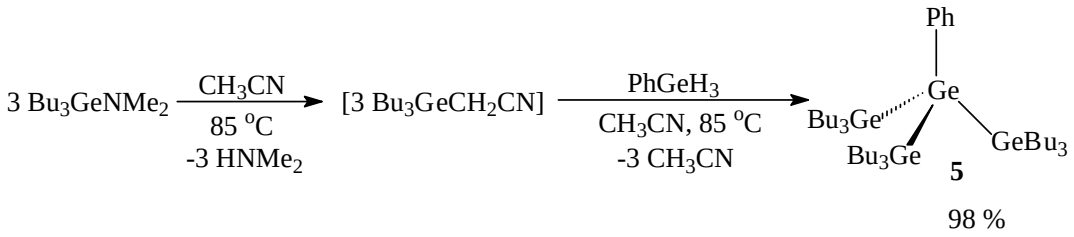

Scheme 3.4: Synthesis of compound **5**

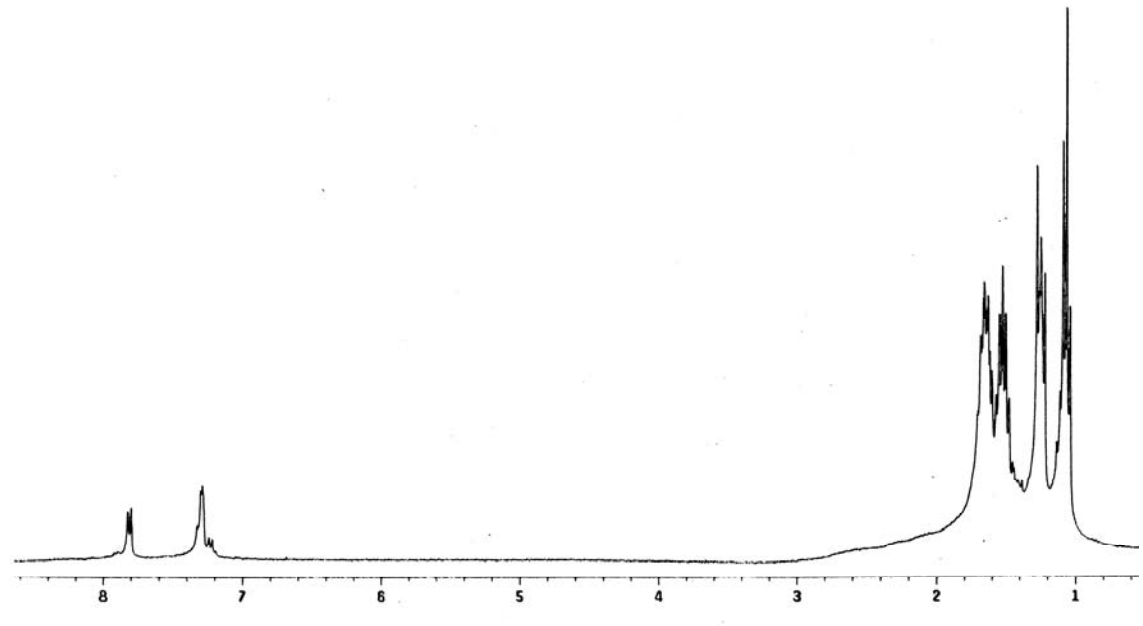

Figure 3.5: ^{1}H NMR of compound **5**

The stepwise synthesis of linear oligogermanes was achieved by the attachment of a β-ethoxy ethyl side group at the terminus of the Ge-Ge chain and was described in Chapter 2. Cleavage of this moiety with DIBAL-H followed by treatment of the resulting hydride with a germanium amide in CH_3CN solution resulted in the incorporation of an additional Ge atom into the backbone. This methodology is also applicable for the stepwise synthesis of branched oligogermanes. The branched tetragermane $PhGe(GeBu_2CH_2CH_2OEt)_3$ (**6**) was prepared in 96 % yield starting from $PhGeH_3$ and the synthon $Bu_2Ge(NMe_2)CH_2CH_2OEt$ (**6a**) in CH_3CN as shown in Scheme 3.5. The formation of the Ge-Ge bonds in **6** again proceeded via initial conversion of **6a** to the α-germylnitrile of **6a** upon reaction of the amide with CH_3CN, which then reacted with Ph_3GeH to furnish the product. The ^1H NMR spectrum of **6** exhibits resonances at δ 3.59 and 3.31 ppm for the protons of the methylene groups adjacent to the oxygen atom of the ethoxyethyl group (Figure 3.6 and 3.7).

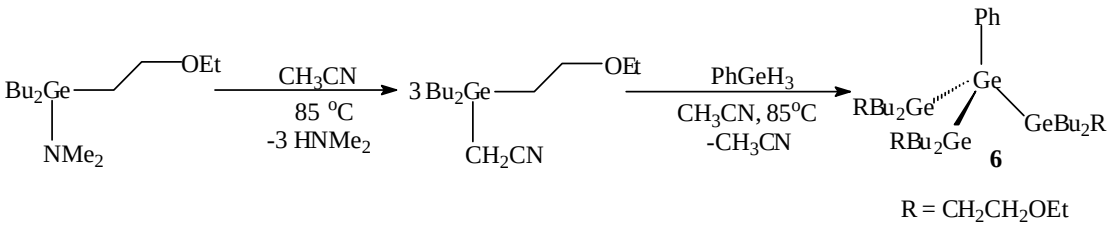

Scheme 3.5: Synthesis of tetragermane **6**

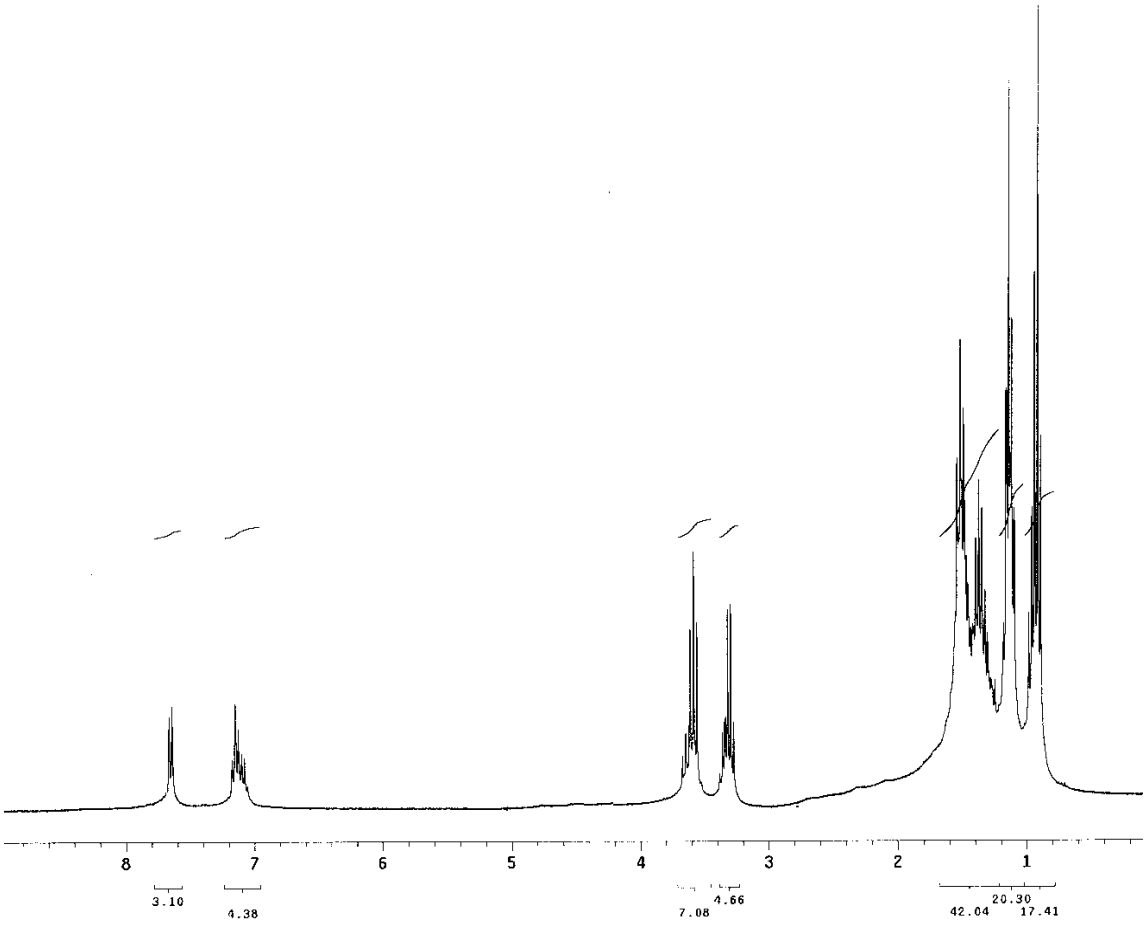

Figure 3.6: ^{1}H NMR of PhGe($GeBu_2CH_2CH_2OEt)_3$ (**6**)

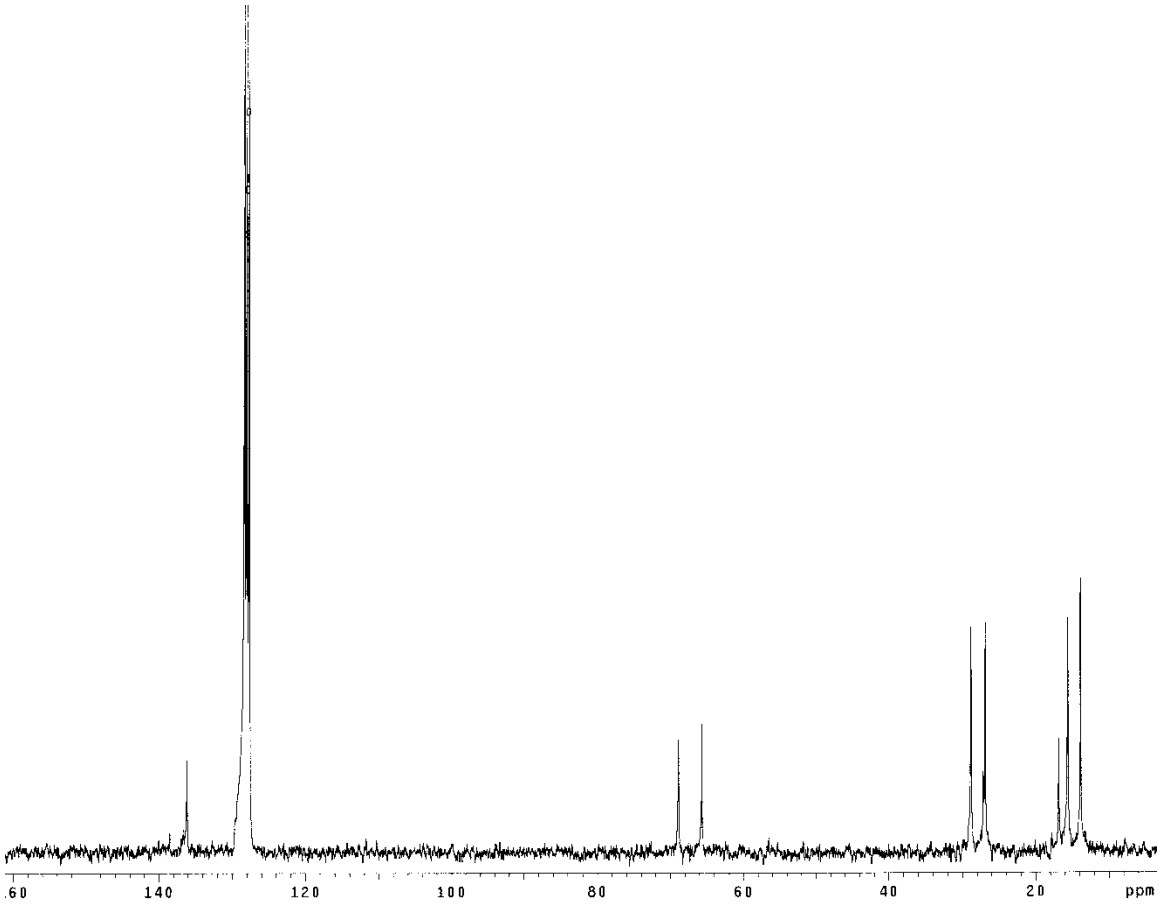

Figure 3.7: ^{13}C NMR of compound **6**

Reaction of **6** with 3 equivalents of DIBAL-H furnishes the intermediate hydride **7**, which was not isolated. Rather, the crude product mixture was dissolved in CH_3CN and treated with 3 equivalents of **6a–c** to generate the branched heptagermanes **8a-c** in moderate to good yields after purification by silica gel column chromatography (Scheme 3.6). The ^1H NMR spectra of **8a** and **8b** exhibit resonances for the methylene groups adjacent to the oxygen atoms which are shifted from those of **5**, appearing at δ 3.67 and

3.41 ppm for **8a** and δ 3.36 and 3.23 ppm for **8b**. The resonances for these methylene groups in the phenyl derivative **8c** are similar to those of **5** appearing at δ 3.59 and 3.32 ppm.

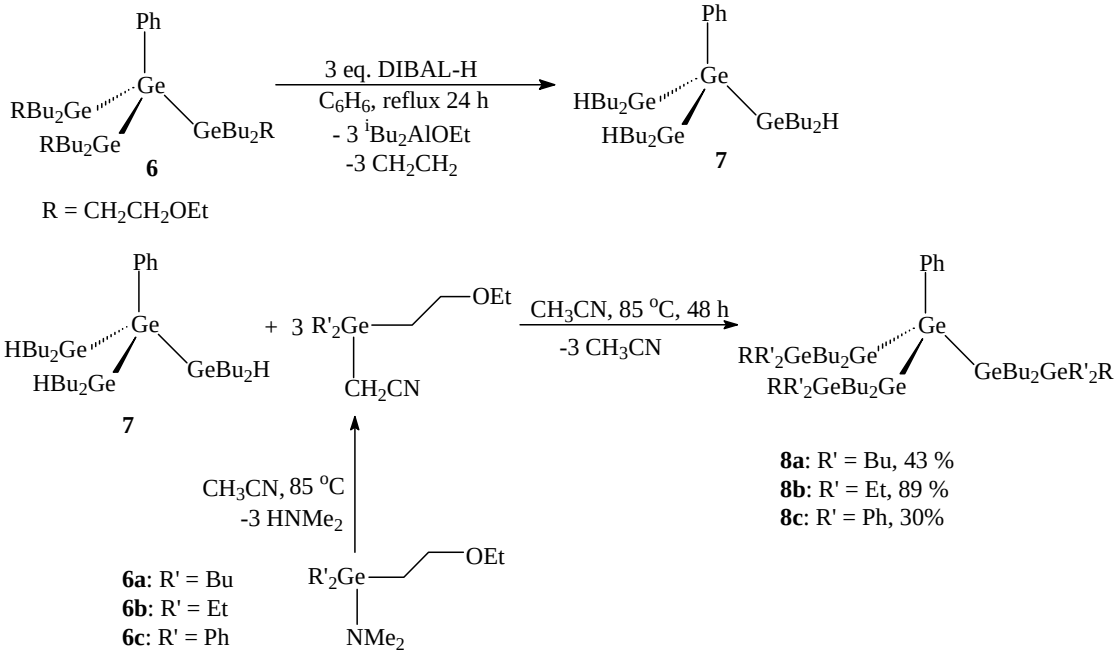

Scheme 3.6: Synthesis of heptagermanes **8a**, **8b** and **8c**

The hydride **7** is a potential building block for the synthesis of highly branched dendritic compounds, where the branching can be extended by reaction of **7** with three-equivalents of germanium amide since it possesses three hydrides. In the synthesis of compound **11**, the starting chloride was prepared by reacting $PhGeH_2Cl$[114] with two equivalents of Ph_3GeNMe_2 in acetonitrile solution. The resulted branched precursor chloride $PhGe(Cl)(GePh_3)_2$ (**9**) was converted to the corresponding amide $PhGe(NMe_2)(GePh_3)_2$ (**10**) with the reaction of $LiNMe_2$ in benzene. The hydride **7** was

treated with three equivalents of amide **10** in acetonitrile to furnish dendrimer compound **11** (Scheme 3.7).

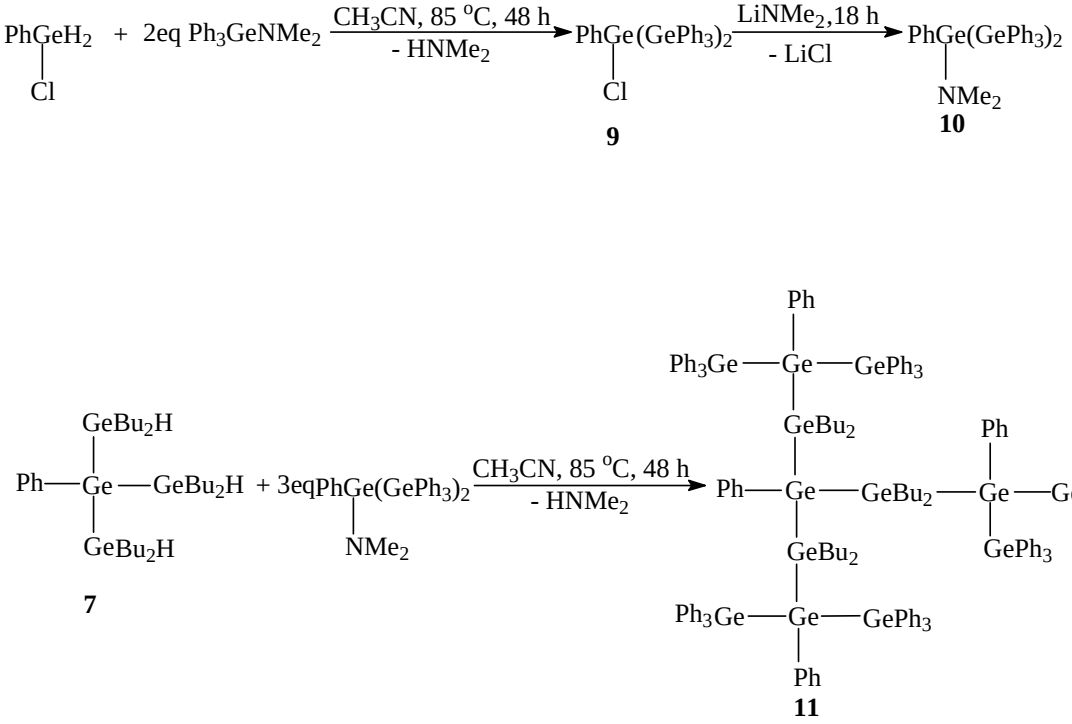

Scheme: 3.7: Synthesis of dendrimer **11**

The formation of compound **11** was confirmed by NMR and elemental analysis. The ^{1}H NMR spectrum of **11** contains three distinct doublets at δ 7.60 (*J* = 7.2 Hz), δ 7.50 (*J* = 7.6 Hz), and δ 7.25 (*J* = 7.6 Hz) ppm due to the *ortho* protons of the peripheral monophenyl, central monophenyl and triphenyl groups respectively. The absorption data compound **11** was also obtained and the UV/visible spectrum of **11** is shown in Figure 3.8. A broad peak is present as a shoulder with absorbance maximum at 254 nm arising from σ→σ* transition.. The absorption values of compound **11** are similar to λ_{max} values of hexagermanes $Me_{14}Ge_6$ (255 nm)[91], $Et_{14}Ge_6$ (258 nm),[81] and $(Me_2Ge)_6$ (250 nm),[88] but

lower in energy compared to those of $Ph(GeEt_2)_6Ph$ (264 nm),[74] $Ph_3Ge(GeEt_2)_4GePh_3$ (278 nm)[74] and $(Ph_2Ge)_6$ (270 nm).[88]

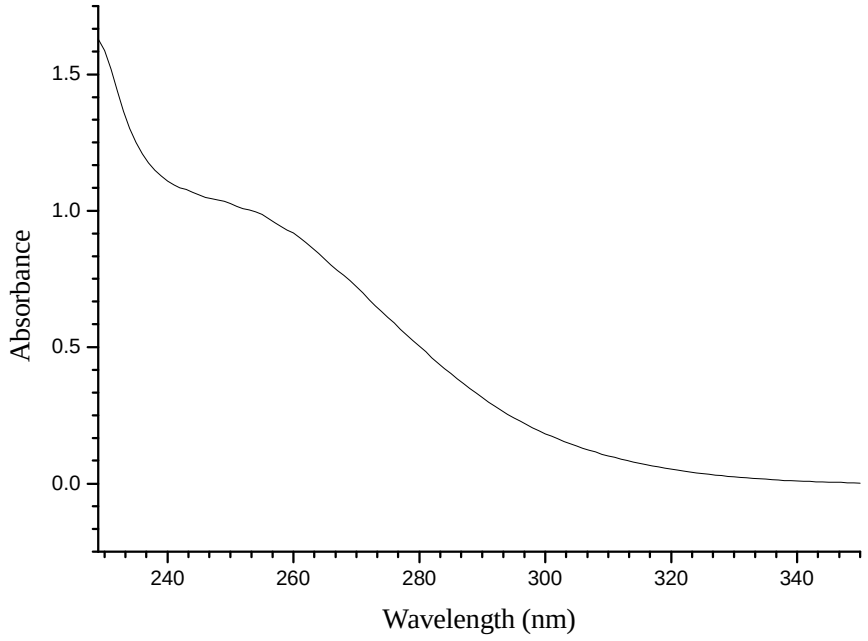

Figure 3.8: UV/visible spectrum of **11**

CONCLUSIONS

The hydrogermolysis reaction is useful in the synthesis of linear oligogermanes as well as branched oligogermanes. The first structurally characterized branched oligogermane $PhGe(GePh_3)_3$ (**1**) has been synthesized, and the phenyl group attached to the central germanium can be selectively removed by triflic acid to give **2**. Subsequent treatment of **2** with $LiAlH_4$ produces $HGe(GePh_3)_3$ (**3**), which is unreactive towards the hydrogermolysis reaction. The functionally substituted branched tetragermane

$PhGe(GeBu_2CH_2CH_2OEt)_3$ was also prepared and characterized. This material can be used as a starting material for the synthesis of highly branched oligomers using the hydrogermolysis reaction coupled with our hydride protection/deprotection strategy, and was used for the preparation of the heptagermanes $PhGe(GeBu_2GeR_2CH_2CH_2OEt)_3$ (R = Bu, Et, Ph) and a highly branched dendritic tridecagermane $PhGe(GeBu_2(Ge(GePh_3)_2Ph)_3$.

EXPERIMENTAL

All manipulations were carried out under an inert N_2 atmosphere with standard Schlenk, syringe, and glovebox techniques.[116] All nondeutarated solvents were purchased from Aldrich and were purified with the use of a Glass Contour solvent purification system. Reagent $PhGeH_3$ was prepared by reaction of $PhGeCl_3$ (Gelest, Inc.) with $LiAlH_4$ with slight modification of the literature method.[142] NMR spectra were recorded on a Varian Gemini 2000 spectrometer operating at 300.0 MHz (^1H), 282.3 (^{19}F), or 75.5 MHz (^{13}C). The ^{19}F NMR spectra were referenced to $C_6H_5CF_3$ set at δ -63.72 ppm while ^1H and ^{13}C NMR spectra were referenced to the C_6D_6 solvent. UV/visible spectra were recorded on a Hewlett Packard Agilent UV/visible spectroscopy system. Elemental analyses were conducted by Midwest Microlab, LLC (Indianapolis, IN).

Synthesis of $PhGe(GePh_3)_3$ (1)

To a solution of Ph_3GeH (0.191g, 1.25 mmol) in acetonitrile (10 mL) was added a solution of Ph_3GeNMe_2[143] (1.31 g, 3.76 mmol) in acetonitrile (20 mL). The reaction mixture was sealed in a Schlenk tube and then heated in an oil bath at 85 °C for 48 h. There reaction was allowed to cool and the solvent was removed *in vacuo*. Distillation of the crude product mixture (135 °C, 0.001 Torr) yielded 1.131 g (85 %) of **1** colorless crystals (mp 264 °C). ^{1}H NMR (C_6D_6, 25 °C): δ 7.66 (d, J = 7.5, 2H, *ortho*-H ($(C_6H_5)_3Ge)_3Ge(C_6\mathit{H}_5)$), 7.26 (d, J = 7.5 Hz, 18H, *ortho*-H ($(C_6\mathit{H}_5)_3Ge)_3Ge(C_6\mathit{H}_5)$), 7.07 (m, 3H *meta*-H and *para*-H ($(C_6H_5)_3Ge)_3Ge(C_6\mathit{H}_5)$), 6.94 (m, 27H, *meta*-H and *para*-H ($(C_6\mathit{H}_5)_3Ge)_3Ge(C_6H_5)$), ^{13}C NMR ($C_6D_6$, 25 °C): δ138.9 (*ipso*-($(\mathit{C}_6H_5)_3Ge)_3Ge(C_6H_5)$), 138.6 (*ipso*-($(C_6H_5)_3Ge)_3Ge(\mathit{C}_6H_5)$), 136.6 (*ortho*-($(\mathit{C}_6H_5)_3Ge)_3Ge(C_6H_5)$), 134.9 (*ortho*-($(C_6H_5)_3Ge)_3Ge(\mathit{C}_6H_5)$), 128.9 (*para*-($(\mathit{C}_6H_5)_3Ge)_3Ge(C_6H_5)$), 128.6 (para-($(C_6H_5)_3Ge)_3Ge(\mathit{C}_6H_5)$), 128.5 (meta-($(\mathit{C}_6H_5)_3Ge)_3Ge(C_6H_5)$), 128.2 (meta-($(C_6H_5)_3Ge)_3Ge(\mathit{C}_6H_5)$) ppm. UV/vis ($CH_2Cl_2$): λ_{max} 256 nm ($\varepsilon = 5.1 \times 10^4$ L mol^{-1}). *Anal*. Calcd for $C_{60}H_{50}Ge_4$: C, 67.90; H, 4.75 Found: C, 67.43; H, 4.69.

Small scale synthesis of $(F_3CO_2SO)Ge(GePh_3)_3$ (2)

To a solution of $PhGe(GePh_3)_3$ (**1**) (0.090 g, 0.085 mmol) in $CDCl_3$ (0.5 mL) in a screw- cap NMR tube was added neat triflic acid (7.4 μL, 0.013 g, 0.084 mmol) with a micropipette. The reaction mixture was kept at room temperature for 4 H, after which time the ^{19}F NMR spectrum of the solution exhibited a single resonance at δ -77.7 ppm indicating complete consumption of $HOSO_2CF_3$ and formation of $(F_3CO_2SO)Ge(GePh_3)_3$

(**2**). The solution was transferred to a conical flask and the volatiles were removed in vacuo to yield 0.082 g (80 %) of **2** as a white solid. IR (nujol mull) 1305 (s, $\nu_{as}(SO_3)$), 1261 (m, $\nu_{as}(SO_3)$), 1237 (s), 1200 (s, $\nu_s(CF_3)$), 1150 (s, $\nu_{as}(CF_3)$), 1094(s), 1024 (m), 998 (m), 937 (s, $\nu_s(SO_3)$) cm^{-1}.

Small scale synthesis of $HGe(GePh_3)_3$ (3)

The sample of compound (**2**) was dissolved in Et_2O (5 mL) and treated with a solution of $LiAlH_4$ (0.0039 g, 0.10 mmol) in Et_2O (5 mL). The solution was stirred for 4 h at the room temperature and the volatiles were removed *in vacuo*. The crude product mixture was dissolved in benzene (5 mL) and filtered through Celite. The Celite pad was washed with benzene (3 × 2 mL) and the solvent was removed *in vacuo* to yield **3** (0.054 g, 64 % based on **1**) as a white solid (mp 210 °C). ^1H NMR (C_6D_6, 25 °C): δ 7.26 (d, *J* = 8.1, 18H, *ortho*-H ((C_6H_5)$_3$Ge)$_3$GeH), 7.15-6.92 (m, 27H, m*eta*-H and *para*-H ((C_6H_5)$_3$Ge)$_3$GeH)), 4.58 (s, 1H, Ge-*H*) ppm. ^{13}C NMR (C_6D_6, 25 °C): δ136.5 (*ipso*-C), 128.8 (*ortho*-C), 128.6 (*para*-C), 127.5 (*meta*-C) ppm. IR (Nujol mull), 1953 (*v* Ge-H) cm^{-1}. *Anal*. Calcd for $C_{54}H_{46}Ge_4$: C, 65.83; H, 4.71 Found: C, 65.27; H, 4.62.

Preparative scale synthesis of $HGe(GePh_3)_3$ (3)

To a solution of (**1**) (0.200 g, 0.188 mmol) in CH_2Cl_2 (1.1 mL) was added triflic acid (0.017 mL, 0.029 g, 0.19 mmol) under a stream of N_2. The reaction mixture was sealed in a Schlenk tube and stirred for 4 h. The volatiles were removed *in vacuo* to yield

a white solid. The ^{19}F NMR in benzene-d_6 exhibited a single line at δ -77.7 ppm. The solid product was dissolved in Et_2O (10 mL) and treated with $LiAlH_4$ (0.0080 g, 0.21 mmol) in Et_2O (5 mL). The reaction mixture was stirred for 18 h at 25 °C and the solvent was removed *in vacuo* to yield 0.171 g (92 %) of **3** as a white solid. The spectral attributes of the product were identical with those described above.

Synthesis of $PhGe(Ge^nBu_3)_3$ (5)

To a solution of $Bu^n{}_3GeNMe_2$ (0.819g, 2.84 mmol) in acetonitrile (15 mL) was added a solution of Ph_3GeH (0.132 g, 0.864 mmol) in acetonitrile (5 mL). The reaction mixture was stirred at 85 °C for 72 h, and volatiles were removed *in vacuo* to yield a colorless oil. The crude product mixture was vacuum distilled at 140 ºC (0.01 Torr) to yield 0.747 g (89 %) of 5 as a colorless oil. ^1H NMR (C_6D_6, 25 °C): δ 7.77 (d, *J* = 7.8 Hz, 1H, *para*-H), 7.68 (d, *J* = 7.8 Hz, 2H, *ortho*-H), 7.08 (t, 2H *J* = 7.5 Hz, *meta*-H), 1.54-1.24 (m, 36H, $CH_2CH_2CH_2CH_3$), 1.11-1.06 (m, 18H, $-CH_2CH_2CH_2CH_3$), 0.97-0.82 (m, 27H, $-CH_2CH_2CH_2CH_3$) ppm. ^{13}C NMR (C_6D_6, 25 °C): δ136.22 (*ipso*-C), 128.41 (*ortho*-C), 128.19 (*meta*-C), 127.38 (*para*-C), 28.92($-CH_2CH_2CH_2CH_3$), 27.00 ($-CH_2CH_2CH_2CH_3$), 15.31 ($-CH_2CH_2CH_2CH_3$), 13.94 ($-CH_2CH_2CH_2CH_3$)ppm. UV/vis (hexane): λ_{max} 233 nm ($\varepsilon = 1.8 \times 10^5$ L mol^{-1}). *Anal*. Calcd for $C_{42}H_{86}Ge_4$: C, 57.23; H, 9.83 Found: C, 56.77; H, 9.44.

Synthesis of $PhGe(GeBu_2CH_2CH_2OEt)_3$ (6)

To a solution of $PhGeH_3$ (2.00 g, 1.31 mmol) in CH_3CN (10 mL) was added a solution of $Bu_2Ge(NMe_2)CH_2CH_2OEt$ (**6a**) (1.195 g, 3.932 mmol) in CH_3CN (30 mL). The reaction mixture was sealed in a Schlenk tube and heated at 85 °C for 72 h. The volatiles were removed in vacuo to yield viscous yellow oil. The crude product was distilled in a Kugelrohr oven (180 °C, 0.050 Torr) to furnish **5** (1.163 g, 95 %) as a colorless viscous oil. ^{1}H NMR (C_6D_6, 25 °C): δ 7.66 (d, *J* = 6.3 Hz, 2H, *ortho*-H), 7.18-7.08 (m, 3H, m*eta*-H and *para*-H (C_6H_5Ge)), 3.59 (t, *J* = 7.2 Hz, 6H, $GeCH_2CH_2O$-), 3.31 (q, *J* = 7.2 Hz, 6H, $-OCH_2CH_3$), 1.55-1.32 (m, 36H, $-CH_2CH_2CH_2CH_3$) 1.14 (t, *J* = 7.2 Hz, 18H, $-CH_2CH_2CH_2CH_3$) 0.96 (t, *J* = 7.2 Hz, 6H, $GeCH_2CH_2O$-), 0.91 (t, *J* = 7.2 Hz, 9H, $-OCH_2CH_3$) ppm. ^{13}C NMR (C_6D_6, 25 °C): δ 138.4 (*ipso*-C_6H_5), 136.1 (*ortho*-C_6H_5), 128.4 (*para*-C_6H_5), 127.6 (*meta*-C_6H_5), 68.8 ($-OCH_2CH_3$), 65.7 ($-GeCH_2CH_2$-), 28.8 ($GeCH_2CH_2CH_2CH_3$), 27.1 ($GeCH_2CH_2O$-), 26.9 ($GeCH_2CH_2CH_2CH_3$), 16.8 ($GeCH_2CH_2CH_2CH_3$), 16.0 ($-OCH_2CH_3$), 13.8 ($GeCH_2CH_2CH_2CH_3$) ppm. *Anal*. Calcd for $C_{42}H_{86}Ge_4O_3$: C, 54.27; H, 9.33. Found: C, 53.79; H, 9.88.

Synthesis of $PhGe(GeBu_2GeBu_2CH_2CH_2OEt)_3$ (8a)

To a solution of **5** (0.280 g, 0.301 mmol) in benzene (25 mL) was added a 1.0 M solution of DIBAL-H in hexanes (0.903 mL, 0.903 mmol). The reaction mixture was refluxed for 24 h and the volatiles were removed *in vacuo* to yield a thick oil that was dissolved in acetonitrile (25 mL). The resulting solution was treated with $Bu_2Ge(NMe_2)CH_2CH_2OEt$ (**5a**) (0.275 g, 0.905 mmol) in CH_3CN (10 mL) and the

reaction mixture was sealed in a Schlenk tube and heated at 85 °C for 48 h. The volatiles were removed *in vacuo* to yield a thick yellow oil that was eluted through a 1.5 in × 1.5 in. silica gel column with 40 mL of a 1:20 (v/v) mixture of Et_2O: hexane as the eluent. The volatiles were removed from the eluent in vacuo to furnish **8a** (0.193 g, 43 %) as a colorless oil. ^{1}H NMR (C_6D_6, 25 °C): δ 7.73 (d, *J* = 7.5 Hz, 2H, *ortho*-C_6H_5), 7.28-7.17 (m, 3H, m*eta*-C_6H_5 and *para*-C_6H_5 (C_6H_5Ge)), 3.67 (t, *J* = 7.8 Hz, 6H, $GeCH_2CH_2O$-), 3.41 (q, *J* = 6.8 Hz, 6H, -OCH_2CH_3), 1.62-1.12 (m, 78H, -$GeCH_2CH_2CH_2CH_3$ and $GeCH_2CH_2O$-), 1.03-0.97 (m, 45H, $GeCH_2CH_2CH_2CH_3$ and –OCH_2CH_3)ppm. ^{13}C NMR (C_6D_6, 25 °C): δ 139.2 (*ipso*-C_6H_5), 136.2 (*ortho*-C_6H_5), 128.4 (*para*-C_6H_5), 128.2 (*meta*-C_6H_5), 68.9 (-OCH_2CH_3), 65.8 (-$GeCH_2CH_2$-), 29.0 ($GeCH_2CH_2CH_2CH_3$), 28.8 ($GeCH_2CH_2CH_2CH_3$), 27.3 ($GeCH_2CH_2O$-), 27.1 ($GeCH_2CH_2CH_2CH_3$), 26.9 ($GeCH_2CH_2CH_2CH_3$), 16.0 ($GeCH_2CH_2CH_2CH_3$), 15.7 ($GeCH_2CH_2CH_2CH_3$), 14.8 (-OCH_2CH_3), 13.9 ($GeCH_2CH_2CH_2CH_3$ and $GeCH_2CH_2CH_2CH_3$) ppm. *Anal*. Calcd for $C_{66}H_{140}Ge_7O_3$: C, 53.20; H, 9.47. Found: C, 53.52; H, 9.54.

Synthesis of $PhGe(GeBu_2GeEt_2CH_2CH_2OEt)_3$ (8b)

To a solution of **5** (0.370 g, 0.398 mmol) in benzene (20 mL) was added a 1.0 M solution of DIBAL-H in hexanes (1.19 mL, 1.19 mmol). The reaction mixture was heated at reflux for 24 h and the volatiles were removed *in vacu*o to yield a thick oil that was dissolved in CH_3CN (30 mL). The resulting solution was treated with $Et_2Ge(NMe_2)CH_2CH_2OEt$ (**5b**) (0.295 g, 1.19 mmol) in CH_3CN (15 mL) and the reaction was sealed in a Schlenk tube and heated at 85 °C for 48 h. The volatiles were removed *in*

vacuo to yield a thick colorless oil that on eluted through a 1.5 in. × 1.5 in. silica gel column with 40 mL of a 1:10 (v/v) mixture of Ether: hexane as the eluent. The volatiles were removed from the eluent *in vacuo* and the resulting yellow oil was distilled in a Kugelrohr oven (120 °C, 0.050 Torr) to furnish **8b** (0.470 g, 89 %) as a pale yellow oil. ^{1}H NMR (C_6D_6, 25 °C): δ 7.72 (d, *J* = 6.6 Hz, 2H, *ortho*-C_6H_5), 7.27-7.21 (m, 3H, m*eta*-C_6H_5 and *para*-C_6H_5 (C_6H_5Ge)), 3.36 (t, *J* = 6.9 Hz, 6H, -OCH_2CH$_3$), 3.23 (q, *J* = 7.2 Hz, 6H, -GeCH$_2$CH_2O-), 1.61-1.39 (m, 24H, -GeCH$_2$CH_2CH_2CH$_3$), 1.31-1.08 (m, 24H, GeCH_2CH$_2$CH$_2$CH$_3$ and GeCH_2CH$_3$), 1.06-0.98 (m, 45H, GeCH$_2$CH$_2$CH$_2$CH_3, GeCH$_2$CH_3, and OCH$_2$CH_3), 0.82 (t, *J* = 7.5 Hz, 6H, GeCH_2CH$_2$O-) ppm. ^{13}C NMR (C_6D_6, 25 °C): δ 136.6 (*ipso*-C_6H_5), 136.1 (*ortho*-C_6H_5), 128.2 (*para*-C_6H_5), 127.6 (*meta*-C_6H_5), 67.3 (-OCH$_2$CH$_3$), 65.9 (-GeCH$_2$$CH_2$-), 28.8 (GeCH$_2CH_2$$CH_2CH_3$), 27.3 (Ge$CH_2CH_2$O-), 27.0 (GeCH$_2$$CH_2CH_2CH_3$), 15.9 (Ge$CH_2CH_2CH_2CH_3$), 15.3 (Ge$CH_2CH_3$), 14.8 (-OCH$_2$$CH_3$), 13.9 (GeCH$_2CH_2CH_2$$CH_3$), 8.6 (-GeCH$_2$$CH_3$) ppm. *Anal*. Calcd for $C_{54}H_{116}Ge_7O_3$: C, 49.07; H, 8.85. Found: C, 49.42; H, 8.71.

Synthesis of PhGe(GeBu$_2$GePh$_2$CH$_2$CH$_2$OEt)$_3$ (8c)

To a solution of (**5**) (0.200 g, 0.215 mmol) in benzene (25 mL) was added a 1.0 M solution of DIBAL-H in hexanes (0.646 mL, 0.646 mmol). The reaction mixture was heated at reflux for 24 h and the volatiles were removed *in vacuo* to yield a thick oil that was dissolved in CH_3CN (25 mL). The resulting solution was treated with $Ph_2Ge(NMe_2)CH_2CH_2OEt$ (**5c**) (0.222 g, 0.645 mmol) in CH_3CN (10 mL) and the reaction mixture was sealed in a Schlenk tube and heated at 85 °C for 48 h. The volatiles

were removed *in vacuo* to yield a thick yellow oil that was eluted through a 1.5 in. × 1.5 in. silica gel column with 40 mL of a 1:20 (v/v) mixture of E_2O: hexane as the eluent. The volatiles were removed from the eluent *in vacuo* and the resulting yellow oil was distilled in a Kugelrohr oven (120 °C, 0.050 Torr) to furnish **8c** (0.105 g, 30 %) as a pale yellow oil. ^{1}H NMR (C_6D_6, 25 °C): δ 7.74 (d, *J* = 6.6 Hz, 2H, *ortho*-C_6H_5 at $Ge_{central}$), 7.66 (d, *J* = 7.5 Hz, 12H, *ortho*-C_6H_5 at $Ge_{peripheral}$), 7.28-7.14 (m, 21H, *meta*-C_6H_5 and *para*-C_6H_5), 3.59 (t, *J* = 7.5 Hz, 6H, $GeCH_2CH_2O$-), 3.31 (q, *J* = 6.9 Hz, 6H, -OCH_2CH_3), 1.54-1.33 (m, 24H, -$GeCH_2CH_2CH_2CH_3$), 1.22-1.11 (m, 18H, $GeCH_2CH_2CH_2CH_3$ and $GeCH_2CH_2O$-), 0.95 (t, *J* = 7.2 Hz, 9H, -OCH_2CH_3), 0.92 (t, *J* = 7.2 Hz, 18H, $GeCH_2CH_2CH_2CH_3$) ppm. ^{13}C NMR (C_6D_6, 25 °C): δ 139.5 (*ipso*-C_6H_5), 138.6 (*ipso*-C_6H_5), 136.6 (*ortho*-C_6H_5), 136.1 (*ortho*-C_6H_5), 128.5 (*para*-C_6H_5), 128.3 (*para*-C_6H_5), 127.9 (*meta*-C_6H_5), 127.7 (*meta*-C_6H_5), 68.8 (-OCH_2CH_3), 65.7 (-$GeCH_2CH_2$-), 29.0 ($GeCH_2CH_2CH_2CH_3$), 27.2 ($GeCH_2CH_2O$-), 26.9 ($GeCH_2CH_2CH_2CH_3$), 15.9 ($GeCH_2CH_2CH_2CH_3$), 14.8 (-OCH_2CH_3), 13.8 ($GeCH_2CH_2CH_2CH_3$) ppm. *Anal*. Calcd for $C_{78}H_{116}Ge_7O_3$: C, 58.19; H, 7.26. Found: C, 58.79.42; H, 7.57.

Synthesis of $PhClGe(GePh_3)_2$ (9)

To a solution of $PhGeH_2Cl$[114] (0.100 g, 0.534 mmol) in acetonitrile (10 mL) was added a solution of Ph_3GeNMe_2[143] (0.371 g, 1.068 mmol) in acetonitrile (15 mL). The reaction mixture was sealed in a Schlenk tube and then heated in an oil bath at 85 °C for 48 h. The reaction mixture was allowed to cool and the solvent was removed *in vacuo* to yield **9** as a white solid (0.401 g, 94.8 %). ^{1}H NMR (C_6D_6, 25 °C): δ 7.61 (d, *J* = 7.4,

12H, *ortho*-H ($(C_6H_5)_3Ge)_2GeCl(C_6H_5)$), 7.43 (d, *J* = 7.6 Hz, 2H, *ortho*-H ($(C_6H_5)_3Ge)_2GeCl(C_6H_5)$), 7.09-7.04 (m, 18H *meta*-H and *para*-H ($(C_6H_5)_3Ge)_2GeCl(C_6H_5)$), 7.021 (m, 3H, *meta*-H and *para*-H ($(C_6H_5)_3Ge)_2GeCl(C_6H_5)$), ^{13}C NMR ($C_6D_6$, 25 °C): δ 134.9 (*ipso*-($(C_6H_5)_3Ge)_2GeCl(C_6H_5)$), 134.5 (*ipso*-($(C_6H_5)_3Ge)_2GeCl(C_6H_5)$), 134.1 (*ortho*-($(C_6H_5)_3Ge)_2GeCl(C_6H_5)$), 130.6 (*ortho*-($(C_6H_5)_2Ge)_2GeCl(C_6H_5)$), 130.3 (*para*-($(C_6H_5)_2Ge)_2GeCl(C_6H_5)$), 128.9 (*para*-($(C_6H_5)_3Ge)_2GeCl(C_6H_5)$), 128.6 (*meta*-($(C_6H_5)_3Ge)_2GeCl(C_6H_5)$), 128.1 (*meta*-($(C_6H_5)_3Ge)_2GeCl(C_6H_5)$) ppm.

Synthesis of $PhGe(GePh_3)_2NMe_2$ (10)

To a solution of **9** (0.463 g, 0.584 mmol) in benzene (15 ml) was added a solution of $LiNMe_2$ (0.031 g, 0.613 mmol) in benzene (15 ml). The reaction mixture was stirred for 18 h, and then filtered through Celite to yield a clear solution. The volatiles were removed *in vacuo* to yield $PhGe(GePh_3)_2NMe_2$ as a yellow semi-solid (0.402 g, 86 %). ^{1}H NMR (C_6D_6, 25 °C): δ 2.74 (s, 6H, -N(CH_3)$_2$).

Synthesis of $PhGe(GeBu_2(Ge(GePh_3)_2Ph)_3$ (11)

To a solution of **5** (0.077 g, 0.083 mmol) in benzene (20 mL) was added a 1.0 M solution of DIBAL-H in hexanes (0.250 mL, 0.250 mmol). The reaction mixture was heated at reflux for 24 h and the volatiles were removed *in vacu*o to yield a thick oil that was dissolved in CH_3CN (25 mL). The resulting solution was treated with $PhGe(NMe_2)(GePh_3)_2$ (**10**) (0.201 g, 0.249 mmol) in CH_3CN (15 mL) and the reaction mixture was sealed in a Schlenk tube and heated at 85 °C for 48 h. The volatiles were

removed *in vacuo* to yield a thick yellow oil that was eluted through a 1.5 in. × 1.5 in. silica gel column with 40 mL of a 1:20 (v/v) mixture of E_2O: benzene as the eluent. The volatiles were removed from the eluent *in vacuo* and the resulting pale yellow solid was distilled in a Kugelrohr oven (110 °C, 0.040 Torr) to furnish **11** (0.105 g, 30 %) as a pale yellow solid. ^{1}H NMR (C_6D_6, 25 °C): δ 7.6 (d, *J* = 7.2 Hz, 2H, *ortho*-PhGe($GeBu_2$(Ge($GePh_3$)$_2C_6H_5$)$_3$), 7.50 (d, *J* = 7.6 Hz, 6H, *ortho*-C_6H_5Ge($GeBu_2$(Ge($GePh_3$)$_2$Ph))$_3$), 7.25 (d, *J* = 7.6 Hz, 36H, *ortho*-PhGe($GeBu_2$(Ge(Ge(C_6H_5)$_3$)$_2$Ph))$_3$), 7.11-6.99 (m, 63H, *meta*-and *para*-C_6H_5Ge($GeBu_2$(Ge($GePh_3$)$_2$Ph))$_3$), 1.52-1.47 (m, 12H, -$GeCH_2CH_2CH_2CH_3$), 1.37-1.33 (m, 12H, -$GeCH_2CH_2CH_2CH_3$), 1.15-1.11 (m, 12H, $GeCH_2CH_2CH_2CH_3$), 0.92 (t, *J* = 7.6 Hz, 18H, $GeCH_2CH_2CH_2CH_3$) ppm. *Anal*. Calcd for $C_{156}H_{164}Ge_{13}$: C, 62.79; H, 5.54. Found: C, 62.70; H, 5.49.

X-ray Structure determination for (1)

Diffraction intensity data were collected with a Siemens P4/CCD diffractometer. Crystallographic details and details of the X-ray study are shown in Table 3.1. Absorption corrections were applied to all data by using SADABS. The structure was solved with the use of direct methods, completed by difference Fourier synthesis, and refined by full-matrix least-squares procedures on F^2. All non-hydrogen atoms were refined with anisotropic displacement coefficients, and hydrogen atoms were treated as idealized contributions. All software and sources of scattering factors are contained in the

SHEXTL (5.10) program packaged (G. Sheldrick, Bruker XRD, Madison, WI).The ORTEP diagram was drawn with the ORTEP3 program (L. J. Farrugia, Glasgow)

Table 3.3: Crystal data and structure refinement for $PhGe(GePh_3)_3$ (**1**)

Formula	$C_{67}H_{58}Ge_4$
Formula weight (g mol^{-1})	1153.49
Crystal size (nm)	0.30 × 0.15 × 0.10
Crystal system	Monoclinic
Space group	$P2_1/c$
a (Å)	12.6857(8)
b (Å)	18.497(1)
c (Å)	23.226(2)
α (deg)	90
β (deg)	98.340(1)
γ (deg)	90
V ($Å^3$)	5392.1(6)
Z	4
Density $_{calc}$ (g cm^{-1})	1.421
abs coeff (nm^{-1})	2.250
F(000)	2352
θ range (deg)	1.62 to 27.95
Index ranges	$-16 \leq h \leq 16$, $-23 \leq k \leq 23$, $-30 \leq l \leq 30$
No. of reflns collected	49681
No of independent reflns	12299 (R_{int} = 0.0348)
Completeness to θ = 25.00 ˚ (%)	100.0
Abs corr	Multiscan/APEXII SADABS
Max and min transmission	0.8063 and 0.5518
Refinement method	Full-matrix least squares on F^2
No. of data/restraints/parameters	12299/0/641
Goodness-of-fit on F^2	1.014
temp (K)	173(2)
Radiation	Mo Kα
wavelength (Å)	0.71073
R	0.0326
R_w	0.0703
Largest peak and hole (e $Å^{-3}$)	1.540 and -1.247

X-ray Structure determination for (3)

Table 3.4: Crystal data and structure refinement for $HGe(GePh_3)_3$ (**3**)

Formula	$C_{54}H_{46}Ge_4$
Formula weight (g mol^{-1})	985.27
Crystal size (mm)	0.20 × 0.10 × 0.10
Crystal system	Monoclinic
Space group	$P2_1/c$
a (Å)	17.1845(5)
b (Å)	11.2369(3)
c (Å)	24.8346(7)
α (deg)	90
β (deg)	108.380(2)
γ (deg)	90
V ($Å^3$)	4550.9(2)
Z	4
Density $_{calc}$ (Mg m^{-3})	1.438
abs coeff (mm^{-1})	3.309
F(000)	1992
θ range (deg)	2.71 to 64.09˚
Index ranges	$-17 \leq h \leq 19$, $-13 \leq k \leq 12$, $-26 \leq l \leq 27$
No.of reflns collected	30305
No of independent reflns	7027 (R_{int} = 0.0334)
Completeness to θ = 25.00 ˚ (%)	96.8
Abs corr	Multi-scan
Max and min transmission	0.8063 and 0.5518
Refinement method	Full-matrix least squares on F^2
No.of data/restraints/parameters	12299/0/641
Goodness-of-fit on F^2	1.014
temp (K)	173(2)
Radiation	Mo Kα
wavelength (Å)	0.71073
R	0.0326
R_w	0.0703
Largest peak and hole (e $Å^{-3}$)	1.540 and -1.247

CHAPTER FOUR

PHYSICAL CHARACTERIZATION OF OLIGOGERMANES

INTRODUCTION

The development of molecular wires having tunable properties and size is of significance in the areas of molecular electronics and nanotechnology.[144-147] Most attention has centered on the investigation of purely organic systems such as linear oligo- or polyphenylenes and oligothiophenes, where π-conjugation controls the efficacy of electronic communication.[148-151] A variety of transition-metal containing systems have also been explored for this purpose, from discrete self-assembled moieties and complexes connected via π-conjugated spacers[152-155] to covalent assemblies of multimetallic complexes.[156-159] The possibility of using catenated compounds of the heavier group 14 elements has also been investigated, and wires based on arrays of Si, Ge, or Sn centers might be expected to have interesting properties that could be used as electronic models for enhancing the understanding of one-dimensional semiconducting nanowires of these elements.

As has been addressed with silicon[9-19] and tin[20-34,36-37,160] oligomers and polymers, as well as in some sporadic reports on the related germanium congeners, [85,87-88,95,132,161] the optical and electronic properties of these compounds are intimately related to their structure. The electronic properties of linear chains of R_2E units (E = Si, Ge, Sn) have been described to arise from σ conjugation of the sp^3 hybrid orbitals.[1-3] Therefore, one can "coarse-tune" the electronic properties of these molecules by changing the number of bonded group 14 atoms in the backbone of the molecule. For example, the absorbance maximum (λ_{max}) in a series of perethylated germanes $Et(GeEt_2)_nEt$ (*n* = 2-6) undergoes a red shift with increasing chain length, varying from 202 nm for the digermane to 258 nm for the hexagermane.[81] Similarly, in the series $Me(GeMe_2)_nMe$ (*n* = 2-6), the absorption

maximum varies from 194 nm for the dimer (n = 2) to 255 nm for the hexamer (n = 6), and the oxidation potential for the series was also shown to decrease with increasing Ge-Ge chain length, from 1.28 V for the dimer to 0.53 V for the hexamer.[87] For the same series of permethylated oligomers the ionization potential was also shown to decrease in energy with increasing chain length.[88]

The study of ^{73}Ge NMR of oligogermanes is of interest because the ^{73}Ge NMR resonances for oligogermanes can be correlated with the substitution pattern at germanium and with the connectivity of the germanium centers. The acquisition of meaningful ^{73}Ge NMR data has, until recently, only been accomplished with difficulty due to a variety of factors. The highly oblate charge distribution at the ^{73}Ge nucleus is indicated by its large quadruple moment ($q = - 0.2 \times 10^{-28}$ m^2), which typically result in the appearance of broad resonances upon interaction of the quadruple moment with the electric field gradient at the nucleus. The line broadening can be extreme, except in compounds where the germanium atom is symmetrically substituted, such as GeR_4 (R= Me, Et, Pr^n, Bu^n, OMe),[162] $GePh_4$[163] and GeX_4 (X = Cl, Br, I).[164] The resonance frequency at a magnetic field strength of 2.3488 T (^{1}H = 100 MHz) is 3.488 MHz, and therefore a dedicated low-frequency probe is required for observation of the ^{73}Ge nucleus. An additional complication involves acoustic ringing, which arises from transient responses in the probe resulting from the radio frequency pulse; however, several pulse sequences have been developed to suppress this problem.[165-168]

The advent of high-field instruments and advanced software technology has recently allowed the acquisition of ^{73}Ge NMR data for numerous non-symmetric compounds. These include the vinyl and alkynyl species $Me_xGe(CH=CH_2)_{4-x}$[169] and $Me_xGe(C\equiv H)_{4-x}$,[170] the heteroaromatic germanes R_xGeMe_{4-x} (R = 2-furyl, 2-thienyl, 4,5-dihydro-2-furyl),[171] various Ge-substituted germacyclohexanes,[172] several hypervalent germanium compounds,[173-175] and a number of arylgermanes Ar_xGeH_{4-x}.[176-178] The ^{1}J(Ge-H) coupling constants for several of these Ar_xGeH_{4-x} compounds have recently been determined , including those for (*p*-$MeOC_6H_4$)GeH_3 (97 Hz), (*p*-$H_3CC_6H_4$)GeH_3 (96 Hz), $MesGeH_3$ (95 Hz), $PhGeH_3$ (98 Hz), Ph_2GeH_2 (94 Hz), and Ph_3GeH (98 Hz).[178] These Ge-H coupling constants are similar to that observed for GeH_4 (97.6 Hz).[166] In 1999, the first ^{73}Ge NMR data for compounds containing Ge-Ge bonds was reported.[179] Resonances for $Me_3GeGeMe_3$, $Ph_3GeGePh_3$, and $(Ph_3Ge)_3GeH$ were observed at δ -59, -67, and -314 ppm, where the latter peak corresponds to the central germanium atom of $(Ph_3Ge)_3GeH$. A resonance corresponding to the Ph_3*Ge*- atoms was not observed.

The impact of the organic supporting ligands on the electronic properties of these catenates has not yet been fully addressed. For instance, it is highly desirable to understand how the variation of the organic substituents affects the fine tuning of the electronic and electrochemical behavior properties of these systems. The focus of this chapter is to expand on our previous findings concerning the synthesis of these systems (described in Chapters 2 and 3) and describe our findings regarding the impact of the variation of the composition of these molecules on their optical and electronic attributes by considering a combination of experimental data and density functional theoretical calculations.[132,180] This chapter describes the ^{73}Ge NMR characterization of several of the

organogermanium compounds described in Chapters 2 and 3, which we have synthesized using hydrogermolysis reaction.[181]

RESULTS AND DISCUSSION

Computational Studies

In order to facilitate the discussion of the electronic properties of the oligogermanes, it is useful to examine the results of computational studies performed on a comprehensive set of 51 derivatives ranging from digermanes to octagermanes that are either known or hypothetical compounds (shown in Table 4.1). In these studies, all the compounds were subjected to semiempirical quantum mechanical PM3-geometry optimization prior to single-point density functional calculations (DFT) using the B3LYP/6-31G* basis set. Higher-level calculations on several derivatives were also explored (ab initio HF/3-21G geometry optimization followed by DFT B3LY/6-311G**), which gave identical trends but were significantly more computationally expensive (in some cases, prohibitively). Therefore only the results for the smaller, but complete, set using the B3LYP/6-31G* basis will be addressed, as these are also in qualitative agreement with the experimental absorbance and voltammetry investigations. Selected frontier orbitals (HOMO and LUMO) are shown for some parent oligogermanes in Figure 4.1, along with the calculated energies of the orbitals for $R_3Ge(GeR_2)_nGeR_3$ (n = 0-6; R = H,Me) derivatives.

Table 4.1: Summary of structural and electronic properties of various oligogermanes from density functional calculations (B3LYP/6-31G*, SPARTAN06)

R = $-CH_2CH_2OCH_2CH_3$ [a]PM3 geometry optimization

Entry	Compound	HOMO (eV)	LUMO (eV)	Eox (eV)	Avg.Ge-Ge (Å) Calcd[a]
	Ge-Ge				
1	$H_3Ge\text{-}GeH_3$	-7.67	+0.40	8.07	2.393
2	$Me_3Ge\text{-}GeMe_3$	-6.07	+1.52	7.59	2.425
3	$Et_3Ge\text{-}GeEt_3$	-5.33	+1.59	6.92	2.429
4	$Pr^n{}_3Ge\text{-}Ge^nPr_3$	-5.22	+1.61	6.83	2.438
5	$Bu^n{}_3Ge\text{-}Ge^nBu_3$	-5.14	+1.66	6.80	2.438
6	$Pr^i{}_3Ge\text{-}Ge^iPr_3$	-5.58	+1.56	7.14	2.461
7	$Bu^t{}_3Ge\text{-}Ge^tBu_3$	-6.04	+1.11	7.15	2.511
8	$Ph_3Ge\text{-}GePh_3$	-5.45	-0.66	4.79	2.468
9	$F_3Ge\text{-}GePh_3$	-6.93	-1.17	5.76	2.475
10	$H_3Ge\text{-}GePh_3$	-6.17	-0.52	5.65	2.429
11	$CF_3Ge\text{-}GePh_3$	-6.73	-0.99	5.74	2.480
12	$Me_3Ge\text{-}GePh_3$	-5.71	-0.39	5.32	2.447
13	$Et_3Ge\text{-}GePh_3$	-5.46	-0.35	5.11	2.449
14	$Pr^n{}_3Ge\text{-}GePh_3$	-5.41	-0.34	5.07	2.450
15	$Bu^n{}_3Ge\text{-}GePh_3$	-5.38	-0.34	5.04	2.450
16	$Pr^i{}_3Ge\text{-}GePh_3$	-5.56	-0.30	5.26	2.461
17	$Bu^t{}_3Ge\text{-}GePh_3$	-5.76	-0.45	5.31	2.489
18	$RMe_2Ge\text{-}GePh_3$	-5.70	-0.39	5.31	2.448
19	$REt_2Ge\text{-}GePh_3$	-5.51	-0.37	5.14	2.449
20	$R^nBu_2Ge\text{-}GePh_3$	-5.45	-0.36	5.09	2.450
21	$RPh_2Ge\text{-}GePh_3$	-5.56	-0.59	4.97	2.463
	Ge-Ge-Ge				
22	$(\mu\text{-}H_2Ge)[GeH_3]_2$	-7.33	+0.14	7.47	2.387
23	$(\mu\text{-}Me_2Ge)[GeMe_3]_2$	-5.74	+1.16	6.90	2.416
24	$(\mu\text{-}Et_2Ge)[GeEt_3]_2$	-5.34	+1.38	6.72	2.423
25	$(\mu\text{-}Bu^n{}_2Ge)[Ge^nBu_3]_2$	-5.33	+1.01	6.33	2.424
26	$(\mu\text{-}Bu^n{}_2Ge)[GePh_3]_2$	-5.57	-0.61	4.96	2.442
27	$(\mu\text{-}Ph_2Ge)[GePh_3]_2$	-5.41	-0.52	4.89	2.456
28	$(\mu\text{-}Ph_2Ge)[GeMe_3]_2$	-5.48	-0.23	5.25	2.431
29	$(\mu\text{-}Ph_2Ge)[GeEt_3]_2$	-5.12	-0.18	4.94	2.437
30	$(\mu\text{-}Ph_2Ge)[Ge^nBu_3]_2$	-5.07	-0.17	4.90	2.440
31	$(\mu\text{-}Ph_2Ge)[GePh_2R]_2$	-5.49	-0.52	4.97	2.453

32	(μ-Ph_2Ge)[$GeEt_2R]_2$	-5.23	-0.19	5.04	2.439
33	(μ-Ph_2Ge)[$GeBu_2R]_2$	-5.18	-0.10	5.08	2.435
34	(μ-Bu_2Ge)[$GePh_2R]_2$	-5.43	-0.35	5.08	2.436
	Ge-Ge-Ge-Ge				
35	(μ-H_2Ge)$_2$[$GeH_3]_2$	-7.01	-0.11	6.90	2.384
36	(μ-Me_2Ge)$_2$[$GeMe_3]_2$	-5.38	+0.96	6.34	2.412
37	(μ-Et_2Ge)$_2$[$GeEt_3]_2$	-5.00	+0.99	5.99	2.416
38	(μ-$Bu^n{}_2$Ge)$_2$[$Ge^nBu_3]_2$	-4.83	+1.10	5.93	2.416
39	(μ-Ph_2Ge)$_2$[$GePh_3]_2$	-5.12	-0.54	4.58	2.457
40	**R**$Bu^n{}_2$Ge(μ-Ge^nBu_2)$GePh_3$	-5.41	-0.37	5.04	2.435
41	**R**$Bu^n{}_2$Ge(μ-$Ge^nBu_2)_2GePh_3$	-5.20	-0.38	4.82	2.428
42	$REt_2GeGePh_2Ge^nBu_2GePh_3$	-5.22	-0.38	4.84	2.438
43	$RBu^n{}_2GeGePh_2Ge^nBu_2GePh_3$	-5.19	-0.38	4.81	2.439
	Higher oligogermanes				
44	(μ-H_2Ge)$_3$[$GeH_3]_2$	-6.78	-0.34	6.44	2.383
45	(μ-Me_2Ge)$_3$[$GeMe_3]_2$	-5.07	+0.82	5.89	2.409
46	(μ-H_2Ge)$_4$[$GeH_3]_2$	-6.61	-0.50	6.01	2.382
47	(μ-Me_2Ge)$_4$[$GeMe_3]_2$	-4.96	+0.64	5.60	2.408
48	(μ-H_2Ge)$_5$[$GeH_3]_2$	-6.49	-0.62	5.87	2.382
49	(μ-Me_2Ge)$_5$[$GeMe_3]_2$	-4.84	+0.54	5.38	2.408
50	(μ-H_2Ge)$_6$[$GeH_3]_2$	-6.39	-0.70	5.69	2.382
51	(μ-Me_2Ge)$_6$[$GeMe_3]_2$	-4.73	+0.47	5.20	2.407

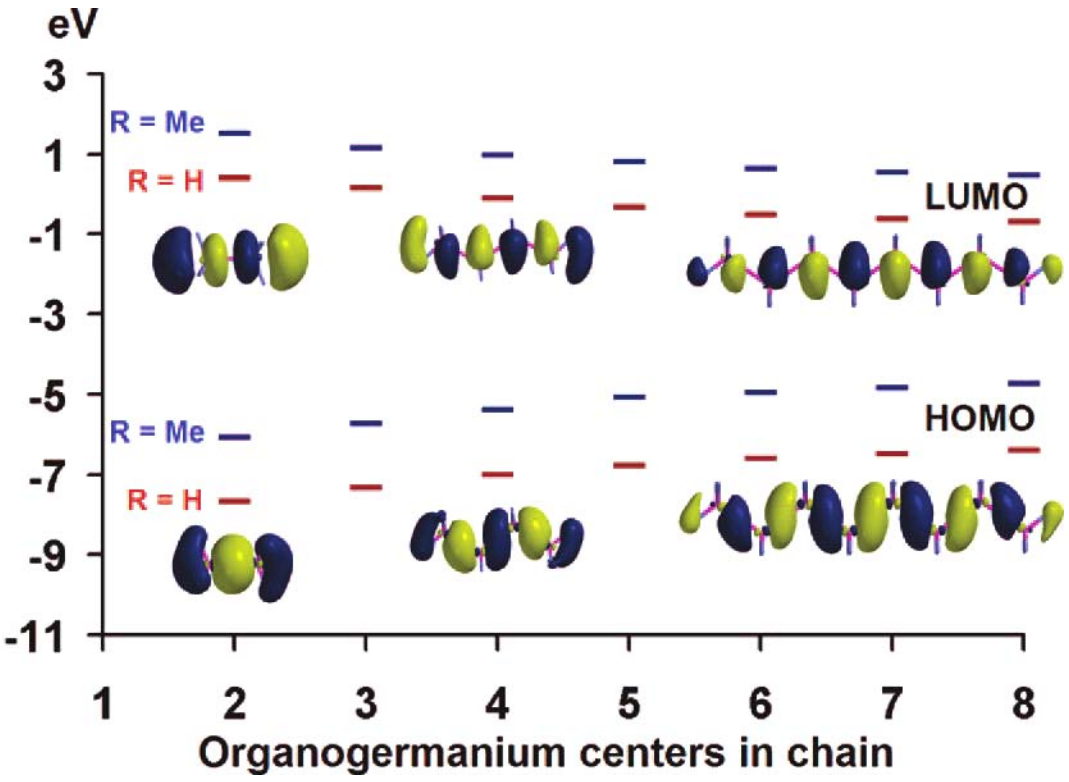

Figure 4.1: Relative energies (eV) of frontier orbitals for $R_3Ge(GeR_2)_nGeR_3$ (n = 0-6): (red lines) R = H; (blue lines) R = Me. The orbital plots for n = 0, 2, 6 are also shown.

With the exception noted below for aryl derivatives, the main feature of the corresponding frontier orbitals for the substituted oligogermanes mirror those for the simple $H_3Ge(GeR_2)_nGeH_3$ (n = 0-6) series in that the HOMO is σ bonding while the LUMO is σ* antibonding in nature. As will be elaborated on, the relatively low symmetry of the oligogermanes (giving rise to a larger number of molecular orbitals of the same symmetry) combined with the close energy separation of the valence 4s and 4p orbitals on germanium results in extensive mixing. Of the compounds studied, the homoleptic digermanes Ge_2R_6 can be differentiated from the higher oligomers by symmetry

considerations. For instance, the Ge_2R_6 series has idealized D_{3d} symmetry which renders one 4p orbital on each germanium atom (p_z, along the internucler C_3 axis) available for σ-bonding interactions and a pair of degenerate 4p orbitals per germanium ($p_{x,y}$ orthogonal to the C_3 axis) available for π-bonding interactions. In contrast, for the homoleptic $R_3Ge(GeR_2)_nGeR_3$ (n = 1-6) series, the highest possible symmetry is C_{2v} for odd values of n and C_{2h} for even values of n. Because of this, only one 4p orbital that is orthogonal to the plane of the molecule participates in π-bonding interactions, while the other two 4p orbitals participate in σ-bonding interactions (*vide infra*).

The main contribution to the frontier orbitals (HOMO and LUMO) for a representative series of oligogermanes $H_3Ge(GeR_2)_nGeH_3$ (n = 0-3) are summarized in Table **4.2**. The HOMO of Ge_2H_6 is a mainly germanium-based σ orbital with only 10 % bonding contribution from an A_{1g} hydrogen group orbital, where the germanium component is comprised mainly (96 %) of two out-of-phase Ge $4p_z$ orbitals mixed with a small amount (4 %) of two in-phase Ge 4s orbitals (bottom left, Table 4.2). The LUMO of Ge_2H_6 is a germanium-based σ* orbital (only 1 % bonding contribution from the A_{2u} hydrogen group orbital) where the germanium component is constructed from a mixture of mainly (68 %) two out-of-phase 4s orbitals mixed with a significant contribution (32 %) of two in-phase Ge $4p_z$ orbitals (top left, Table 4.2).

Table 4.2: Summery of LUMO and HOMO composition from DFT calculations

[a] Nonstandard coordinate system employed for simplicity (x, y normally in molecular plane)

LUMO

	Ge_2H_6 (D_{3d})		Ge_3H_8 (C_{2v})		Ge_4H_{10} (C_{2h})[a]		Ge_5H_{12} (C_{2v})	
	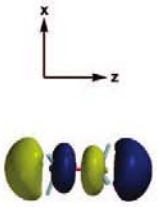		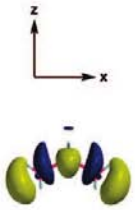		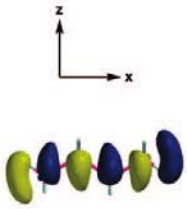		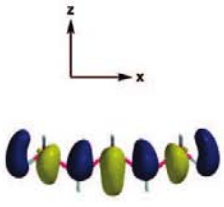	
	A_{2u}, 0.39 eV	%	A_1, 0.14 eV	%	B_u, -0.11 eV	%	A_1, -0.34 eV	%
s		68	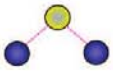	65	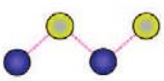	65	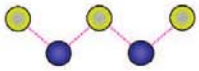	63
p_x	----	0	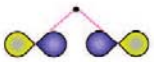	13	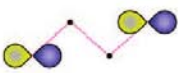	8	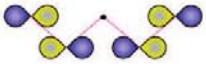	6
p_z	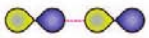	32	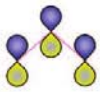	22	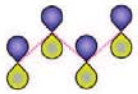	27	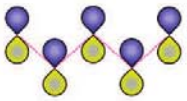	31

HOMO

	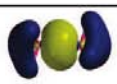		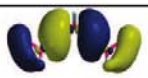		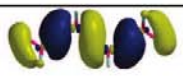		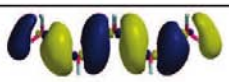	
	A_{1g}, -7.68 eV	%	B_2, -7.33 eV	%	A_g, -6.78 eV	%	B_2, -6.78 eV	%
s		4	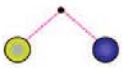	3	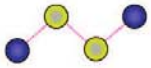	4	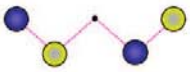	5
p_x	----	0	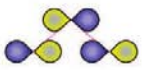	85	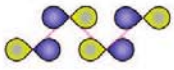	90	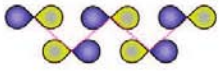	87
p_z		96	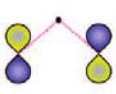	12	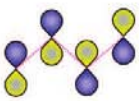	6	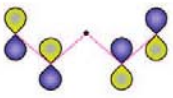	8

For the higher oligogermanes of the form Ge_nH_{2n+2}, the HOMO is germanium based and is comprised mainly (85-91 %) of a molecular orbital composed of out-of-phase $4p_x$ (see Table 4.2 for coordinate system) atomic orbitals. These are mixed with 5-12 % of a molecular orbital comprised of a partly out-of-phase in-plane $4p_z$ atomic orbitals (see Table 4.2 for coordinated system) that have one node in the yz plane and also with 2-5 % of a molecular orbital containing *n* 4s atomic orbitals that are partly "out of phase" with *n*-2 nodes. The LUMO of the higher oligogermanes, Ge_nH_{2n+2}, is also a mixture of three components. In this case, the major component (ca. 65 %) is a molecular orbital comprised of out-of-phase 4s atomic orbitals mixed with 22-30 % of a molecular orbital constructed from in-phase $4p_z$ atomic orbitals. The smallest component (6-13 %) of the LUMO is a set of partly out-of phase $4p_x$ orbitals (x directed along the internuclear axis) that has *n*-1 nodes. To a first approximation with the smallest component of mixing being ignored, the HOMO is essentially out-of-phase $4p_x$ in character while the LUMO represents an in-phase combination of sp hybrid orbitals.

The relative energies of the HOMO and LUMO vary in the expected manner according to the chain length, and the Ge-Ge bond distances, which are guided by the steric bulk of the attached substituents and by the inductive effects of peripheral groups bound to the oligogermane core. Thus, the HOMO energy increases (becomes destabilized) as the proportion of electron-rich R_2Ge^{II} centers increases relative to the terminal R_3Ge^{III} centers. Electron donating groups bound to germanium destabilize the HOMO by making the chain more electron rich, as exemplified by comparing the relative energies of the HOMO in $R_3Ge(GeR_2)_nGeR_3$ (*n* = 0-6; R = H versus R = Me) in Figure

4.1. Similarly, the energy of the HOMO increases along the series Me < Et < Pr^n < Bu^n due to the inductive effects of replacing C-H with C-alkyl groups.

With increasing chain length, the LUMO becomes stabilized via conjugation, as expected from the σ* character. As found for the HOMO, the substitution of electron-donating substituents destabilizes the LUMO via inductive effects, as indicated by a comparison of the CH_3 versus H groups in Figure 4.1. It is also noteworthy that for the new compounds described here replacing a germanium-alkyl group with the CH_2CH_2OEt group has only a very small stabilizing effect on the energies of the frontier orbitals, an exception being the replacement of the CH_3 group with the CH_2CH_2OEt group, where the inductive (destabilizing) effects become important.

Phenyl substitution has a significant impact on the frontier orbitals of oligogermanes, since the phenyl group acts as a better σ donor than either methyl groups or hydrogens and is sufficiently bulky to increase the Ge-Ge bond distance. Therefore, this substitution is expected to significantly raise the energy of the HOMO; however, conjugation with the phenyl group orbitals partially offsets the expected destabilization. Furthermore, the LUMO and next-higher virtual orbitals of the aryl-substituted oligogermanes, which consist of two group orbitals per phenyl ring, are almost exclusively composed of linear combinations of phenyl-based π* orbitals rather than being germanium-based σ*, as these are in-phase sp hybrid orbitals which are higher in energy. Thus, the variation in LUMO energy is very small through the series of aryl-substituted oligogermanes.

As expected, The HOMO-LUMO energy gap in oligogermanes can be coarsely tuned by varying the degree of catenation, with longer chains giving rise to smaller energy gaps. Changing the nature of substituents bound to the oligogermane core changes the relative energy of the HOMO to a greater extent than the energy of the LUMO and therefore provides a simple means for fine-tuning the HOMO-LUMO energy gap of these compounds. Both of these conclusions were also observed experimentally as described below.

Absorption and Electrochemical Characteristics.

Cyclic volatammograms for the various oligogermanes were obtained in CH_3CN solution using 1.0 M $[Bu_4N][PF_6]$ as the supporting electrolyte. Irreversible oxidation waves were observed in all cases, as exemplified for the $Ph_3Ge(GeBu_2)_nGeBu_2CH_2CH_2OEt$ (**2**, n = 0; **3**, n = 1; **4**, n = 2) series shown in Figure 4.2. The values for the oxidation waves are shown in Table 4.3**.** These are for the anodic waves, as the expected cathodic return waves were absent, and are the average values of four independent measurements, which were generally reproducible with errors of less than ±30 mV. The irreversibility of the oxidation waves is in accord with previous finding of electrochemical measurements on permethyloligogermanes.[85,182] Chain contraction of oligogermanes has also been reported to occur via germylene extrusion and heterolytic Ge-Ge bond cleavage,[91] and similar reactions may be responsible for the irreversible process in the compounds described here. Regardless, the relative oxidation potentials of the series of oligogermanes measured in these studies parallel the results found from the DFT calculations, in that the oxidation potential decreases with an increasing proportion of R_2Ge centers along the oligogermane backbone. Thus, the

oxidation potentials of the series **2-4** decrease on traversing from the digermane (1589 mV) to the trigermane (1546 mV) and to the tetragermane (1474 mV). Frontier orbital diagrams for the series **2-4** are shown in Table 4.4.

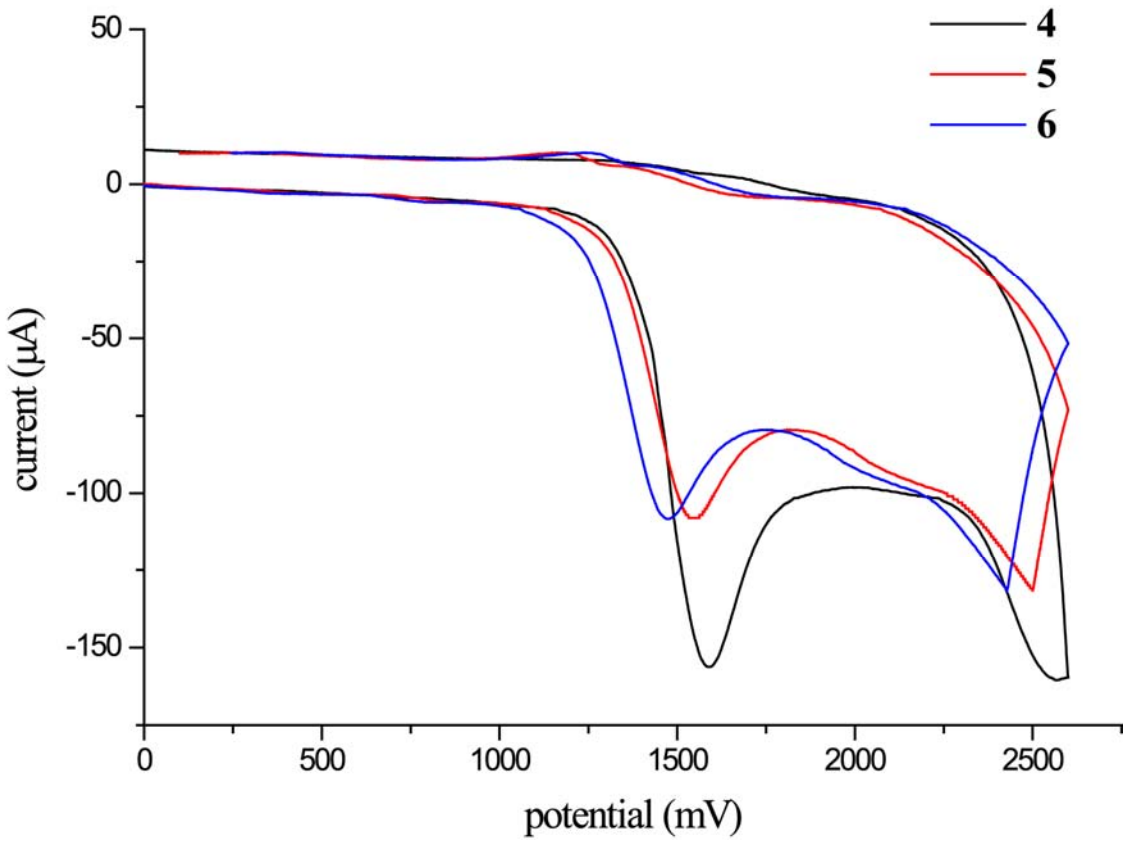

Figure 4.2: Cyclic voltammograms for CH_3CN solutions of $Ph_3Ge(GeBu_2)_nGeCH_2CH_2OEt$ obtained at 150 mV/s using $(^nBu_4N)(PF_6)$ as the supporting electrolyte: (black line) n = 0 (**2**); (red line) n = 1(**3**); (blue line) n = 2 (**4**).

Table 4.3: Absorption, electrochemical data, and calculated HOMO/LUMO energy levels (B3LYP/6-31G*) for oligogermanes **1-6** and **7** (R = CH_2CH_2OEt)

Compound	**λ_{max} (nm)**	**Eox (mV)**	**HOMO (eV)**	**LUMO (eV)**
$REt_2GeGePh_2GeEt_2R$ (1a)	243	1577 ± 22	- 5.23	- 0.19
$RBu_2GeGePh_2GeBu_2R$ (1b)	243	1500 ± 18	- 5.18	- 0.10
$RPh_2GeGePh_2GePh_2R$ (1c)	247	1609 ± 24	- 5.49	- 0.52
$Ph_3GeGeBu_2R$ (2)	224	1590 ± 19	- 5.45	- 0.36
$Ph_3Ge(GeBu_2)_2R$ (3)	232	1546 ± 16	- 5.41	- 0.37
$Ph_3Ge(GeBu_2)_3R$(4)	245	1474 ± 21	- 5.20	- 0.38
$Ph_3GeGeBu_2GePh_2R$ (5)	232	1525 ± 26	- 5.43	- 0.35
$Ph_3GeGeBu_2GePh_2GeEt_2R$ (6a)	248	1483 ± 17	- 5.22	- 0.38
$Ph_3GeGeBu_2GePh_2GeBu_2R$ (6b)	248	1462 ± 19	- 5.19	- 0.38
$Ph_3GeGePh_3$ (7a)	240	1576 ± 13	- 5.45	- 0.66
$Pr^i_3GeGePh_3$ (7b)	235	1635 ± 12	- 5.56	- 0.30
$Et_3GeGePh_3$ (7c)	231	1587 ± 17	- 5.46	- 0.35
$Bu_3GeGePh_3$(7d)	232	1588 ± 11	- 5.38	-0.34

Table 4.4: Frontier orbitals for $Ph_3Ge(GeBu_2)_nL$ (R = CH_2CH_2OEt), *n* = 0 (**2**), 1 (**3**), 2 (**4**).

n = 0, (**2**)	*n* = 1, (**3**)	*n* = 2, (**4**)
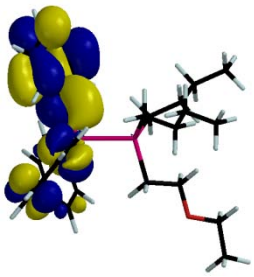	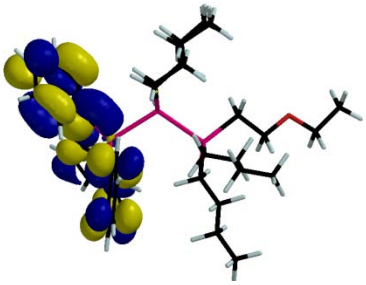	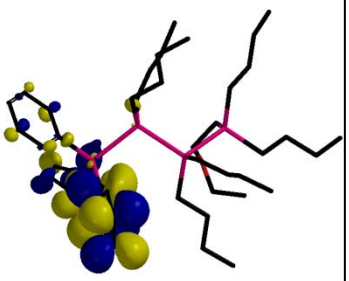
LUMO (+1) -0.09 eV	LUMO (+1) +0.13 eV	LUMO (+1) +0.13 eV
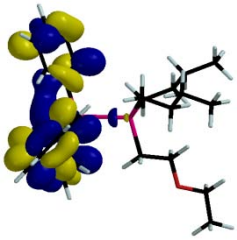	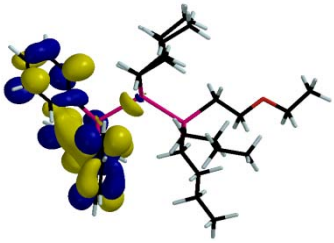	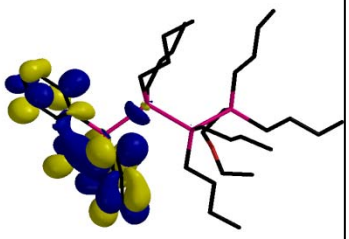
LUMO -0.36 eV	LUMO -0.37 eV	LUMO -0.38 eV
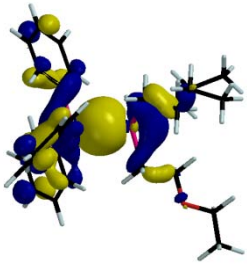	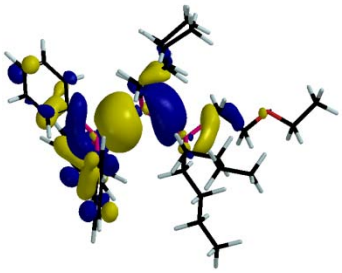	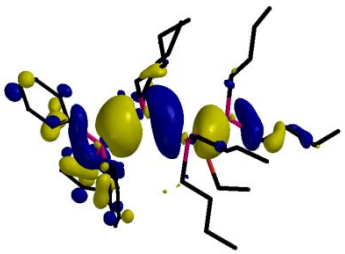
HOMO -5.45 eV	HOMO -5.41 eV	HOMO -5.20 eV
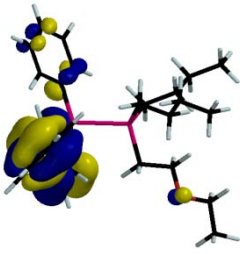	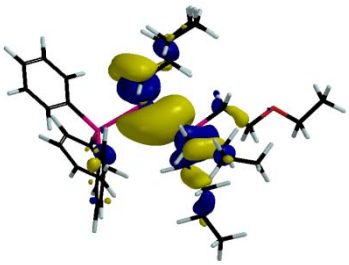	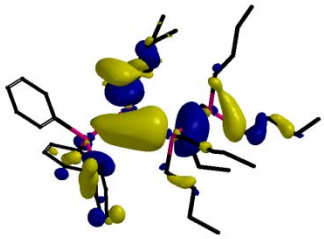
HOMO (-1) -6.67 eV	HOMO (-1) -5.99 eV	HOMO (-1) -5.98 e

Several other trends in the oxidation potential of these systems are noteworthy. First, the observed oxidation potentials of the trigermanes **3** (1546 mV) and **5** (1525 mV) agree with the results predicted from the DFT calculations, that the presence of a phenyl substituent increases the relative energy of the HOMO compared to the presence of an alkyl substituent. Additionally, for the two tetragermanes **6a** and **6b** there is a small decrease in the oxidation potential with increasing inductive potential effects on exchanging ethyl substituents in **6a** (1483 mV) with the butyl groups of **6b** (1462 mV), which was also expected on the basis of the DFT calculation. The frontier orbital diagrams for compound **6a**, **6b** and for **7a**, **7b**, and **7d** are shown in Table 4.5 and 4.6 respectively. Finally for the four digermanes $R_3GeGePh_3$ investigated in this study, the oxidation potential of **7a** (R = Ph), **7c** (R = Et) and **7d** (R = Bu) are all lower than that of **7b** (R = Pr^i). This results also agrees with the DFT calculations in that **7b** has the lowest lying HOMO in the series, which is presumably a steric consideration. Compound **7b** was calculated to have the longest Ge-Ge distance among the four digermanes (Table 4.1). This has also been observed experimentally, as the Ge-Ge distance in **7b** is 2.4637(7) Å[161] versus those for **7a** [2.437(2) Å],[62] **7c** [2.4253(7) Å],[95] and **7d** [2.4212(8) Å (average of two independent molecules)].[95]

Table 4.5: Frontier orbitals for $Ph_3GeGeBu_2GePh_2GeEt_2CH_2CH_2OEt$ (**6a**) and $Ph_3GeGeBu_2GePh_2GeBu_2CH_2CH_2OEt$ (**6b**)

6a	**6b**
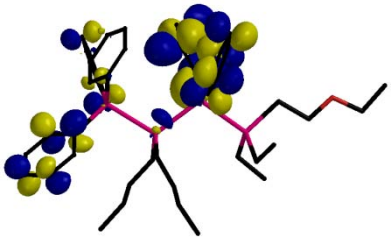	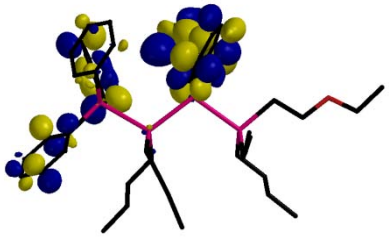
LUMO (+1) -0.27 eV	LUMO (+1) -0.29 eV
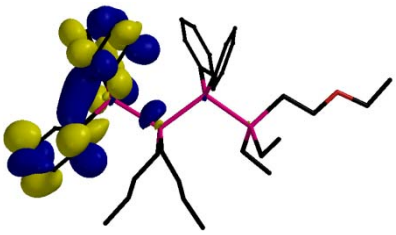	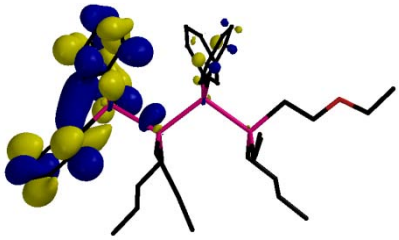
LUMO -0.38 eV	LUMO -0.38 eV
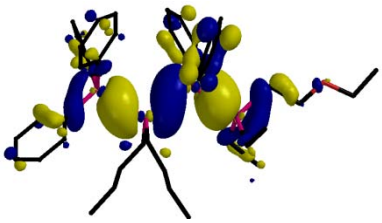	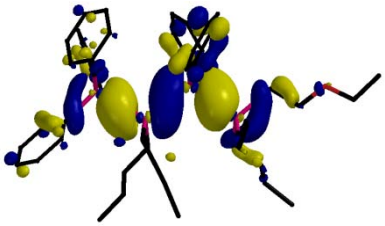
HOMO -5.22 eV	HOMO -5.19 eV
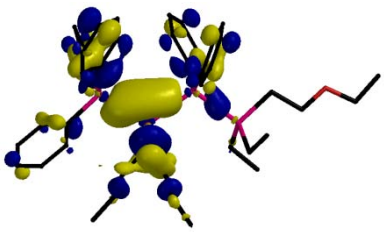	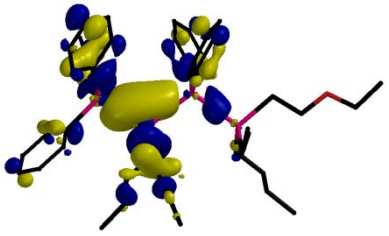
HOMO (-1) -5.91 eV	HOMO (-1) -5.90 eV

Table 4.6: Frontier orbital diagrams for $Ph_3GeGePh_3$ (**7a**), $Ph_3GeGePr^i_3$ (**7b**) and $Ph_3GeGeEt_3$ (**7c**)

7a	**7b**	**7c**
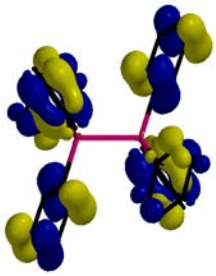	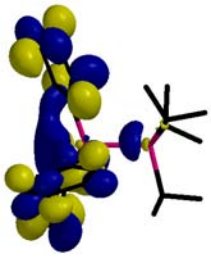	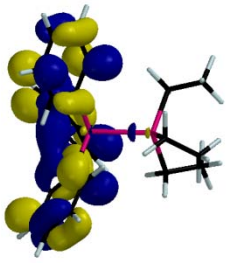
LUMO (+1) -0.21 eV	LUMO (+1) -0.27 eV	LUMO (+1) -0.08 eV
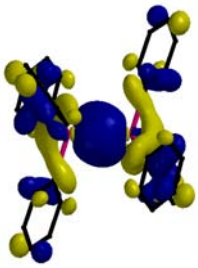	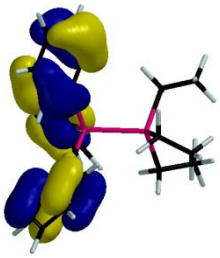	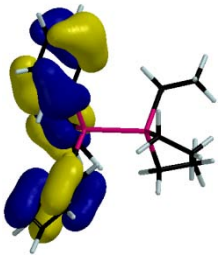
LUMO -0.66 eV	LUMO -0.30 eV	LUMO -0.35 eV
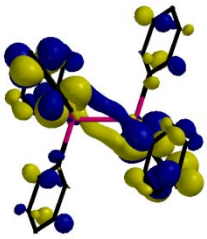	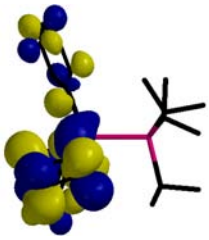	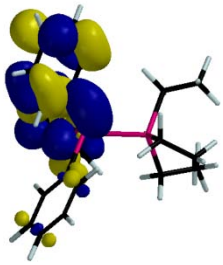
HOMO -5.45 eV	HOMO -5.56 eV	HOMO -5.46 eV
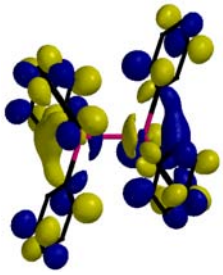	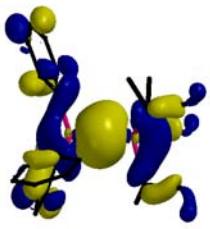	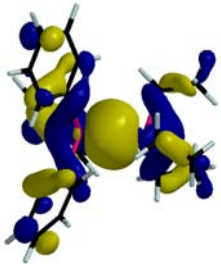
HOMO (-1) -6.64 eV	HOMO (-1) -6.30 eV	HOMO (-1) -6.67 eV

Absorption data for oligogermanes **1-7** are collected in Table 4.3, and UV/visible spectra for the three related series **1a-c**, **2-4**, and **7a-d** are shown in Figures 4.3-4.5, respectively. The absorption bands for the digermanes **7a-d** and the butylated series **3-5** are broad, and the absorbance maxima (λ_{max}) range from 221 to 245 nm. As expected on the basis of similar studies conducted for a series of permethylated[87] and perethylated[81] germanium oligomers as well as a related group of butylated tin species,[20] the position of the absorbance maximum among the oligomers **3-5** undergoes a red shift with increasing chain length. These findings agree with previous observations on related systems and with the magnitude of the HOMO/LUMO gap calculated by DFT (*vide supra*). The relative position of the LUMO remains approximately the same among the three molecules, but increasing the number of germanium atoms in the chain results in an overall destabilization of the energy of the HOMO, thus shifting the energy of the electronic transition to lower energy.

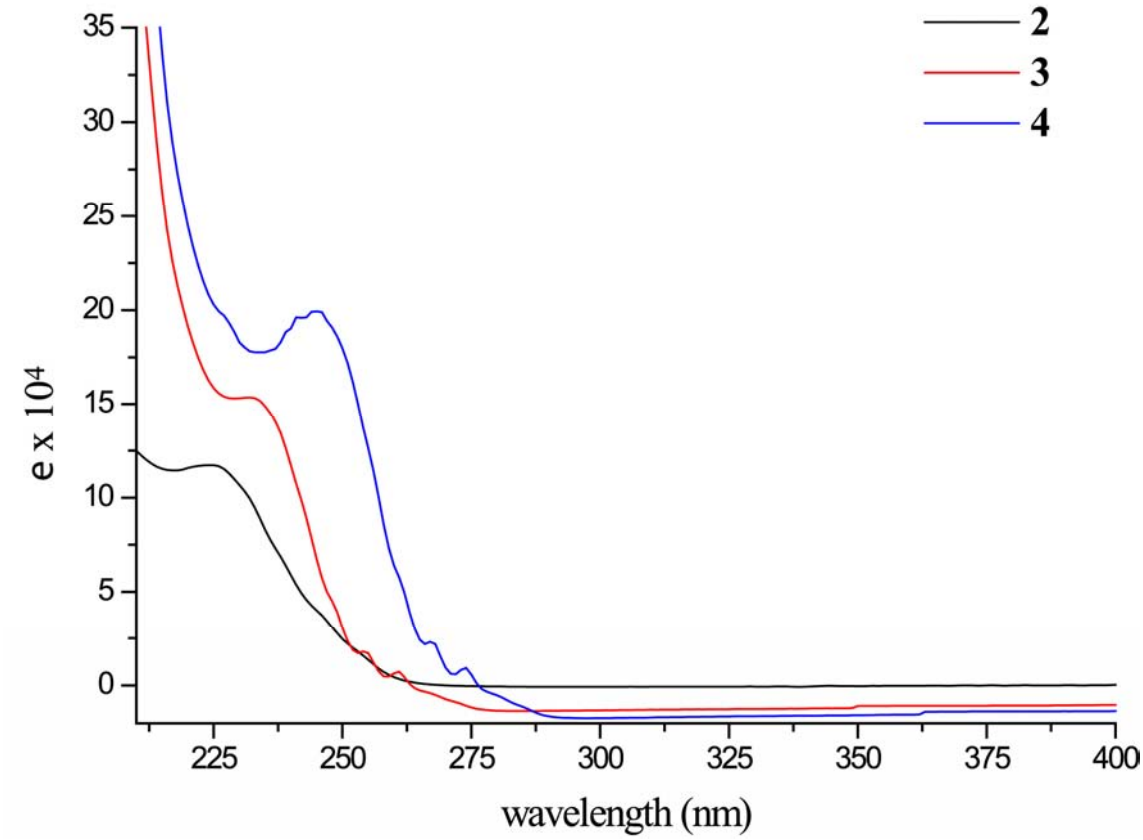

Figure 4.3: UV/visible spectra in CH_3CNsolution: $Ph_3GeGeBu_2CH_2CH_2OEt$ (black line, **2**); $Ph_3GeGeBu_2GeBu_2CH_2CH_2OEt$ (red line, **3**); $Ph_3GeGeBu_2GeBu_2GeBu_2CH_2CH_2OEt$ (blue line, **4**)

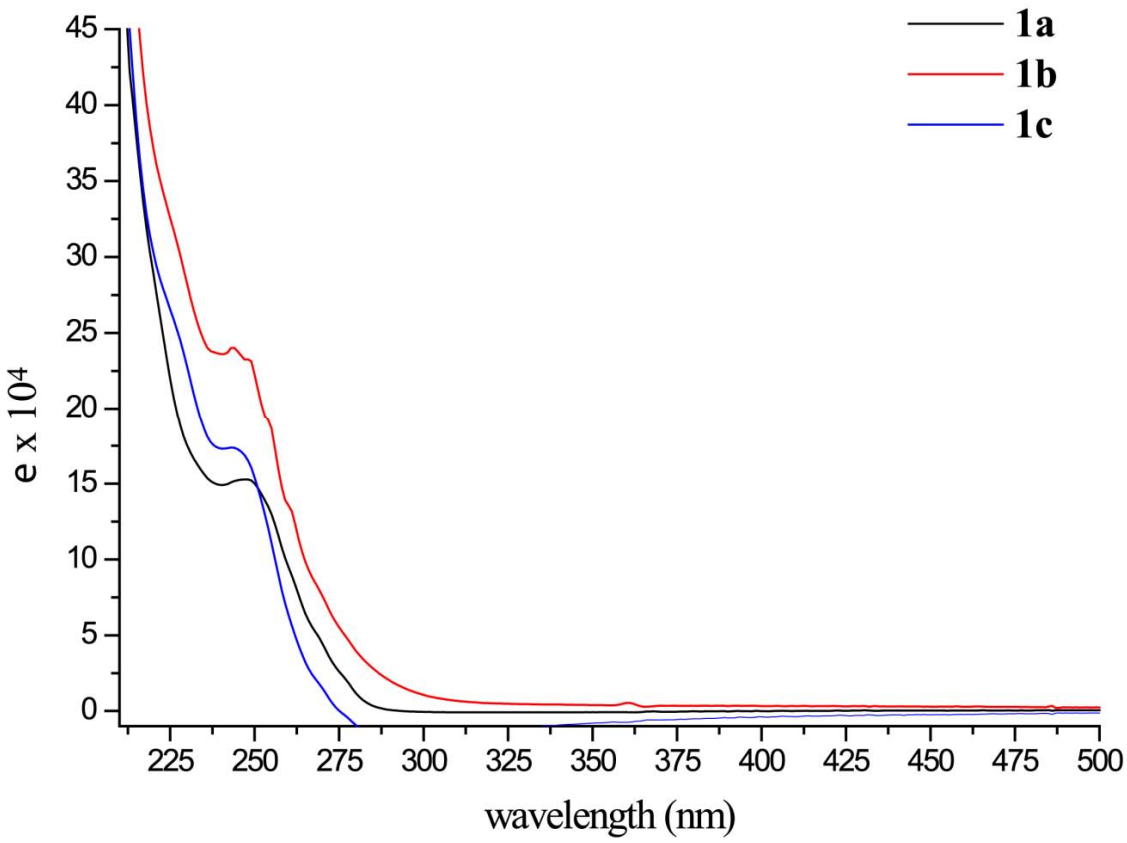

Figure 4.4: UV/visible spectra in CH_3CNsolution: $RPh_2GeGePh_2GePh_2R$ (black line, **1c**); $REt_2GeGePh_2GeEt_2R$ (red line, **1b**); $RBu_2GeGePh_2GeBu_2R$ (blue line, **1a**) ,(R = $CH_2CH_2OCH_2CH_3$)

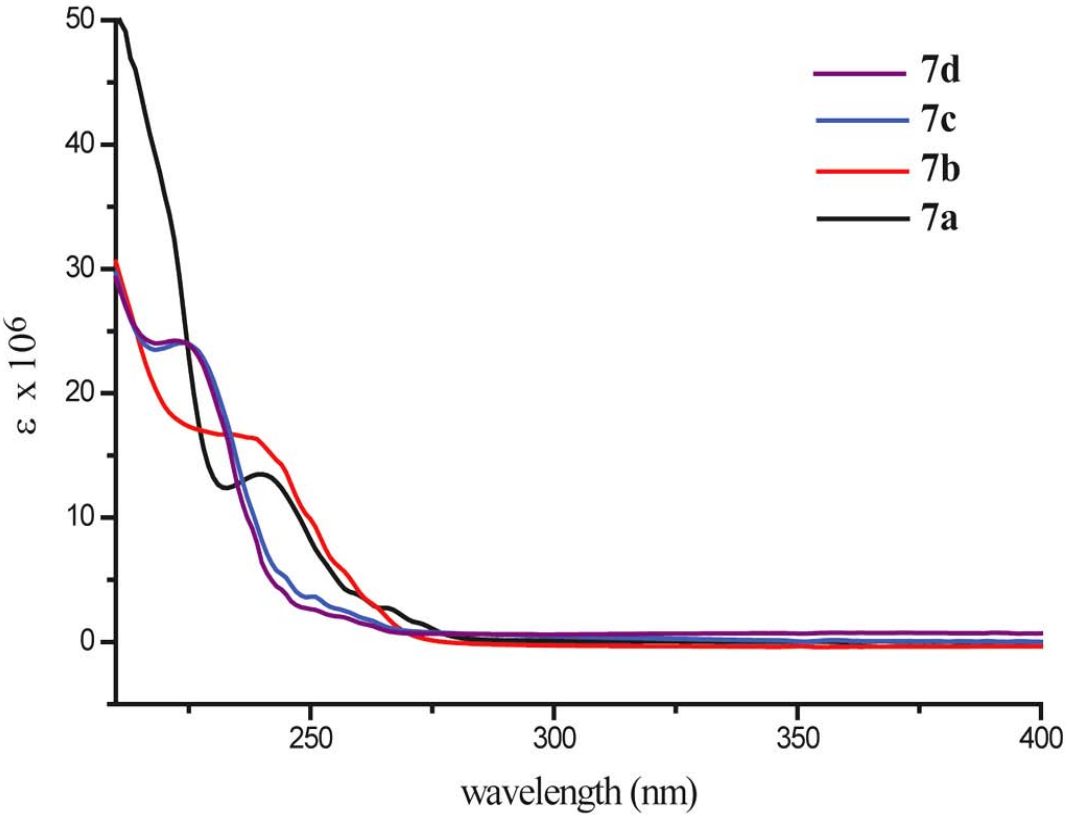

Figure 4.5: UV/visible spectra in CH_3CNsolution: $Ph_3GeGePh_3$ (black line, **7a**); $Pr^i_3GeGePh_3$ (red line, **7b**); $Et_3GeGePh_3$ (blue line, **7c**); $Bu_3GeGePh_3$ (purple line, **7d**)

For the series of digermanes $R_3GeGePh_3$, the absorbance maximum of the phenyl-substituted derivative **7a** (R = Ph) is significantly red-shifted relative to the alkyl-substituted species **7b-d**. This trend parallels the results found in the DFT calculations (see Table 4.1) and can be attributed to the lower energy and greater number of low-lying virtual orbitals from the phenyl group substituents in **7a** relative to the alkyl-substituted derivatives **7b-d**. The three compounds **7b-d** all have similar absorption characteristics, as predicted from the DFT calculations, where the energetic differences between the frontier orbitals on traversing the series of these three compounds is negligible. Likewise, the series of trigermanes **1a-c** all have approximately the same HOMO/LUMO separation and their λ_{max} values fall into the narrow range of 243-247 nm. However, the absorbance bands **1a-c** are all significantly broader and tail off into the visible region when compared to those of compounds **1**, **4-6** and **7**. This results in the trigermanes **1a-c** being slightly pale yellow while the remaining nine species are colorless.

The tetragermane, $Ph_3GeGeEt_2GeEt_2GeEt_2CH_2CH_2OEt$ (**8)** exhibits observable absorbance maxima in its electronic spectrum that appear as shoulders on the CH_3CN solvent peak at 235 nm arising from the $\sigma\rightarrow\sigma^*$ transition. The position of λ_{max} for the relative butyl analogue **4** is 245 nm. These values are similar to those of other similar species including the tetragermane $Et_3Ge(GeEt_2)_2GeEt_3$ (λ_{max} = 234 nm) and the hexagermane $Et_3Ge(GeEt_2)_4GeEt_3$ (λ_{max} = 258 nm).[81] The related tin containing congeners exhibit a more substantial red shift of their absorbance maxima, as illustrated for the related tetrastannane $Bu_3Sn(SnBu_2)_2SnOCH_2CH_2OEt$, which has a λ_{max} at ca. 275 nm, and the hexastanane $Bu_3Sn(SnBu_2)_4SnCH_2CH_2OEt$, which exhibits at 310 nm.[20]

Absorption characteristics of branched oligogermanes

The UV/visible spectra observed for branched oilgogermanes are shown in Figure 4.6, 4.7 and 4.8 while the λ_{max} values are collected in Table 4.7. The UV/visible spectrum of **9** ($PhGe(GePh_3)_3$), exhibits a clearly defined absorption maximum at 256 nm resulting from the $\sigma \rightarrow \sigma^*$ transition. The presence of branching in oligomeric and polymeric group 14 compounds has been shown experimentally and theoretically to result in a red shift of the λ_{max} due to an enhancement of the σ-delocalization present in these systems versus their linear analogues.[123-125,183] The absorbance maximum of **9** can be compared to those for the $\sigma \rightarrow \sigma^*$ transitions in Ge_3Ph_8 and Ge_4Ph_{10} observed at 249 and 282 nm, respectively.[57] The position of the λ_{max} for **9** is very similar to that of the trigermane rather than the tetragermane, which is as expected since the structure of **9** can be regarded as one having three overlapping Ge_3 chains, and the red shift of the λ_{max} for **9** versus that of Ge_3Ph_8 can be attributed to its branched structure.

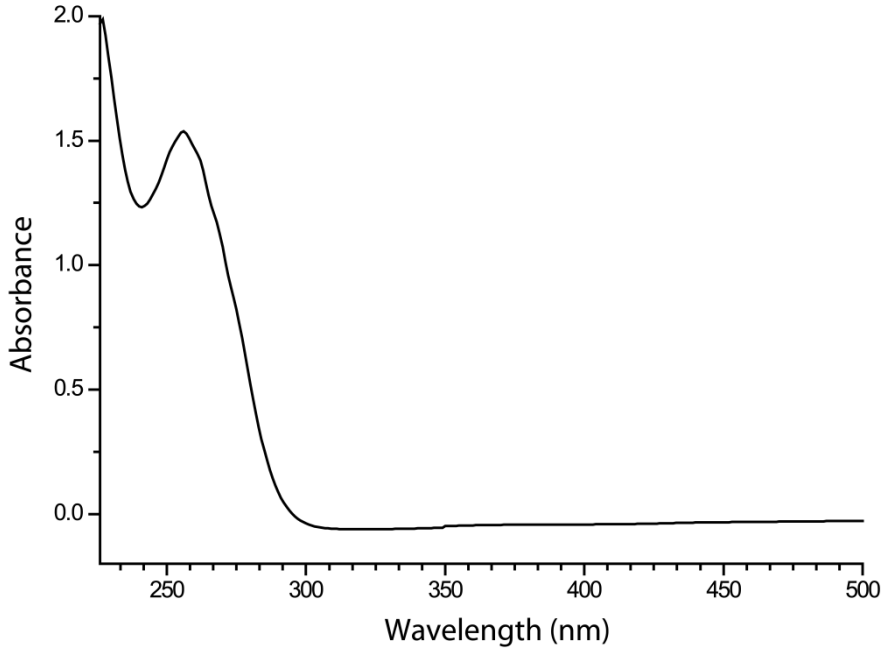

Figure 4.6: UV/visible spectrum of $PhGe(GePh_3)_3$ **(9)** in hexane

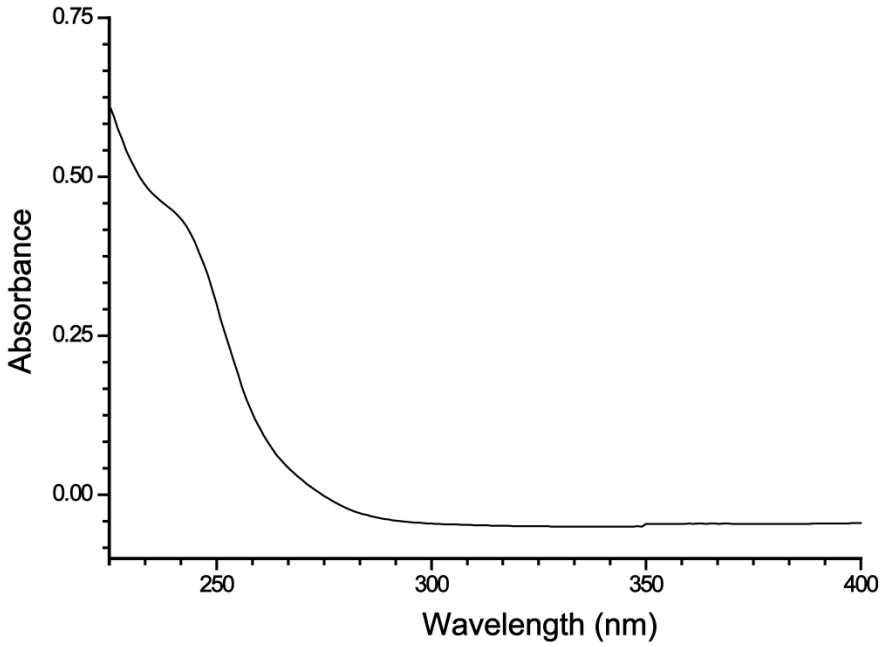

Figure 4.7: UV/visible spectrum of $PhGe(GeBu_3)_3$ **(10)** in hexane

Table 4.7: Absorption data for branched oligogermanes **9- 12** (in hexane)

Compound	λ_{max} (nm)	ε (L mol^{-1} cm^{-1})
$PhGe(GePh_3)_3$ (**9**)	256	5.1×10^4
$PhGe(GeBu_3)_3$ (**10**)	233	1.8×10^5
$PhGe(GeBu_2CH_2CH_2OEt)_3$ (**11**)	234	1.83×10^4
$PhGe(GeBu_2Bu_2CH_2CH_2OEt)_3$ (**12a**)	241	2.64×10^4
$PhGe(GeBu_2Et_2CH_2CH_2OEt)_3$ (**12b**)	242	1.83×10^4
$PhGe(GeBu_2Ph_2CH_2CH_2OEt)_3$ (**12c**)	247	3.31×10^4

The UV/visible spectrum of **10** exhibits an absorption maximum at 233 nm, which is higher in energy than that of the phenyl substituted species $PhGe(GePh_3)_3$ (**11**), which was observed at 256 nm.[132] As shown for linear oligogermanes, the presence of phenyl versus alkyl substituents stabilizes both the HOMO and the LUMO , resulting in a lower energy for the $\sigma \rightarrow \sigma^*$ electronic transition.[180] Therefore, the λ_{max} for **10** is expected to be blue shifted relative to that for **9**.

The UV/visible spectrum of **11** exhibits a broad absorption maximum centered at 234 nm (Figure 4.8). This feature appears at higher energy than that observed for compound **9**, which is likely due to the presence of the electron-withdrawing phenyl groups bound to the germanium atoms in **9** versus the inductively electron-donating butyl and ethoxyethyl groups in **11**, resulting in a larger σ→σ* gap in **11** versus that for compound **9**.

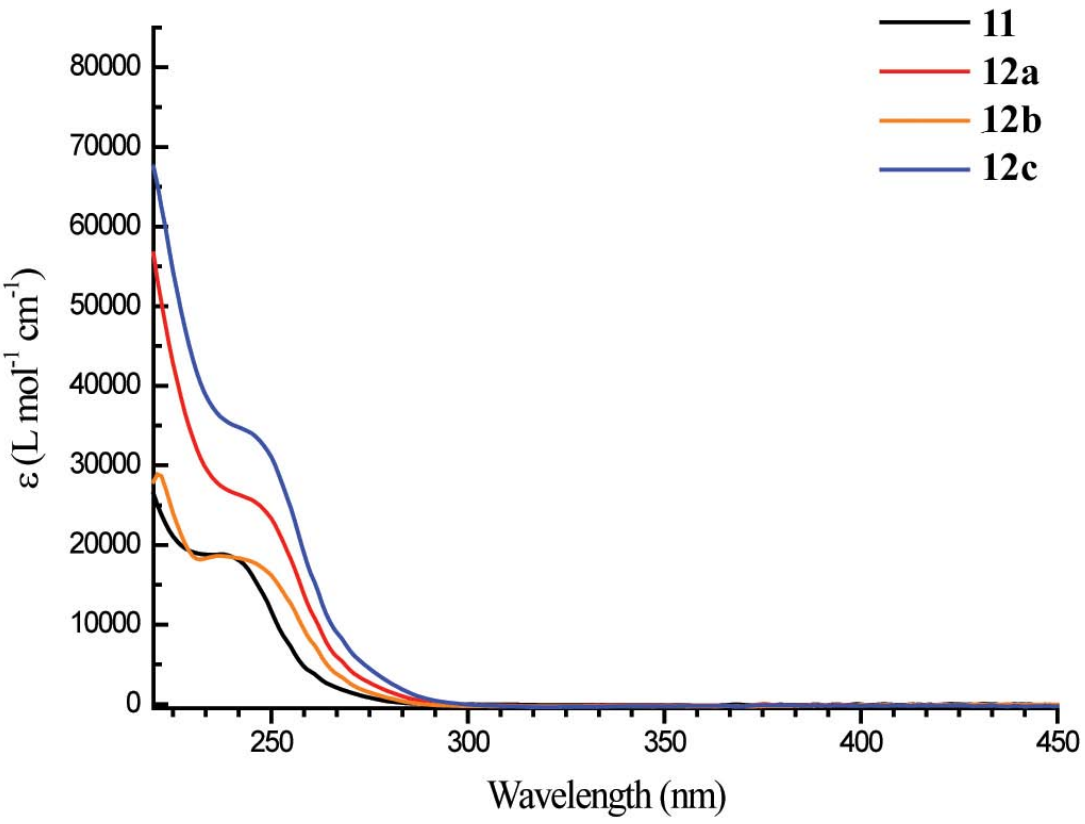

Figure 4.8: Overlaid UV/visible spectra (in hexane) of $PhGe(GeBu_2CH_2CH_2OEt)_3$ (**11**) and $PhGe(GeBu_2GeR_2CH_2CH_2OEt)_3$ (**12a**: R = Bu; **12b**: R = Et; **12c**: R = Ph).

The absorption maxima of **12a-c** are shown in Figure 4.8 and all are slightly red – shifted relative to that of **11**, having λ_{max} values of 240 (**12a**), 236 (**12b**), and 242 (**12c**) nm. The extension of each of the three arms of the oligomer by one germanium atom thus appears to have a small but measureable effect on the energy difference between the σ and σ* orbitals in these molecules. The λ_{max} values of **11** and **12a-c** are all broadened and red-shifted relative to that of the linear tetragermane $Ph_3GeGe(Et_2)_3CH_2CH_2OEt$, which was observed at 235 nm.[95] However, these values are similar in energy to that of the butylated derivative $Ph_3Ge(GeBu_2)_3CH_2CH_2OEt$ (241 nm).[95] The combination of inductive effects from the attached organic groups in the linear oligomers and branching present in compounds **11** and **12a-c** therefore appear to have varying contributions to the overall relative energies of the σ and σ* orbitals in these systems.

^{73}Ge Spectral Investigations

Although observation of the ^{73}Ge nucleus by NMR spectroscopy is challenging for the reasons described in the introduction, a significant amount of information has been accumulated in the last several years, including chemical shifts, coupling constants, and relaxation times for various compounds that do not have a symmetric environment about the germanium atom. In contrast to simple germanes, ^{73}Ge NMR data for compounds containing Ge-Ge single bonds are relatively scarce. Chemical shift data for 16 different compounds are collected in Table 4.8, and some trends in these values can be identified. Resonances for germanium atoms bearing hydride substituents appear upfield relative to those having methyl or ethyl substituents, while the expected number of

signals for some of the compounds was not observed. For example, the branched germanium hydride $(Ph_3Ge)_3GeH$, exhibits a peak for the central germanium atom at δ -314 ppm,[184] but no resonance was observed for the germanium atoms of the peripheral Ph_3*Ge*- groups.

Table 4.8: Previously determined ^{73}Ge NMR chemical shift data

Compound	δ ^{73}Ge (ppm)[b]	Ref
Ge_2H_6	- 311.8 (95.5)	185
Ge_2D_6	- 318.0	184
Ge_3H_8	- 298 (94), - 310 (90)	185
Ge_4H_{10}	- 284, - 300	185
MeH_2GeGeH_3	- 306.2 (90.0)	185
$Me_2HGeGeMe_2H$	- 209	185
$Me_2HGeGeH_3$	- 127, - 296 (85)	185
$Me_2ClGeGeH_3$	- 280.5	184
Me_3GeGeH_3	- 47.7, - 295.6 (90.7)	185
$(MeH_2Ge)_2GeMeH$	- 125, - 206.2	185
$Me_3GeGeMe_3$	- 59	184
$Et_3GeGeEt_3$	- 34.7	186
$Ph_3GeGePh_3$	- 67	184
$(Ph_3Ge)_3GeH$	- 314	184
$H_3GeGeH_2Mn(CO)_5$	- 291.8	184
$H_3GeGeMeHMn(CO)_5$	- 277.9	184

[a] Chemical shifts are relative to $GeMe_4$

[b] Experimental ^1J (Ge–H) coupling constants are given in parentheses.

We have obtained ^{73}Ge NMR data for several linear and branched oligogermanes that we have prepared via the hydrogermolysis reaction. The structures of these species are shown in Figure 4.9, and chemical shifts and half-height line widths for these compounds are collected in Table 4.9. An acquisition time of 0.01 s, zero-filling, and a line broadening of 20 were used for all spectra, except for the digermane $Bu^s_3GeGePh_3$ (**7e**), where an acquisition time of 0.1 was employed. The lines are broad, as expected, and this is in part a result of the short acquisition time used. The chemical shifts reported in Table 4.9 have an associated error of ±3 ppm. Spectra for several samples were run using longer acquisition times, but this did not allow for the acquisition of a sufficient number of scans to obtain a reasonable signal-to-noise ratio. No correction was applied in cases where the resonances overlap, but the chemical shift data obtained in spectra where overlapping resonances occur were run several different times and the data were consistently reproducible.

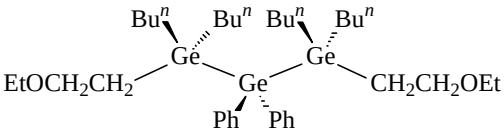

1b

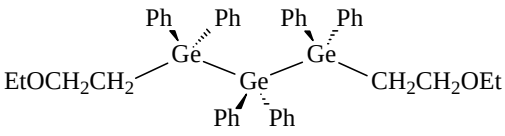

1c

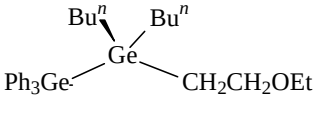

2

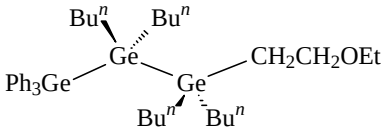

3

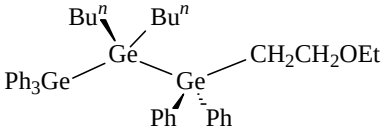

5

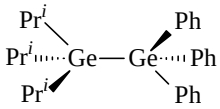

7b

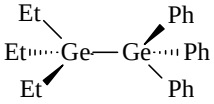

7c

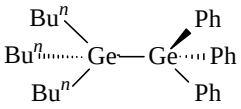

7d

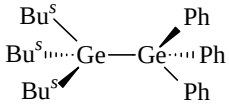

7e

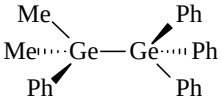

7f

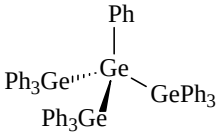

9

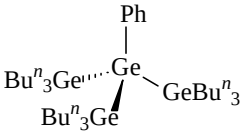

10

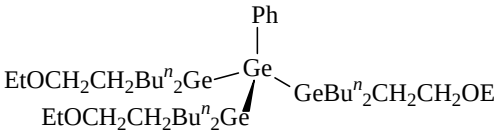

11

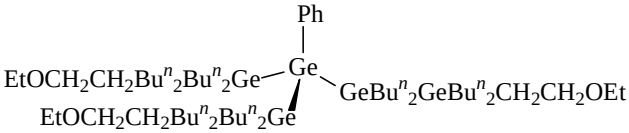

12a

Figure 4.9: Structures of the compounds used for ^{73}Ge NMR study

Table 4.9: ^{73}Ge NMR data for various oligogermanes (L = CH_2CH_2OEt)

Compound	Δ (pm)	$\Delta\nu_{1/2}$ (Hz)	Assignment
$LGeBu^n_2GePh_2GeBu^n_2L$ (**1b**)	– 111	180	$LGeBu^n_2\mathit{Ge}Ph_2GeBu^n_2L$
$LGePh_2GePh_2GePh_2L$ (**1c**)	– 121	170	$LGePh_2\mathit{Ge}Ph_2GePh_2L$
$Ph_3GeGeBu^n_2L$ (**2**)	– 57	90	$Ph_3Ge\mathit{Ge}Bu^n_2L$
	– 64	330	$Ph_3\mathit{Ge}GeBu^n_2L$
$Ph_3GeGeBu^n_2GeBu^n_2L$ (**3**)	– 57	310	$Ph_3GeGeBu^n_2\mathit{Ge}Bu^n_2L$
	– 63	310	$Ph_3\mathit{Ge}GeBu^n_2GeBu^n_2L$
$Ph_3GeGeBu^n_2GePh_2L$ (**5**)	– 54	120	$Ph_3GeGeBu^n_2\mathit{Ge}Ph_2L$
	– 65	390	$Ph_3\mathit{Ge}GeBu^n_2GePh_2L$
$Pr^i_3GeGePh_3$ (**7b**)	– 56	80	$Pr^i_3\mathit{Ge}GePh_3$
	– 65	240	$Pr^i_3Ge\mathit{Ge}Ph_3$
$Et_3GeGePh_3$ (7**c**)	– 64	270	$Et_3Ge\mathit{Ge}Ph_3$
$Bu^n_3GeGePh_3$ (**7d**)	– 58	100	$Bu^n_3\mathit{Ge}GePh_3$
	– 65	340	$Bu^n_3Ge\mathit{Ge}Ph_3$
$Bu^s_3GeGePh_3$ (**7e**)	– 52	30[b]	$Bu^s_3\mathit{Ge}GePh_3$
$PhMe_2GeGePh_3$ (**7f**)	– 65	90	$PhMe_2Ge\mathit{Ge}Ph_3$
$PhGe(GePh_3)_3$ (**9**)	– 202	290	$Ph\mathit{Ge}(GePh_3)_3$
$PhGe(GeBu^n_3)_3$ (**10**)	– 33	100	$PhGe(\mathit{Ge}Bu^n_3)_3$
	– 195	240	$Ph\mathit{Ge}(GeBu^n_3)_3$
$PhGe(GeBu^n_2L)_3$ (**11**)	– 43	90	$PhGe(\mathit{Ge}Bu^n_2L)_3$
	– 203	380	$Ph\mathit{Ge}(GeBu^n_2L)_3$
$PhGe(GeBu^n_2GeBu^n_2L)_3$ (**12a**)	– 38	110	$PhGe(GeBu^n_2\mathit{Ge}Bu^n_2L)_3$
	– 209	320	$Ph\mathit{Ge}(GeBu^n_2GeBu^n_2L)_3$

[a] Chemical shifts are relative to external $GeMe_4$ by substitution. Chemical shift values are ±3 ppm, and $\Delta\nu_{1/2}$ are ±10 %. No correction for overlapping peaks was applied. Acquisition time = 0.01 s.

[b] Acquisition time = 0.1 s

From the chemical shifts observed for the digermanes **2**, **7b-7f**, it is apparent that trialkyl-substitued germanium atoms resonate at slightly lower field than triphenyl-substituted germanium atoms, and these findings are consistent with the results of previous ^{73}Ge NMR spectral investigations of simple alkyl- and aryl-germanes.[162-163,166,185-189] The ^{73}Ge NMR spectra obtained for the digermanes **7b-7f** are shown in Figures 4.10-4.14. The single ^{73}Ge NMR resonance observed for compound **7e** at δ -52 ppm corresponds to the *sec*-butyl-substituted germanium atom, while the single features present in the ^{73}Ge NMR spectra of **7c** at δ -64 ppm correspond to the triphenyl-substituted germanium atom. Compound **7d** exhibits a peak for each type of germanium atom, and the resonance for the tri-*n*-butyl-substituted germanium atom appears at δ -58 ppm, while that for the triphenyl-substituted germanium atom appears upfield at δ -65 ppm. The spectrum of the digermane **7f** exhibits a single peak for the Ph_3*Ge*- atom at δ -65 ppm, while that for **7b** contains two resonances corresponding to each type of germanium atom.

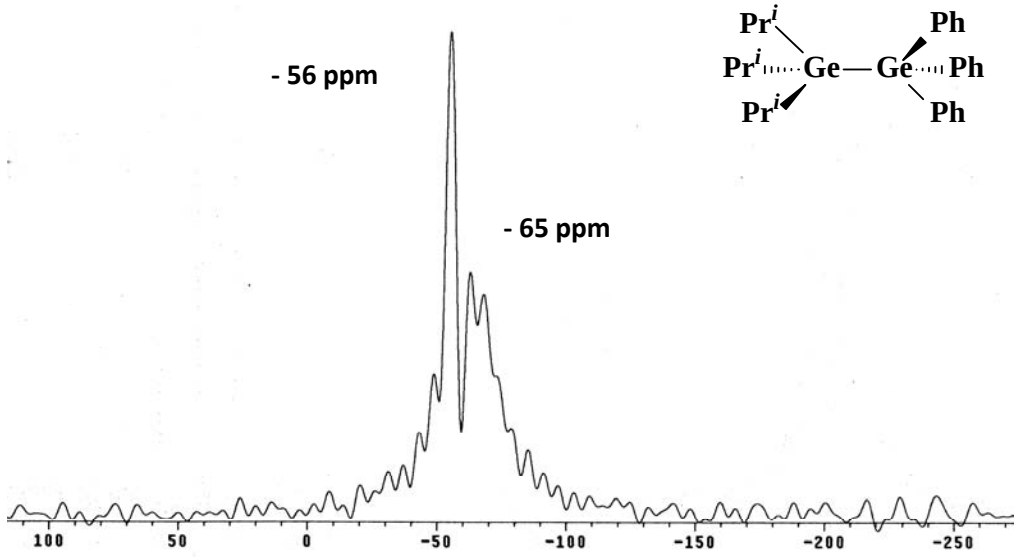

Figure 4.10: ^{73}Ge NMR spectra of $Pr^i_3GeGePh_3$ (**7b**)

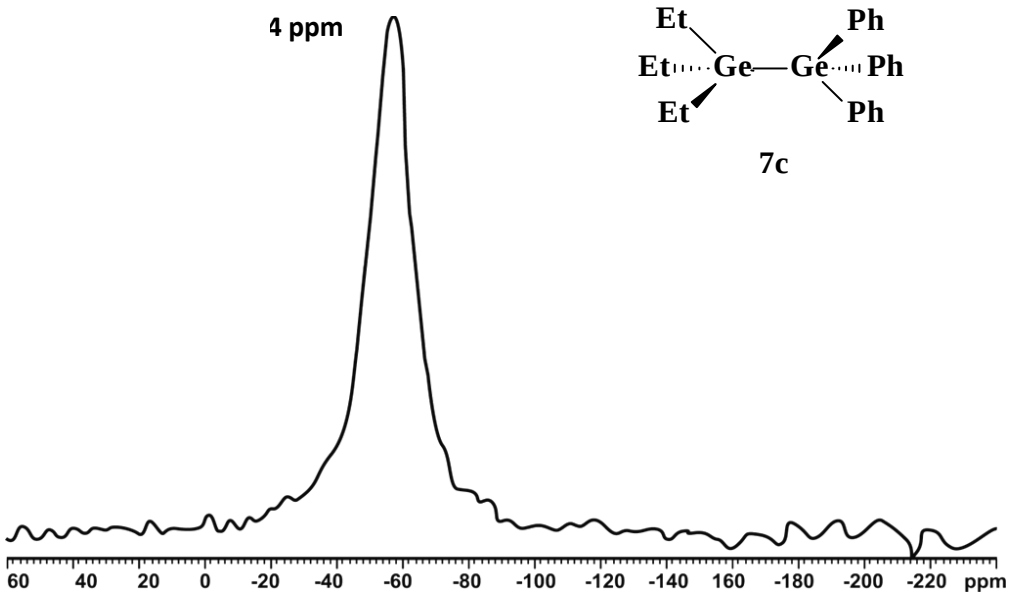

Figure 4.11: ^{73}Ge NMR spectra of $Et_3GeGePh_3$ (**7c**)

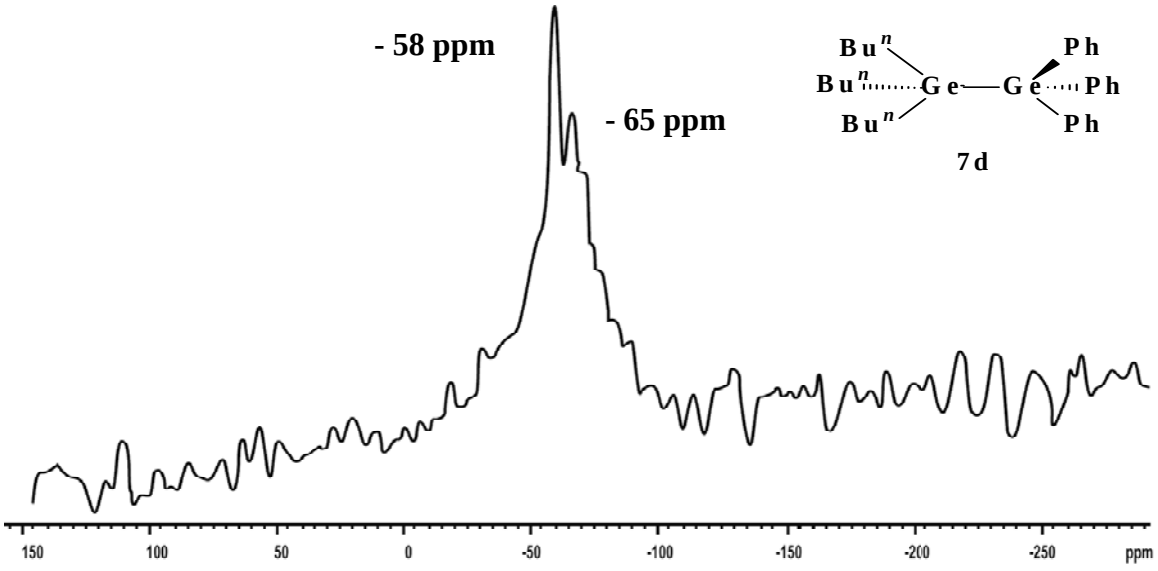

Figure 4.12: ^{73}Ge NMR spectra of $Bu^n_3GeGePh_3$ (**7d**)

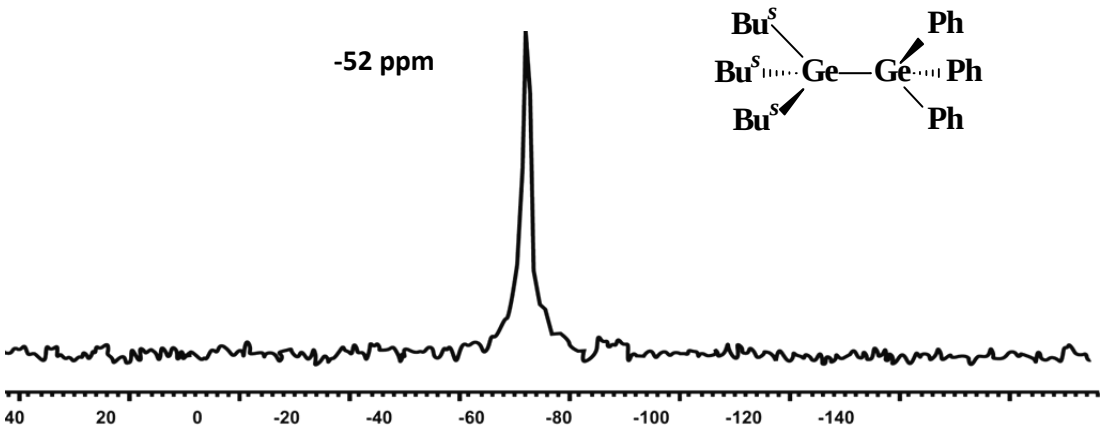

Figure 4.13: ^{73}Ge NMR spectra of $Bu^{s}_{3}GeGePh_3$ (**7e**)

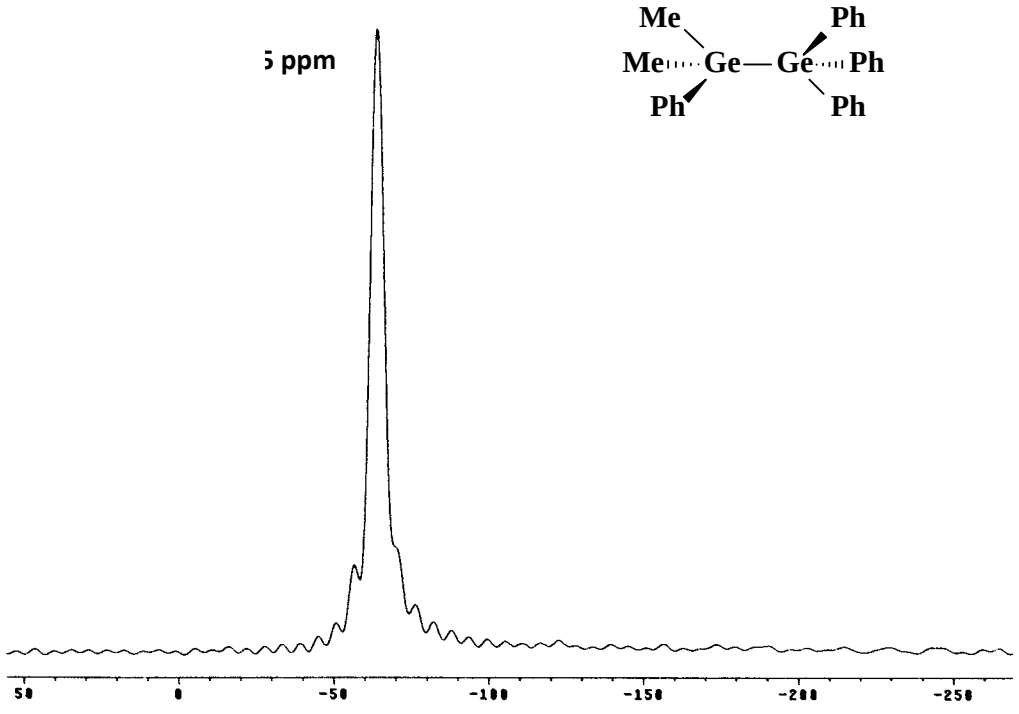

Figure 4.14: ^{73}Ge NMR spectra of $PhMe_2GeGePh_3$ (**7f**)

Although chemical shifts observed in ^{73}Ge NMR spectroscopy are highly sensitive to the substitution pattern at germanium, it has been demonstrated that there is not a linear correlation between inductive effects and ^{73}Ge NMR chemical shift values.[185-186,188] For example, the tetraalkyl germanes GeR_4 exhibit chemical shifts of δ 0.0 (R = Et), 2.4 (R = Pr^n), and 6.0 (R = Bu^n) ppm.[162] However, among the digermanes **7b-7e**, the observed chemical shift values exhibit a consistent upfield shift as the calculated inductive (σ_1) and polar (σ*) substituent constants[190] of the alkyl groups become more negative, and the relationship between δ (^{73}Ge) for the R_3Ge- groups and each of these constant is nearly linear (Figure 4.15 and Figure 4.16).

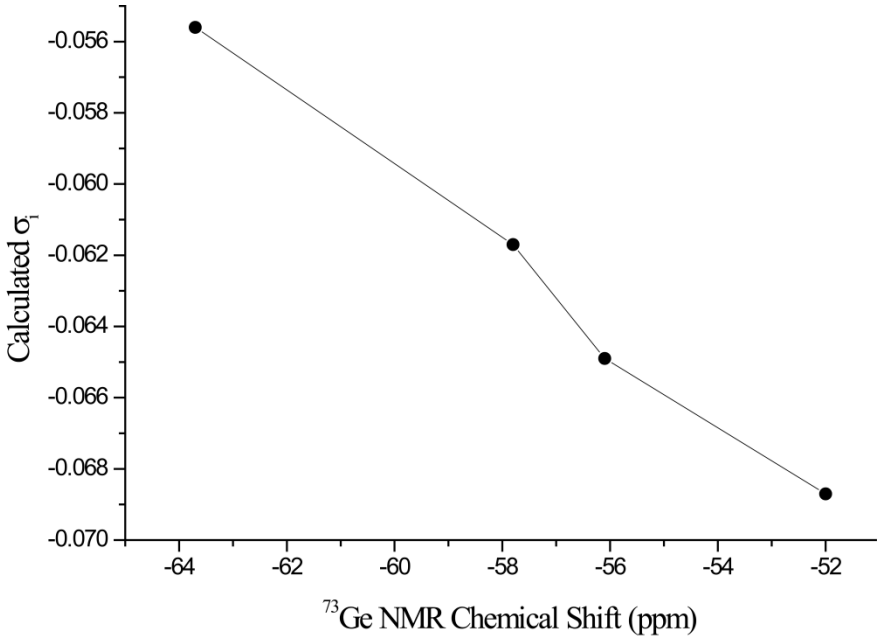

Figure 4.15: Plots of the ^{73}Ge NMR chemical shift (in ppm) of **7b-7e** versus the calculated inductive substituent constant

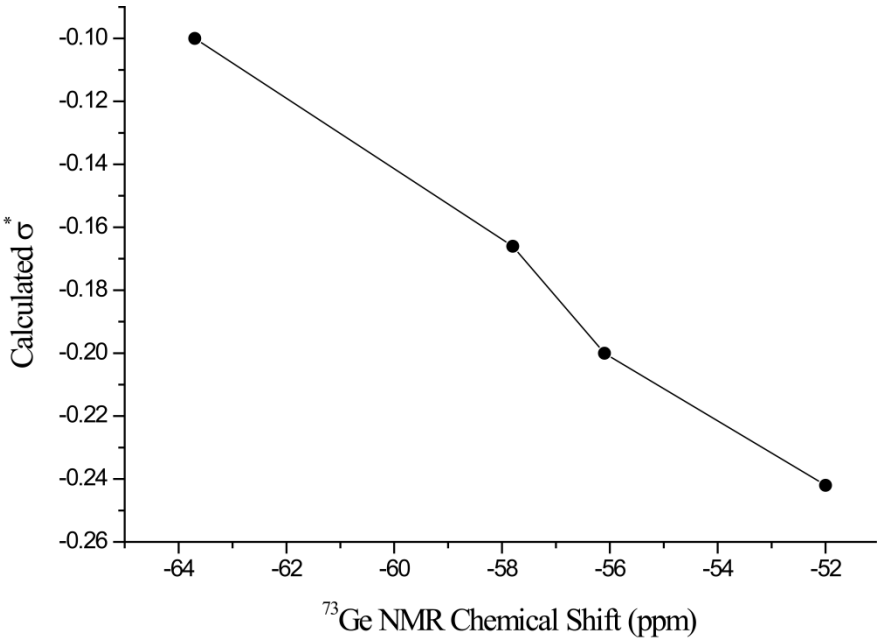

Figure 4.16: Plots of the ^{73}Ge NMR chemical shift (in ppm) of **7b-7e** versus the calculated polar substituent constant.

Germanium^{73}Ge NMR spectra for the two linear compounds $Ph_3GeGeBu^n_2CH_2H_2OEt$ (**2**) and $Ph_3GeGeBu^n_2GePh_2CH_2CH_2OEt$ (**5**) and the branched oligomers $PhGe(GeBu^n_2CH_2CH_2OEt)_3$ (**11**) and $PhGe(GeBu^n_2GeBu^n_2CH_2CH_2OEt)_3$ (**12a**) are shown in Figures 4.17 and 4.18, respectively. The digermane **2** exhibits two resonances in its ^{73}Ge NMR spectrum at δ -57 and -64 ppm, where the former resonance corresponds to the alkyl-substituted germanium atom and the latter corresponds to the triphenyl-substituted germanium atom. The spectrum of **5** exhibits a resonance for two of the three-germanium atoms, with a feature for the terminal Ph_3*Ge*- atom at δ -54 ppm and a signal at -65 ppm that corresponds to the –*Ge*$Ph_2CH_2CH_2OEt$ atom. This resonance is shifted upfield relative to the triphenyl-substituted germanium atoms due to the presence of the ethoxyethyl substituent.

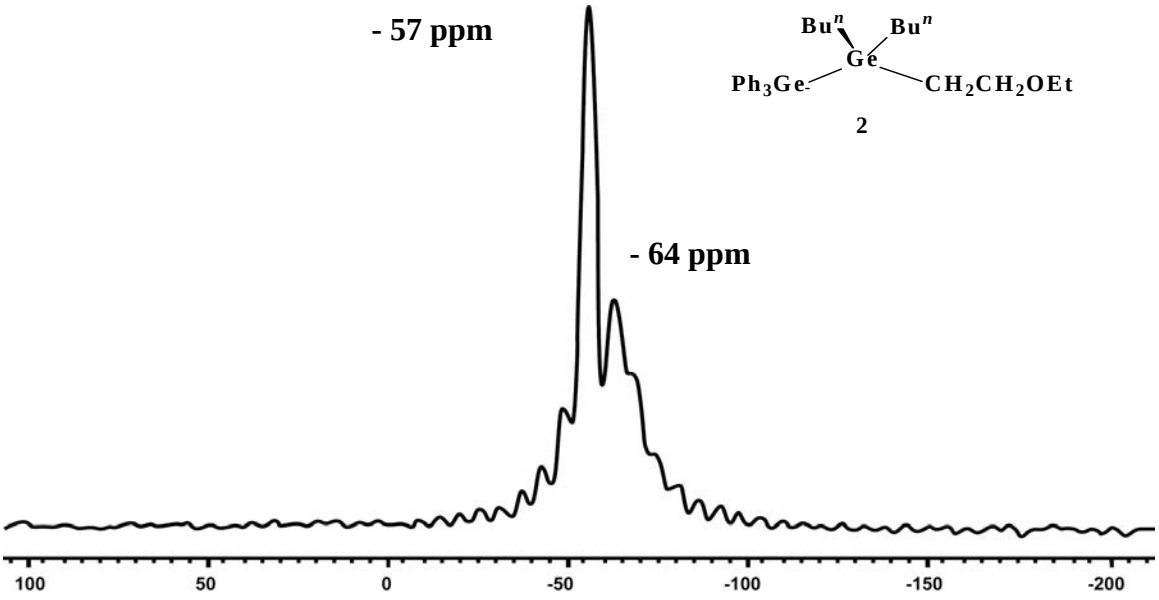

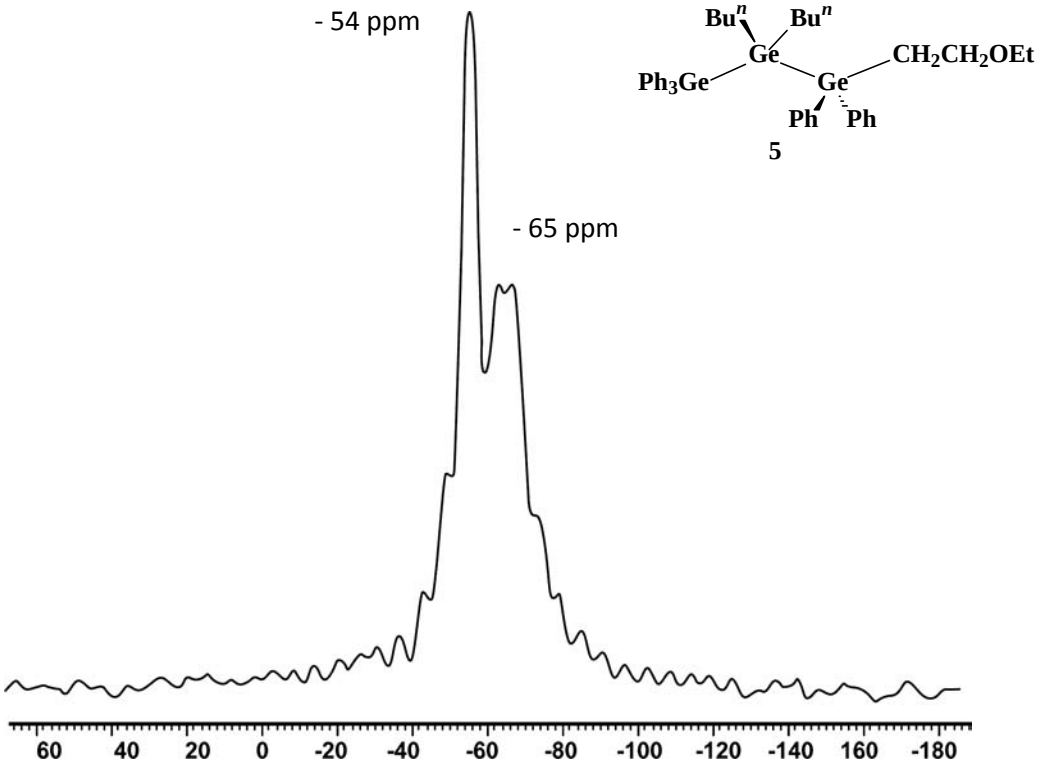

Figure 4.17: ^{73}Ge NMR spectra of $Ph_3GeGeBu^n_2CH_2CH_2OEt$ (**2**) and $Ph_3GeGeBu^n_2GePh_2CH_2CH_2OEt$ (**5**)

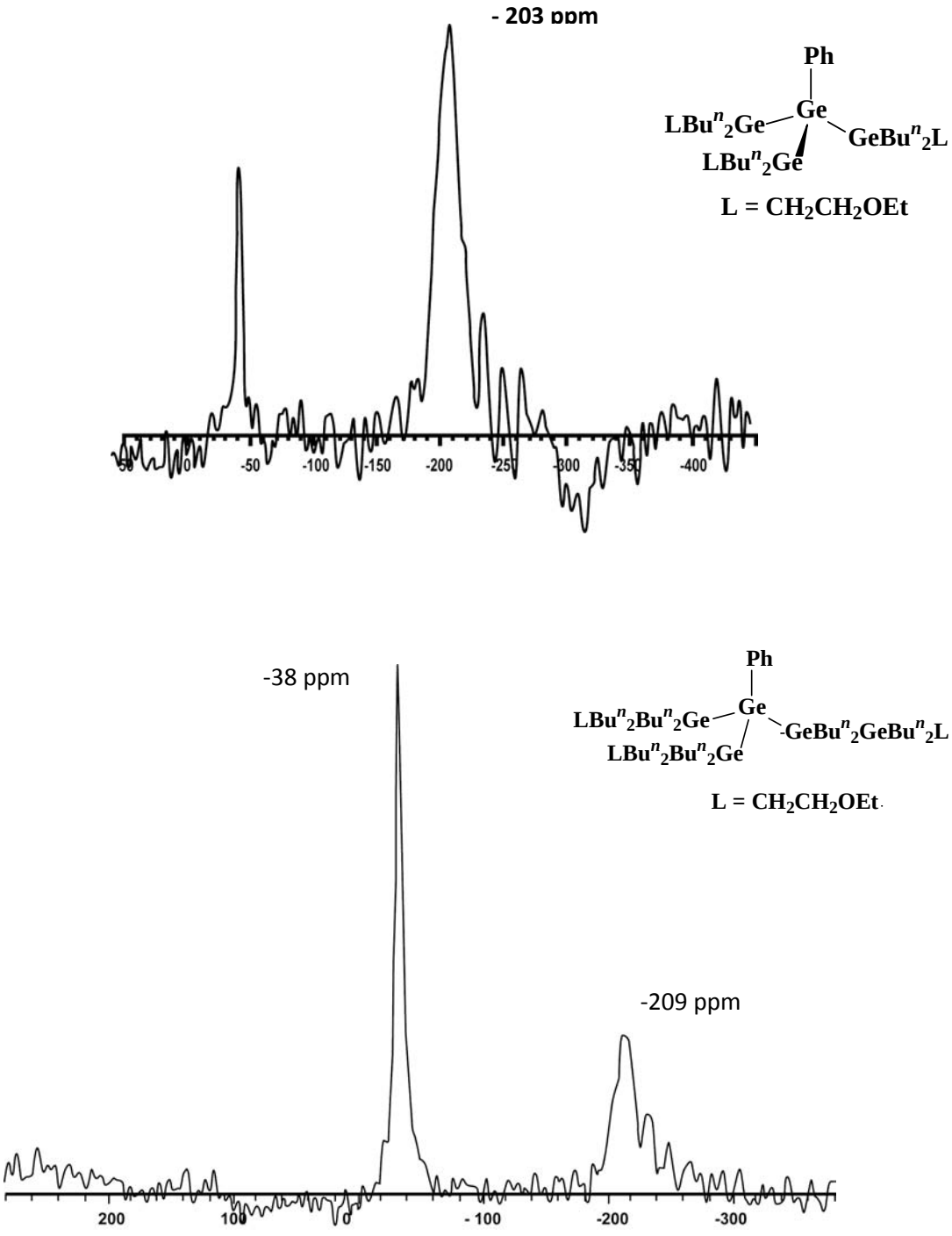

Figure 4.18: ^{73}Ge NMR spectra of PhGe(GeBu$^n_2$CH$_2$CH$_2$OEt)$_3$ (**11**) and PhGe(GeBu$^n_2$GeBu$^n_2$CH$_2$CH$_2$OEt)$_3$ (**12a**).

The number of germanium-germanium bonds to each germanium atom can have a pronounced effect on the ^{73}Ge chemical shift in these compounds. Both of the germanium atoms in the digermanes **2** and **7b-7f**, as well as the terminal germanium atoms in the higher oligomers **1b**, **1c**, **2**, **3**, **5**, **9-11**, and **12a** are bound to only one other germanium atom. Resonances for these germanium atoms range from δ -33 ppm in **10** to δ -65 ppm in **5**, which compare with the previously determined values of δ -35, -59, and -67 ppm for the compounds $R_3GeGePh_3$ (R = Et,[186] Me,[184] Ph[184] respectively). Trends for the resonances corresponding to the terminal germanium centers in **3**, **5**, **1b**, **1c**, and **9-12a** are similar to those observed for the digermanes **7b-7f**, in that phenyl substituents result in an upfield shift of the observed ^{73}Ge NMR resonances. The trigermanes **3**, **5**, **1b**, **1c** and the branched species **12a** each contain a germanium atom that is attached to two other germanium atoms, and for compound **1b** and **1c** resonances corresponding to the central phenyl substituted germanium atoms were observed at δ -111 and -121 ppm (respectively). Resonances for the germanium atoms bound to two other germanium centers in compounds **3**, **5** and **12a** were not observed. The upfield shift for these peaks in **1b** and **1c** verses those observed for germanium centers bound to only one germanium atom (*vide supra*) is a result of the increased shielding resulting from attachment to two germanium atoms. This effect is more evident in the data collected for the branched oligogermanes **9-11** and **12a** where the central germanium atoms in these species are substantially more shielded due to their being connected to three other germanium atoms. Resonances for these atoms are shifted upfield and range from δ -195 to -209 ppm, and a similar chemical shift was reported for the central germanium atom of $(Ph_3Ge)_3GeH$ at δ -314 ppm.[184]

CONCLUSIONS

The synthesis of oligogermanes with controllable number of germanium atoms and organic substitution patterns has been described. Examination of the experimental electronic properties and the results of density functional calculations reveal that the HOMO in each of these molecule is a σ orbital resulting mainly from the out-of-phase linear combination of p orbitals on germanium, but with a small contribution from mixing of the 4s and the orthogonal 4p orbitals. For oligogermanes without phenyl substituents, the LUMO is σ* in nature but is extensively mixed, mainly between the out-of-phase linear combination of $4p_z$ orbitals. The net result is that the LUMO can be adequately described as being due to an in-phase but spatially inverted linear combination of sp hybrid orbitals.

The HOMO/LUMO gap can be tuned in a predictable way by changing the length of the Ge-Ge chain in these compounds, as well as by altering the organic groups along the germanium backbone, where increasing the chain length is the most effective means for decreasing the HOMO/LUMO gap. Variation of the σ-donor abilities of the groups bound to germanium provides a means to more finely tune this energy difference, since the relative energy of the HOMO is more affected by such a change than that of the LUMO. For phenyl substituted oligogermanes, the LUMO is derived from linear combinations of phenyl group π* orbitals, rather than being germanium-based, which significantly alters the electronic properties of these compounds. However, the electronic tunability according to the findings of the aliphatic series is still preserved, as seen experimentally from UV/visible spectroscopic and electrochemical measurements. For consideration of the use of oligogermanes as viable candidates for molecular wires, it

would be desirable to improve the air and electrochemical stability and, to this end, we are currently investigating new ligand systems that would promote reversibility by constraining Ge-Ge bond dissociation.

The ^{73}Ge NMR resonance for oligogermanes can be correlated with the substitution pattern at germanium and also with the connectivity of the germanium centers. Germanium centers bound to only one additional germanium atom give rise to peaks in the approximate range δ -30 to -65 ppm, while the more shielded germanium centers which are connected to two or three additional germanium atoms exhibit resonances in the respective ranges of δ -100 to -120 and δ -195 to -210 ppm. In all cases, resonances for alkyl-substituted germanium atoms appear downfield from their phenyl-substituted analogues, which is consistent with previous findings for related systems. Due to the limitation that some substitution patterns do not allow an observable ^{73}Ge NMR resonance, ^{73}Ge NMR spectroscopy is not as versatile a technique as that for the corresponding group 14 elements carbon, silicon, tin, and lead. However, the investigations described here indicate that structural information can be obtained using this method, and the compilation of a database of ^{73}Ge NMR spectral data is a worthwhile endeavor.

EXPERIMENTAL

All the compounds used for these studies were synthesized using hydrogermolysis reaction and the synthetic procedures have been described in Chapters 2 and 3.[132,161,180-181] Cyclic voltagrams were obtained using a Bioanalytical Systems Epsilon

Electrochemical workstation with a glassy-carbon-disk working electrode, a platinum-wire counter electrode, and a Ag/AgCl reference electrode, using 1.0 M $[Bu_4N]PF_6$ in CH_3CN as the supporting electrolyte. UV/visible spectra were obtained using a Hewlett-Packard Agilent UV/visible spectrophotometer. Elemental analyses were conducted by Desert analytics or Midwest Microlabs. Germanium-73 NMR spectra of the products (50 mg/mL in benzene-d_6) were recorded on a Varian INOVA 500 MHz spectrometer using a 10 mm low gamma broadband probe at 17.43 MHz with the Carr-Purcell-Maiboom-Gill (CPMG) pulse sequence[191-192] to reduce baseline roll. The following parameters were used with proton decoupling during acquisition: spectral with = 100 000 Hz, acquisition time = 0.01 s (except 0.1s for compound **2**), delay time = 0 s, line broadening factor = 20, number of transients = 1×10^6 to 1×10^7. This pulse sequence was found to give peaks widths within ca. 5 % of those obtained using the slandered pulse sequence up to peak widths of ca. 800 Hz. Based on multiple runs of the same sample, the error in the chemical shifts is estimated to be ±3 ppm. The error in half-height line widths is ca.10 %. No correction was applied to the measurement of overlapping peaks. The spectra were reference to external $GeMe_4$ by substitution.

CHAPTER FIVE

STRUCTURE, SPECTRAL, AND ELECTROCHEMICAL INVESTIGATIONS OF PARA-TOLYL-SUBSTITUTED OLIGOGERMANES.

INTRODUCTION

It has been demonstrated in the previous chapters that both the number of catenated atoms and the electronic attributes of the attached organic substituents of oligogermanes affect the relative energies of the frontier orbitals in these systems. This has been demonstrated by characterizing the oligogermane systems using UV/visible spectroscopy and cyclic voltammetry, in conjunction with computational (DFT) studies. We have shown that the magnitude of the σ→σ* electronic transition, which corresponds to the promotion of an electron from the HOMO σ bonding orbital to the LUMO σ* anti-bonding orbital, decreases upon increasing the Ge-Ge chain length and /or by increasing the number of inductively electron donating organic substituents. In general, this effect results from the destabilization of the HOMO, and these two structural effects also diminish the oxidation potential of these systems. The oxidation waves exhibited in the cyclic voltammograms of all oligogermanes observed to date are irreversible, indicating that a chemical reaction is occurring after the oxidation event takes place.[85,180,182]

The majority of the oligogermanes that we have synthesized and described in previous chapters are either liquids or amorphous solids at room temperature, with the exception of several phenyl-substituted digermanes and the branched tetragermane $(Ph_3Ge)_3GePh$. The majority of oligogermanes Ge_nR_{2n+2} that have been characterized using X-ray crystallography (n = 2-5) contain phenyl substituents, although the yields of the reactions leading to these products are generally low (0.5-45 %).[25,48,57,61,69,95,105,161,181] Due to our desire to use our oligogermane systems as precursors for the synthesis of germanium-based nanomaterials, we were interested in preparing new systems that could be structurally characterized. This chapter focuses on the preparation of *para*-tolyl-

substituted oligogermanes, where the *para*-methyl group of the tolyl substituents can be used for an initial assessment of the purity of the products using ^{1}H NMR spectroscopy. We have prepared and structurally characterized four new tolyl-substituted oligogermanes containing between two and four germanium atoms in the chain, and these compounds have been further characterized using UV/visible spectroscopy and cyclic voltammetry. We have observed, for the first time, multiple irreversible oxidation events in the cyclic voltammograms of these oligogermanes, and have postulated the pathway of their decomposition after the oxidation event takes place.

Results and Discussion

The starting materials for the synthesis of *para*-tolyl substituted germanium compounds, Tol_3GeCl and Tol_2GeBr_2 (Tol = *p*-$H_3CC_6H_4$), were prepared by the Grignard reaction. Compound Tol_3GeCl was prepared by the reaction of TolMgCl with $GeCl_4$ while Tol_2GeBr_2 was prepared from the reaction of TolMgBr and $GeBr_4$. Carefully controlled reaction conditions were employed to prevent the formation of product mixtures including oligogermanes. While the preparation of $GeCl_4$ with 3 equivalents of TolMgCl yielded primarily the desired triaryl product Tol_3GeCl, the preparation of the diaryl material Tol_2GeBr_2 was complicated by the concomitant formation of Tol_3GeBr and $TolGeBr_3$. Separation of the three components of the product mixture was difficult, and as a result the product mixture was treated directly with excess $LiAlH_4$ to yield a mixture of the corresponding arylgermanium hydrides R_nGeH_{4-n} (n = 1-3). The three hydrides could be readily separated by fractional vacuum distillation and Tol_2GeH_2 was

obtained in 8 % yield based on $GeBr_4$. The ^1H NMR spectrum of Tol_2GeH_2 contains a singlet at δ 5.22 ppm corresponding to the two equivalent hydric protons, and the IR spectrum of this material contains a symmetric Ge-H stretching band at 2050 cm^{-1}. The amide reagent Tol_3GeNMe_2 was prepared from the salt metathesis reaction of Tol_3GeCl with $LiNMe_2$ in 76 % yield. The ^1H NMR spectrum of this material exhibits a singlet at δ 2.84 ppm corresponding to the protons of the amide methyl groups.

The digermane $Tol_3GeGePh_3$ (**1**) and the trigermanes $Tol_3GeGePh_2GeTol_3$ (**2**) and $Tol_3GeGeTol_2GeTol_3$ (**3**) were prepared using the amide Tol_3GeNMe_2 via the hydrogermolysis reaction in CH_3CN solvent. (Scheme 5.1)

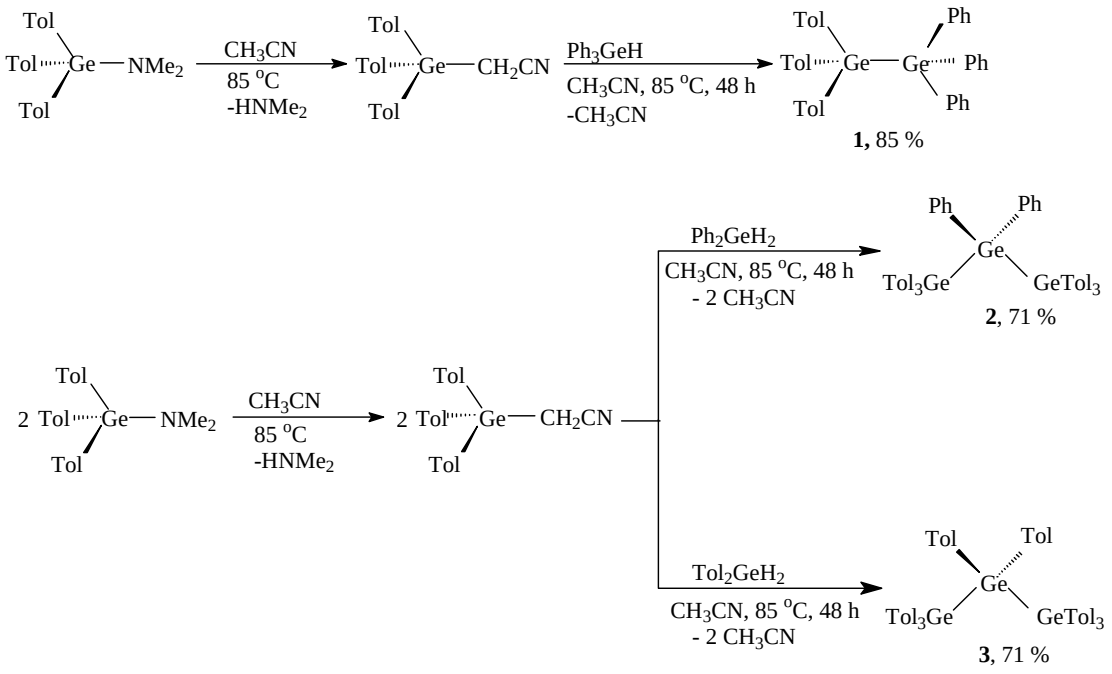

Scheme 5.1: Synthesis of digermane $Tol_3GeGePh_3$ (**1**), and trigermanes $Tol_3GeGePh_2GeTol_3$ (**2**) and trigermane $Tol_3GeGeTol_2GeTol_3$ (**3**).

The ^{1}H NMR spectra of **1** and **2** exhibit similar patterns in the aromatic region that are consistent with expected chemical shift values. In both compounds, resonances for the *ortho*-protons of the tolyl rings are shifted downfield relative to those for the *ortho*-protons of the phenyl rings, while resonances for the *meta*-protons appear upfield relative to those of the phenyl groups. In addition, resonances for the *ipso*-carbons of the tolyl groups in the ^{13}C NMR spectra of **1** and **2** appear downfield relative to those of the phenyl groups. Singlets for the methyl protons of **1** and **2** are observed at δ 2.02 and 2.07 ppm, respectively, while the pertolyl-substituted trigermane **3** exhibits two methyl group resonances at δ 2.09 and 1.99 ppm, where the singlet corresponding to the central tolyl substituents appears upfield at δ 1.99 ppm (Figure 5.1 and 5.2).

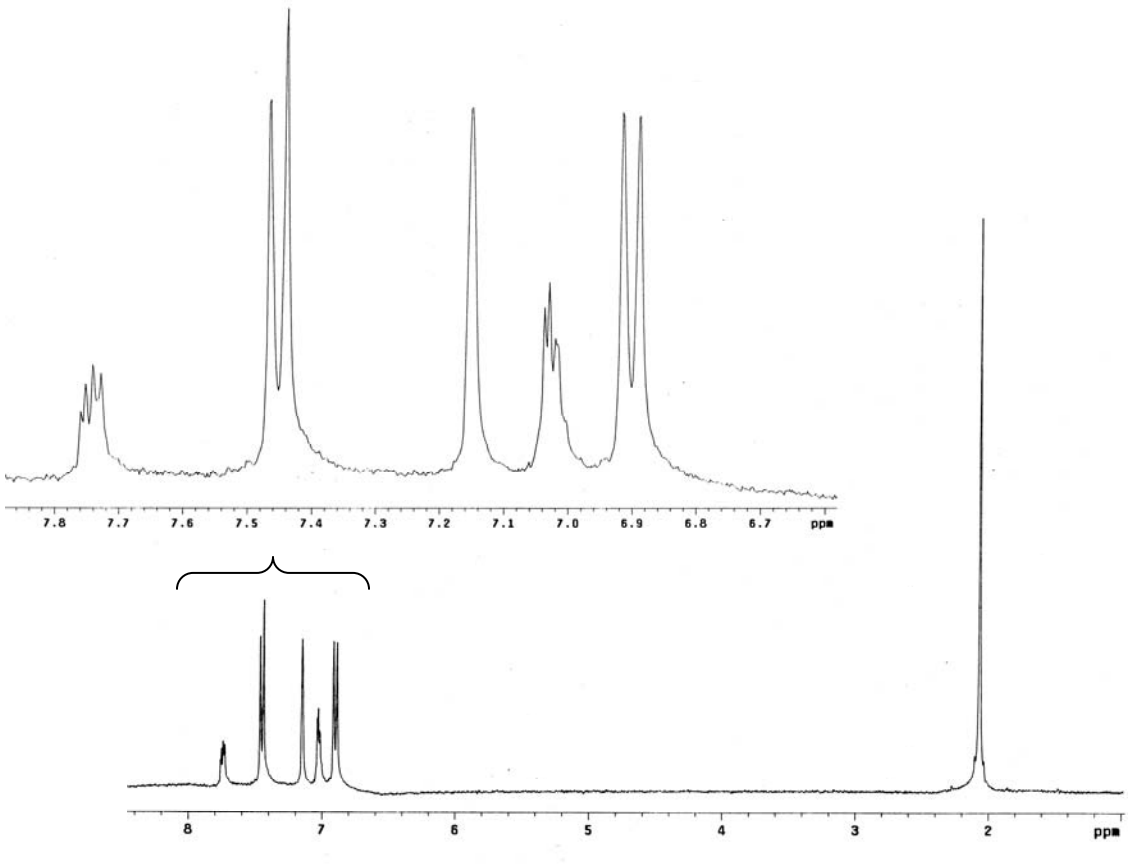

Figure 5.1: ^{1}H NMR of compound **2**

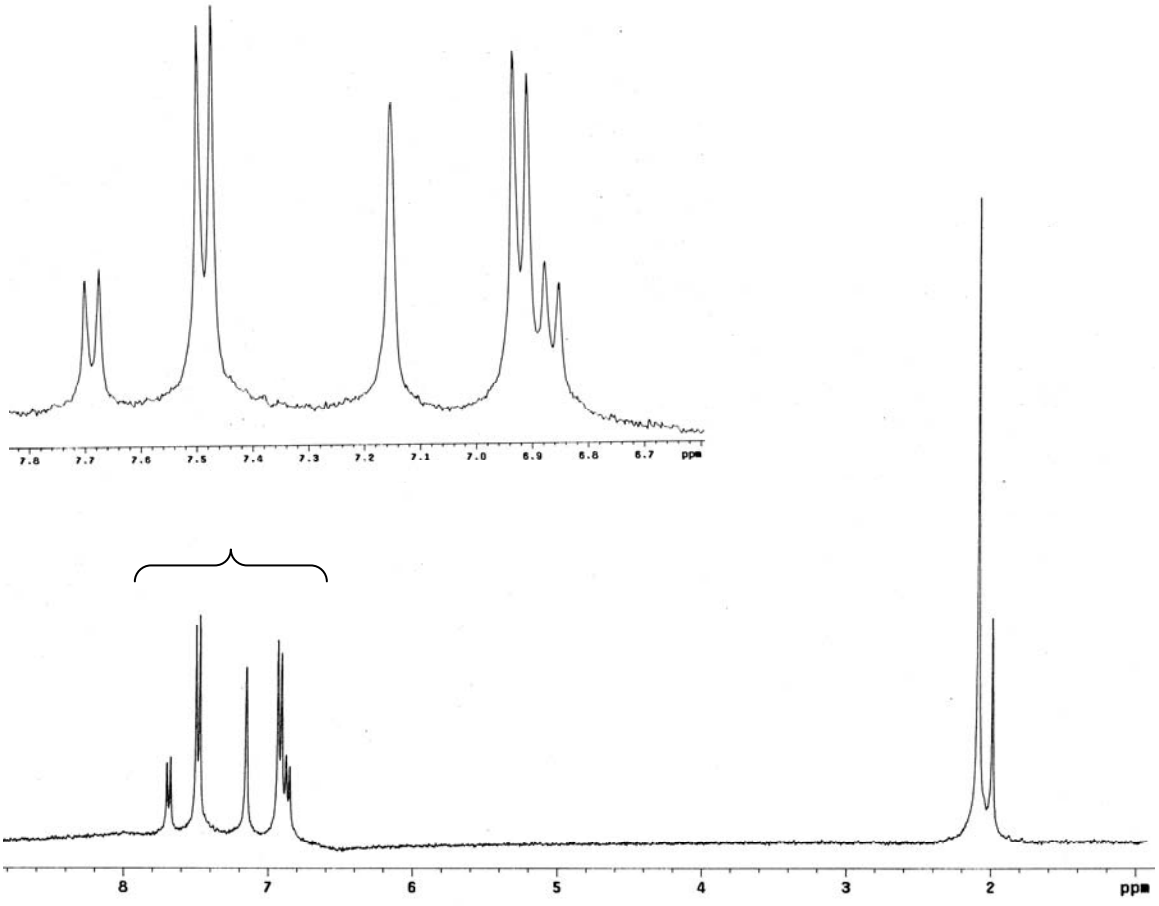

Figure 5.2: ^{1}H NMR of compound **3**

The crystal structures of **1-3** were determined and an ORTEP diagram of **1**·2C_6H_6 is shown in Figure 5.3 while selected bond distances and angles are collected in Table 5.1. Curiously, the Ge-Ge bond distance in **1** measures 2.408 Å, which is shorter than the reported Ge-Ge bond length in the related perphenyl digermane $Ph_3GeGePh_3$·2C_6H_6 (**4**·2C_6H_6) of 2.446(1) Å,[61] as well as that in the unsolvated form of **4** (2.437(2) Å).[62] A survey of twenty five structurally characterized digermanes [61-62,67,69,90,95-96,105,161,181,193-204] reveals that the Ge-Ge bond distance in **1** is the third shortest Ge-Ge bond length to be reported, where only $Cl_3CCOOPh_2GeGePh_2OOCCCl_3$ (**5**)[69] and (2,6-$Dipp_2C_6H_3$)H_2GeGeH_2($C_6H_3Dipp_2$-2,6) (Dipp = 2,6-diisopropylphenyl)[197] have shorter

bond lengths of 2.393(2) and 2.402(1) Å, respectively. The short bond length in the later compound is not surprising despite the presence of the bulky aryl groups at each germanium atom, since the other two substituents are sterically unencumbering hydrogen atoms. The bond length in **5** is constricted because the carbonyl oxygen atoms in each of the trichloroacetato ligands are coordinated to the opposite Ge atom to yield a hypervalent five-coordinate Ge center in each case.[69] The structure of $Ge_2Tol_6 \cdot C_6H_6$ was recently determined and this compound also has a short Ge-Ge distance that measures 2.419(1) Å.[205]

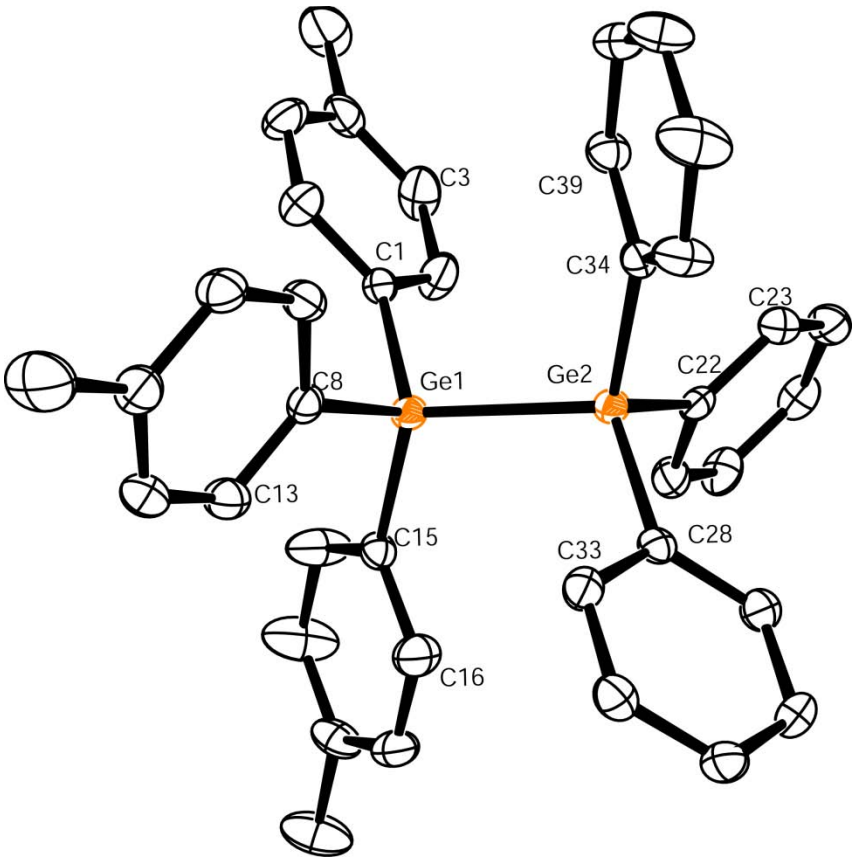

Figure 5.3: ORTEP diagram of $Tol_3GeGePh_3$ (**1**$\cdot 2C_6H_6$). The two benzene molecules are not shown.

Table 5.1: Selected bond distances (Å) and angles (deg) for $Tol_3GeGePh_3 \cdot 2C_6H_6$ (**1**$\cdot 2C_6H_6$).

Ge(1)-Ge(2)	2.408(1)	C(1)-Ge(1)-C(8)	109.64(9)
Ge(1)-C(1)	1.942(2)	C(1)-Ge(1)-C(15)	109.76(9)
Ge(1)-C(8)	1.942(2)	C(8)-Ge(1)-C(15)	108.94(9)
Ge(1)-C(15)	1.935(2)	C(22)-Ge(2)-C(28)	109.89(9)
Ge(2)-C(22)	1.941(2)	C(22)-Ge(2)-C(34)	110.32(9)
Ge(2)-C(28)	1.940(2)	C(28)-Ge(2)-C(34)	109.97(8)
Ge(2)-C(34)	1.939(2)	C(1)-Ge(1)-Ge(2)	108.47(8)
		C(8)-Ge(1)-Ge(2)	109.72(7)
		C(15)-Ge(1)-Ge(2)	110.30(7)
		C(22)-Ge(2)-Ge(1)	109.18(7)
		C(28)-Ge(2)-Ge(1)	110.47(7)
		C(34)-Ge(2)-Ge(1)	106.97(7)

The short Ge-Ge bond distances in **1**$\cdot 2C_6H_6$ and $Ge_2Tol_6 \cdot C_6H_6$ might be attributed to electronic effects, since the *para*-methyl group of the tolyl substituents presumably renders the germanium atoms more electron rich via inductive effects relative to a triphenylsubstituted germanium center. However, the constriction of the Ge-Ge bond distance in **1**$\cdot 2C_6H_6$ and $Ge_2Tol_6 \cdot C_6H_6$ is drastic compared to that in $Ph_3GeGePh_3 \cdot 2C_6H_6$, and similar short Ge-Ge bond lengths were not observed in **2**$\cdot C_7H_8$ and **3**$\cdot C_7H_8$ (*vide infra*). Crystal packing effects combined with electronic effects from the tolyl substituents also are likely to contribute to the contracted bond distances in these molecules.

The structure of the trigermane **2**·C_7H_8 is shown in Figure 5.4 and selected bond distances and angles are collected in Table 5.2. Structurally characterized linear trigermanes are rare, and to our knowledge the structures of only six other such species have been previously reported.[57,76-77,206-208] The average Ge-Ge bond distance in **2**·C_7H_8 is 2.4328(5) Å, which is shorter than the average Ge-Ge bond length in Ge_3Ph_8 [**6**, 2.440(2) Å][57] but is similar to the average Ge-Ge bond distance of 2.429(1) Å in $Ph_3GeGeMe_2GePh_3$ (**7**).[76] However, the contraction of the Ge-Ge bond length in **2**·C_7H_8 compared to those in **6** is not as pronounced as that observed between **1**·$2C_6H_6$ and $Ph_3GeGePh_3$, further suggesting that interplay of electronic and steric effects in the trigermane **2**·C_7H_8 have a combined effect on the Ge-Ge bond distance. The Ge-Ge-Ge bond angle at Ge(2) in **2**·C_7H_8 measures 114.80(2)^o, which is more acute than those in both **6** [121.3(1)˚][57] and **7** [120.3(1)˚][76] but is similar to those in the halide –substituted trigermanes X^{t}Bu$_2$GeGe^{t}Bu$_2$Ge^{t}Bu$_2$X [X = Br,[208] 113.6(1)˚; X = I,[207] 115.4(1)˚]. The C(22)-Ge(2)-C(28) bond angle in **2**·C_7H_8 which measures 106.2(1)˚ is also more acute than the corresponding bond angle at the central germanium atom in both **6** [108.7(4)˚][57] and **7** [109.2(2)˚],[76] which can be attributed to the steric effects of the six terminal tolyl groups.

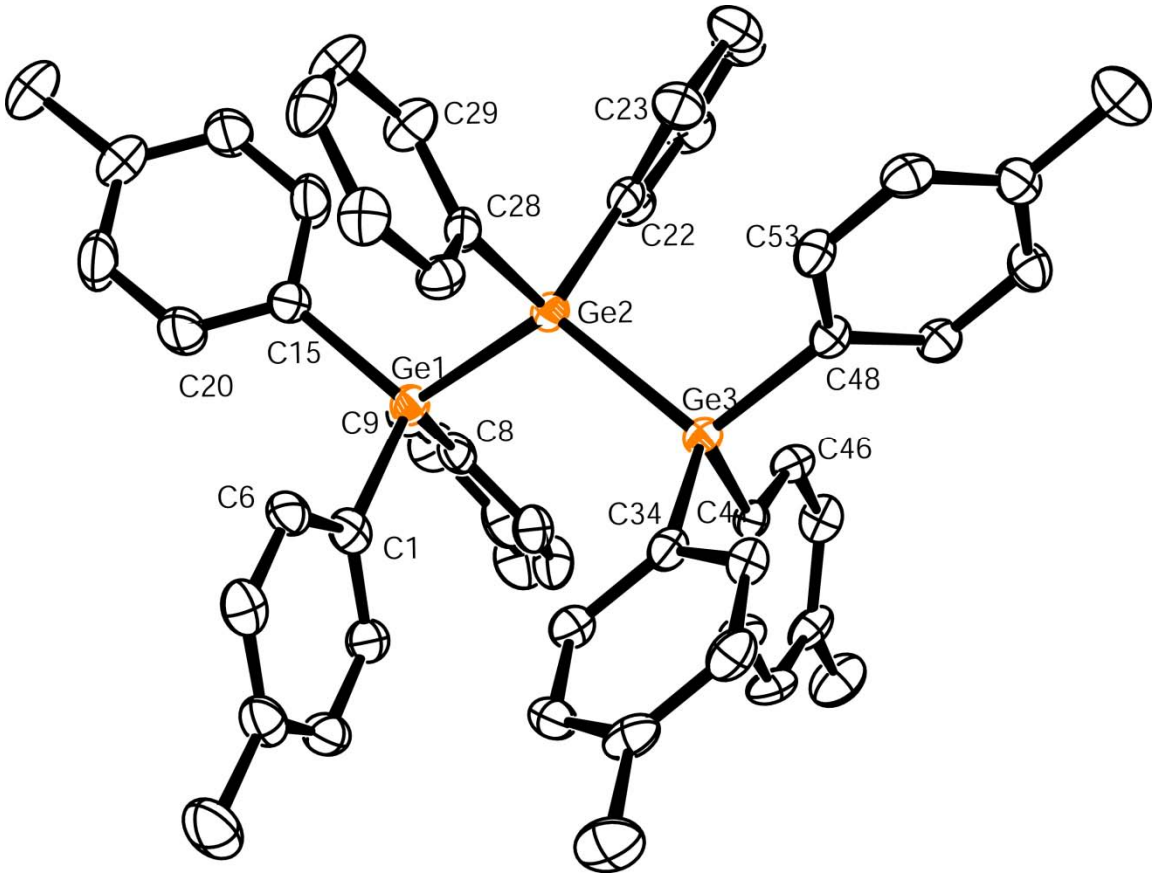

Figure 5.4: ORTEP diagram of $Tol_3GeGePh_2GePh_3$ (**2**·C_7H_8). The toluene molecule is not shown.

Table 5.2: Selected bond distances (Å) and angles (deg) for $Tol_3GeGePh_2GePh_3 \cdot C_7H_8$ (**2**$\cdot C_7H_8$).

Ge(1)-Ge(2)	2.4318(5)	Ge(1)-Ge(2)-Ge(3)	114.80(2)
Ge(2)-Ge(3)	2.4338(4)	C(1)-Ge(1)-C(8)	110.0(1)
Ge(1)-C(1)	1.958(3)	C(1)-Ge(1)-C(15)	108.1(1)
Ge(1)-C(8)	1.959(3)	C(8)-Ge(1)-C(15)	105.8(1)
Ge(1)-C(15)	1.966(3)	C(22)-Ge(2)-C(28)	106.2(1)
Ge(2)-C(22)	1.958(3)	C(34)-Ge(3)-C(41)	108.7(1)
Ge(2)-C(28)	1.955(3)	C(34)-Ge(3)-C(48)	107.6(1)
Ge(3)-C(34)	1.957(3)	C(41)-Ge(3)-C(48)	109.0(1)
Ge(3)-C(41)	1.945(3)	C(1)-Ge(1)-Ge(2)	106.7(8)
Ge(3)-C(48)	1.944(3)	C(8)-Ge(1)-Ge(2)	117.36(9)
		C(15)-Ge(1)-Ge(2)	108.52(9)
		C(22)-Ge(2)-Ge(1)	111.50(9)
		C(28)-Ge(2)-Ge(1)	113.93(8)
		C(22)-Ge(2)-Ge(3)	105.28(8)
		C(28)-Ge(2)-Ge(3)	113.93(8)
		C(34)-Ge(3)-Ge(2)	117.53(8)
		C(41)-Ge(3)-Ge(2)	106.95(8)
		C(48)-Ge(3)-Ge(2)	106.81(8)

The structure of the pertolyl-substituted trigermanes **3**·C_7H_8 is shown in Figure 5.5 and selected bond distances and angles are given in Table 5.3. The Ge-Ge bond distances in **3**·C_7H_8 are longer than those in **2**·C_7H_8 and **7** due to the additional steric crowding imposed by the two central tolyl substituents. The average Ge-Ge bond distance in **3**·C_7H_8 is 2.4404(5) Å, a value nearly identical to that of trigermane **6** [2.440(2) Å].[57] The central Ge-Ge-Ge bond angle in **3**·C_7H_8 of 117.54(1)˚ is more acute than those in both **6** [121.3(1)˚][57] and **7** [120.3(1)˚][76], but is more obtuse than the corresponding angle in **2**·C_7H_8 [114.80(2)˚]. The central C(23)-Ge(2)-C(30) angle in **3**·C_7H_8 measures 106.45(9)˚, which is slightly more obtuse than that in **2**·C_7H_8 [106.2(1)˚], but is more acute than the corresponding angles in both **6** [108.7(4)˚][57] and **7** [109.2(2)˚].[76] Therefore, the effects resulting from the presence of tolyl groups versus phenyl groups at the central germanium atom in the three trigermanes **2**·C_7H_8, **3**·C_7H_8 and **6** depend on the identity of the substituents attached to the terminal germanium atoms. The trigermane **3**·C_7H_8, which contains eight tolyl substituents and thus is the most sterically encumbered of these three molecules, has the longest Ge-Ge bond distances but intermediate Ge-Ge-Ge and C-Ge-C bond angles at the central germanium atom. The trigermane **7**, which contains sterically unencumbering methyl substituents at the central germanium atom, has the shortest Ge-Ge bond distances among the three molecules and the most obtuse bond angles at the central germanium atom.

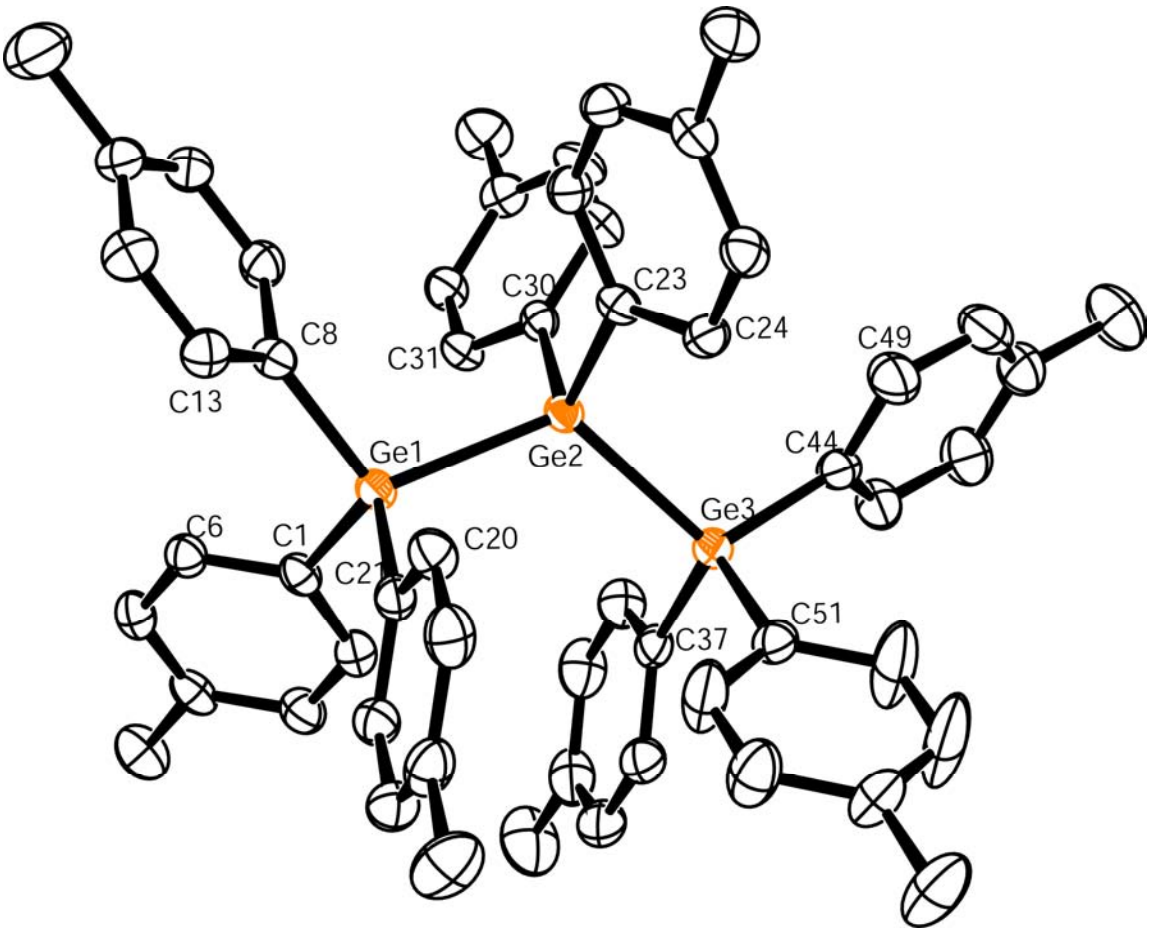

Figure 5.5: ORTEP diagram of $Tol_3GeGeTol_2GeTol_3.C_7H_8$ (**3**·C_7H_8). The toluene molecule is not shown.

Table 5.3: Selected bond distances (Å) and angles (deg) for $Tol_3GeGeTol_2GeTol_3 \cdot C_7H_8$ (**3**$\cdot C_7H_8$).

Ge(1)-Ge(2)	2.4450(4)	Ge(1)-Ge(2)-Ge(3)	117.54(1)
Ge(2)-Ge(3)	2.4359(5)	C(1)-Ge(1)-C(8)	108.33(9)
Ge(1)-C(1)	1.951(2)	C(1)-Ge(1)-C(21)	108.02(9)
Ge(1)-C(8)	1.951(2)	C(8)-Ge(1)-C(21)	108.5(1)
Ge(1)-C(21)	1.953(2)	C(23)-Ge(2)-C(30)	106.45(9)
Ge(2)-C(23)	1.958(2)	C(37)-Ge(3)-C(44)	107.0(1)
Ge(2)-C(30)	1.960(2)	C(37)-Ge(3)-C(51)	108.8(1)
Ge(3)-C(37)	1.950(2)	C(44)-Ge(3)-C(51)	107.4(1)
Ge(3)-C(44)	1.962(2)	C(1)-Ge(1)-Ge(2)	114.30(7)
Ge(3)-C(51)	1.949(2)	C(8)-Ge(1)-Ge(2)	108.32(6)
		C(21)-Ge(1)-Ge(2)	109.24(6)
		C(23)-Ge(2)-Ge(1)	106.21(6)
		C(30)-Ge(2)-Ge(1)	108.76(6)
		C(23)-Ge(2)-Ge(3)	109.94(7)
		C(30)-Ge(2)-Ge(3)	107.42(7)
		C(37)-Ge(3)-Ge(2)	109.16(7)
		C(44)-Ge(3)-Ge(2)	110.08(7)
		C(51)-Ge(3)-Ge(2)	114.09(7)

The synthesis of tetragermane $Tol_3GeGePh_2GePh_2GeTol_3$ (**11**) was achieved in four steps starting from hexaphenyldigermane (Scheme 5.2). Using a variation of a published procedure, a single phenyl group was cleaved from each germanium atom in $Ph_3GeGePh_3$ (**4**) using trichloroacetic acid to yield the 1,2-dichloroacetato derivative **5**,[69] and this was subsequently converted to the 1,2-dichloride **8** using concentrated hydrochloric acid.[69] The synthesis of **8** by the action of anhydrous HCl on $Ph_3GeGePh_3$ under pressure has also been described.[67] Treatment of **8** with $LiAlH_4$ furnished the 1,2-dihydride **10** in 79 % yield. The ^1H NMR spectrum of **10** contains a singlet for the two equivalent hydride protons at δ 5.58 ppm, and the Ge-H stretching frequency was observed at 2033cm^{-1} in

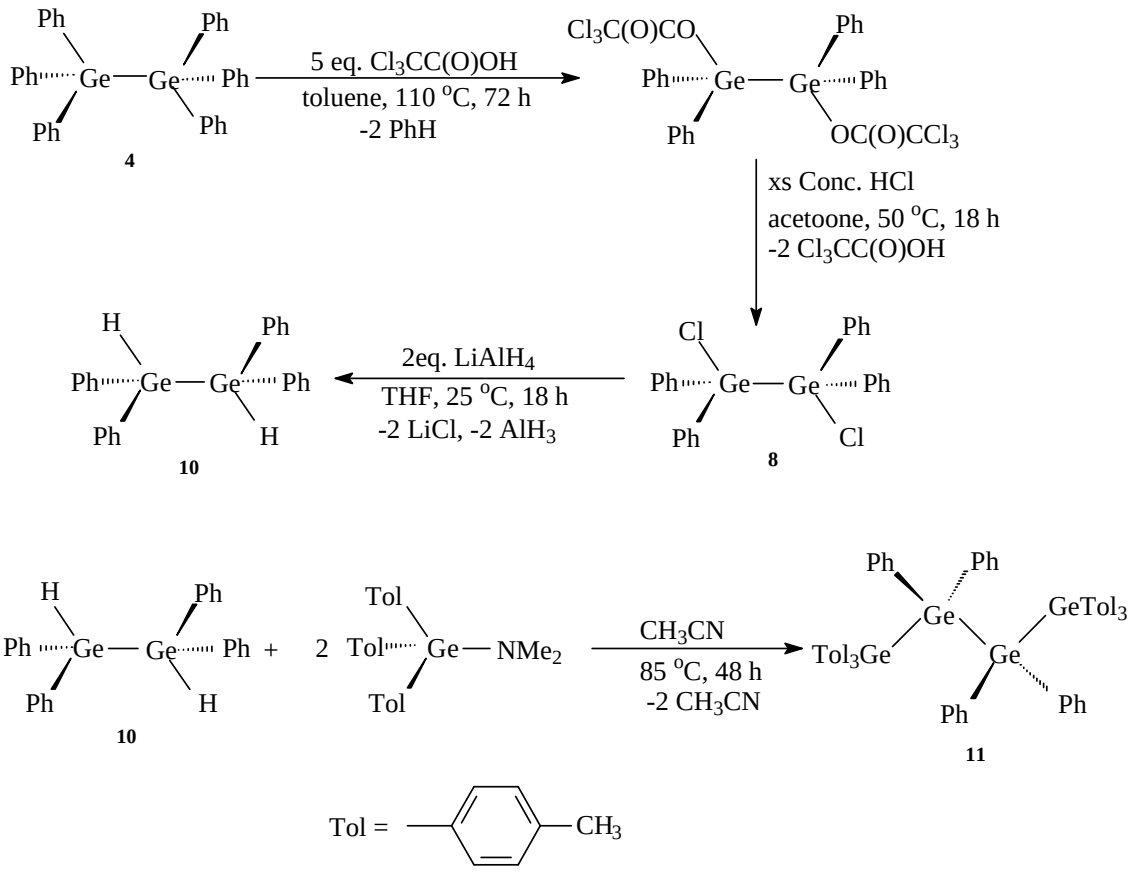

Scheme 5.2: Stepwise synthesis of tetragermane $Tol_3GeGePh_2GePh_2GeTol_3$ (**11**)

the IR spectrum of **10**. The synthesis of **10** has been achieved by other methods,[209-211] including by the hydrolysis of Ph_2GeHLi[211] and also by the catalytic dehydrocoupling of Ph_2GeH_2,[210] and the spectral data obtained for **10** agree with the reported values. The tetragermane **11** was prepared from **10** and two equivalents of Tol_3GeNMe_2 in 80 % yield via the hydrogermolysis reaction in CH_3CN , which again proceeds via the *in situ* generation of the reactive Tol_3GeCH_2CN intermediate. Similar to what was observed in the ^1H NMR spectra of **1** and **2** , resonances for the *ortho*-protons of the tolyl substituents of **11** are shifted downfield from those of the phenyl substituents while those for the *meta*-protons are shifted upfield .

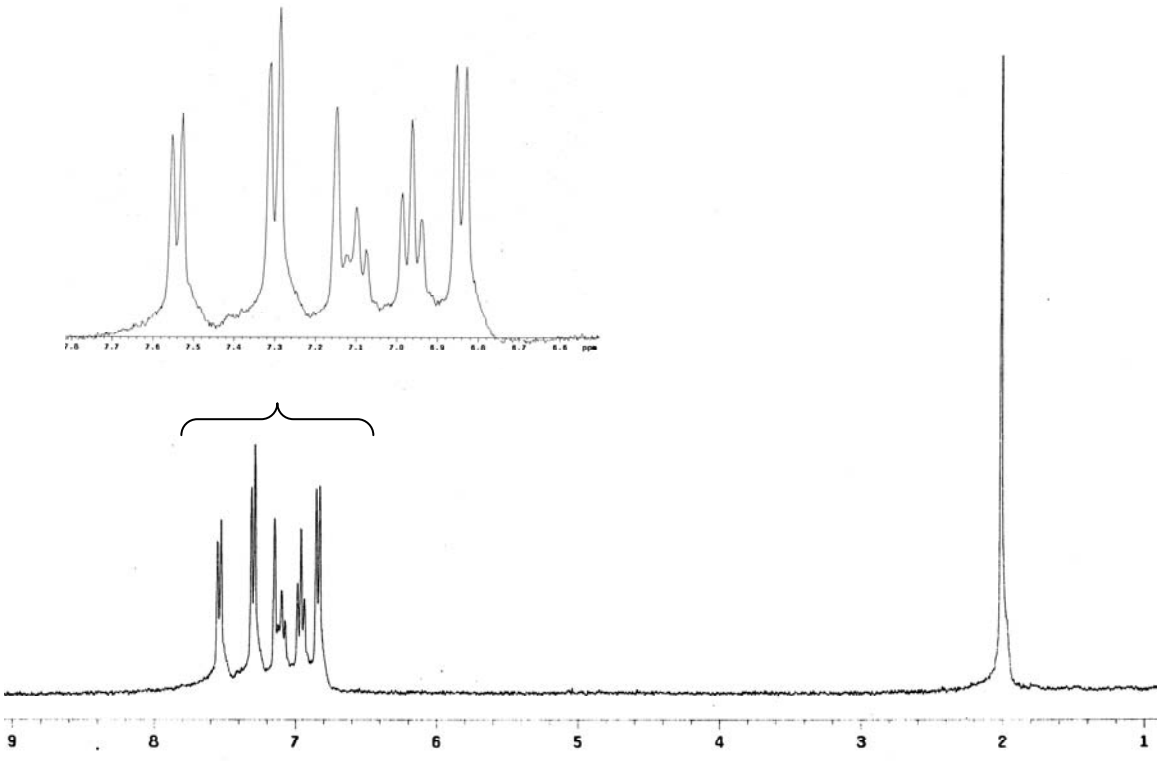

Figure 5.6: ^1H NMR of compound **11**

Structurally characterized tetragermanes are rare,[57,76-77,207-208,212] and compounds that have been characterized by this method include $Ge_4Ph_{10}\cdot 2C_6H_6$ (**12**$\cdot 2C_6H_6$),[49] 1,4-dichloro-1,1,2,2,3,3,4,4-octaphenyltetragermane,[77] and 1,4-diido-1,1,2,2,3,3,4,4-octaphenyltetragermane.[212] An ORTEP diagram of the tetragermane **11** is shown in Figure 5.7 and the selected bond distances and angles for **11** are collected in Table 5.4. Compound **11** crystallizes with two independent molecules in the unit cell, where one of the molecules (molecule 1) is completely ordered and the other (molecule 2) is disordered. Both molecules of **11** are located on a crystallographic inversion center, and the germanium atoms of molecule 2 are disordered over two positions with occupancies of 85.6 and 14.4 %. The bond distances given for molecule 2 are a weighted average of the two positions. The average Ge-Ge bond distance in **11** is 2.455(3) Å which is slightly shorter than the average Ge-Ge bond length in the perphenyl-substituted tetragermane **12**$\cdot 2C_6H_6$ (2.462(2) Å).[49]

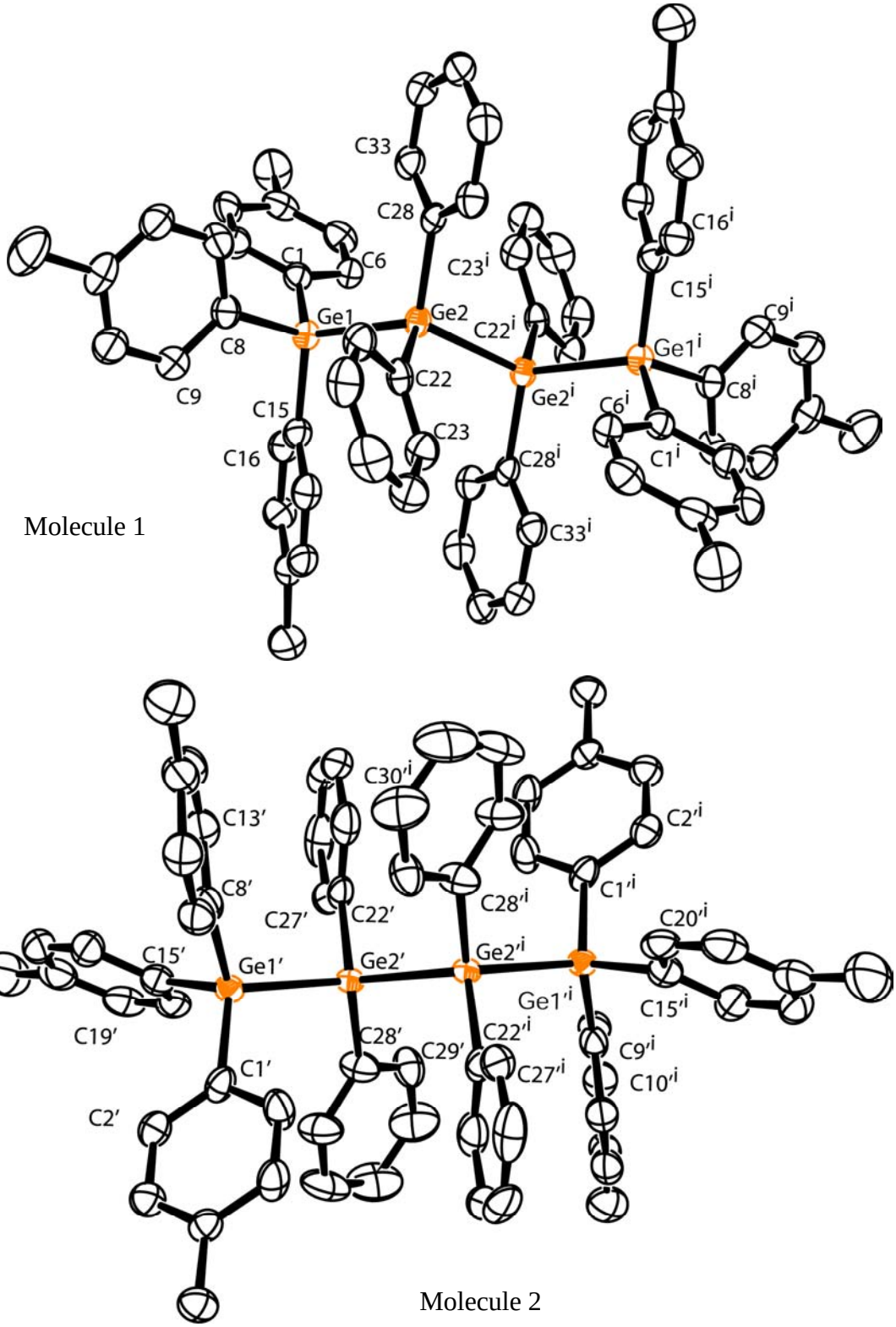

Figure 5.7: ORTEP diagram of $Tol_3GeGePh_2GePh_2GeTol_3 \cdot C_7H_8$ (**11**). The toluene molecule is not shown.

Table 5.4: Selected bond distances (Å) and angles (deg) for $Tol_3GeGePh_2GePh_2GeTol_3$ (**11**).

Molecule 1		*Molecule 2*[a]	
Ge(1)-Ge(2)	2.4490(8)	Ge(1′)-Ge(2′)	2.4460(3)
Ge(2)-Ge(2^{i})	2.457(1)	Ge(2′)-Ge(2′i)	2.448(3)
Ge(1)-C(1)	1.961(4)	Ge(1′)-C(1)	1.953(5)
Ge(1)-C(8)	1.960(4)	Ge(1′)-C(8)	2.008(5)
Ge(1)-C(15)	1.964(5)	Ge(1′)-C(15)	1.947(6)
Ge(2)-C(22)	1.971(4)	Ge(2′)-C(22)	1.980(5)
Ge(2)-C(28)	1.974(4)	Ge(2′)-C(28)	1.981(5)
Ge(1)-Ge(2)-Ge(2^{i})	115.53(3)	Ge(1′)-Ge(2′)-Ge(2′^{i})	118.9(2)
C(1)-Ge(1)-C(8)	108.1(1)	C(1)-Ge(1′)-C(8)	106.6(2)
C(1)-Ge(1)-C(15)	107.5(2)	C(1)-Ge(1′)-C(15)	113.0(2)
C(8)-Ge(1)-C(15)	109.4(2)	C(8)-Ge(1′)-C(15)	106.8(2)
C(22)-Ge(2)-C(28)	106.2(2)	C(22)-Ge(2′)-C(28)	111.2(2)
C(1)-Ge(1)-Ge(2)	116.5(1)	C(1)-Ge(1′)-Ge(2′)	110.8(1)
C(8)-Ge(1)-Ge(2)	106.2(1)	C(8)-Ge(1′)-Ge(2′)	114.2(1)
C(15)-Ge(1)-Ge(2)	109.1(1)	C(15)-Ge(1′)-Ge(2′)	105.5(2)
C(22)-Ge(2)-Ge(1)	103.5(1)	C(22)-Ge(2′)-Ge(1′)	103.8(2)
C(28)-Ge(2)-Ge(1)	110.7(1)	C(28)-Ge(2′)-Ge(1′)	108.2(2)
C(22)-Ge(2)-Ge(2^{i})	108.6(1)	C(22)-Ge(2′)-Ge(2′^{i})	107.8(1)
C(28)-Ge(2)-Ge(2^{i})	111.5(1)	C(28)-Ge(2′)-Ge(2′^{i})	106.5(2)

[a] The germanium atoms in molecule 2 of **11** are disordered over two positions with occupancies of 85.6 and 14.4 %. Distances and angles including Ge(1′) and Ge (2′) are a weighted average based on the two occupancies.

As observed for the digermane **1**·$2C_6H_6$ and the trigermanes **2**·C_7H_8 and **3**·C_7H_8 versus their perphenyl analogs, the steric and electronic effects of the tolyl groups in **11**

versus the phenyl groups in **12**·2C_6H_6 have an effect on the structural parameters. The terminal Ge-Ge bonds in both molecules of **11** [2.4490(8) and 2.460(3) Å] are shorter than those in the perphenyl tetragermane **12**·2C_6H_6 [2.463(2) Å],[49] and the internal Ge-Ge distances in the molecules of **11** [2.457(1) and 2.448(3) Å] are also shorter than that of **12**·2C_6H_6 [2.461(3) Å].[49] Furthermore, the crystallographically unique Ge-Ge-Ge bond angle in both molecules of **11** [115.53(3) and 118.9(2)˚] are more acute than that in **12**·2C_6H_6 [121.3(1)˚].[49]

Table 5.5: Torsion angles (deg) along the Ge(1)-Ge(2) and Ge(2)-Ge(2^i) bond in molecule 1 of $Tol_3GeGePh_2GePh_2GeTol_3$ (**11**).

C(1)-Ge(1)-Ge(2)-Ge(2^i)	72.8(1)	Ge(1)-Ge(2)-Ge(2^i)-C(22^i)	64.3(1)
C(1)-Ge(1)-Ge(2)-C(28)	55.1(1)	C(28)-Ge(2)-Ge(2^i)-C(22^i)	63.3(1)
C(8)-Ge(1)-Ge(2)-C(28)	65.3(1)	C(28)-Ge(2)-Ge(2^i)-Ge(1^i)	52.4(1)
C(8)-Ge(1)-Ge(2)-C(22)	48.2(1)	C(22)-Ge(2)-Ge(2^i)-Ge(1^i)	64.3(1)
C(15)-Ge(1)-Ge(2)-C(22)	69.6(1)	C(22)-Ge(2)-Ge(2^i)-C(28^i)	63.3(1)
C(15)-Ge(1)-Ge(2)-Ge(2^i)	49.0(1)	Ge(1)-Ge(2)-Ge(2^i)-C(28^i)	52.4(1)

The overall geometry of **11** approximates that of *n*-butane, and is also similar to that of the tetragermane **12**·2C_6H_6. Torsion angles for molecule 1 of **11** about the Ge(1)-Ge(2) and Ge(2)-Ge(2^i) bonds are collected in Table 5. The two terminal Tol_3Ge- groups in molecule 1 are disposed in an anti-conformation about the central Ge(2)-Ge(2^i) bond and the dihedral angle is exactly 180˚. The environment about the central Ge(2)-Ge(2^i) bond in molecule 1 of **11** is symmetric due to the presence of a crystallographic inversion center. However, although the phenyl group containing C(8) and Ge(2^i) deviates from the ideal value of 180˚ by 13.2˚. The structure of **12**·2C_6H_6 exhibits a similar arrangement

along the terminal Ge(1)-Ge(2) bond, but the dihedral angle in **12**·$2C_6H_6$ is distorted by only 7.4˚, and the greater distortion in **11** is attributed to the increased steric bulk of the tolyl substituents.

UV/visible spectra and cyclic voltammetry

The series of four oligogermanes **1-3** and **11** were characterized using cyclic voltammetry in CH_2Cl_2 solution with 0.1M $[Bu_4N][PF_6]$ as the supporting electrolyte. Voltammograms for each of the four species are shown in Figure 5.8, average values for the oxidation waves for four separate runs and Ge-Ge bond distance data are collected in Table 5.6, and the proposed electrochemical decomposition pathways for **1-3** and **11** are shown in Scheme 5.3. The voltammograms for each of these Ge_nAr_{2n+2} compounds exhibit a total of *n*-1 irreversible oxidation waves. This is significant, since oligogermanes that have been previously characterized by this method typically exhibit only one irreversible oxidation wave[180,182,213-214] due to decomposition of the oligogermanes after the oxidation event occurs. However, the multiple waves observed for **2**, **3**, and **11** suggest that in the case of these three compounds, the species generated after oxidation is stable and undergoes either one (compounds **2** and **3**) or two subsequent one-electron oxidation process.

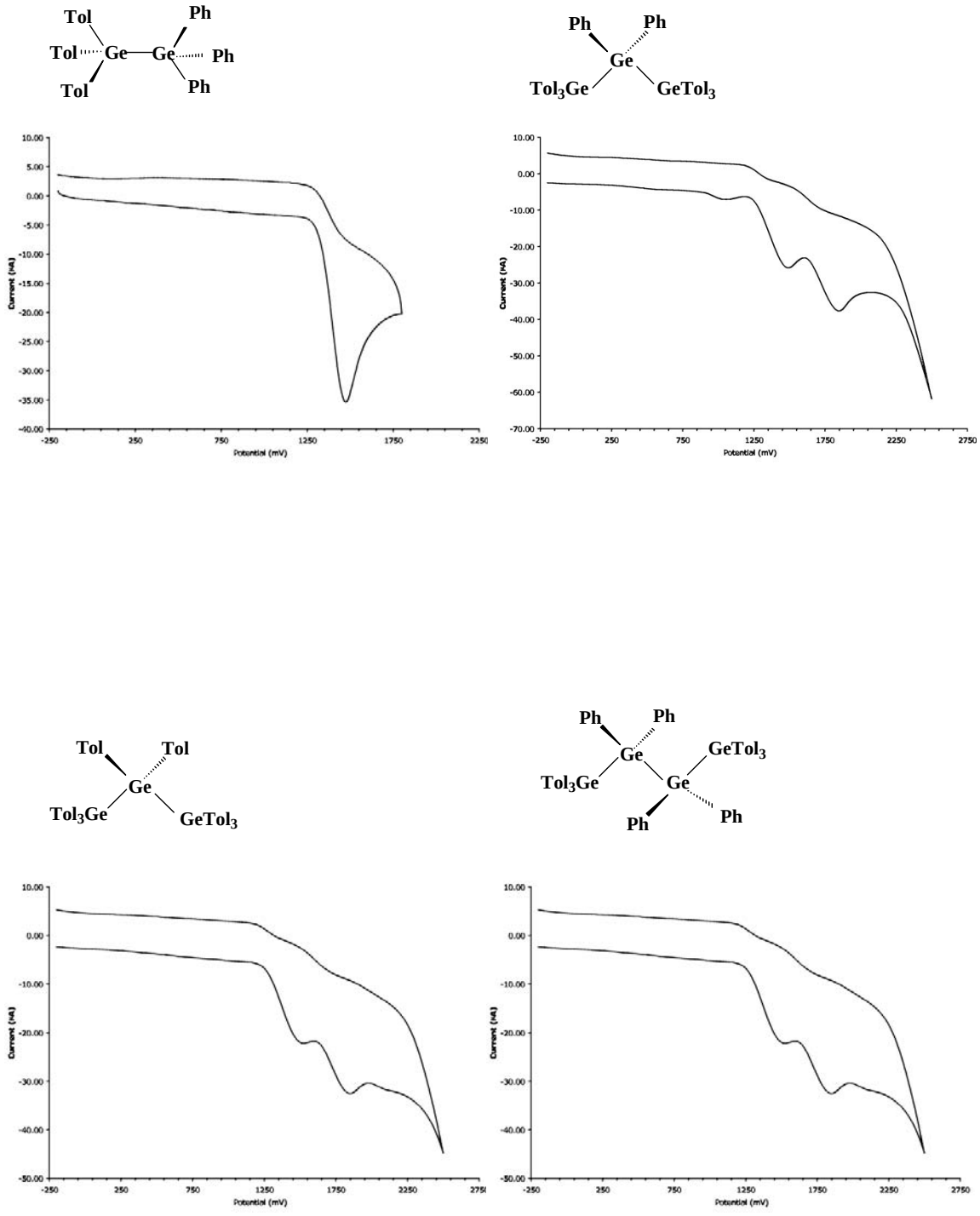

Figure 5.8: Cyclic voltammograms for CH_2Cl_2 solutions of compound **1**, **2**, **3**, and **11** obtained using $[^nBu_4N][PF_6]$ as the supporting electrolyte

Table 5.6: Oxidation potentials, absorbance maxima and Ge-Ge bond distances for compounds **1-3**, **11**, Ge_2Tol_6 and Ge_nPh_{2n+2} (n = 2-4) in CH_2Cl_2 solution using 0.1 M $[Bu_4N][PF_6]$ as the supporting electrolyte.

Compound	*Eox (mV)*	λ_{max} *(nm)*	$d_{Ge\text{-}Ge}$ *(Å)*
$Tol_3GeGePh_3$ (**1**)	1483 ± 17	240	2.408(1)
$Tol_3GeGePh_2GeTol_3$ (**2**)	1498 ± 14	251	2.4328(5)[a]
	1860 ± 15		
$Tol_3GeGeTol_2GeTol_3$ (**3**)	1542 ± 11	253	2.4405(5)[a]
	1865 ± 13		
$Tol_3GeGePh_2GePh_2GeTol_3$ (**11**)	1398 ± 14	285	2.455(3)[a]
	1718 ± 11		
	2242 ± 18		
Ge_2Tol_6	1757 ± 18	241	2.419(1)[b]
Ge_2Ph_6 (**4**)	1958 ± 19	240	2.446(1)[c]
Ge_3Ph_8 (**6**)	1696 ± 12	238[d]	2.440(2)[d]
	2052 ± 15		
Ge_4Ph_{10} (**12**)	1644 ± 22	282[d]	2.462(2)[d]
	2060 ± 17		
	2450 ± 18		

[a] Average value
[b] Data taken from ref. [48].
[c] Data taken from ref. [68].
[d] Data taken from ref. [39].

The oxidation potentials among the three digermanes **1**, Ge_2Tol_6, and Ge_2Ph_6 can be correlated with the Ge-Ge bond distances in these compounds. The single irreversible oxidation wave for **1** was observed at 1483 ± 17 mV, and this can be compared to that of

a commercial sample of Ge_2Ph_6 (1958 ± 19 mV) and a sample of Ge_2Tol_6 (1757 ± mV) prepared from Tol_3GeH and Tol_3GeNMe_2. Compound **1** exhibits the least positive oxidation potential among these three species and also has the shortest Ge-Ge bond distance. The electronic and steric attributes of the substituents both have an effect on the Ge-Ge bond length as well as on the relative energies of the frontier molecular orbitals[180], and since tolyl substituents are more inductively electron-donating and also more sterically encumbering than phenyl substituents, the trends in both oxidation potential and Ge-Ge bond length are as expected.

Compounds **2** and **3** both exhibit two irreversible oxidation waves in their cyclic voltammograms. The first (least positive) oxidation wave was observed at 1498 ± 14 mV for **2** and 1542 ± 11 mV for **3**, while the second oxidation waves for **2** (1860 ± 15 mV) and **3** (1865 ± 13 mV) were observed at nearly identical potentials, and two oxidation waves were also observed for a sample of Ge_3Ph_8 at 1696 ± 12 mV and 2052 ± 15 mV. As found for the three digermanes described above, the same correlation of the potential of the first oxidation wave with bond length was observed for the trigermanes **2**, **3**, and Ge_3Ph_8. The Ge-Ge bond distances in **2** are 2.4318(5) and 2.4338(4) Å (av. 2.4328(5) Å) and are shorter the corresponding distances in **3**, which measure 2.4450(4) and 2.4395(5) Å (av. 2.4405(5) Å). The average Ge-Ge bond distance in Ge_3Ph_8 is similar to that of **3** and measures 2.440(2) Å.[49]

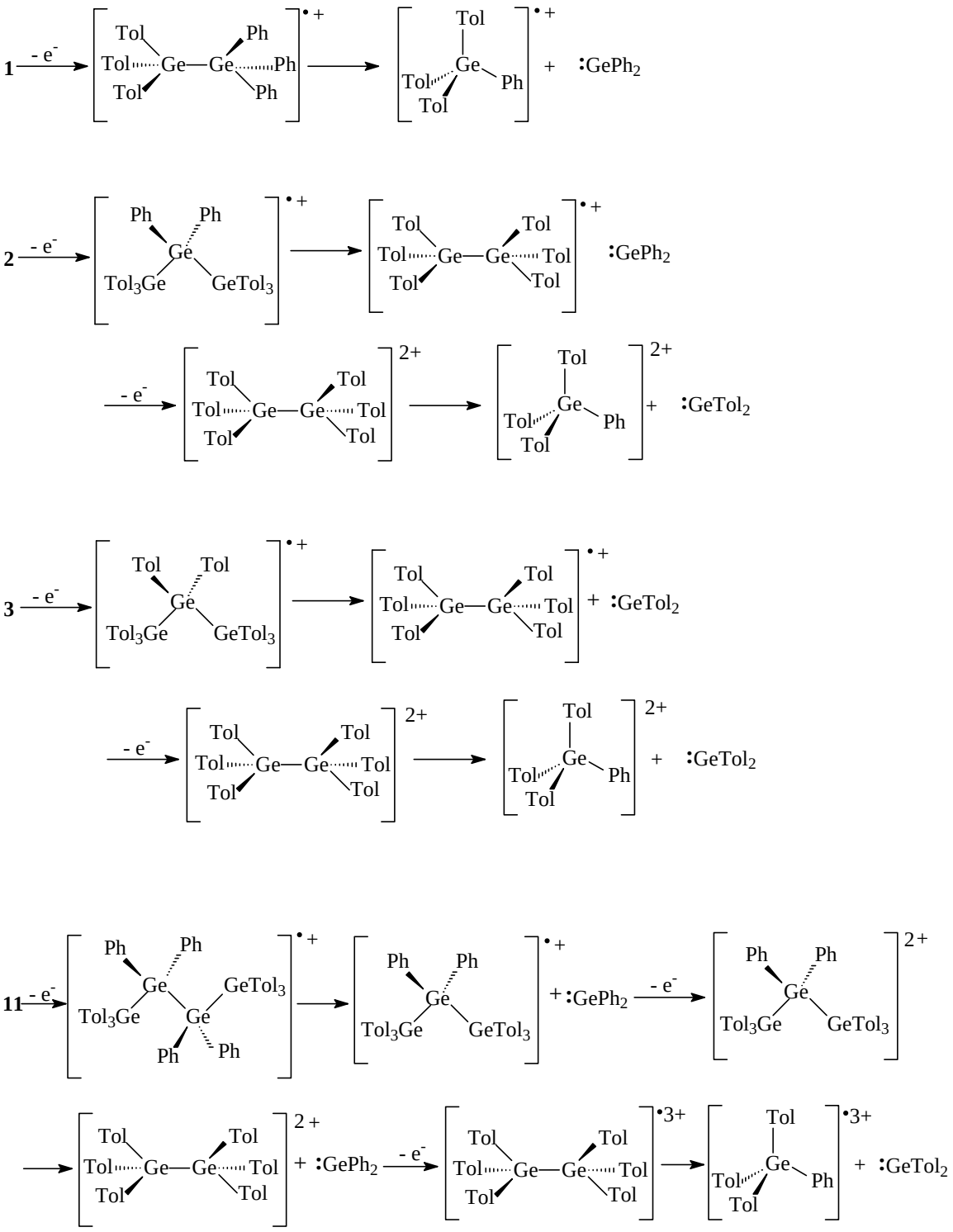

Scheme 5.3: The proposed electrochemical decomposition pathways for compound **1**, **2**, **3**, and **11**.

The data obtained for these digermanes and trigermanes suggests that the decomposition of the oligogermane via germylene extrusion is occurring in these systems. The loss of :GeR_2 fragments has been detected via trapping with 2,3-dimethyl-1,3-butadiene from the photolysis of oligo[91] and polygermanes,[215] and has also been postulated to occur in reactions of oligogermanes with tetracyanoethylene.[214,216] It should be noted, however, that homolytic Ge-Ge bond cleavage has also been observed as a competing process. The similarity of the potentials of the second oxidation waves in **2** and **3** suggests that the same chain contraction product is being generated from both molecules after the first oxidation event takes place. We propose that this species is $Ge_2Tol_6^{\cdot+}$, which is generated by the loss of :$GePh_2$ from **2** and :$GeTol_2$ from **3**. The oxidation potential for the digermane Ge_2Tol_6 at 1757 ± 18 mV is also consistent with this statement, since the positively charged species $Ge_2Tol_6^{\cdot+}$ generated from **2** (1860 ± 15 mV) and **3** (1865 ± 13 mV) is expected to have a more positive oxidation potential than the neutral species Ge_2Tol_6 due to its single positive charge.

The first oxidation wave for Ge_3Ph_8 is at a more positive potential than that of both **2** and **3**, which is consistent with the observations for the three digermanes **1** and Ge_2Tol_6, and Ge_2Ph_6 described above. The first oxidation of Ge_3Ph_8 results in extrusion of :$GePh_2$ to generate $Ge_2Ph_6^{\cdot+}$ and this species undergoes an additional oxidation event at 2052 ± 15 mV, which more positive than the oxidation wave for the neutral compound Ge_2Ph_6 at 1958 ± 19 mV. The second oxidation wave for Ge_3Ph_8 also occurred at a more positive potential than that for **2** and **3**, which is consistent with the oxidation wave of Ge_2Ph_6 being at a higher potential than both **1** and Ge_2Tol_6.

The CV for the tetragermane **11** exhibits three distinct waves at 1398 ± 14, 1718 ± 11, and 2242 ± 18 mV, indicating the sequential generation of two stable oligogermane decomposition products. The CV of Ge_4Ph_{10} also exhibits three oxidation waves that each appear at more positive potentials (1644 ± 22, 2060 ± 117, and 2450 ± 18 mV) than the corresponding waves for **11**, which is again consistent with the results obtained for the phenyl-substituted digermanes and trigermanes versus their tolyl-containing analogs. The presence of three oxidation waves for **11** and Ge_4Ph_{10} suggests that three germylene fragments are released from the Ge-Ge backbone, since this type of decomposition has been observed in photolysis studies of oligogermanes.[91,214-216] The first two germylenes resulting from the sequential oxidations of **11** are most likely $:GePh_2$, since the internal germanium atoms are phenyl substituted and are more susceptible to elimination. In the perphenyl-substituted tetragermane Ge_4Ph_{10}, all three of the germylenes released are $:GePh_2$, but the third oxidation of **11** results in the generation of the radical trivalent cation $Tol_3GeGeTol_3^{\cdot 3+}$, and this species then subsequently decomposes via elimination of the germylene $:GeTol_2$.

The UV/visible spectra of **1**-**3** and **11** are shown in Figure 5.9 and the λ_{max} values are collected in Table 5.10. The expected trend among the di, tri, and tetragermanes was observed, where the position of λ_{max} is red shifted with increasing catenation. The absorbance maximum corresponding to the $\sigma \rightarrow \sigma^*$ transition in the tetragermanes **11** at 285 nm ($\varepsilon = 3.43 \times 10^4$ L mol^{-1} cm^{-1}) is at lower energy than those of the trigermanes **2** and **3** and the digermane **1**. In addition to the band at 285 nm, three additional features at 274, 268, and 260 nm are present in the UV/visible spectrum of **11**, which are assigned to electronic transitions between the π and π^* orbitals of the aryl ligands. Similar $\pi \rightarrow \pi^*$

transitions for compounds **1-3** are also likely to occur, but the peaks for these transitions were not visible due to their overlap with the intense λ_{max} feature resulting from the $\sigma \rightarrow \sigma^*$ electronic transition. The red shift of the λ_{max} for **11** versus those for **1-3** allows these additional absorbance features to be observed in **11**. The λ_{max} for Ge_4Ph_{10} was reported at 282 nm (ε 3.98 × 10^4 L mol^{-1} cm^{-1}), and a second defined feature was also observed at 228 nm.[49] The λ_{max} for **2** (251 nm, ε 3.17 × 10^4 L mol^{-1} cm^{-1}) and **3** (253 nm, ε 2.55 × 10^4 L mol^{-1} cm^{-1}) appear at nearly the same wavelength, and are red shifted relative to that of **1** but are blue shifted relative to that of **11**. Both absorbance maxima are red shifted relative to the reported λ_{max} for Ge_3Ph_8 at 238 nm (ε 3.16 × 10^4 L mol^{-1} cm^{-1})[49]; however, the λ_{max} for **1** and Ge_2Ph_2[74] were both observed 240 nm.

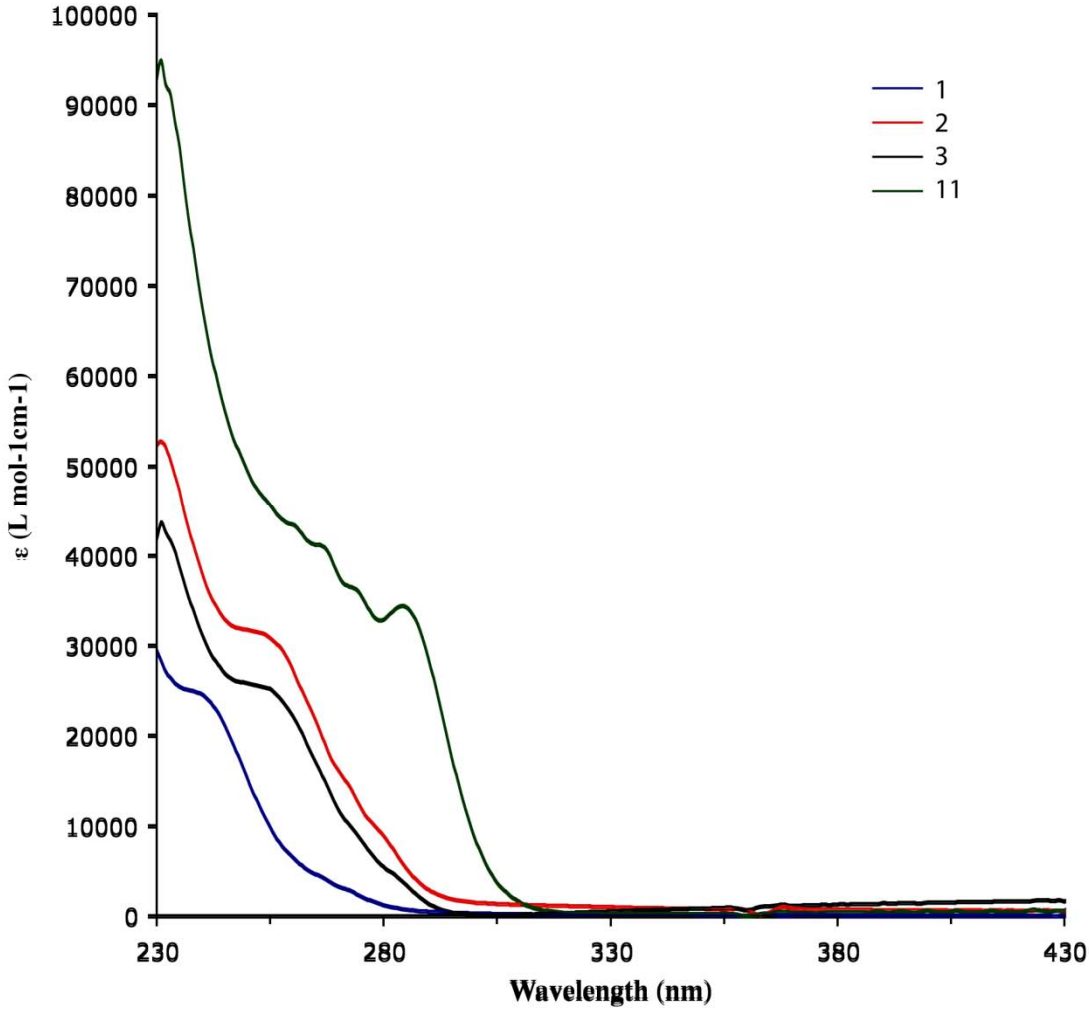

Figure 5.9: UV/visible spectra of **1-3** and **11**. (blue line = $Ph_3GeGeTol_3$, purple line = $Tol_3GeGePh_2GePh_2GeTol_3$, red line = $Tol_3GeGePh_2GeTol_3$, black line = $Tol_3GeGeTol_2GeTol_3$)

CONCLUSIONS

The series of *para*-tolyl-substituted oligogermanes $Tol_3GeGePh_3$ (**1**), $Tol_3GeGePh_2GeTol_3$ (**2**), $Tol_3GeGeTol_2GeTol_3$ (**3**), and $Tol_3GeGePh_2GePh_2GeTol_3$ (**11**) can be prepared via the hydrogermolysis reaction using Tol_3GeNMe_2 and Tol_2GeH_2 as synthetic building blocks. The structures of these four compounds differ from their perphenyl-substituted analogs, in both the Ge-Ge bond distances and, in the case of **2**, **3** and **11**, in the Ge-Ge-Ge bond angles, due to the different steric and electronic effects of the tolyl substituents. In general, the Ge-Ge bond distances are shorter and the Ge-Ge-Ge bond angles are more acute when tolyl substituents are introduced along the Ge-Ge backbone in place of phenyl substituents.

The incorporation of tolyl substituents also has an effect on the oxidation potential and UV/visible absorbance maxima in these compounds. Oligogermanes **1-3** and **11**, which have the general formula Ge_nAr_{2n+2} (Ar = *p*-$CH_3C_6H_4$ or Ph), exhibit *n*-1 oxidation waves in their cyclic voltammograms. This has not been observed previously, as oligogermanes typically exhibit only one irreversible oxidation wave regardless of the degree of catenation. We suggest that the first oxidation event for **1-3** results in extrusion of the germylene $:GeTol_2$, and the resulting electrochemical by-products for **2** and **3** are stable and undergo a second oxidation event with concomitant extrusion of a second germylene fragment.

Experimental

General considerations

All manipulations were performed under an atmosphere of nitrogen using standard Schlenk, syringe, and glovebox techniques.[116] The reagents *p*-$CH_3C_6H_4Cl$, elemental Mg, TolMgBr (1.0 M solution in THF), Ph_3GeH, $LiNMe_2$, trichloroacetic acid, and $LiALH_4$ were purchased from Aldrich. The compounds $GeBr_4$, $GeCl_4$, and Ge_2Ph_6 were purchased from Gelest, Inc. Solvents were purified using a Glass Contour Solvent Purification System. NMR spectra were recorded in C_6D_6 at room temperature using a Varian Gemini 2000 spectrometer operating at 300 MHz (^1H) or 75.5 MHz (^{13}C) and were referenced to the C_6D_6 solvent. Cyclic voltammograms were obtained using a Bioanalytical Systems Epsilon Electrochemical Workstation with a glassy-carbon working electrode, a platinum wire counter electrode, and an Ag/AgCl reference electrode using 1.0 M $[Bu_4N][PF_6]$ as the supporting electrolyte. UV/visible spectra were obtained using a Hewlett-Packard Agilent UV/visible spectroscopy system. IR spectra were recorded using a Hewlett-Packard Infrared Spectrometer. Elemental analyses were obtained by Midwest Microlabs or Galbraith Laboratories.

Synthesis of Tol_3GeCl

A flame-dried 3-necked flask equipped with a reflux condenser was charged with magnesium metal (4.30 g, 177 mmol). A solution of *p*-$CH_3C_6H_4Cl$ (14.92 g, 117.9 mmol) in THF (100 mL) was placed in a dropping funnel. The magnesium metal was coated

with approx. 15 mL of the *p*-$CH_3C_6H_4Cl$ solution and a crystal of iodine was added to the flask. The mixture was gently heated with a heat gun until the iodine color had faded, and the remaining *p*-$CH_3C_6H_4Cl$ solution was added dropwise over 45 min. The resulting reaction mixture was refluxed for 2 h, was allowed to cool, and then was added to a solution of $GeCl_4$ (8.43 g, 39.3 mmol) in THF (50 mL). The reaction mixture was refluxed for 90 min, was allowed to cool, and then was carefully poured over a 20 % aqueous HCl solution at 0 ^oC. The THF layer was separated and the aqueous layer was extracted with ether (3 × 50 mL). The combined THF layer and ethereal extracts were dried over anhydrous $MgSO_4$. The suspension was filtered and the volatiles were removed *in vacuo* to yield a viscous oil. The crude product was distilled *in vacuo* (125 ^oC, 0.05 torr) to remove impurities to yield Tol_3GeCl (12.425 g, 83 %) as a white solid. ^1H NMR δ 7.66 (d, *J* = 7.8 Hz, 6H, *o*-$H_3CC_6H_4$), 7.00 (d, *J* = 7.8 Hz, 6H, *m*-$H_3CC_6H_4$), 2.06 (s, 9H, $H_3CC_6H_4$) . ^{13}C NMR 140.6 (*ipso*-($H_3CC_6H_4$), 134.6 (*o*-$H_3CC_6H_4$), 130.0 (*p*-$H_3CC_6H_5$), 129.8 (*m*-$H_3CC_6H_4$), 21.4 (*p*-$H_3CC_6H_4$) ppm. *Anal*. Calcd. For $C_{21}H_{21}ClGe$: C,66.10; H, 5.55. Found: C, 66.25; H, 5.61.

Synthesis of Tol_3GeNMe_2

To a solution of Tol_3GeCl (1.951 g, 5.117 mmol) in benzene (20 mL) was added a suspension of $LiNMe_2$ (0.280 g, 5.49 mmol) in benzene (10 mL). The reaction mixture was stirred for 18 h and then filtered through Celite. The volatiles were removed *in vacuo* to yield Tol_3GeNMe_2 (1.51 g, 76 %) as a thick colorless oil. ^1H NMR δ 7.71 (d, *J* = 7.8 Hz, 6H, *o*-$H_3CC_6H_4$), 7.09 (d, *J* = 7.8 Hz, 6H, *m*-$H_3CC_6H_4$), 2.84 (s, 6H, $N(CH_3)_2$), 2.11

(s, 9H, $H_3CC_6H_4$). ^{13}C NMR: 139.1 (*ipso*-$H_3CC_6H_4$), 135.5 (*o*-$H_3CC_6H_4$), 129.4 (*p*-$H_3CC_6H_4$), 41.7 ($N(CH_3)_2$), 21.4 (*p*-$H_3CC_6H_4$) ppm. *Anal*. Calcd. for $C_{23}H_{27}GeN$: C, 70.80; H, 6.98. Found C, 71.21; H, 7.08.

Synthesis of Tol_2GeBr_2[217] and Tol_2GeH_2[218]

To a solution of $GeBr_4$ (5.00 g, 12.7 mmol) at 0 ^oC in ether (70 mL) was added a solution of TolMgBr in THF (1.0 M, 25.5 mL) dropwise via syringe. The resulting reaction mixture was refluxed for 3 h, was allowed to cool, and was carefully poured over a 0.1 M aqueous HBr solution. The aqueous layer was separated and extracted with ether (3 × 25 mL). The organic layer and the combined ether extract were dried over anhydrous $MgSO_4$. The volatiles were removed *in vacuo* after filtration to yield a viscous liquid. The crude reaction mixture (1.85 g) in ether (30 mL) was treated with a suspension of $LiAlH_4$ (0.34 g, 8.94 mmol) in ether (30 mL) at 0 ^oC. The reaction mixture was subsequently refluxed for 3 h and then was quenched with 1 M aqueous HCl at -78 ^oC. The temperature was raised to 25 ^oC and the reaction mixture was stirred for 30 min. The solution was cooled to -78 ^oC and the ether layer was cannulated into a separate flask. The remaining aqueous layer was extracted with ether (2 × 15 mL) and the combined ether solution was dried over anhydrous $MgSO_4$. The volatiles were removed *in vacuo* to yield a colorless liquid that was distilled *in vacuo* (65 ^oC, 0.10 torr) to yield Tol_2GeH_2 (0.25 g, 8 % based on $GeBr_4$). ^{1}H NMR δ 7.43 (d, J = 7.5 Hz, 4H, *o*-$H_3CC_6H_4$), 6.99 (d, J = 7.5 Hz, 4H, *m*-$H_3CC_6H_4$), 5.52 (s, 2H, GeH), 2.07 (s, 6H, $H_3CC_6H_4$). ^{13}C NMR 139.8

(*ipso*-$H_3CC_6H_4$), 136.5 (*o*-$H_3CC_6H_4$), 131.7 (*p*-$H_3CC_6H_4$), 130.6 (*m*-$H_3CC_6H_4$), 22.4 (*p*-$H_3CC_6H_4$) ppm. *Anal*. Calcd. For $C_{14}H_{16}Ge$: C, 65.43; H, 6.28. Found: C, 65.22; H, 6.37.

Synthesis of $Tol_3GeGePh_2GeTol_3$ (2)

To a solution of $PhGeH_2$ (0.10 g, 0.44 mmol) in acetonitrile (10 mL) in a Schlenk tube was added a solution of Tol_3GeNMe_2 (0.34 g, 0.87 mmol) in acetonitrile (10 mL). The tube was sealed and the reaction mixture was stirred in an oil bath at 90 ^oC for 48 h. The volatiles were removed *in vacuo* to yield a white solid that was distilled in a Kugelrohr oven (125 ^oC, 0.05 torr). The material remaining in the distillation flask was recrystallized from hot toluene to yield **2** (0.283g of (71 %) as colorless crystals. ^1H NMR (C_6D_6, 25 °C): δ 7.78-7.74 (m, 6H, *m*-C_6H_5 and *p*-C_6H_5), 7.46 (d, *J* = 7.5 Hz,12H, *o*- $H_3CC_6H_4$), 7.05-7.03 (m, 4H, *o*-C_6H_5), 6.91 (d, *J* = 7.5 Hz, 12H, *m*-$H_3CC_6H_4$), 2.07 (s, 18H, -CH_3). ^{13}C NMR (C_6H_6, 25 °C): 139.1 (*ipso*-$H_3CC_6H_4$), 137.0 (*o*-$H_3CC_6H_4$), 136.2 (*o*-C_6H_5), 134.9 (*ipso*-C_6H_5), 129.4 (*p*-C_6H_5), 128.6 (*p*-$H_3CC_6H_4$), 128.3 (*m*-$H_3CC_6H_4$), 127.9 (*m*-C_6H_5), 21.3 (*p*-$H_3CC_6H_4$) ppm. *Anal*. Calcd for $C_{61}H_{60}Ge_3$ (**2**.C_7H_8): C, 72.45; H, 5.98. Found: C, 72.39; H, 6.01.

Synthesis of $Tol_3GeGeTol_2GeTol_3$ (3)

To a solution of H_2GeTol_2 (0.175 g, 0.681 mmol) in acetonitrile (10 mL) in a Schlenk tube was added a solution of Tol_3GeNMe_2 (0.531 g, 1.36 mmol) in acetonitrile (10 mL). The tube was sealed and the reaction mixture was stirred in an oil bath at 90 ^oC

for 48 h. The volatiles were removed *in vacuo* to yield a pale yellow solid that was recrystallized from a hot benzene/hexane mixture (1:1, 10 mL) to yield **3** (0.283 g, 71 %) as a colorless crystals. ^{1}H NMR: δ 7.69 (d, *J* = 7.8 Hz, 4H, *o*-Ge($C_6H_4CH_3)_2$), 7.49 (d, *J* = 7.8 Hz, 12H, *o*-Ge($C_6H_4CH_3)_3$), 6.93 (d, *J* = 7.8 Hz, 12H, m-Ge($C_6H_4CH_3)_3$), 6.87 (d, *J* = 7.8 Hz, 4H, *m*-Ge($C_6H_4CH_3)_2$), 2.09 (s, 18H, Ge($C_6H_4CH_3)_3$), and 1.99.12 (s, 6H, Ge($C_6H_4CH_3)_2$). ^{13}C NMR: 138.3 (*ipso*-Ge($C_6H_4CH_3)_3$), 138.2 (*ipso*-Ge($C_6H_4CH_3)_2$), 137.0 (*o*-Ge($C_6H_4CH_3)_2$), 136.4 (*o*-Ge($C_6H_4CH_3)_3$), 135.4 (*p*-Ge($C_6H_4CH_3)_2$), 135.2 (*p*-Ge($C_6H_4CH_3)_3$), 129.4 (*m*-Ge($C_6H_4CH_3)_3$), 129.3 (*m*-Ge($C_6H_4CH_3)_2$), 21.4 (-Ge($C_6H_4CH_3)_3$), 21.3 (Ge($C_6H_4CH_3)_2$) ppm. *Anal*. Calcd for $C_{56}H_{56}Ge_3$ (**3**): C, 71.01; H, 5.96. Found: C, 70.91; H, 5.96.

Synthesis of $Cl_3(O)COPh_2GeGePh_2OC(O)CCl_3$ (5)

To a solution of $Ph_3GeGePh_3$ (2.000 g, 2.866 mmol) in toluene (3.6 mL) was added a solution of $Cl_3CC(O)OH$ (2.34 g, 14.32 mmol) in toluene (3.0 mL). The reaction mixture sealed in a Schlenk tube and was heated at 110 ^{o}C for 72 h in an oil bath. The resulting solution was cooled to room temperature and layered with hexane to yield a white precipitate which was filtered and washed with a mixture of hexane and toluene (1:1) to yield 5 (1.712 g, 76 %) as a white solid. IR (Nujol mull): 1644.8 cm-1 (ν_{co})

Synthesis of $ClPh_2GeGePh_2Cl$ (8)

To a solution of **5** (1.050 g, 1.349 mmol) in acetone (8.75 mL) was added 3 mL of concentrated hydrochloric acid. The reaction mixture was stirred under N_2 at 50 ^oC for 18 h in an oil bath. The resulting dark red solution was cooled to -28 ^oC using a dry ice/*ortho*-xylene mixture to yield ochre-colored crystals which were washed with a mixture of hexane and acetone (1:1). Recrystallization of the crude product with a mixture of Et_2O and hexane (2:1) yielded **8** (0.382 g, 54 %) as needle-shaped colorless crystals. ^1H NMR δ 7.77-7.73 (*m*, 8H, *o*-C_6H_5), 7.03-7.01 (*m*,12H, *m*-C_6H_5 and *p*-C_6H_5) ppm. ^{13}C NMR δ 136.0 (*ipso*-C_6H_5), 134.1 (*o*-C_6H_5), 130.8 (*p*-C_6H_5), 129.1 (*m*-C_6H_5) ppm.

Synthesis of $HPh_2GeGePh_2H$ (10)

To a solution of **8** (0.110 g, 0.209 mmol) in THF (10 mL) was added a suspension of $LiAlH_4$ (0.016 g, 0.416 mmol) in THF (10 mL). The resulting mixture was stirred for 18 h under N_2. The solvent was removed in vacuo yielding a white solid that was washed with benzene (2 × 3 mL). The product was dried *in vacuo* to yield 10 (0.075 g, 79 %) as a white solid. ^1H NMR δ 7.54-7.50 (*m*, 8H, *o*-C_6H_5), 7.08-7.04 (*m*, 12H, *m*-C_6H_5 and *p*-C_6H_5), 5.58 (*s*, 2H, Ge*H*) ppm. ^{13}C NMR δ 136.0 (*ipso*-C_6H_5), 135.7 (*o*-C_6H_5), 129.1 (*p*-C_6H_5), 128.7 (*m*-C_6H_5) ppm. IR (Nujol mull): 2033 cm^{-1}.

Synthesis of $Tol_3GeGePh_2GePh_2GeTol_3$ (11)

To a solution of 10 (0.075 g, 0.165 mmol) in acetonitrile (5 mL) in a Schlenk tube was added a solution of Tol_3GeNMe_2 (0.128 g, 0.330 mL) in CH_3CN (5 mL). The tube was sealed and the reaction mixture was stirred in an oil bath at 90 ^oC for 48 h. The volatiles were removed *in vacuo* to yield a pale yellow solid that was recrystallized from a hot benzene/hexane mixture (1:1, 10 mL) to yield 11 (0.150 g, 80 %) as colorless crystals. ^1H NMR δ 7.55 (d, *J* = 7.5 Hz, 12H, *o*-$C_6H_4CH_3$), 7.31 (d, *J*=7.2 Hz, 8H, *o*-C_6H_5), 7.11 (t, *J* = 7.2 Hz, 4H, *p*-C_6H_5), 6.97 (t, *J* = 7.2 Hz, 8H, *m*-C_6H_5), 6.85 (d, *J* = 7.5 Hz, 12H, *m*-$C_6H_4CH_3$), 2.02 (s, 18H, $C_6H_4CH_3$) ppm. ^{13}C NMR δ 138.4 (*ipso*-$H_3CC_6H_4$), 137.2 (*o*-C_6H_5), 136.2 (*o*-$CH_3C_6H_4$), 135.1 (*ipso*-C_6H_5), 129.5 (*p*-C_6H_5), 129.4 (*p*-$H_3CC_6H_4$), 128.4 (*m*-$H_3CC_6H_4$), 127.9 (*m*-C_6H_5), 21.3 (*p*-$H_3CC_6H_4$) ppm. *Anal*. Calcd. For $C_{80}H_{78}Ge_4$ ($7.2C_7H_8$): C,72.23; H, 5.91. Found: C, 72.38; H, 6.05.

X-ray crystal structure of compounds 1-3 and 11

Diffraction intensity data were collected with a Siemens P4/CCD diffractometer. Crystallographic data and details are shown in Table X. Absorption corrections were applied for all data using SADABS. The structures were solved using direct methods, completed by difference Fourier syntheses, and refined on full-matrix least squares procedures on F^2. All ordered non-hydrogen atoms were refined with anisotropic displacement coefficients and hydrogen atoms were treated as idealized contributions. Solvent molecules were removed using SQUEEZE for compounds **2** and **3**. All software and sources of scattering factors are contained in the SHEXTL (5.10) program package

(G. Sheldrick, Bruker XRD, Madison, WI). ORTEP diagrams were drawn using the ORTEP3 program (L.J. Farrugia, Glasgow).

Table 5.7: Crystal data and structure refinement details for **1**·$2C_6H_6$

Compound	**1**·$2C_6H_6$
Empirical formula	$C_{51}H_{48}Ge_2$
Temperature (K)	150(2)
Wavelength (Å)	0.71073
Crystal system	Triclinic
Space group	P-1
a (Å)	8.884(5)
b (Å)	10.428(6)
c (Å)	21.52(1)
α (˚)	89.200(8)
β (˚)	79.094(8)
γ (˚)	81.806(8)
Volume (Å^3)	1937(2)
Z,*Z´*	2.0
Calculated density (g/cm^3)	1.315
Absorption coefficient (mm^{-1})	1.584
F(000)	794
Crystal size (mm)	0.25 × 0.18 × 0.12
Crystal size and shape	Colorless block
θ range for data collection (o)	1.93-28.31
Index ranges	$-11 \leq h \leq 11$ $-13 \leq k \leq 13$ $-28 \leq l \leq 28$
Reflections collected	42 366
Independent reflections	9055 (R_{int} = 0.0456)
Completeness to θ	25.00 (99.9%)
Absorption correction	Multi-scan
Maximum and minimum transmission	0.8327 and 0.6929
Refinement method	Full-matrix least-squares on F^2
Data/restraints/parameters	9055/0/454
Goodness of fit on F^2	1.053
Final R indices ($I > 2\sigma(I)$)	
R_1	0.0320
wR_2	0.0701
Final R indices (all data)	
R_1	0.0534
wR_2	0.0750
Largest difference in peak and hole (e Å^{-3})	0.433 and -0.295

Table 5.8: Crystal data and structure refinement details for **2**·C_7H_8

Compound	**2**·2C_7H_8
Empirical formula	$C_{61}H_{60}Ge_3$
Temperature (K)	120(2)
Wavelength (Å)	0.71073
Crystal system	Monoclinic
Space group	$P2_1/n$
a (Å)	13.7610(5)
b (Å)	26.044(1)
c (Å)	14.1583(5)
α (˚)	90
β (˚)	90
γ (˚)	90
Volume (Å^3)	5069.6(3)
Z,*Z´*	4,0
Calculated density (g/cm^3)	1.324
Absorption coefficient (mm^{-1})	2.374
F(000)	2088
Crystal size (mm)	0.15 × 0.10 × 0.10
Crystal size and shape	Colorless block
θ range for data collection (o)	3.39-66.11
Index ranges	$-15 \leq h \leq 13$
	$-28 \leq k \leq 29$
	$-14 \leq l \leq 16$
Reflections collected	26 445
Independent reflections	8224 (R_{int} = 0.0502)
Completeness to θ	60.00 (99.4%)
Absorption correction	Multi-scan
Maximum and minimum transmission	0.7972 and 0.7171
Refinement method	Full-matrix least-squares on F^2
Data/restraints/parameters	8224/0/520
Goodness of fit on F^2	1.032
Final R indices ($I > 2\sigma(I)$)	
R_1	0.0367
wR_2	0.0773
Final R indices (all data)	
R_1	0.0544
wR_2	0.0813
Largest difference in peak and hole (e Å^{-3})	0.591 and -0.347

Table 5.9: Crystal data and structure refinement details for **3**·C_7H_8

Compound	**2**·2C_7H_8
Empirical formula	$C_{63}H_{64}Ge_3$
Temperature (K)	150(2)
Wavelength (Å)	0.71073
Crystal system	Triclinic
Space group	P-1
a (Å)	11.563(2)
b (Å)	13.825(2)
c (Å)	17.739(3)
α (˚)	86.381(2)
β (˚)	88.798(2)
γ (˚)	72.552(2)
Volume (Å^3)	2702.3(8)
Z,*Z´*	2,0
Calculated density (g/cm^3)	1.277
Absorption coefficient (mm^{-1})	1.695
F(000)	1076
Crystal size (mm)	0.35 × 0.15 × 0.08
Crystal size and shape	Colorless block
θ range for data collection (o)	3.55-28.20
Index ranges	$-15 \leq h \leq 15$
	$-17 \leq k \leq 18$
	$-23 \leq l \leq 23$
Reflections collected	69 956
Independent reflections	12 152 (R_{int} = 0.0431)
Completeness to θ	25.00 (99.8%)
Absorption correction	Multi-scan
Maximum and minimum transmission	0.8763 and 0.5884
Refinement method	Full-matrix least-squares on F^2
Data/restraints/parameters	12152/0/540
Goodness of fit on F^2	1.075
Final R indices ($I > 2\sigma(I)$)	
R_1	0.0374
wR_2	0.0915
Final R indices (all data)	
R_1	0.0448
wR_2	0.0968
Largest difference in peak and hole (e Å^{-3})	1.070 and -0.666

Table 5.10: Crystal data and structure refinement details for **11**

Compound	**11**
Empirical formula	$C_{66}H_{62}Ge_4$
Temperature (K)	150(2)
Wavelength (Å)	0.71073
Crystal system	Triclinic
Space group	P-1
a (Å)	11.582(4)
b (Å)	13.114(4)
c (Å)	19.527(6)
α (˚)	83.531(5)
β (˚)	79.175(4)
γ (˚)	72.021(4)
Volume (Å^3)	2766(1)
Z,*Z*′	2,0
Calculated density (g/cm^3)	1.375
Absorption coefficient (mm^{-1})	2.192
F(000)	1172
Crystal size (mm)	0.25 × 0.21 × 0.11
Crystal size and shape	Colorless block
θ range for data collection (o)	1.64-27.51
Index ranges	$-12 \leq h \leq 14$
	$-12 \leq k \leq 16$
	$-25 \leq l \leq 24$
Reflections collected	15 530
Independent reflections	9778 (R_{int} = 0.0335)
Completeness to θ	25.00 (83.2%)
Absorption correction	Multi-scan
Maximum and minimum transmission	0.7945 and 0.6102
Refinement method	Full-matrix least-squares on F^2
Data/restraints/parameters	9778/0/656
Goodness of fit on F^2	1.026
Final R indices ($I > 2\sigma(I)$)	
R_1	0.0499
wR_2	0.1110
Final R indices (all data)	
R_1	0.0691
wR_2	0.1237
Largest difference in peak and hole (e Å^{-3})	0.808 and -0.487

REFERENCES

(1) Balaji, V.; Michl, J. *Polyhedron* **1991**, *10*, 1265-1284.

(2) Miller, R. D.; Michl, J. *Chem. Rev.* **1989**, *89*, 1359-1410.

(3) Ortiz, J. V. *Polyhedron* **1991**, *10*, 1285-1297.

(4) Zeigler, J. M. *Synthetic Metals* **1989**, *28*, 581-591.

(5) Seki, S.; Tagawa, S. *Polym. J.* **2007**, *39*, 277-293.

(6) Kepler, R. G.; Zeigler, J. M.; Harrah, L. A.; Kurtz, S. R. *Phys. Rev. B* **1987**, *35*, 2818-2822.

(7) Mochida, K.; Nagano, S.-s.; Maeyama, S.; Kodaira, T.; Watanabe, A.; Ito, O.; Matsuda, M. *Bull. Chem. Soc. Jpn.* **1997**, *70*, 713-716.

(8) Weinert, C. S. *Dalton Trans.* **2009**, 1691-1699.

(9) Jones, R. G.; Benfield, R. E.; Cragg, R. H.; Swain, A. C.; Webb, S. J. *Macromolecules* **1993**, *26*, 4878-4887.

(10) Benfield, R. E.; Cragg, R. H.; Jones, R. G.; Swain, A. C. *J. Chem.Soc., Chem. Commun.* **1992**, 1022-1024.

(11) Kimata, Y.; Suzuki, H.; Satoh, S.; Kuriyama, A. *Chem. Lett.* **1994**, 1163-1164.

(12) Bratton, D.; Holder, S. J.; Jones, R. G.; Wong, W. K. C. *J.Organomet. Chem.* **2003**, *685*, 60-64.

(13) Shankar, R.; Saxena, A.; Brar, A. S. *J. Organomet. Chem.* **2002**, *650*, 223-230.

(14) Zuev, V. V.; Skvortsov, N. K. *J. Polym. Sci. A: Polym. Chem.* **2003**, *41*, 3761-3767.

(15) Kimata, Y.; Suzuki, H.; Satoh, S.; Kuriyama, A. *Organometallics* **1995**, *14*, 2506-2511.

(16) Hengge, E. F. *J. Inorg. Organomet. Polym.* **1993**, *3*, 287-303.

(17) Kashimura, S.; Ishifune, M.; Yamashita, N.; Bu, H.-B.; Takebayashi, M.; Kitajima, S.; Yoshiwara, D.; Kataoka, Y.; Nishida, R.; Kawasaki, S.; Murase, H.; Shono, T. *J. Org. Chem.* **1999**, *64*, 6615-6621.

(18) Miller, R. D.; Jenkner, P. K. *Macromolecules* **1994**, *27*, 5921-5923.

(19) Lacave-Goffin, B.; Hevesi, L.; Devaux, J. *J. Chem. Soc., Chem. Commun.* **1995**, 769-770.

(20) Sita, L. R. *Organometallics* **1992**, *11*, 1442-1444.

(21) Sita, L. R.; Terry, K. W.; Shibata, K. *J. Am. Chem. Soc.* **1995**, *117*, 8049-8050.

(22) Sommer, R.; Schneider, B.; Neumann, W. P. *Justus Liebigs Ann.Chem.* **1966**, *692*, 12-21.

(23) Sita, L. R. *Acc. Chem. Res.* **1994**, *27*, 191-197.

(24) Sita, L. R. *Adv. Organomet. Chem.* **1995**, *38*, 189-243.

(25) Adams, S.; Dräger, M. *J. Organomet. Chem.* **1985**, *288*, 295-304.

(26) Adams, S.; Dräger, M.; Mathiasch, B. *J. Organomet. Chem.* **1987**, *326*, 173-186.

(27) Imori, T.; Lu, V.; Cai, H.; Tilley, T. D. *J. Am. Chem. Soc.* **1995**, *117*, 9931-9940.

(28) Imori, T.; Tilley, T. D. *J. Chem. Soc., Chem. Commun.* **1993**, 1607-1609.

(29) Choffat, F.; Smith, P.; Caseri, W. *J. Mater. Chem.* **2005**, *15*, 1789-1792.

(30) Deacon, P. R.; Devylder, N.; Hill, M. S.; Mahon, M. F.; Molloy, K. C.; Price, G. J. *J. Organomet. Chem.* **2003**, *687*, 46-56.

(31) Thompson, S. M.; Schubert, U. *Inorg. Chim. Acta.* **2004**, *357*, 1959-1964.

(32) Babcock, J. R.; Sita, L. R. *J. Am. Chem. Soc.* **1996**, *118*, 12481- 12482.

(33) Lu, V.; Tilley, T. D. *Macromolecules* **1996**, *29*, 5763-5764.

(34) Lu, V. Y.; Tilley, T. D. *Macromolecules* **2000**, *33*, 2403-2412.

(35) Thompson, S. M.; Schubert, U. *Inorg. Chim. Acta.* **2004**, *357*, 1959-1964.

(36) Mochida, K.; Hayakawa, M.; Tsuchikawa, T.; Yokoyama, Y.; Wakasa, M.; Hayashi, H. *Chem. Lett.* **1998**, 91-92.

(37) Okano, M.; Matsumoto, N.; Arakawa, M.; Tsuruta, T.; Hamano, H. *Chem. Commun.* **1998**, 1799-1800.

(38) Winkler, C. A.; Ber, C. *Chem. Ber.* **Chem. Ber**, *19*, 210-211.

(39) Winkler, C. A. *J. Prakt. Chem.* **1886**, *142*, 177-229.

(40) Winkler, C. A. *J. Prakt. Chem.* **1887**, *36*, 177-209.

(41) Morgan, G. T.; Drew, H. D. K. *J. Chem. Soc.* **1925**, *127*, 1760-1768.

(42) Dräger, M.; Ross, L.; Simon, D. *Rev. Silicon Germanium Tin Lead Cmpds.* **1983**, *7*, 299-445.

(43) Glockling, F. *The Chemistry of Germanium*; Academic Press: London, UK, 1969.

(44) Lesbre, M.; Mazerolles, P.; Satgé, J. *The Organic Compounds of Germanium.*; Wiley Interscience: London, UK, 1971.

(45) Rivière, P.; Rivière-Baudet, M.; Satgé, J. *Comprehensive Organometallic Chemistry;*. Abel, E. W., Eds.; Pergamon: New York, 1982; Vol. 2, pp 399-518.

(46) Rivière, P.; Rivière-Baudet, M.; Satgé, J. *In Comprehensive Organometallic Chemistry II*; Wilkinson, G., Ed.; Pergamon: New York, 1995; Vol. 2, pp 137-216.

(47) Weinert, C. S. In *Comprehensive Organometallic Chemistry III*; Crabtree, R. H., Mingos, D. M. P., Eds.; Elsevier: Oxford, UK, 2007; Vol. 3, pp 699-808.

(48) Roller, S.; Dräger, M. *J. Organomet. Chem.* **1986**, *316*, 57-65.

(49) Roller, S.; Simon, D.; Dräger, M. *J. Organomet. Chem.* **1986**, 27-40

(50) Neumann, W. P.; Kühlein, K. *Tetrahedron Lett.* **1963**, *4*, 1541-1545.

(51) Azemi, T.; Yokoyama, Y.; Mochida, K. *J. Organomet. Chem.* **2005**, *690*, 1588-1593.

(52) Yokoyama, Y.; Hayakawa, M.; Azemi, T.; Mochida, K. *J. Chem. Soc., Chem. Commun.* **1995**, 2275.

(53) Triplett, K.; Curtis, M. D. *J. Organomet. Chem.* **1976**, *107*, 23-32.

(54) Kraus, C. A.; Flood, E. A. *J. Am. Chem. Soc.* **1932**, *54*, 1635-1644.

(55) Brown, M. P.; Fowles, G. W. A. *J. Chem. Soc.* **1958**, 2811-2814.

(56) Glockling, F.; Hooton, K. A.; Kotz, J. C.; Laubengayer, A. W. *Inorg. Synth.* **1966**, *8*, 31-34.

(57) Roller, S.; Simon, D.; Dräger, M. *J. Organomet. Chem.* **1986**, 27-40.

(58) Glockling, F.; Hooton, K. A. *J. Chem. Soc.* **1962**, 3509-3512.

(59) Seyferth, D. *J. Am. Chem. Soc.* **1957**, *79*, 2738-2740.

(60) Harris, D. M.; Nebergall, W. H.; Johnson, O. H.; Rochow, E. G.; Tolivaisa, N. *Inorg. Synth.* **1957**, *5*, 72-74.
(61) Dräger, M.; Ross, L. *Z. Anorg. Allg. Chem.* **1980**, *469*, 115 - 122.
(62) Dräger, M.; Ross, L. *Z. Anorg. Allg. Chem.* **1980**, *460*, 207-216.
(63) Metlesics, W.; Zeiss, H. *J. Am. Chem. Soc.* **1960**, *82*, 3321-3323.
(64) Kühlein, K.; Neumann, W. P. *Liebigs Ann. Chem.* **1967**, *702*, 17-23.
(65) Bulten, E. J.; Noltes, J. G. *Tetrahedron Lett.* **1966**, 3471-3476.
(66) Höfler, F.; Brandstätter, E. *Monatshefte für Chemie / Chemical Monthly* **1975**, *106*, 893-904.
(67) Häberle, K.; Dräger, M. *Z. Naturforsch.* **1987**, *42B*, 323-329.
(68) Glocklin.F; Houston, R. E. *J. Chem. Soc.,Dalton Trans.* **1973**, 1357-1359.
(69) Simon, D.; Haberle, K.; Drager, M. *J. Organomet. Chem.* **1984**, *267*, 133-142.
(70) Riviere, P.; Castel, A.; Guyot, D.; Satge, J. *J. Organomet. Chem.* **1985**, *290*, C15-C18.
(71) Cooke, J. A.; Dixon, C. E.; Netherton, M. R.; Kollegger, G. M.; Baines, R. M. *Syn. React. Inorg. Met.-Org. Chem.* **1996**, *26*, 1205-1217.
(72) Castel, A.; Rivière, P.; Satgé, J.; Ahbala, M.; Abdennadher, C.; Desor, D. *Main Group Met. Chem.* **1993**, *16*, 291-303.
(73) Kraus, C. A.; Brown, C. L. *J. Am. Chem. Soc.* **1930**, *52*, 4031-4035.
(74) Castel, A.; Rivière, P.; Saint-Roch, B.; Satgé, J.; Malrieu, J. P. *J. Organomet. Chem.* **1983**, *247*, 149-160.
(75) Bulten, E. J.; Noltes, J. G. *Tetrahedron Lett.* **1967**, 1443-1447.
(76) Dräger, M.; Simon, D. *J. Organomet. Chem.* **1986**, *306*.
(77) Häberle, K.; Dräger, M. *J. Organomet. Chem.* **1986**, *312*, 155-165.
(78) Rivière, P.; Satgé, J. *Synth. React. Inorg. Met.-Org. Chem.* **1971**, *1*, 13-20.
(79) Tanabe, M.; Hanzawa, M.; Ishikawa, N.; Osakada, K. *Organometallics* **2009**, *28*, 6014–6019.
(80) Kumada, M.; Sakamoto, S.; Ishikawa, M. *J. Organomet. Chem.* **1969**, *17*, 235-240.
(81) Bulten, E. J.; Noltes, J. G. *J. Organomet. Chem.* **1969**, *16*, P8–P10.

(82) Bulten, E. J.; Noltes, J. G. *Recl. TraV. Chim. Pays-Bas.* **1972**, *91*, 1041-1056.

(83) Glockling, F.; Hooton, K. A. *J. Chem. Soc. A* **1963**, 1849-1854.

(84) Glockling, F.; Light, J. R. C. *J. Chem. Soc. A* **1967**, 623-627.

(85) Mochida, K.; Hodota, C.; Hata, R.; Fukuzumi, S. *Organometallics* **1993**, *12*, 586-588.

(86) Mochida, K.; Hata, R.; Chiba, H.; Seki, S.; Yoshida, Y.; Tagawa, S. *Chem. Lett.* **1998**, 263-264.

(87) Okano, M.; Mochida, K. *Chem. Lett.* **1990**, 701-704.

(88) Mochida, K.; Hata, R.; Shimoda, M.; Matsumoto, F.; Kurosu, H.; Kojima, A.; Yoshikawa, M.; Masuda, S.; Harada, Y. *Polyhedron* **1996**, *15*, 3027-3032.

(89) Mochida, K.; Hata, R.; Chiba, H.; Seki, S.; Yoshida, Y.; Tagawa, S. *Chem. Lett.* **1998**, 263-264.

(90) Baumgartner, J.; Fischer, R.; Fischer, J.; Wallner, A.; Marschner, C.; Flörke, U. *Organometallics* **2005**, *24*, 6450-6457.

(91) Mochida, K.; Chiba, H.; Okano, M. *Chem. Lett.* **1991**, 109-112.

(92) Rivierebaudet, M. *Main Group Met. Chem.* **1995**, *18*, 353-385.

(93) Bochkarev, M. N.; Vyazankin, N. S.; Bochkarev, L. N.; Razuvaev, G. A. *J. Organomet. Chem.* **1976**, *110*, 149-157.

(94) Creemers, H. M. J. C.; Noltes, J. G. *J. Organomet. Chem.* **1967**, *7*, 237-247.

(95) Subashi, E.; Rheingold, A. L.; Weinert, C. S. *Organometallics* **2006**, *25*, 3211-3219.

(96) Weidenbruch, M.; Grimm, F.-T.; Herrndorf, M.; Schäfer, A.; Peters, K.; von Schnering, H. G. *J. Organomet. Chem.* **1988**, *341*, 335-343.

(97) Bulten, E. J.; Noltes, J. G. *Tetrahedron Lett.* **1966**, 4389-4392.

(98) Rivière-Baudet, M.; Rivière, P. *J. Organomet. Chem.* **1976**, *116*, C49-C52

(99) Rivière-Baudet, M. *Main Group Met. Chem.* **1995**, 353-385.

(100) Lappert, M. F.; Power, P. P.; Sanger, A. R.; Srivatava, R. C. *Metal and Metalloid Amides*; Ellis Horwood Ltd: Chichester, England, 1980.

(101) Ohlsson, B.; Ullenius, C.; Jagner, S.; Grivet, C.; Wenger, E.; E.P.Kündig *J. Organomet. Chem.* **1989**, *365*, 243-267.

(102) M, W.; M, N.; J, F. H.; A, M. *J. Organomet. Chem.* **1982**, 228-238.

(103) Weidenbruch, M.; Grimm, F.-T.; Herrndorf, M.; S&tier, A.; Peters, K.; Schnering, H. G. v. *J. Organomet. Chem.* **1988**, *341*, 335-343.

(104) Yarosh, O. G.; Voronkov, M. G.; Zhilitskaya, L. V.; Yarosh, N. O.; Albanov, A. I.; Korotaeva, I. M. *Russ. J. Gen. Chem* **2005**, *75*, 714-718.

(105) Párkányi, L.; Kálmán, A.; Sharma, S.; Nolen, D. M.; Pannell, K. H. *Inorg. Chem* **1994**, *33*, 180-182.

(106) March, J. *Adv. Org. Chem.*; John Wiley & Sons: New York, 1992.

(107) Rivière-Baudet, M.; Rivière-Baudet, A.; Britten, J. F.; Onyszchuk, M. *J. Organomet. Chem.* **1992**, *423*, C5-C8.

(108) Wraage, K.; Lameyer, L.; Stalke, D.; Roesky, H. *Angew. Chem. Int. Ed.* **1999**, 522-523.

(109) Wraage, K.; Schmidt, H.-G.; Noltemeyer, M.; Roesky, H. W. *Eur. J. Inorg. Chem.* **1999**, 863-867.

(110) Walding, J. L.; Fanwick, P. E.; Weinert, C. S. *Inorg. Chim. Acta.* **2005**, *358*, 1186–1192.

(111) Chorley, R. W.; Hitchcock, P. B.; Lappert, M. F.; Leungtt, W.-P.; Power, P. P.; Olmstead, M. M. *Inorg. Chim. Acta.* **1992**, *198-200*, 203-209.

(112) Lappert, M. F.; Slade, M.; Atwood, J.; Zaworotko, M. J. *J. Chem. Soc., Chem. Commun.* **1980**, 621-622.

(113) Emsley, J. *The Elements*; Oxford: New York, 1991.

(114) Ohshita, J.; Toyoshima, Y.; Iwata, A.; Tang, H.; Kunai, A. *Chem. Lett.* **2001**, 886-887.

(115) Marchand, A.; Gerval, P. *J. Organomet. Chem.* **1978**, *162*, 162, 365-387.

(116) Shriver, D. F.; Drezdzon, M. A. *The Manipulation of Air-Sensitive Compounds*; 2nd ed.; Wiley: New York, 1986.

(117) Ohshita, J.; Toyoshima, Y.; Iwata, A.; Tang, H.; Kunai, A. *Chem. Lett.* **2001**, 886-887.

(118) Weidenbruch, M.; Grimm, F.-T.; Herrndorf, M.; Schäfer, A.; Peters, K.; Schnering, H. G. v.; *J. Organomet. Chem.* **1988**, *341*, 335.

(119) Highsmith, R. E.; Sisler, H. H. *Inorg. Chem.* **1969**, *8*, 1029-1032.

(120) Rijkens, F.; Janssen, M. J.; Vanderke.Gj *Recueil Des Travaux Chimiques Des Pays-Bas* **1965**, *84*, 1597.

(121) Duffaut, N.; Dunogues, J.; Calas, R. *J. Organomet. Chem.* **1978**, *149*, 57-63.

(122) Riviere, P.; Satge, J.; Dousse, G.; Riviere-Baudet, M.; Couret, C. *J. Organomet. Chem.* **1974**, *72*, 339-350.

(123) Watanabe, A. *J. Organomet. Chem.* **2003**, *685*, 122-133.

(124) Hatanaka, Y.; Okada, S.; Onozawa, S.; Suzuki, Y.; Tanaka, M. *Chem. Lett.* **2001**, 600-601.

(125) Watanabe, A.; Miike, H.; Tsutsumi, Y.; Matsuda, M. *Macromolecules* **1993**, *26*, 2111-2116.

(126) Mitchell, T. N.; El-Behairy, M. *J. Organomet. Chem.* **1977**, *141*, 43-48.

(127) Kobayashi, K.; Kawanisi, M.; Hitomi, T.; Kozima, S. *J. Organomet Chem.* **1982**, *233*, 299-311.

(128) Willemsens, L. C.; van der Kerk, G. J. M. *J. Organomet. Chem.* **1964**, *2*, 260-264.

(129) Babcock, J. R.; Sita, L. R. *J. Am. Chem. Soc.* **1996**, *118*, 12481-12482.

(130) Riviĕre, P.; Satge, J.; Soula, D. *J. Organomet. Chem.* **1973**, *63*, 167-174.

(131) Häberle, K.; Dräger, M. *Z. Anorg. Allg. Chem.* **1987**, *551*, 116-122.

(132) Amadoruge, M. L.; Golen, J. A.; Rheingold, A. L.; Weinert, C. S. *Organometallics* **2008**, *27*.

(133) Ross, L.; Dräger, M. *J. Organomet. Chem.* **1980**, *199*, 195-204.

(134) Ross, L.; Dräger, M. *Z. Anorg. Allg. Chem.* **1984**, *519*, 225-232.

(135) Dräger, M.; Ross, L. *Z. Anorg. Allg. Chem.* **1981**, *476*, 95-104.

(136) Uhlig, W. *J. Organomet. Chem.* **1991**, *409*, 377-383.

(137) Katz, S. M.; Reichl, J. A.; Berry, D. H. *J. Am. Chem. Soc.* **1998**, *120*, 9844-9849.

(138) Angus-Dunne, S. J.; Chin, L. E. P. L.; Burns, R. C.; Lawrance, G. A. *Trans. Met. Chem.* **2006**, *31*, 268-275.

(139) Bürger, H.; Burczyk, K.; Blaschette, A. *Monatsh. Chem.* **1970**, *101*, 102-119.

(140) Miles, M. G.; Doyle, G.; Cooney, R. P.; Tobias, R. S. *Spectrochim.Acta A* **1969**, *25*, 1515-1526.

(141) Johnston, D. H.; Shriver, D. F. *Inorg. Chem.* **1993**, *32*, 1045-1047.

(142) Meyer, J. M.; Allred, A. L. *J. Phys. Chem.* **1968**, *72*, 3043-3045.

(143) Rivière, P.; Rivière-Baudet, M.; Couret, C.; Satgé, J. *Synth. React.Inorg. Met. Org. Chem.* **1974**, *4*, 295-307.

(144) Petty, M. C. *Molecular Electronics: From Principles to Practice* Hoboken, NJ, 2007.

(145) James, D. K.; Tour, J. M. *Top. Curr. Chem.* **2005**, *257*, 33-62.

(146) Balzani, V.; Venturi, M.; Credi, A. *Molecular Devices and Machines-A Journey into the Nano World*; Wiley-VCH: Weinheim, Germany, 2003.

(147) Tour, J. M. *Molecular Electronics: Commercial Insights, Chemistry, Devices, Architecture, and Programming*; World Scientific: Hackensack, NJ, 2003.

(148) Cohen, R.; Stokbro, K.; Martin, J. M. L.; Ratner, M. A. *J. Phys.Chem C* **2007**, *111*, 14893-14902.

(149) Finch, C. M.; Sirichantaropass, S.; Bailey, S. W.; Grace, I. M.; Garcia-Suarez, V. M.; Lambert, C. J. *J. Phys. Condens. Mat.* **2008**, *20*, 022203.

(150) Grave, C.; Risko, C.; Shaporenko, A.; Wang, Y.; Nuckolls, C.; Ratner, M. A.; Rampi, M. A.; Zharnikov, M. *Adv. Funct. Mater.* **2007**, *17*, 3816-3828.

(151) Hutchison, G. R.; Ratner, M. A.; Marks, T. J. *J. Am. Chem. Soc.* **2005**, *127*, 16866-16881.

(152) Roth, S.; Carroll, D. *One Dimensional Metals: Conjugated Polymers, Organic Crystals, Carbon Nanotubes*; Wiley-VCH: Weinheim, Germany, 2004.

(153) Nakamura, A.; Ueyama, N.; Yamaguchi, K., Eds *Organometallic Conjugation: Structures, Reactions, and Functions of d-d and d-π Conjugated Systems*; Springer: New York, 2002.

(154) Coe, B.; Curati, N. *Comments Inorg. Chem.* **2004**, *25*, 147-184.

(155) Paul, F.; Lapinte, C. *Coord. Chem. Rev.* **1998**, *178-180*, 431-509.

(156) Ying, J.-W.; Cordova, A.; Ren, T. Y.; Xu, G.-L.; Ren, T. *Chem.Eur. J. Inorg. Chem.* **2007**, *13*, 6874-6882.

(157) Ren, T. *Organometallics* **2005**, *24*, 4854-4870.

(158) Shi, Y.; Lee, G. T.; Wang, G.; Ren, T. *J. Am. Chem. Soc.* **2004**, *126*, 10522-10533.

(159) Berry, J. F.; Cotton, F. A.; Murillo, C. A. *Organometallics* **2004**, *23*, 2503-2506.

(160) Holder, S. J.; Jones, R. G.; Benfield, R. E.; Went, M. J. *Polymer* **1996**, *37*, 3477-3479.

(161) Amadoruge, M. L.; DiPasquale, A. G.; Rheingold, A. L.; Weinert, C. S. *J. Organomet. Chem.* **2008**, *693*, 1771-1778.

(162) Kaufmann, J.; Sahm, W.; Schwenk, A. *Z. Naturforsch. A* **1971**, *26A*, 1384–1389.

(163) Takeuchi, Y.; Harazono, T.; Kakimoto, N. *Inorg. Chem.* **1984**, *23*, 3835–3836.

(164) Kidd, R. G.; Spinney, H. G. *J. Am. Chem. Soc.* **1973**, *95*, 88–90.

(165) Belton, P. S.; Cox, I. J.; Harris, R. K. *J. Chem. Soc., Faraday Trans.* **1985**, *81*, 63–75.

(166) Mackay, K. M.; Watkinson, P.; J.; Wilkins, A. L. *J. Chem. Soc., Dalton Trans.* **1984**, 133–139.

(167) Patt, S. L. *J. Magn. Reson.* **1982**, *49*, 161–163.

(168) Wilkins, A. L.; Thomson, R. A.; Mackay, K. M. *Main Group Met. Chem.* **1990**, *13*, 219–236.

(169) Takeuchi, Y.; Inagaki, H.; Tanaka, K.; Yoshimura, S. *Magn. Reson. Chem.* **1989**, *27*, 72–74.

(170) Liepins, E.; Petrova, M. V.; Bogoradovsky, E. T.; Zavgorodny, V. S. *J. Organomet. Chem.* **1991**, *410*, 287–291.

(171) Liepins, E.; Zicmane, I.; Ignatovich, L. M.; Lukevics, E. *J. Organomet. Chem.* **1991**, *389*, 23–28.

(172) Takeuchi, Y.; Shimoda, M.; Tanaka, K.; Tomoda, S.; Ogawa, K.; Suzuki, H. *J. Chem. Soc., Perkin Trans.* **1988**, *2*, 7–13.

(173) Kupce, E.; Ignatovich, L. M.; Lukevics, E. *J. Organomet. Chem.* **1989**, *372*, 189–191.

(174) Kupce, E.; Lukevics, E. *J. Magn. Reson.* **1988**, *79*, 325–327.

(175) Yoder, C. H.; Agee, T. M.; Schaeffer, C. D.; Carroll, M. J.; Fleisher, A. J.; DeToma, A. S. *Inorg. Chem.* **2008**, *47*, 10765–10770.

(176) Takeuchi, Y.; Yamamoto, H.; Tanaka, K.; Ogawa, K.; Harada, J.; Iwamoto, T.; Yuge, H. *Tetrahedron* **1998**, *54*, 9811–9822.

(177) Takeuchi, Y.; Tanaka, K.; Aoyagi, S.; Yamamoto, H. *Magn. Reson. Chem.* **2002**, *40*, 241–243.

(178) Riedmiller, F.; Wegner, G. L.; Jockisch, A.; Schmidbaur, H. *Organometallics* **1999**, *18*, 4317–4324.

(179) Thomson, R. A.; Wilkins, A. L.; Mackay, K. M. *Phosphorus, Sulfur, Silicon* **1999**, *150-151*, 319–324.

(180) Amadoruge, M. L.; Gardinier, J. R.; Weinert, C. S. *Organometallics* **2008**, *27*, 3753-3760.

(181) Amadoruge, M. L.; Yoder, C. H.; Hope Conneywerdy, J.; Heroux, K. R., A. L; Weinert, C. S. *Organometallics* **2009**, *28*, 3067-3073.

(182) Okano, M.; Mochida, K. *Chem. Lett.* **1990**, 701-704.

(183) Seki, S.; Acharya, A.; Koizumi, Y.; Saeki, A.; Tagawa, S.; Mochida, K. *Chem. Lett.* **2005**, *34*, 1690–1691.

(184) Thomson, R. A.; Wilkins, A. L.; Mackay, K. M. 1999; Vol. 150-151, p 319-324.

(185) Wilkins, A. L.; Watkinson, P. J.; Mackay, K. M. *J. Chem. Soc., Dalton Trans.* **1987**, 2365-2372.

(186) Liepins, E.; Zicmane, I.; Lukevics, E. *J. Organomet. Chem.* **1988**, *341*, 315-333.

(187) Zicmane, I.; Liepins, E.; Lukevics, E.; Gar, T. K. *Zh. Obsch. Khim.* **1982**, *52*, 896–899.

(188) Mackay, K. M.; Thomson, R. A. *Main Group Met. Chem.* **1987**, *10*, 83–108.

(189) Takeuchi, Y.; Takayama, T. *Annu. Rep. NMR Spectrosc.* **2005**, *54*, 155–200.

(190) Hanson, P. *J. Chem. Soc., Perkin Trans.* **1984**, *2*, 101–108.

(191) Carr, H. Y.; Purcell, E. M. *Phys. Rev.* **1954**, *94*, 630.

(192) Meiboom, S.; Gill, D. *Rev. Sci. Instrum.* **1958**, *29*, 688-691.

(193) Puff, H.; Heisig, H.; Schuh, W.; Schwab, W. *J. Organomet. Chem.* **1986**, *303*, 343-350.

(194) Puff, H.; Kök, T. R.; Nauroth, P.; Schuh, W. *J. Organomet. Chem***. 1985**, *281*, 141-148.

(195) Dräger, M.; Häberle, K. *J.Organomet. Chem.* **1985**, *280*, 183-196.

(196) Liu, Y. X.; Ballweg, D.; Muller, T.; Guzei, I. A.; Clark, R. W.; West, R. *J. Am. Chem. Soc.* **2002**, *124*, 12174-12181.

(197) Spikes, G. H.; Fettinger, J. C.; Power, P. P. *J. Am. Chem. Soc.* **2005**, *127*, 12232 - 12233.

(198) Schäfer, H.; Saak, W.; Weidenbruch, M. *J. Organomet. Chem.* **2000**, *604*, 211 - 213.

(199) Setaka, W.; Sakamoto, K.; Kira, M.; Power, P. P. *Organometallics* **2001**, *20*, 4460 - 4462.

(200) Mallela, S. P.; Geanangel, R. A. *Inorg. Chem.* **1991**, *30*, 1480 - 1482.

(201) Renner, G.; Kircher, P.; Huttner, G.; Rutsch, P.; Heinze, K. *Eur. J. Inorg. Chem.* **2000**, 879 - 887.

(202) Farwell, J. D.; Fernandes, M. A.; Hitchcock, P. B.; Lappert, M. F.; Layh, M.; Omondi, B. *Dalton Trans.* **2003**, 1719 - 1729.

(203) Bender IV, J. E.; Litz, K. E.; Giarikos, D.; Wells, N. J.; Banaszak Holl, M. M.; Kampf, J. W. *Chem. Eur. J.* **1997**, *3*, 1793-1796.

(204) J.E. Bender IV, J. E.; Banaszak Holl, M. M.; Mitchell, A.; Wells, N. J.; Kampf, J. W. *Organometallics* **1998**, *17*, 5166-5171.

(205) Ng, M. C. C.; Craig, D.; Harper, J. B.; van-Eijck, L.; Stride, J. A. *Chem. Eur. J.* **2009**, *15*, 6569-6572.

(206) Amadoruge, M. L.; Weinert, C. S. *Chem. Rev.* **2008**, *108*, 4253-4294.

(207) Weidenbruch, M.; Hagedorn, A.; Peters, K.; Schnering, H. G. v. *Angew. Chem. Int. Ed. Engl.* **1995**, *34*, 1085-1086.

(208) Weidenbruch, M.; Hagedorn, A.; Peters, K.; Schnering, H. G. v. *Chem. Ber.* **1996**, *129*, 401-404.

(209) Castel, A.; Riviere, P.; Satge, J.; Ko, H. Y. *Organometallics* **1990**, *9*, 205-210.

(210) Aitken, C.; Harrod, J. F.; Malek, A.; Samuel, E. *J. Organomet. Chem.* **1988**, *349*, 285-291.

(211) Castel, A.; Rivière, P.; Satgé, J.; Ko, Y.-H. *J. Organomet. Chem.* **1988**, *342*, C1-C4.

(212) Dräger, M.; Simon, D. *Z. anorg. Allg. Chem.* **1981**, *472*, 120-128.

(213) Mochida, K.; Hodota, C.; Hata, R.; Fukuzumi, S. *Organometallics* **1993**, *12*, 586-588.

(214) Mochida, K.; Shimizu, H.; Kugita, T.; Nanjo, M. *J. Organomet. Chem.* **2003**, *673*, 84-94.

(215) Mochida, K.; Chiba, H. *J. Organomet. Chem.* **1994**, *473*, 45-54.

(216) Mochida, K.; Shimizu, H.; Nanjo, M. *Chem. Lett.* **2000**, 1226-1227.

(217) Schwarz, R.; Lewinsohn, M. *Chem. Ber.* **1931**, *64B*, 2352-2358.

(218) Mochida, K.; Matsushige, N.; Hamashima, M. *Bull. Chem. Soc. Jpn.* **1985**, *58*, 1443-1447.

APPENDICES

APPENDIX A

2,2,3,3,5,5,6,6-OCTA-*P*-TOLYL-1,4-DIOXA-2,3,5,6-TETRAGERMACYCLOHEXANE DICHLOROMETHANE DISOLVATE

The title compound, $C_{56}H_{56}Ge_4O_2 \cdot 2CH_2Cl_2$ or $Tol_8Ge_4O_2 \cdot 2CH_2Cl_2$ (Tol = p-$CH_3C_6H_4$), was obtained serendipitously during the attempted synthesis of a branched oligogermanes from Tol_3GeNMe_2 and $PhGeH_3$. The molecule contains an inversion center in the middle of the Ge_4O_2 ring which is in a chair conformation. The Ge-Ge bond distance is 2.4418(5) Å and the Ge-O bond distances are 1.790(2) and 1.785(2) Å. The torsion angles within the Ge_4O_2 ring are -56.7(1) and 56.1(1)° for the Ge-Ge-O-Ge angles and -43.9(1)° for the O-Ge-Ge-O angle.

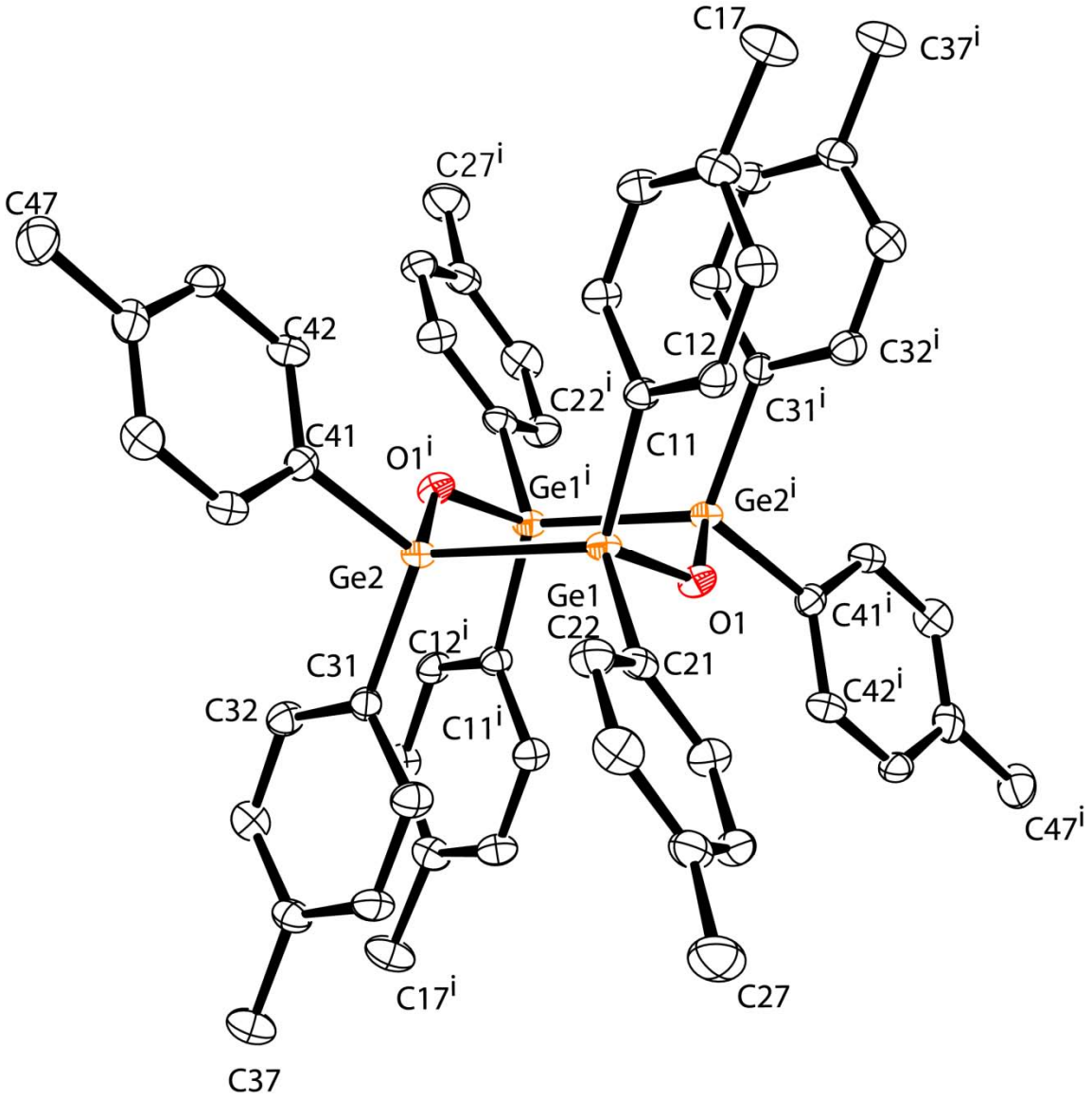

Crystal structure of 2,2,3,3,5,5,6,6-Octa-*p*-tolyl-1,4-dioxa-2,3,5,6-tetragermacyclohexane dichloromethane disolvate, with displacement ellipsoids drawn at the 50 % probability level. Primed atoms are related by the symmetry operator (-x, -y, z+1).

Selected bond distances (Å) and bond angles (deg) of 2,2,3,3,5,5,6,6-Octa-*p*-tolyl-1,4-dioxa-2,3,5,6-tetragermacyclohexane dichloromethane disolvate

Ge1–O1	1.790(2)	O1–Ge1–C21	102.6(1)
Ge1–C21	1.945(3)	O1–Ge1–C11	109.6(1)
Ge1–C11	1.953(3)	C21-Ge1-C11	109.1(1)
Ge1–Ge2	2.4418(5)	O1-Ge1-Ge2	104.82(8)
Ge2–O1^{i}	1.785(2)	C21-Ge1-Ge2	116.8(1)
Ge2C14	1.944(3)	C11-Ge1-Ge2	113.1(1)
Ge2–C31	1.943(3)	O1^{i}-Ge2-C41	102.3(1)
O1–Ge2^{i}	1.785(2)	O1^{i}-Ge2-C31	108.8(1)
		C41-Ge2-C31	110.5(1)
		O1^{i}-Ge2-Ge1	106.2(8)
		C41-Ge2-Ge1	114.5(1)
		C31-Ge2-Ge1	113.7(1)
		Ge2^{i}-O1-Ge1	126.7(1)

Crystal data and structure refinement details of 2,2,3,3,5,5,6,6-Octa-*p*-tolyl-1,4-dioxa-2,3,5,6-tetragermacyclohexane dichloromethane disolvate

Empirical formula	$C_{56}H_{56}Ge_4O_2 \cdot 2CH_2Cl_2$
Temperature (K)	123
Wavelength (Å)	0.71073
Crystal system	Triclinic
Space group	$P\bar{1}$
a (Å)	10.781(1)
b (Å)	11.905(1)
c (Å)	12.295(1)
α (˚)	110.941(1)
β (˚)	94.766(1)
γ (˚)	109.069(1)
Volume (Å^3)	1356.8(2)
Z,*Z*′	1
Calculated density (Mg/m^3)	1.495
F(000)	620
Crystal size (mm)	0.33 × 0.33 × 0.24
Crystal size and shape	Colorless block
θ range for data collection (o)	2.4-25.5°
Index ranges	$-12 \leq h \leq 13$
	$-14 \leq k \leq 14$
	$-14 \leq l \leq 14$
Independent reflections	5003
Absorption correction	Multi-scan
Maximum and minimum transmission	0.471 and 0.558
Refinement method	Full-matrix least-squares on F^2
Final R indices (all data)	
R_1	0.039
wR_2	0.128

APPENDIX B

Absorption data, and calculated HOMO/LUMO energy levels (B3LYP/6-31G*) for oligogermanes 1-6 and 7 (R = CH_2CH_2OEt) in Chapter 4.

Compounds	**λ_{max} $\times 10^{-19}$ J**	**HOMO $\times 10^{-19}$ J**	**HOMO $\times 10^{-20}$ J**	**(HOMO-LUMO) gap $\times 10^{-19}$J**
$REt_2GeGePh_2GeEt_2R$ **(1a)**	8.179	-8.379	- 3.044	8.075
$RBu_2GeGePh_2GeBu_2R$ **(1b)**	8.179	-8.299	- 1.602	8.139
$RPh_2GeGePh_2GePh_2R$ **(1c)**	8.047	-8.796	- 8.331	7.963
$Ph_3GeGeBu_2R$ **(2)**	8.873	-8.732	- 5.768	8.155
$Ph_3Ge(GeBu_2)_2R$ **(3)**	8.567	-8.668	- 5.928	8.075
$Ph_3Ge(GeBu_2)_3R$ **(4)**	8.112	-8.331	- 6.088	7.722
$Ph_3GeGeBu_2GePh_2R$ **(5)**	8.567	-8.699	- 5.608	8.139
$Ph_3GeGeBu_2GePh_2GeEt_2R$ **(6a)**	8.014	-8.363	- 6.088	7.755
$Ph_3GeGeBu_2GePh_2GeBu_2R$ **(6b)**	8.014	-8.315	- 6.088	7.706
$Ph_3GeGePh_3$ **(7a)**	8.281	-8.732	- 1.057	7.674
$Pr^i{}_3GeGePh_3$ **(7b)**	8.457	-8.908	- 4.806	8.427
$Et_3GeGePh_3$ **(7c)**	8.604	-8.748	- 5.608	8.187
$Bu_3GeGePh_3$ **(7d)**	8.567	-8.620	- 5.447	8.075

A

VITA

Monika Lakshmie Amadoruge

Candidate for the Degree of

Doctor of Philosophy

Dissertation: RATIONAL SYNTHESIS OF LINEAR AND BRANCHED OLIGOGERMANES

Major Field: Chemistry

Biographical:

Personal Data:

Born in Sri Lanka, Colombo.

Education:

2005-2010 Completed the requirements for the Doctor of Philosophy in Chemistry at Oklahoma State University, Stillwater, Oklahoma in July, 2010.

1998-2003 B.Sc. Special Degree in Chemistry with first class honors, University of Kelaniya (Sri Lanka).

Professional Memberships:

American Chemical Society

Name: Monika Lakshmie Amadoruge Date of Degree: July, 2010

Institution: Oklahoma State University Location: Stillwater, Oklahoma

Title of Study: RATIONAL SYNTHESIS OF LINEAR AND BRANCHED OLIGOGERMANES

Pages in Study: 247 Candidate for the Degree of Doctor of Philosophy

Major Field: Chemistry

Scope and Method of Study:

Group 14 catenates are important because of their intrinsic optical and electronic properties which entirely depends on their structure. However, study of this structure-property relationship in germanium catenates have been less developed compared with silicon and tin analogues due to the lack of synthetic methods to provide the pure compounds in high yield. The purpose of this study was to develop a method to synthesize discrete oligogermanes in good yields and to investigate the correlation between their structure and physical properties. We have developed a method to synthesize oligogermanes in good yields using the hydrogermolysis reaction and those compounds were characterized using ^{1}H NMR, ^{13}C NMR, ^{73}Ge NMR, elemental analyses, UV/vis, CV and X-ray crystallography.

Findings and Conclusions:

We have developed a rational synthetic procedure for the synthesis of oligogermanes using a germanium amide and a germanium hydride. This reaction proceeds in the presence of acetonitrile via the formation of α-germyl nitrile, which is the active species of the reaction. Therefore, acetonitrile acts as a solvent as well as a reagent. Along with the hydrogermolysis reaction and the hydride protection/deprotection strategy, we have prepared a myriad of new compounds including both linear and branched oligomers. Using these combined methods, we can systematically change the number of germanium atoms in the molecule as well as the identity of the substituents. The optical properties and the electronic properties that we found correlate with the theoretically calculated values using DFT. Therefore, this synthetic methodology allows both “coarse-tuning” and “fine-tuning” of the properties of the molecule by varying the number of catenated germanium atoms and the identity of the organic substituents respectively.

ADVISER’S APPROVAL: Dr. Charles S. Weinert